



TAP 2017

22nd International Transport and Air Pollution Conference

Poster Proceedings

Contents: (click titles to navigate)

1. On-board measurements to assess in-cabin vehicle air quality in Paris
2. Clean Air Project Bolivia – Long-Term Impacts
3. Incentives System for Purchase of Ecological Vehicles in the Republic of Croatia - Analyses of Existing System and Proposal for More Efficient One
4. Coherent structure induced dispersion of exhaust plume from heavy-duty truck
5. Using an iterative Markov Chain process to develop driving cycles based on large-scale GPS data: a case study in Beijing
6. Global Sensitivity Analysis in the Simulation of Road Traffic Emissions at Metropolitan Scale
7. The Role of Changing Costs in Uptake of Hybrid and Electric Vehicles: A UK Case Study Comparing Diffusion Projection Methodologies
8. Developing a high-resolution traffic emission inventory for the metropolitan area of Nanjing, China
9. Particulate emissions of Light Duty Vehicles in the future
10. Emission of PM10 and coarse particles from “silent” asphalt
11. Algebraic and geometric aspects of traffic control models on complex networks
12. SmartAQnet – spatial/temporal high-resolution detection of air quality by new data products
13. Particle Dispersion from Railway Rolling Stock: Preliminary Results from Wind Tunnel Experiments and CFD
14. Computer Vision in Modern Intelligent Transport System
15. A real-world driving monitoring for 44T Natural Gas & Diesel Heavy Duty Trucks: Equilibre Project first results
16. Effects of Driving Behaviour on Fuel Consumption
17. Research of Emissions with Gas PEMS and PN PEMS
18. Fuel Consumption and Emissions of Four Modern Passenger Cars under Real-World Driving Conditions
19. Diesel Particle Filter Tampering Detection during a Vehicle Periodic Technical Inspection
20. Are GPFs effective for reducing genotoxic emissions of GDI vehicles?
21. Drone-based measurement systems offer promising new methods for measuring Air Pollution Spatial Distribution – example results from a pilot study conducted in the Misox Valley of the Swiss Alps
22. Assessment of urban hybrid buses performance in a megacity network
23. Emission Inventory of Non-Road Mobile Machineries (NRMM) – First results for the Republic of Croatia
24. The Influence of Passenger Car Population and Their Activities on NOX and PM Emissions (Data from Croatia)
25. Urban Public Transport Systems Analysed in Terms of Land Use Considering CO2 Emissions: the Case of Vienna, Austria
26. Photocatalytic tunnel coatings: evaluation of their efficiency with time
27. Consumer Acceptance and Societal Climate Benefits of Electric Vehicles: Insights from Individual Travel Patterns in China, U.S., and Europe
28. Physico-chemical characterization of fine and ultrafine non-exhaust particles generated by road traffic in urban and suburban environment

On-board measurements to assess in-cabin vehicle air quality in Paris

A. MEHEL^{1*}, F. MURZYN², F. JOLY³, B. BRUGE³, Ph. CUVELIER¹ and B. PATTE-ROULAND⁴

¹ ESTACALAB, Department of Mechanical Engineering, ESTACA, 78180, Montigny-Le-Bretonneux, France, amine.mehel@estaca.fr

² ESTACALAB, Department of Mechanical Engineering, ESTACA, 53000, Laval, France

³ AIRPARIF, Paris, 75004, France

⁴ CORIA, UMR 6614 CNRS, University of Rouen, 76801 Saint Etienne du Rouvray, France

Abstract

In urban areas, on-road vehicles are the primary direct emission sources of gaseous (NO_x) and particulate (nanoparticles) pollutants. In particular, near major roads and freeways (Morawska et al., 2008). In the region of Paris, the World Health Organization recommended thresholds of their concentrations are often exceeded. These pollutants are carried from these regions to the surrounding environments. When released in the atmosphere, these particles can infiltrate and accumulate into the vehicle in-cabin. As it can be considered as a micro-environment, passengers are submitted to a non-negligible level of exposure. In the present paper, on-board measurements are conducted around and in Paris (France) to characterize the inside to outside (I/O) ratio of NO_x and ultrafine particles (UFP) concentrations in a car for real-driving conditions. The results clearly show that in-cabin pollutants can accumulate depending not only on the road topologies but also on the stochastic event arising in front of the driven vehicle. It is expected that our measurements would lead to some driving recommendations for people to minimize their expositions to UFP and NO_x in cars.

Keywords: Ultrafine particle, Nox, Air pollution, in-cabin, on-board measurements, infiltration.

Introduction

Gaseous and particulate pollutants are present in urban areas with concentrations that are very high. Indeed, in these areas, on-road vehicles are the primary direct emission sources (Biswas et al., 2008; Morawska et al., 2008; Boulter et al., 2012). These pollutants are transported from these regions with very high concentrations to all over the surrounding local environments where they can infiltrate vehicle in-cabin to cumulate resulting in the exposure of the passengers. Several toxicological and epidemiological studies have associated the exposure to high levels of such toxic ultrafine particles (UFP) and NO_x to the enhancement of respiratory inflammation, allergy and Asthma (Hao et al., 2003) and numerous long-term health problems including lung cancer and cardiovascular diseases (Delfino et al., 2005). Two major pollutant characteristics (among others) are important to assess the exposure to UFP: the concentration and the particle size. It has been shown that the ratio of inside-to-outside concentrations (I/O) during the infiltration process strongly depends on vehicle internal parameters such as vehicle mileage, age, ventilation fan speed/settings and ventilation mode (recirculation on/off) (Hudda et al., 2012). Nevertheless it is also submitted to the external parameters such as the local topology as mentioned in (Goel et al., 2015; Takano and Moonen, 2013). In this study, we investigate the pollutant concentrations combining the two points of view through two approaches: the first one consists of on-board measurements where we measure both in and outdoor pollutant concentrations and the second one considers a study at a small scale in a wind tunnel. In that one, the dispersion process from the emission point (at the tailpipe) and the interaction with the vehicle near-wake flow is discussed. This second approach will help to identify the region of preferential accumulation of such UFP leading to a better understanding on the infiltration process.

1. Experimental method

In the present paper, the first approach is a characterization of the I/O ratio of NO_x and UFP concentrations in a car in real-driving conditions. Outdoor NO_x and UFP mass concentrations as well as UFP Number Concentration (PNC) were sampled through three 4 mm probes mounted on the left side of the vehicle. Similar probes were used for in-cabin air sampling set at the front passenger mouth level. I/O PNC were measured using two TSI P-Trak model 8525 alcohol-based

condensation particle counters (CPC). The PNC for UFP ranging between 20-1000 nm were collected at a rate of 1Hz to provide high temporal resolution results. Particle mass concentrations were measured using two TSI DUST-Trak model 8533 for PM₁, PM_{2.5} and PM₁₀ with a time resolution of 10 seconds. Simultaneous measurements of NO and NO₂ (both in and outside of the vehicle) were carried out using two Thermo Scientific 42i model with 10 seconds time resolution. The instruments were powered by a package of internal batteries and a DC to AC converter. The data were transmitted in real time via the Ecombox GSM based device. An on-board Global Positioning System (GPS) device recorded the location and speed of the vehicle at 1s intervals. Lastly, a synchronised video recordings have been used to get additional information. This means that further analyses can be performed on particular events occurring in front of the vehicle. The vehicle was the light duty Renault Kangoo (model year 2006). It is worthwhile to note that windows were closed for all the runs and the ventilation was set (mid-strength fans) and recirculation was off. Fan speed was kept constant to medium for all the tests. The on-board measurements campaign was conducted in April-July 2016 (sunny weather, temperatures between 5° and 27°). Many routes were tested at different moments of the day (morning, mid-day and evening). In the present paper, we only present the results corresponding to evening for Versailles to Paris (route 1); Cergy to Paris (route 2), Saint Denis to Paris (route 3) and Paris proper (route 4) (Figure 1). Traffic was light to busy depending on road types (highways, urban, ring road). A mean distance of 100 km per route is considered for a mean duration of 3 hours. The measurements were made at vehicle speed ranging from 10 km·h⁻¹ to 130 km·h⁻¹

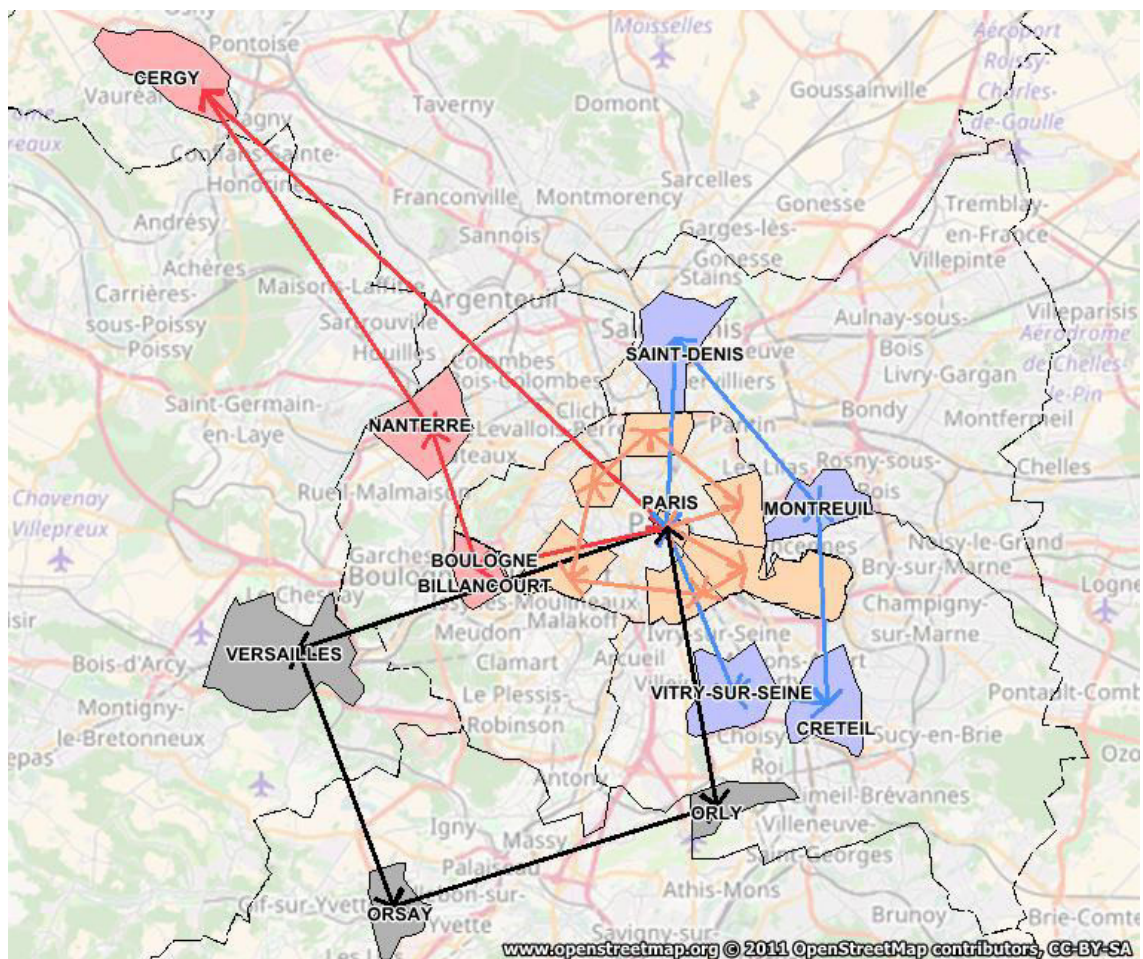


Figure 1: Map of the four routes that were investigated.

3. Results and discussion

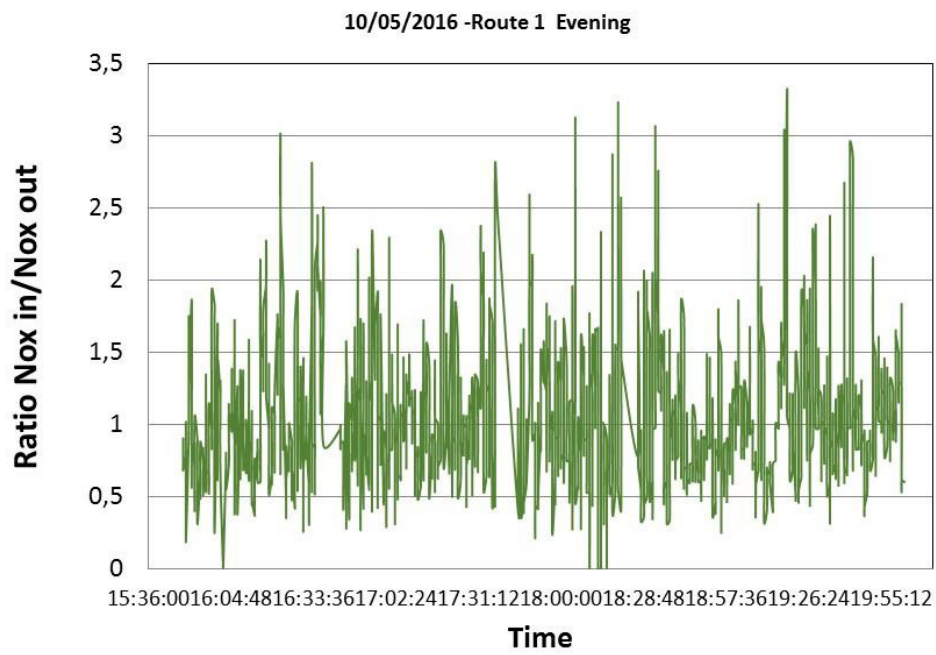
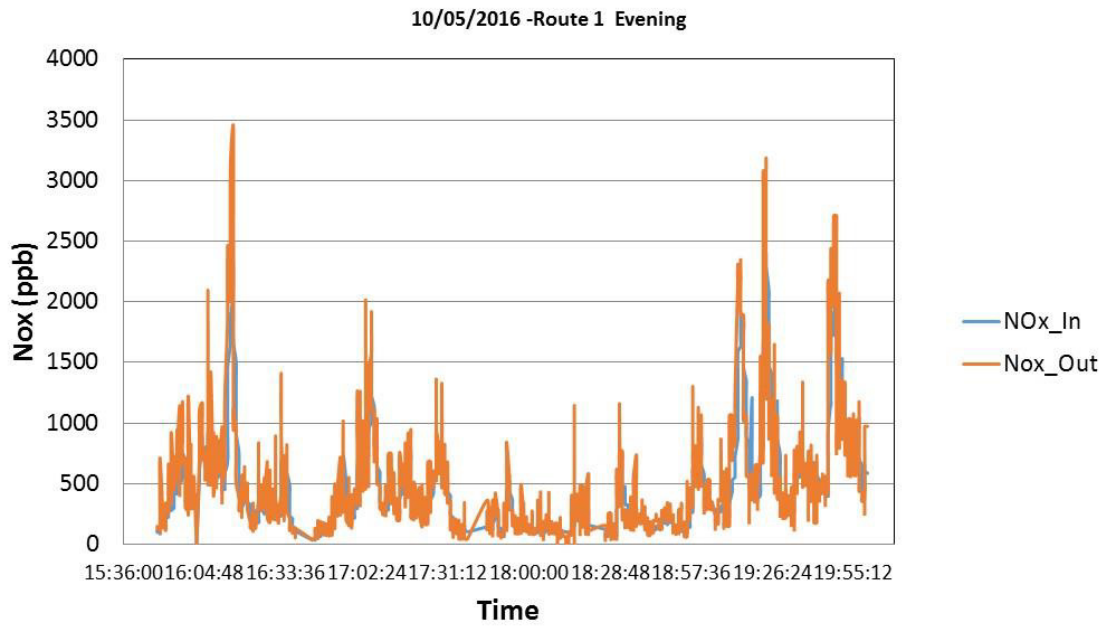


Figure 2: Time evolution of NOx concentrations inside and outside the vehicle cabin (top) and I/O concentrations ratio (bottom) for route 1

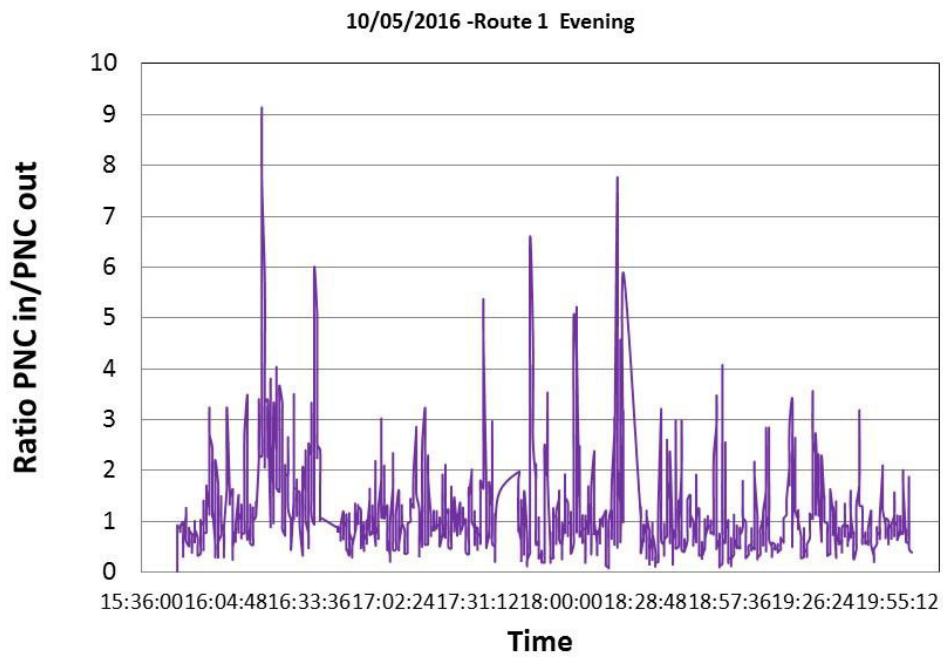
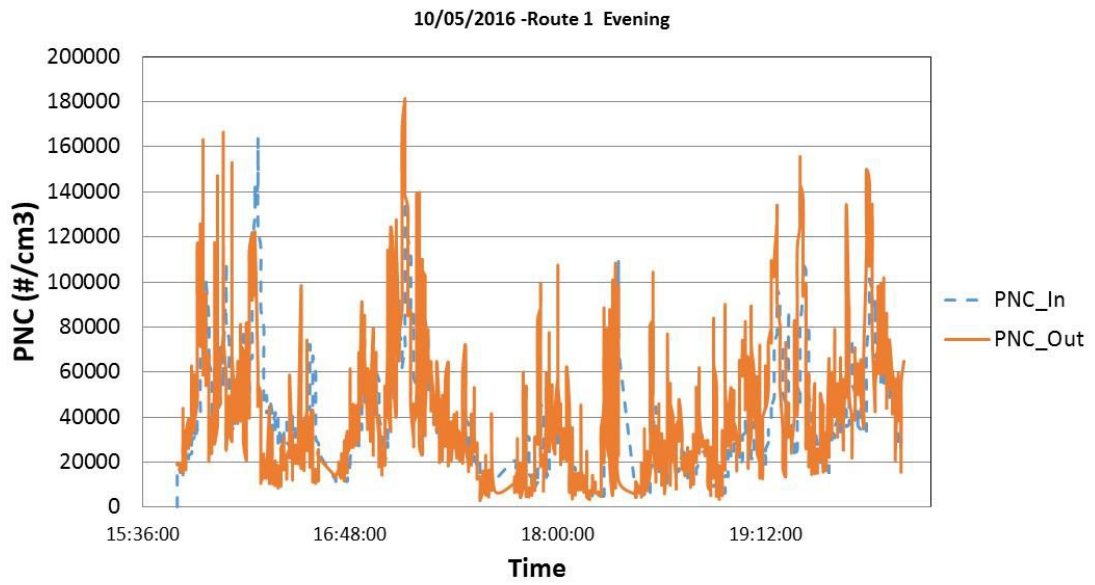


Figure 3: Time evolution of PNC concentrations inside and outside the vehicle cabin (top) and I/O concentrations ratio (bottom) for route 1

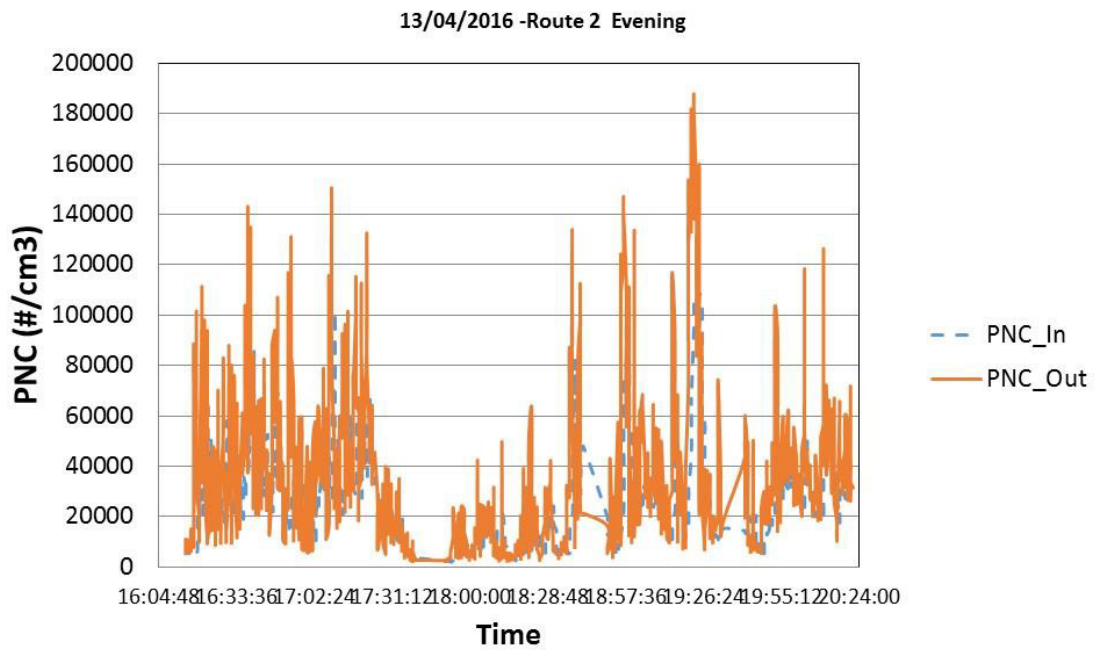
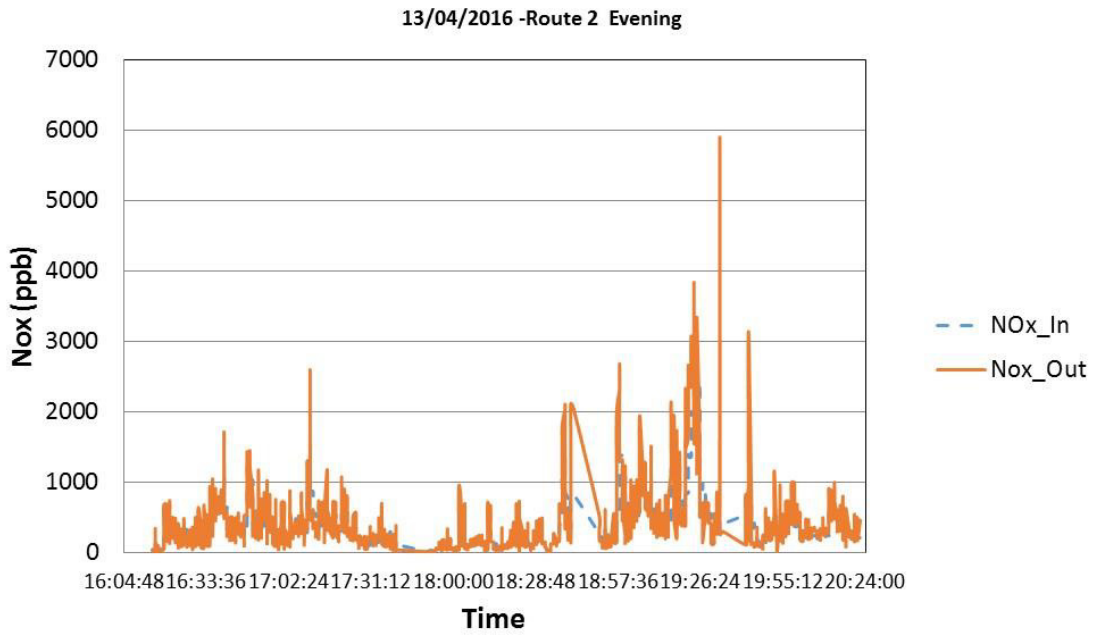


Figure 4: Time evolution of NOx concentrations inside and outside the vehicle cabin (top) and Time evolution of PNC concentrations inside and outside the vehicle cabin (bottom) for route 2

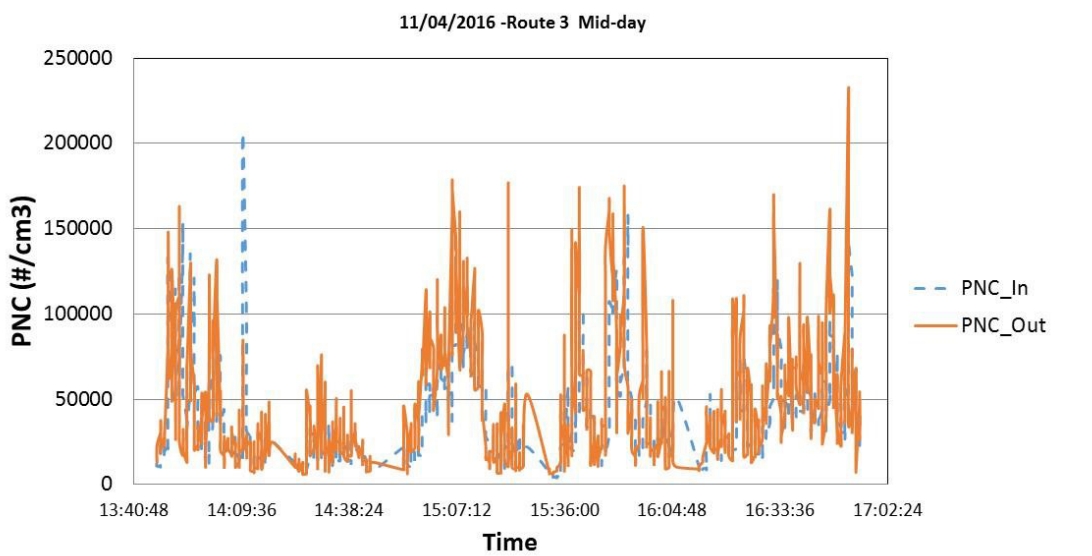
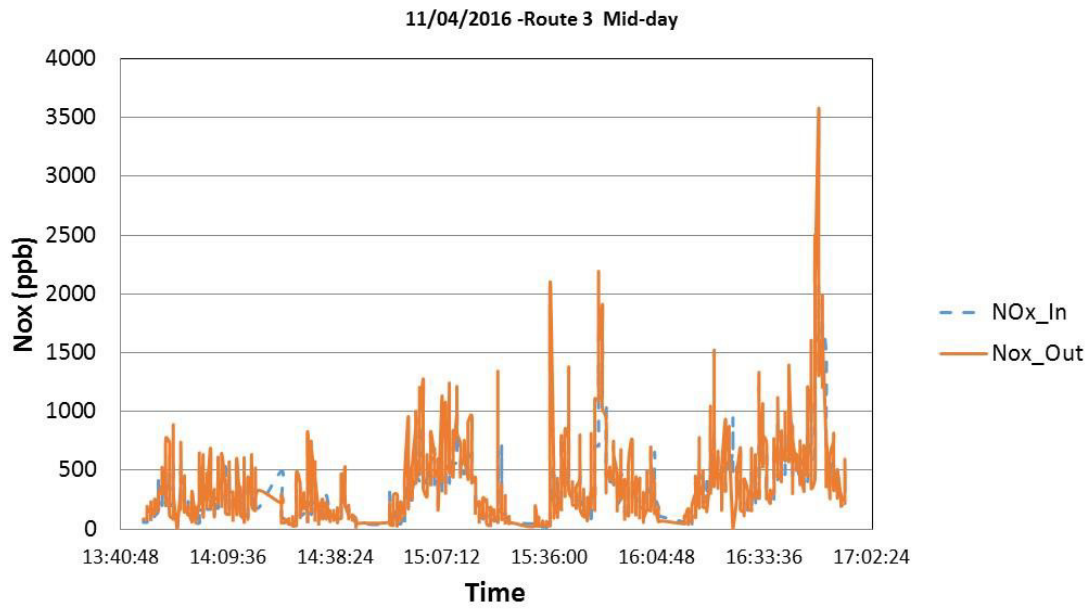


Figure 5: Time evolution of NOx concentrations inside and outside the vehicle cabin (top) and Time evolution of PNC concentrations inside and outside the vehicle cabin (bottom) for route 3

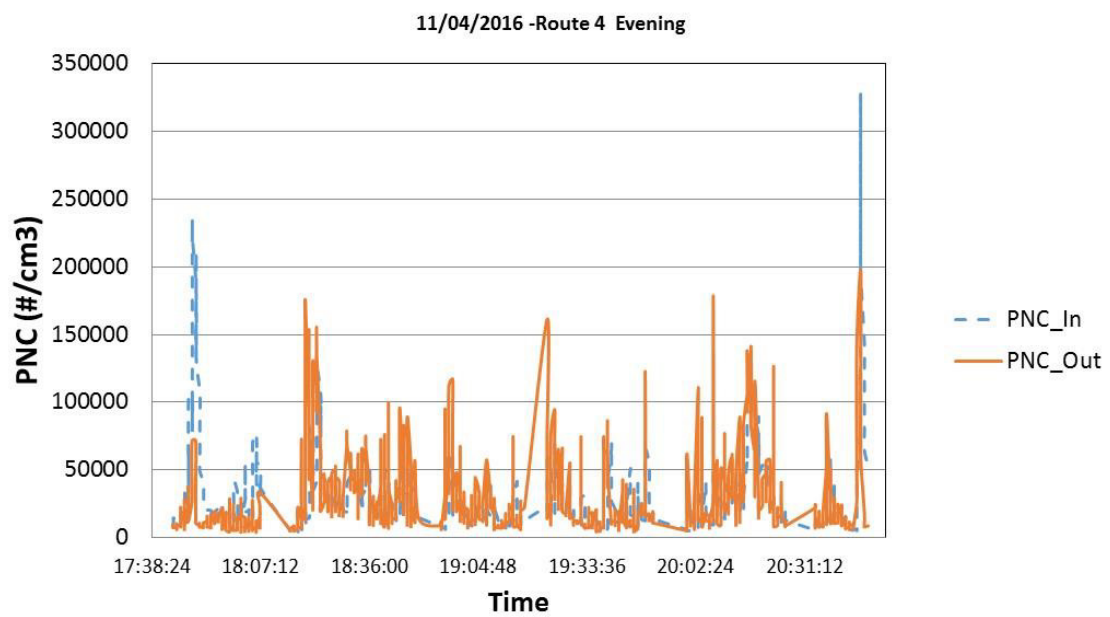
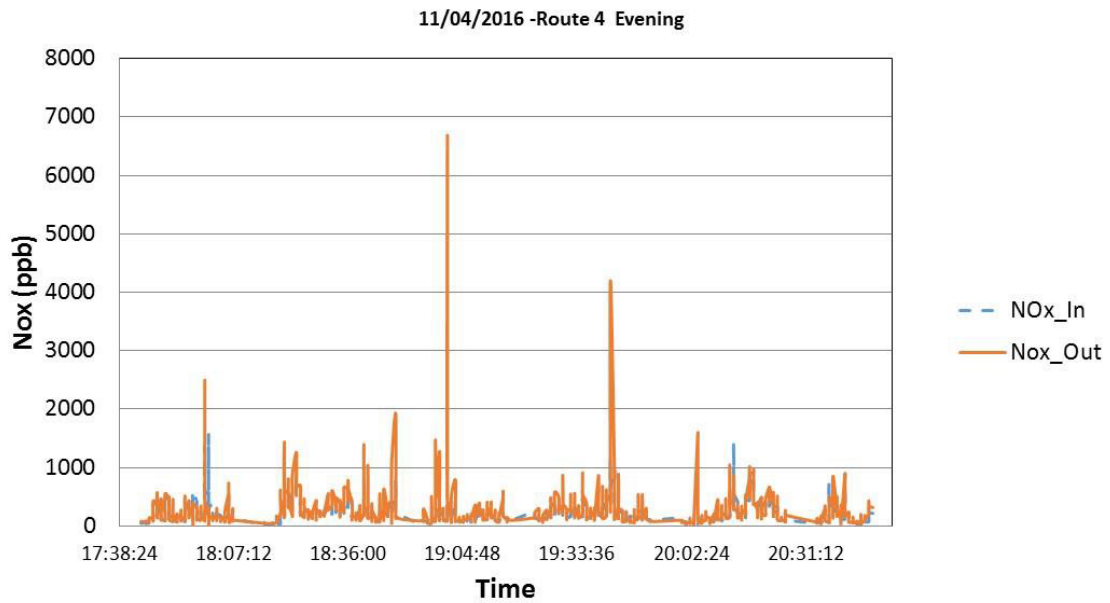


Figure 6: Time evolution of NOx concentrations inside and outside the vehicle cabin (top) and Time evolution of PNC concentrations inside and outside the vehicle cabin (bottom) for route 7

From on-board measurements, time evolution of the concentrations inside and outside vehicle cabin as well as I/O concentrations ratios were obtained. Typical results are presented in Figures 2-6 for NOx and UFP.

Even if the dynamical variation of NOx concentration outside of the vehicle is relatively more important, we still have a fluctuation inside the cabin that is almost the same. Particularly, for peaks which correspond to specific events such as tunnels. This means that when we set the fan ventilation to medium, despite the presence of the cabin filter, most of the gaseous pollutants infiltrate the vehicle in-cabin. The concentrations level inside the cabin can reach 3 times those measured outside (figure 2, bottom) to 7 times for route 4. While the average value of NOx

concentration inside the cabin during the whole test is varying between 1.05 and 1.2 times the one outside. The ratio is more important for routes where the traffic is more important but also where the urban area is more present. The same conclusion could be driven for UFP where their infiltration is followed by an accumulation period that is longer since their deposition or inhalation process takes more time. This could be seen since the peaks of the blue curve are more abundant (figures 2-6). Furthermore, in most of cases, they follow the orange peaks which correspond to the outside UFP concentrations. The average PNC ratio is varying between 1.07 and 1.57 for the whole test. It is also relevant to see that the maximum inside concentration of such nanoparticles can reach 14 times the outside ones (even if it is for short time period) and correspond to weak level of UFP concentrations.

Conclusion

In this study the infiltration process has been studied by conducting on-board measurements. We demonstrate that the pollutants tend to accumulate into the car, particularly for UFP. It is believed that a better understanding of these complex processes (dispersion and infiltration) are needed to improve car cabin air quality and that both approaches (on board measurements and wind tunnel investigations) are required for that.

Acknowledgments

The authors would like to express their gratitude to the Ademe (Environment Agency).

References

- Biswas S, Hu S, Verma V, Herner J, Robertson WJ, Ayala A, Sioutas C., Physical Properties of particulate matter (PM) from late model heavy duty diesel vehicles operating with advanced emission control technologies. *Atmospheric Environment*, 42, 2008.
- Boulter, P. G. , Borken-Kleefeld, J. , Ntziachristos, L., The Evolution and Control of NO_x Emissions from Road Transport in Europe, *The Handbook of Environmental Chemistry*, chap. Urban Air Quality in Europe, 26, 31-53, 2012
- Delfino, R.J., Malik, S., and Sioutas, C., 2005. Potential role of ultrafine particles in associations between airborne particle mass and cardiovascular health. *Environmental Health Perspectives* 113, 934-946.
- Goel, A., & Kumar, P., Zone of influence for particle number concentrations at signalised traffic intersections. *Atmospheric Environment*, 123, 25-38, 2015.
- Hudda, N., Eckel, S. P., Knibbs, L. D., Sioutas, C., Delfino, R. J., and Fruin, S. A., Linking in-vehicle ultrafine particle exposures to on-road concentrations. *Atmospheric Environment* 59, 578-586, 2012.
- Li, N.; Hao, M.Q.; Phalen, R. F.; Hinds, W.C.; Nel, A. E., Particulate air pollutants and asthmas A paradigm for the role of oxidative stress in PM-induced adverse health effects. *Clinical Immunology*, 109, 250-265, 2003
- Morawska, L., Ristovski, Z., Jayaratne, E.R., Keogh, D.U., Ling, X., Ambient nano and ultrafine particles from motor vehicle emissions: characteristics, ambient processing and implications on human exposure. *Atmospheric Environment* 42, 8113-8138, 2008.
- Takano, Y., & Moonen, P., On the influence of roof shape on flow and dispersion in an urban street canyon. *Journal of Wind Engineering and Industrial Aerodynamics*, 123, 107-120, 2013.

Clean Air Project Bolivia – Long-Term Impacts

C.F. Koch¹, R. Villavicencio²

¹Swiss Foundation for Technical Cooperation, Swisscontact, La Paz, Bolivia, freddy.koch@swisscontact.org.

² Swiss Agency for Development and Cooperation, SDC, La Paz, Bolivia, rodrigo.villavicencio@eda.admin.ch

Background

Globally, the transport sector accounts for 24% of greenhouse gas (GHG) emissions and in Latin America and the Caribbean, this percentage rises to 40%. In Bolivia, the transport sector is the largest consumer (40%) of the total energy and the second contributor of emissions, after the land use change. The rapid growth of vehicle fleet entails a significant increase in emissions of greenhouse gases and harmful pollutants, causing the negative effects of climate change and damage to the health of the exposed population.

The project interventions seek to optimize the use of energy resources, reduce pollution, reduce the emission of greenhouse gases and provide better transport services, contributing to the improvement of the quality of life of the population because a city with less pollution and better services is a city with higher quality of life. Especially the vulnerable and marginalized population living in poor and peri-urban areas

The vulnerable population of the cities represents 2.1 million people or 21% of the entire Bolivian population. These are people who work in the streets (kiosqueros, bootblacks, taxi drivers, ...), exposed to the pollution produced by the vehicle park. By their place of residence, far from the urban centers, they have a bad connection to a public transport and / or they use vehicles of bad and very poor technical state or of security that they represent a risk for their lives. A number of scientific studies state that women are the most vulnerable to the exposure of polluted air (especially their work) and, on the other hand, the ones that least move on public transport, in most cases, for fear of abuses, harassment and robbery.

The Clean Air Project

In 1999 Swisscontact started the Urban Ecology Project in Bolivia with a low budget but first actions to improve urban air quality. Based on this effort, in 2003 the Swiss Agency for Development and Cooperation (SDC) decided to start the *Clean Air Project for Bolivia*, with a sister initiative in Peru, based on:

- Focus on pollution caused by vehicles, due to its importance in contributions (>70% of total pollution).
- Lack of institutionality at all levels of government.
- Cities planned for vehicles without considering pedestrians and cyclists.
- Vehicle fleet on average 20 years old (public transport 30 years old). Highly hazardous and polluting.

Timeline of the project

In the Clean Air Project's first phase (3 years), the most important work was to generate social sensitivity (e.g. awareness building campaigns, health impact studies) and set up air quality monitoring networks in Bolivia's four major cities. Later, this network was expanded to another seven cities.

In the second phase (4 years), greater technical and institutional capacities in the municipalities were generated and local offices in charge of air quality management were established.

During the third phase (3 years), the problems of traffic congestion worsened due to the growing number of mostly second-hand vehicles, which led to increased air pollution. The coordinated lobbying among country's major cities towards the national government finally resulted in more restrictive rules on vehicle importation. Thus, air pollution (PM₁₀) today is still above the WHO guidelines (Figure 1) but could be decoupled from the fast-growing density of vehicles (Table 1).

Focus and Principles

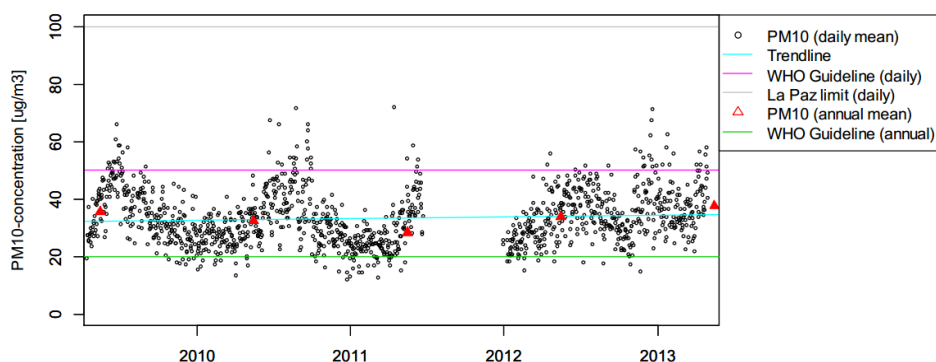


Figure 1. La Paz continuous (daily mean) PM₁₀

Table 1. Increase in Motorization in Bolivia 2003 to 2016

Year	Inhabitants (millions)	Density (veh/1000 inhab.)
2003	8.81	50
2016	10.81	150

Phase IV (2014-2017) of the Clean Air Project achieved the consolidation, institutionalization and scaling up of air quality management in 12 municipalities in Bolivia. The vision was to achieve proper and permanent management in the three lines of intervention (Air Quality Monitoring, Vehicle Inspection Plants and Urban Mobility) of the different political levels according to their competencies, thus ensuring the sustainability of all project interventions.

Focus and Principles

The Project fulfills a role of process facilitator and specialized technical assistance, directed to the different players involved in the implementation of measures aimed at the reduction of air pollution in the cities of Bolivia.

The project focuses on: supporting municipalities and the national government to complete a legal framework on air quality and urban mobility; assisting technically the public and private sectors so that, depending on the roles assigned in the legal framework, they can apply measures of reduction and prevention of air pollution; this approach of intervention, does not generate dependence and allows the Project to leave installed capacities and to leave the system once it works properly.

Components

Awareness building

One of the fundamental pillars of the project from the outset was undoubtedly the sensitization. Little or nothing can be done in Air Quality Management if one does not have a population sensitized and aware of the environment problem.

Among the most successful awareness campaigns that have been carried out are the so-called "Clean Air Weeks", in which vehicle emissions are measured free of charge at different points in the city. These campaigns served to sensitize drivers about the damages caused by vehicular emissions and raise awareness about the technical and economic advantages of preventive maintenance of their mobility. The aim was to introduce drivers to a culture of annual emission control, while the results of the campaigns enrich the statistics on the environmental impact of the car fleet.

With regard to environmental education, a series of publications were published in children's newspapers, training of teachers of schools on the subject, awareness building process aimed mainly at pneumologist and pediatricians, police and journalists.

Air quality monitoring

One of the most important elements of the air pollution problem is to know the air quality situation, which is possible through a tool such as the Air Quality Monitoring Network (MoniCA Network) that allows planning and measure the effectiveness of air quality, mobility and transport quality management measures. The Project helped to implement 12 monitoring networks in different cities of the country, the institutionalization of a national department responsible for air quality and the creation of an Air Quality Reference Laboratory at the most prestigious University in Bolivia. Currently the network operates in a sustainable way and the data generated goes through a quality control by the Reference Laboratory. The Ministry of the Environment has developed 5 annual publications with the air quality information generated by the local Networks and coordinate the quality assurance and quality control of the laboratories.

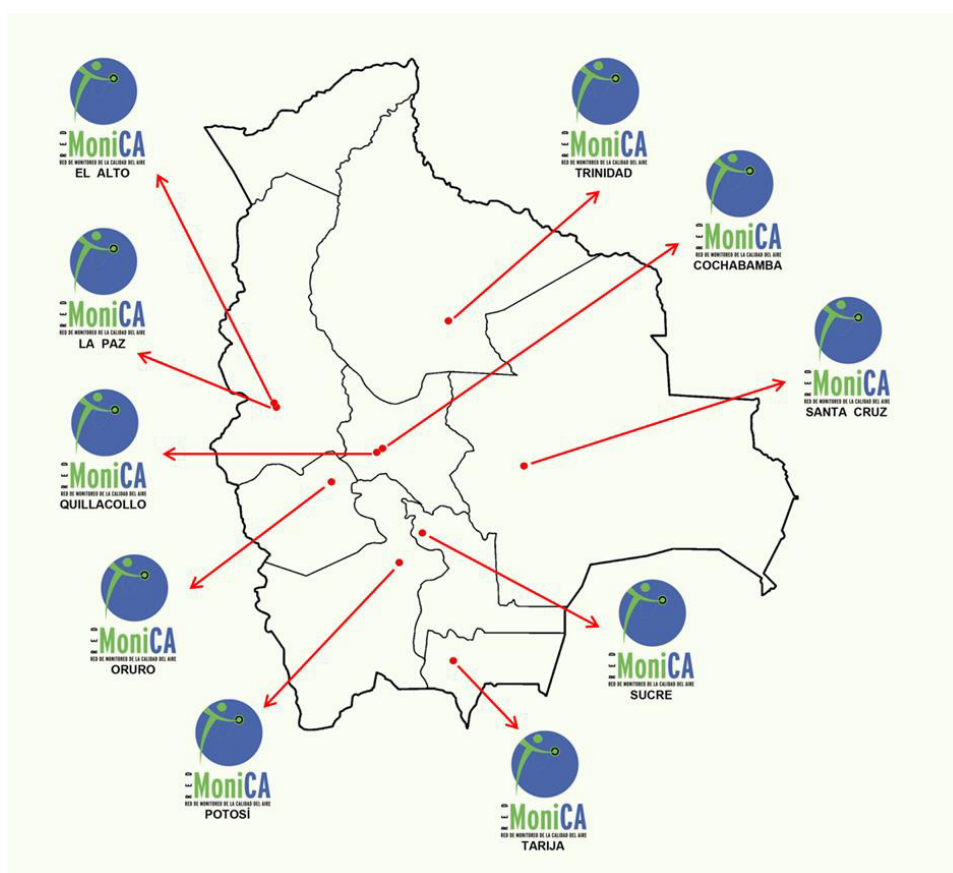


Figure 2. MoniCA Network - Bolivia

Inspection & Maintenance Program

The Bolivian Police, through its Transit Operative Unit, is in charge of the Vehicle Technical Inspection (ITV) Program that is carried out once a year with a mandatory character. The procedure is limited to a visual inspection on a public road, in which the system of lights, electrical system, brakes and accessories is observed. The Vehicle Technical Inspection program is not comprehensive and does not meet many technological requirements to reduce traffic accidents and air pollution.

The Clean Air Project, prompted the building of a new legal framework that allows to migrate to a modern Vehicle Technical Inspection System. In a pilot way, 5 municipalities of Bolivia built their first Programs. The lack of political agreement between governors, does not allow that the new system is still implemented.

Sustainable Urban Mobility

The improvement of transport systems greatly favors the most vulnerable population, such as women, disabled persons and pregnant women, by facilitating access to more efficient, dignified, safe and more space and temporary coverage systems.

The mobility of people in a city is directly related to local economic development. So, with better access to decent and safe transportation, the possibilities of access to employment and education increase, especially the most disadvantaged. In this way, the project supports poverty reduction.

Meanwhile, the municipalities, based on all the knowledge provided by the Clean Air Project, generated institutionalility on two fronts: *Environment* (with specific units of air quality management) and *Urban Mobility* (with a new approach and paradigm, prioritizing pedestrians, cyclists and public transport).

As a result of the process and a newly established legal framework, important actions and plans have been developed:

- 11 cities developed their Sustainable Urban Mobility Plans, and two others are under construction.
- 2 Bus Rapid Systems (BRS) have been implemented in 2 cities and another 4 have finished their studies.
- The state-owned Urban Cablecar Company has been created and currently operates 5 lines, with another 5 under construction.
- Many streets and avenues have been redesigned in favour of pedestrians, some of them are exclusive.
- At least 20 km of bicycle paths are under construction.
- A new Inspection and Maintenance (I&M) Program for vehicles is under discussion. Meanwhile, 4 cities have implemented their pilot programs.
- Each Swiss Franc invested by SDC in urban mobility has so far generated investments by the Bolivian public sector (local & national level) of 89.- CHF.
- Major cities have substantially increased their capacity in terms of Environment and Urban Mobility (number of staff & technical knowledge).

City	Year
PMUS La Paz (AECI)	2011
PROMUT Tarija	2011
PROMUT Sucre	2012
PROMUT Potosí	2012
PROMUT Oruro	2013
PROMUT Trinidad	2014
PROMUT Sacaba	2017
PROMUT Quillacollo	2017
PROMUT Tiquipaya	2016
PROMUT El Alto (IDB/WB)	2017
PMUS Santa Cruz (JICA)	2017

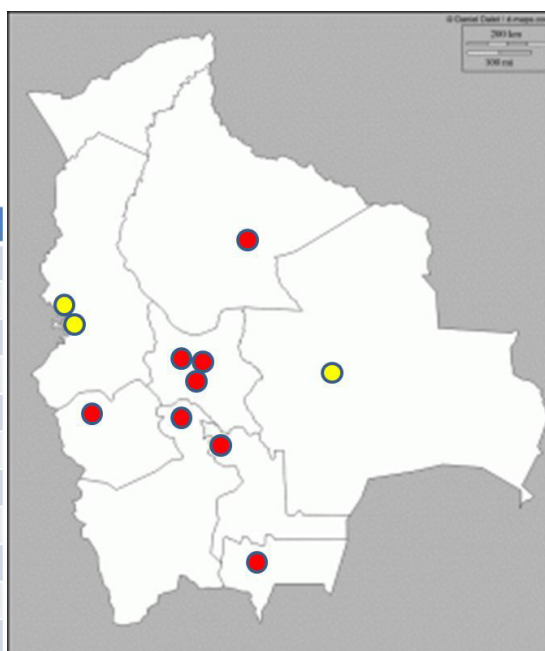


Figure 3. Cities with Urban Mobility Plans

The achievement of the inclusion of economic resources in the Annual Operational Programs (POAs) of the 10 municipalities with which Clean Air currently works, allows an autonomy of management that is the best argument to convince authorities of other municipalities to reproduce the scheme and maximize investments in improving air quality.

Conclusions

Although Bolivia has not yet overcome its problems of air pollution, the country is on the right track and prepared to face new challenges. There is an institutional structure at all levels of the state, as well as a legal framework, which – although not yet complete – allows the development of many actions. The process of implementing air quality improvement systems in developing countries is a long process, so cooperation interventions should last for at least ten years.

The *Clean Air Project* has shown that the construction of tangible solutions can only be reached by collaborating directly with local governments and by empowering the beneficiary population. It is a long and complex road but the results are achievable. At the national level, framework policies contribute and are important, but they do not directly translate into concrete solutions for people.

In urban mobility, thanks to the interventions of the Project, until 2017 public investments have been secured close to USD 1,600 million. This is the first time that these levels of financial resources have been invested to improve urban mobility in Bolivia.

Urban mobility is the main axis of a city's development. If proper planning and implementation of urban development is not done, you end up designing cities to move people only in private vehicles, the antithesis of modern urban mobility principles. In this sense, the intervention of the *Clean Air Project for Bolivia* is considered very successful and at the right time.

Incentives System for Purchase of Ecological Vehicles in the Republic of Croatia – Analyses of Existing System and Proposal for More Efficient One

M. Bunjevac¹, M. Pečet¹ and Z. Lulić¹

¹ Department of IC Engines and Mechanical Handling Equipment, Faculty of Mechanical Engineering and Naval Architecture, University of Zagreb, Ivana Lučića 5, 10000 Zagreb, Croatia

Presenting author email: mb196921@stud.fsb.hr

Abstract

Emissions from road vehicles, i.e. internal combustion engines, are one of the significant sources of Greenhouse Gases (GHG). Because of the harmful effects which vehicles produce, hybrid and electric vehicles are becoming more and more popular every day. Electric vehicles are frequently proposed in terms of solving the problems with GHG emissions and are therefore financially supported through various incentives systems which significantly differ in some countries. The two main aims of this study are the analysis of existing incentives system in the Republic of Croatia and recommendation of a new vehicle incentives system in order to reduce the before mentioned GHG emissions. As the amount of incentives was one of the highest in the EU, the scientific question is: was the incentives system appropriate for the Republic of Croatia and was it possible to achieve higher impact with the same budget? In the paper, several aspects of using EV were analysed, especially their CO₂ emissions depending on the origin of the electrical energy. Emissions from old road vehicles are far greater than emission of new ones and if the incentives were used for co-financing smaller vehicles with internal combustion engine and low CO₂ emissions, a much greater overall GHG reduction would be achieved, which is also shown in the conducted analysis. An additional reason for such decision lies in need for increased safety on the roads in the Republic of Croatia. Namely, the Republic of Croatia still stands above the EU average when it comes to dealing with numbers of road traffic accidents with fatal injuries.

Introduction

Emissions from road vehicles, i.e. internal combustion engines, are one of the significant sources of Greenhouse Gases (GHG). Because of the harmful effects which vehicles produce, hybrid and electric vehicles are becoming more and more popular every day. Electric vehicles are frequently proposed in terms of solving the problems with GHG emissions and are therefore financially supported through various incentives systems which significantly differ in some countries.

Benefit of electric and hybrid vehicles regarding conventional vehicles with internal combustion engines are numerous and these vehicles represent promising, but maybe yet far off future, it is open to a question are they currently the best choice when it comes to reducing GHG in Republic of Croatia. Also question is could it be possible to achieve greater results in GHG reduction with the same finances as well as some additional benefits.

Ministry of Environment and Energy and The Environmental Protection and Energy Efficiency Fund are in charge for carrying out measures for environmental protection and energy efficiency in road traffic. Main goal of implementing measures for energy efficiency in road traffic is encouragement of cleaner transport in Croatia and reduction of air pollution. Project is intended for monitoring goals in improving energy efficiency and GHG reduction in accordance with European commission's "White paper – Roadmap to a single European transport area" [1] and National Environmental Action Plan [2].

According to [3] transport contributes with approximately 33 % in overall energy consumption, while in GHG emission in European Union (EU) transport contributes with 23,2 %, of which 19 % is generated through road traffic, as shown in Figure 1.

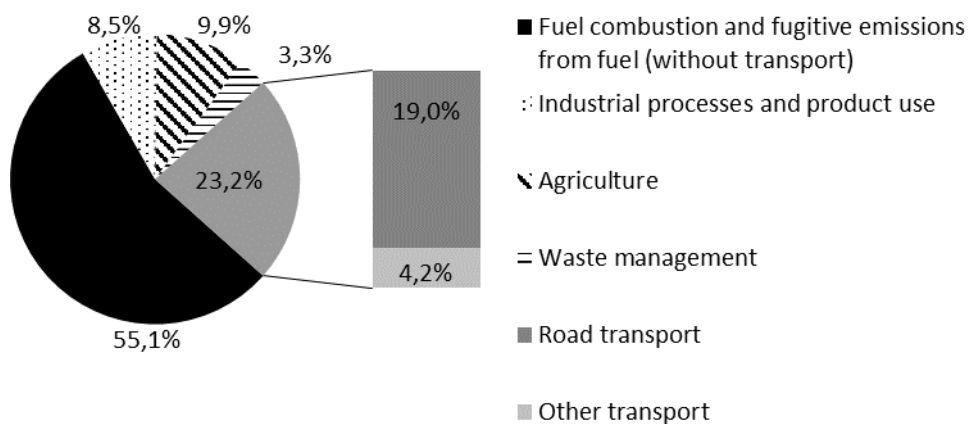


Figure 1: Greenhouse gas emissions, analysis by source sector [3]

CO₂ equivalent

Measurement of life-cycle greenhouse gas emissions involves calculating the global-warming potential of electrical energy sources through life-cycle assessment of each energy source. The findings are presented in units of global warming potential per unit of electrical energy generated by that source. The scale uses the global warming potential unit, the carbon dioxide equivalent (CO_{2e}), and the unit of electrical energy, the kilowatt hour (kWh). The goal of such assessments is to cover the full life of the source, from material and fuel mining through construction to operation and waste management.

In 2014, the Intergovernmental Panel on Climate Change harmonized the carbon dioxide equivalent (CO_{2e}) findings of the major electricity generating sources in use worldwide. This was done by analysing the findings of hundreds of individual scientific papers assessing each energy source. [7]

Old incentive system

Incentive system for electric and hybrid vehicles was authorized by Ministry of Environment and Energy and The Environmental Protection and Energy Efficiency Fund as a measure for GHG reduction and increasing of the energy efficiency. In Table 1 the values of incentives for a specific electric vehicle type are provided.

Table 1: Incentive used in 2014 and 2015

Incentive amount	Vehicle type
70.000,00 HRK ≈ 9.300,00 EUR	Electric vehicles
50.000,00 HRK ≈ 6.700,00 EUR	Plug-in hybrid and electric vehicle with range extender
30.000,00 HRK ≈ 4.000,00 EUR	Hybrid vehicles with emission up to 90 gCO ₂ /km
7.500,00 HRK ≈ 1.000,00 EUR	Electric vehicles with 2 wheels and maximum speed up to 50km/h
10.000,00 HRK ≈ 1.300,00 EUR	Electric motorcycle with maximum speed greater than 50 km/h
15.000,00 HRK ≈ 2.000,00 EUR	Light duty electric quad with output power less than 4 kW
30.000,00 HRK ≈ 4.000,00 EUR	Heavy duty electric quad with output power greater than 4 kW

Carrying out of this co-financing measure was started in 2014. For the incentive itself, an amount of approx. 2 million EUR was provided in order to co-finance 440 vehicles of which 379 were hybrid vehicles, 53 electric vehicles and 8 plug-in hybrid vehicles. From the resources provided, approx. 1,5 million EUR was spent on co-financing 340 vehicles of which 313 were hybrid vehicles, 24 electric vehicles and 3 plug-in hybrid vehicles as shown in Figure 4.

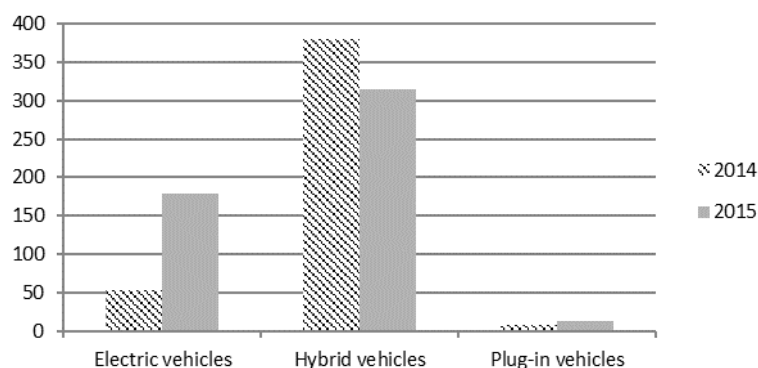


Figure 2: Vehicles obtained throughout the 2014 and 2015 incentives

The second circle of incentive was initiated in 2015. When approx. 2,5 million EUR was approved for co-financing 506 vehicles of which 314 are hybrid vehicles, 179 electric vehicles and 13 plug-in hybrid vehicles. The financial allocation began in February and stopped in April the same year, under the explanation that the full capacity of the incentive was reached.

Methodology

The efficiency grade of the program is based on estimation of GHG emission savings, as well as the realization of additional benefits with comparison between two different incentive systems. In order to present additional benefits which is possible to achieve with different incentive system, it is necessary to determine the vehicle state in Republic of Croatia.

Calculation of electric vehicles emission

Hybrid vehicles are assumed to be less environmentally harmful, while electric ones are believed to be entirely clean. Even though nowadays aim is to gain electric energy through renewable sources such as hydroelectric power plant, solar power plant and wind power plants, thermal power plants are still labelled as one of the basic sources of electrical energy [6]. The most used fuels are coal, natural gas and petroleum. Their main characteristic are their gases, which are the same ones that come from ICE vehicles.

According to [7], every energy source produces CO_{2e} at some point. Values of these emissions are shown in Table 2. EU-mix represents an average CO_{2e} emissions expressed in g/kWh for electric energy production inside the European Union, which is later imported in Republic of Croatia for further distribution and usage.

Table 2: CO_{2e} by electricity source and CO_{2e} for electricity used in Croatia

Energy source	Specific emission of CO _{2e} [g/kWh]	Share in HR [%]	Share of specific CO _{2e} emission by energy source in HR [g/kWh]
Conventional thermal	740-910	24,8	183,5-225,7
Wind	7-56	5,8	0,4-3,2
Nuclear	3,7-110	\	\
Hydro	1-24	39,3	0,4-9,4
Solar	18-180	0,3	0,1-0,5
EU-mix (for 2016)	435	29,8(import)	129,6
			Σ 314,0 – 368,4

Multiplying the percentage of electric energy sources and specific CO_{2e} emissions according to used energy-generating product, gives the overall value of CO_{2e} emissions in grams per kWh produced electric energy. In Table 2, specific CO_{2e} emission subject to source

from which it is obtained is being presented. After the conducted calculation, we come to the value from 314,0 to 368,4 gCO_{2e}/kWh.

For a precise representation of electrical vehicles environmental impact, it is necessary to consider a few electric vehicles subject to their size and thereby specific energetic requests.

In Table 4, some specific energetic requests for certain types of vehicle classes are being shown. According to [8], specific requests for electric vehicle energy is in the range from 0,146 kWh/km for a low-energy-consumption electric vehicle to 0,164 kWh/km for a high-energy-consumption electric vehicle.

Table 3: Examples of electric car consumption based on NEDC [8]

Vehicle	Energy consumption [kWh/km]
Ford Focus Electric 2017	0,164
Nissan Leaf 2016	0,15
Renaul Zoe Q90	0,146
Volkswagen e-Golf	0,127

$$E_{CO_2, EV} = e_{CO_2, EV} \cdot E_{consumption} \quad (1)$$

Where:

$E_{CO_2, EV}$ – specific CO_{2e} emission of electric vehicle, [g/km];

$e_{CO_2, EV}$ – emission factor of electric energy production, [g/kWh];

$E_{consumption}$ – energy consumption of an electric vehicle, [kWh/km].

With equation (1) electric vehicle emission factor [gCO_{2e}/km] can be calculated. This kind of notation is common for ICE vehicles, because it also represents a basis for paying a special kind of charge for environment during vehicle registration in Republic of Croatia.

Proposed incentive system

The proposed incentive system would be based on changing the old vehicles with new ones with ICE. It would be conducted in a way that the new vehicles with a low fuel consumption would replace old ones with higher fuel consumption.

The new vehicles would be co-financed with an amount of approx. 3.000,00 EUR which would represent 20-25% of their initial value. In other words, that means that Republic of Croatia would not, in fact, give the incentive for co-financing the vehicles, but rather give up money gained through VAT and input VAT. In that way, it would be possible to replace significantly more old vehicles with new ones. The incentive would include vehicles with emission levels up to 100 gCO₂/km, emission standard Euro 6 and driven by gasoline engine.

The basic incentive conditions would be: that the incentive resource is given to people that have only one vehicle in their property, that they can prove they are owners of that vehicle for more than 5 years and that the vehicle has been produces before 2000. Furthermore, the replacement of the vehicle would primarily be applied to vehicles with a greater annual mileage in order to ensure removal of larger harmful emission sources.

After they have obtained the incentive right, the owners would be asked to leave a verification of their vehicle destruction to competent institution in order to ensure complete replacement of old vehicles with new ones.

Emission savings

In order to properly demonstrate the emission savings of the GHG, an average emission accordingly to EEA data (The European Environment Agency) [9] is taken in consideration, which for 2000. is 172,2 g/km. In Table 4, an average CO₂ emission by kilometre of distance travelled for a variety of fuels has been shown.

Table 4: Average CO₂ emissions from new passenger cars by fuel (EU) [9]

g CO ₂ /km	2000	2001	2002	2003	2004	2005	2006	2007	2008	2009	2010	2011	2012	2013	2014	2015
All fuels	172.2	169.7	167.2	165.5	163.4	162.4	161.3	158.7	153.6	145.7	140.3	135.7	132.2	126.7	123.4	119.5
Petrol	177.4	175.3	173.5	171.7	170.0	168.1	164.9	161.6	156.6	147.6	142.5	137.6	133.7	128.5	125.6	122.5
Diesel	160.3	159.7	158.1	157.7	156.2	156.5	157.9	156.3	151.2	145.3	139.3	134.5	131.5	126.9	123.2	119.2

Given the fact that incentive of electric and hybrid vehicles is foreseen in a way to replace the ICE vehicles, the emission savings calculation would be conducted in a way that the newly purchased electrical vehicles will change vehicles with 162,4 gCO₂/km emission which represents the value of average CO₂ emissions for 2005. That particular year has been chosen since the average vehicle age for Republic of Croatia is 12 years.

The emission calculation would be led by the principle firstly by showing the reduced specific emission by replacing electric vehicle and replacing with a new ICE vehicle, then by showing the reduction of the overall CO₂ emission on an annual level achieved by old and new incentive system.

$$\Delta E_{EV} = E_{2005} - E_{EV} \quad (2)$$

$$\Delta E_{NV} = E_{2000} - E_{NV} \quad (3)$$

Where:

ΔE_{EV} – specific emission savings reached by co-financing electric vehicles, [g/km];

E_{2005} – average CO₂ emissions for 2005., according to EEA data [9] it is 162,4 [g/km];

ΔE_{NV} – specific emission savings achieved by co-financing new ICE vehicles, [g/km];

E_{2000} – average CO₂ emissions for 2000., according to EEA data [9] it is 172,2 [g/km];

By looking at data from Center for Vehicles of Croatia [4], an average annual number of kilometres of electric vehicles is 6.823 km, while for ICE vehicles that number increases to 12.706 km. The small kilometres number is caused by their relatively short range and battery charging time.

$$E_{EV,annual} = \Delta E_{EV} * s_{EV} * n_{EV} \quad (4)$$

$$E_{NV,annual} = \Delta E_{NV} * s_{NV} * n_{NV} \quad (5)$$

Where:

$\Delta E_{EV,annual}$ – specific emission savings reached by co-financing electric vehicles, [g/km];

$\Delta E_{NV,annual}$ – specific emissions savings reached by co-financing of new ICE vehicles, [g/km];

s_{EV} – annual number of kilometres of an electric vehicle;

s_{NV} – annual number of kilometres of new vehicles;

n_{EV} – number of electric vehicles co-financed by incentive

n_{NV} – number of new ICE vehicles co-financed by incentive.

Vehicle age and roadworthiness of vehicles in Republic of Croatia

According to data from Center for Vehicles of Croatia, Republic of Croatia has 2.010.172 registered vehicles in 2016. From which 1.528.119 is M1 category (motor vehicles for passenger transport which except driver's seat has maximum 8 seats more) [4]. Average vehicle age is 12,76 years with a constant grow.

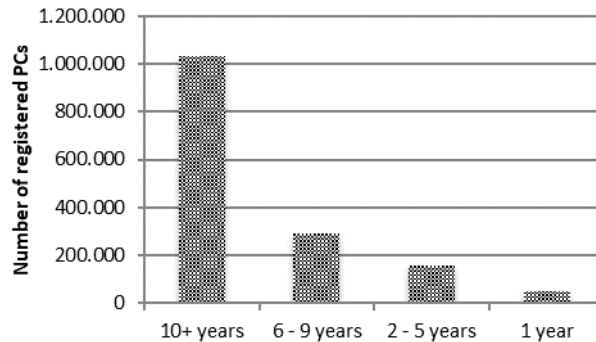


Figure 3: Number of registered passenger cars (PCs) in Croatia by their age

From Figure 3 it can be clearly seen that more than a million vehicles are 10 or more years old. That also means that Republic of Croatia is full of old vehicles, which are both environmentally unfavourable and not safe for traffic. In European Union, average vehicle age is 9,76 years [5]. It can be said that the more the vehicle is old, it consumes more fuel, and thereby releases more toxic and greenhouse gases into environment. Out of that 10-or-more-years-old vehicles, 57.517 is falling within emission class Euro 0 and 98.562 vehicles within Euro 1 which makes 10% out of all M1 category vehicles. [4].

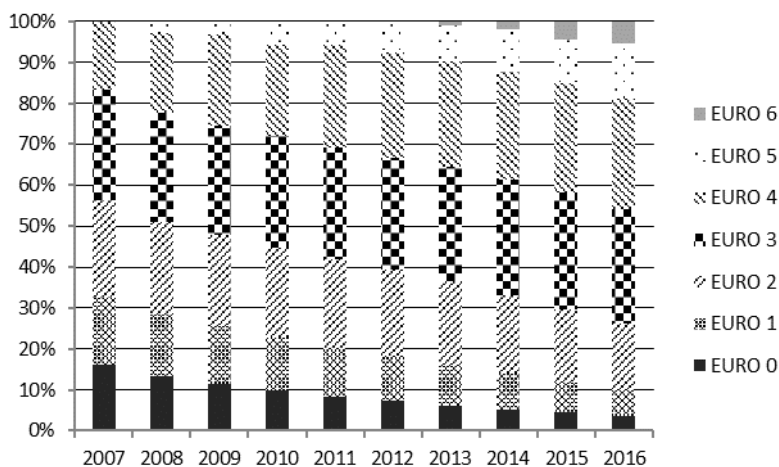


Figure 4: PCs in Croatia by emission standards

Despite the fact that vehicles cause harmful effects on environment, they also represent a danger in traffic. Statistic data from Center for Vehicles of Croatia show that older vehicles are quite more often technically defective which directly affects traffic safety. During the research conducted by the Center for Vehicles of Croatia and Faculty of Mechanical Engineering and Naval Architecture, 166 vehicles have been inspected which have participated in road accidents with fatalities, in which 70 of them (42,17%) have been labelled as unroadworthy (meaning they would fail at PTI). Since average vehicle age in Republic of Croatia is 12,76 years and given the fact that average vehicle age which have participated in car accidents with fatalities is 14,54 years clearly indicates how much old and technically defective vehicles are dangerous in traffic. On Figure 5, a percentage of unroadworthy vehicles and proper vehicles that participated in car accidents is being shown. [4]

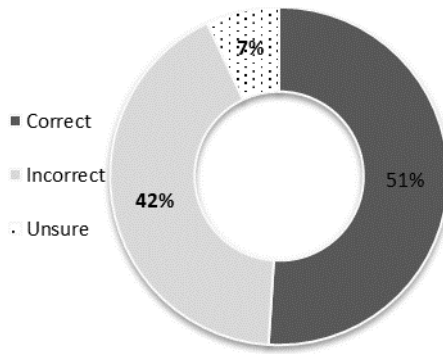


Figure 5: Technically incorrect PCs that where in a traffic accident with fatal injuries

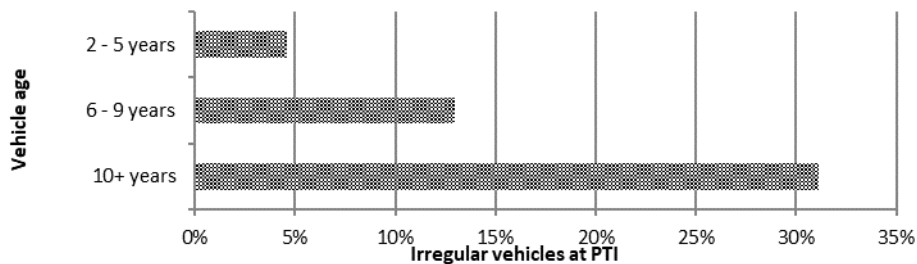


Figure 6: PC irregularities at PTI by vehicle age

On Figure 6, a percentage of irregular vehicles at PTI by their age is being presented. According to the conducted research, it appears that vehicle age impact significantly on death case probability during traffic accident. It was also sighted that death rate increases with vehicle age.

Results

Results of electric vehicle emissions calculation

As indicated earlier, electric vehicles in reality are not vehicles with zero emissions, at least not globally, therefore their real CO_{2e} emission extremely depends on the source of electrical energy.

For a source of energy for electrical energy production, fuel combustion is still being used at least by some point. Every country's sources differ from one another which means that every country has specific gCO_{2e}/kWh emissions. Figure 7 shows gCO_{2e}/kWh emissions accordingly to former mentioned calculations for European Union countries.

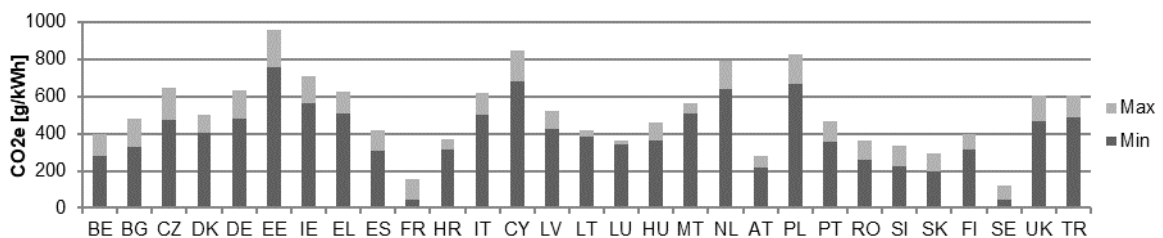


Figure 7: CO_{2e} for electricity production based on source types used in countries across Europe

Altogether with Table 3 and equation (1), it is possible to determine that limiting value of profitability of electric vehicles in terms of CO₂ emissions does exist.

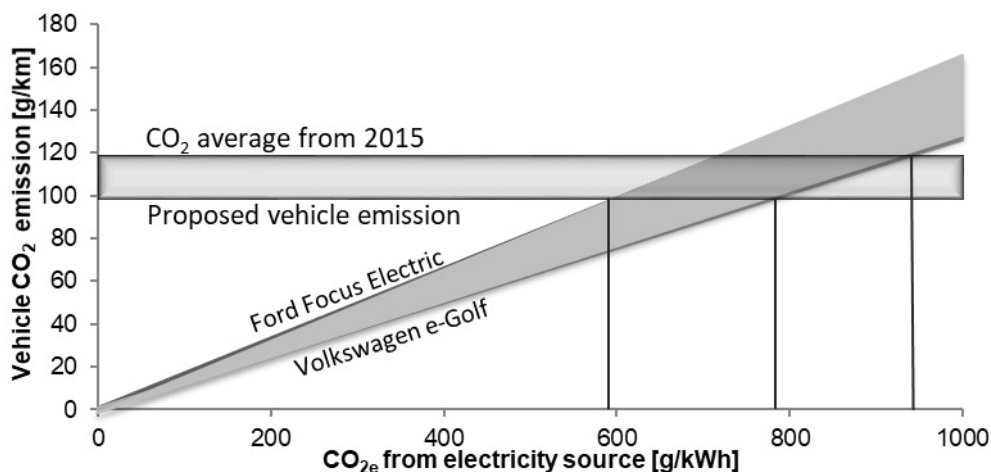


Figure 8: Example of electric vehicle GHG emission based on electricity source

By taking a low-electrical-energy consumption vehicle into account, e.g. VW e-Golf, in Figure 8, it can be observed that replacing the vehicles with ICE vehicles serves as a favourable option, but only if the emission of produced electrical energy is lower than 940 g/kWh. In addition, if we take an electrical vehicle with greater energy consumption, for instance Ford Focus Electric 2017, the cost effectiveness of that kind of vehicles in terms of reducing the GHG emissions, drops down to 600 CO_{2e}/kWh.

Comparing the given data with Figure 7, it can be clearly seen that electrical vehicles are crucial for GHG emission reduction for countries with greater number of renewable energy sources like Austria and Republic of Croatia. The limiting cost effectiveness case of switching the ICE vehicles is Ireland, where 565 to 710 gCO_{2e} is produced for 1 kWh of electrical energy.

In countries like Estonia, Cyprus, Netherlands or Poland, the replacement of ICE vehicles with electric ones is not favourable option because of the high CO_{2e}/kWh electrical energy production. In order for a positive impact of vehicles replacement, it is necessary to provide more electrical energy out of renewable energy sources such as tidal power plants, wind power plant or hydroelectric power plant. Otherwise, a counter-effect would be reached and instead of GHG reduction coming from the electric vehicles, it would be indirectly increased because of the electrical energy production needed for driving electric vehicles.

Results of emission saves calculation

In 2015., an incentive of providing 506 ecologically favourable vehicles was ensured, falling within electric and hybrid vehicles, while in 2014. that number was 340 vehicles, as formerly shown. 3.960.000,00 EUR was spent on that incentive, i.e. 846 new vehicles have been procured. With that amount of money, new incentive would ensure replacement of 1.485 old vehicles and purchasing new ones.

If we take into consideration electrical energy consumption of the newly procured vehicles in the range of 0,127 up to 0,164 kWh/km and CO_{2e} emissions which for Republic of Croatia is from 313,8 to 368,4 gCO_{2e}/kWh, altogether with earlier described equations, it is possible to determine that average CO_{2e} electrical vehicles emissions in Republic of Croatia is between 39,9 and 60,4 gCO_{2e}/km.

According to equation (2), a reduction of 122,5 to 102 gCO₂/km in specific GHG emissions by putting electric vehicle on the road. Additionally, by equation (3), a reduction of 72,2 gCO₂/km has been accomplished in specific GHG emission of replacing old vehicle with a new one. It can be seen that a much greater difference is being made by implementing electric vehicles in traffic.

Even though a significantly higher GHG specific emissions saving has been achieved, it still is not big enough to substitute the savings made with replacing old vehicles with new ones. With equation (4) the saving made on electric vehicles is 707,1 to 588,7 tCO_{2e}/annually, whereas equation (5) shows the savings made by replacing old vehicles with new ones, which is 1362,3 tCO₂/annually.

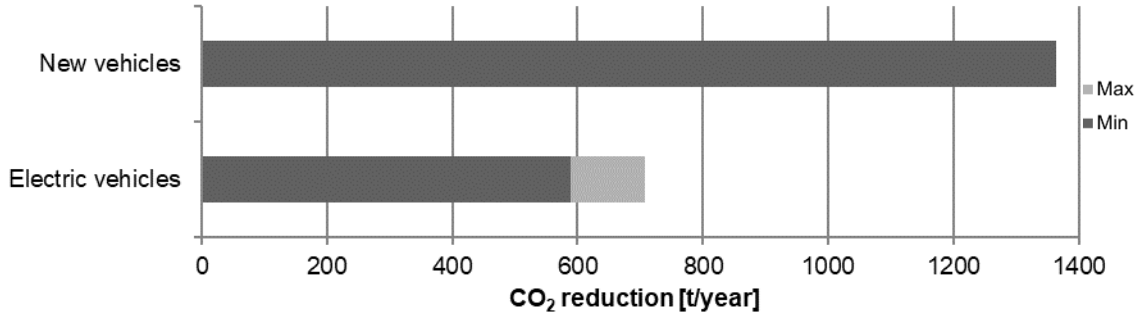


Figure 9: GHG savings (benefit) by implementing new incentive system

It would only be possible for GHG emission savings to be approximately the same for two incentives systems if electric vehicles had the same average number of kilometres as ICE vehicles, which is 12.706.

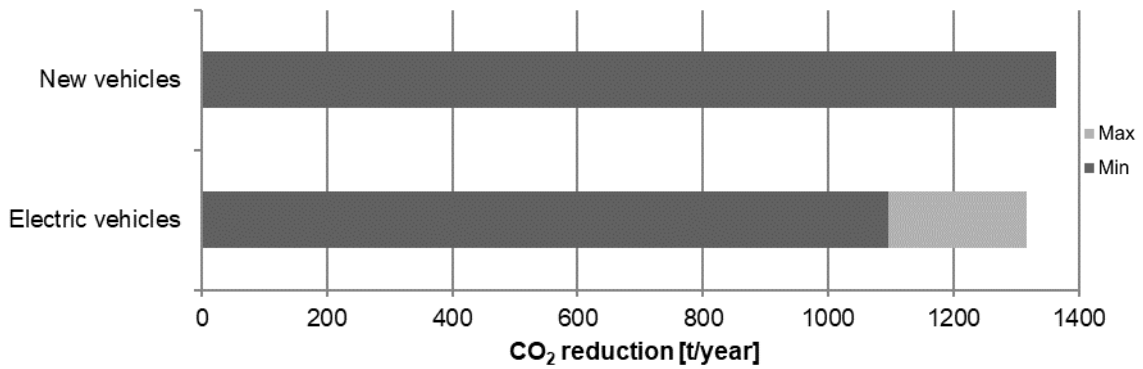


Figure 10: GHG savings (benefit) if electric vehicles were used as conventional vehicles

Conclusion

The new incentive would serve as a step forward in reduction of average vehicle age in Republic of Croatia. The new system is designed in a way not only to provide the market with new vehicles, but also removing the old ones from the traffic. Thus, the average vehicle age is being double effected. The Republic of Croatia is one of the worst positioned countries of European Union by the number of traffic accident fatalities. The new incentive would therefore serve as a more relevant step to traffic safety growth and at the same time, it would promote the public awareness of the consequences related to vehicle age and their technical roadworthiness.

According to the before mentioned, it is easy to conclude that the impact of electrical vehicles on CO_{2e} emissions considerably depends on the way they are obtaining their electrical energy. The limiting value of specific emission of sources of electric energy is in the range from 600 to 900 gCO_{2e}/kWh, which means that all countries with higher specific emission cannot and should not to consider electrical vehicles as a solution that ecologically pays off. The specific electrical energy source emission for Republic of Croatia is less than the limiting value: 314 to 368 gCO_{2e}/kWh. Thereby, a chance of CO₂ emission savings is being made, with the help of electric vehicles implementation into the traffic of Republic of Croatia.

With the vehicle age reduction in Republic of Croatia, the new incentive would also significantly reduce GHG emission, because vehicles with higher GHG emissions would be primarily replaced. A great issue that comes along when talking about electrical vehicles is their source of electrical energy. Electrical energy in most countries is being provided through conventional thermal sources which represent a noteworthy environment impact. Also, a lack of electric vehicles is their relatively small range, which results in half of annual mileage, compared with ICE vehicles. Likewise, the price of electric vehicles is twice the price of vehicles with similar performances which automatically makes them unattainable for most people, even with high incentives.

With all the mentioned put into consideration, it has been concluded that replacement of old vehicles with new ones would have far more GHG emission impact, average vehicle age and by that road safety. Electrical vehicles surely represent the future of road traffic, but before putting them on the road, a different kind of measure would be needed. A kind which deals with GHG reduction as well as traffic safety improvement.

References

- [1] White paper – Roadmap to a single European transport area – towards a competitive and resource efficient transport system, (2011)
https://ec.europa.eu/transport/themes/strategies/2011_white_paper_en
- [2] Ministry of Economy, 3. National Environmental Action Plan,
http://www.mingo.hr/public/3%20Nacionalni_akcijski_plan.pdf
- [3] Greenhouse gas emission statistics,
http://ec.europa.eu/eurostat/statistics-explained/index.php/Greenhouse_gas_emission_statistics
- [4] Center for vehicles of Croatia, Capraška 9, 10 000 Zagreb
- [5] European Automobile Manufacturers Association, 2014.
http://www.acea.be/uploads/statistic_documents/ACEA_PARC_2014_v4.pdf
- [6] Eurostat-European Commission, 2017.
http://ec.europa.eu/eurostat/statistics-explained/index.php/Electricity_production_and_supply_statistics
- [7] IPCC Working Group III, 2014, Mitigation of Climate Change, Annex III: Technology - specific cost and performance parameters
- [8] PUSHEVS,
<http://pushevs.com/electric-car-range-efficiency-nedc/>
- [9] The European Environment Agency (2015), Monitoring CO₂ emissions in cars and vans

Coherent structure induced dispersion of exhaust plume from heavy-duty truck

Georges FOKOUA¹, Amine MEHEL¹ & Frederic MURZYN²

¹ Department of Composite Materials Mechanics and Environment, ESTACA, 78180, Montigny-Le-Bretonneux, France Fax +33 01 76 52 11 43 - email: georges.fokoua@estaca.fr

² Department of Composite Materials Mechanics and Environment, ESTACA, 53061, Laval, France

Abstract

Dispersion of cars exhaust gas is a primary source of air pollution in urban areas. Thus it has become an important subject in automotive field. The present work presents the computational fluid dynamic modelling of the dispersion of exhaust plume induced by coherent structures downstream of heavy-duty truck. In this modelling we use a passive tracer as a pollutant. A standard κ - ϵ two-equation turbulence model was used to reproduce flow motion and Fick's law with convective term for scalar dispersion. A specific goal of this study was to study the effect of the recirculation region near the truck walls on the dispersion of the exhaust plume so two configurations of study were compared and analysed: in the first one, the exhaust gas and the upstream flow were parallel while they were perpendicular in the second configuration. The study has shown no real difference into the two configurations in terms of flow structures for the given input velocities but, we observe a disparity in terms of passive scalar dispersion. Study also evidences a strong correlation between flow structures and the dispersion of the concentration.

Keys-words: NO_x, passive scalar dispersion, Ultrafine Particles, turbulence, CFD

Introduction

Air pollution is responsible for the general enhancement of adverse health effects including respiratory inflammation and cardiovascular diseases (Delfino et al., 2005). The related cost was estimated to 225 billion per year in terms of health expenses and income lost (World bank and IHME, 2016). According to that, it has then become an important issue to prevent and reduce the risk of exposure to toxic pollutants such as NO_x and UltraFine Particles (UFP). These gaseous and solid pollutants are found at very high level in urban/suburban areas where the road traffic is dense and assuming that engine combustion is one of their most important sources. Recent studies have reported very high concentrations of such particles near major roadways (Hudda et al., 2012) with a dominant contribution of nanoparticles.

In the present paper, we are interested in investigating the dispersion of a passive scalar representing a gaseous pollutant such as NO_x downstream of heavy-duty diesel truck exhaust stack. Here it is assumed that passive scalar is a purely diffusive contaminant in a fluid flow with no dynamical effect (such as buoyancy) on the fluid motion itself, however its behavior being important in studying turbulent mixing, combustion and pollution (Warhaft, 2000). The mixing mechanism between exhaust stream and the background air greatly depends on the flow structures, particularly when turbulent coherent structures are present. Indeed, as mentioned by Gautam et al. (2003) and Littera et al. (2017), it is well known that those structures deeply influence the pollutants dynamics and concentrations. Even though this issue has already been studied for several decades, its understanding is still not good enough.

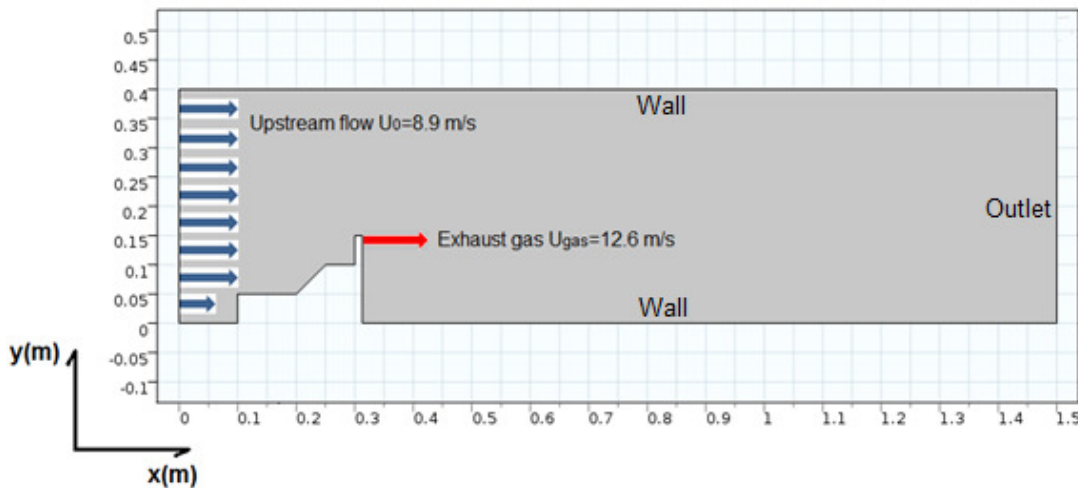
Numerous studies in the literature have focused on experimental and numerical modeling of the dispersion of pollutants in automotive field. But note that it is very difficult to carry out fine studies both qualitative and quantitative because the problem is very complex. The complexity in depicting such phenomena lies in the fact that, there are large number of parameters to be taken into account, among which: the turbulence characteristics (intensity, size of structures, time scales), the modeling of multiphase flow; considering the case with simple diffusion or not (see the study of Gidhagen et al., 2005 for more details); configuration with fast driving vehicle, idle or vehicle in stop (Isella et al., 2008; Ning et al., 2005; Dong et al., 2006); and the influence of road traffic (Chan et al., 2008; Uhrner et al., 2007). The present work focuses only on the CFD, which has many advantages, such as low cost of

money and time, ease in changing boundary condition and high repeatability. FEM software, the COMSOL Multiphysics (COMSOL AB, Sweden) is used to solve a set of transport equations: that is Fick's law for dispersion of passive scalar concentration, incompressible 2D Navier-Stokes equations for flow dynamics (numerical simulations are based on the standard κ - ϵ model) and unsteady heat transfer equation for energy. Simulations are performed into two configurations: on the first hand, the exhaust gas is parallel to the upstream flow while it is perpendicular in the second one. The upstream flow velocity is set to $U_0=8.9$ m/s and the exhaust gas velocity to $U_{gas}=12.6$ m/s. Those two input velocities correspond to the experimental work of Littera et al. (2017). So the paper is organized as follows: section 1 is dedicated to a description of the numerical model, some results and discussion are presented in section 2. A conclusion and the future works end the article.

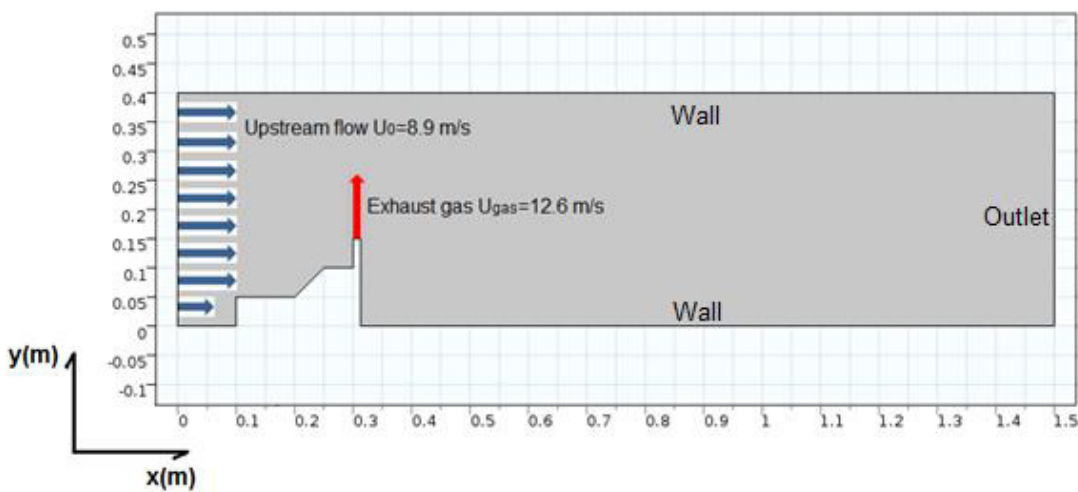
1. Numerical simulation

Calculation domain

Calculation domain consists on a rectangular of about 1.5 m length and 0.4 m height. Inside the rectangular area, a simplified body representing a tractor pulling without trailer is placed (see Figure 1 below, which depicts the two configurations of the study). For meshing strategy we used unstructured triangular prisms and to accurately simulate the boundary layer, the grid around the body was refined to efficiently capture the flow field near the body. The upstream flow and the exhaust gas velocities were set to 8.9 m/s and 12.6 m/s in order to make comparison with the experimental wind tunnel studies of Littera et al. (2017).



(a)



(b)

Figure 1 Vehicle model and coordinate system: (a) first configuration of study and (b) second configuration of study

Numerical model

Finite Element Method helped to discretize the governing equations using FEM software, the COMSOL Multiphysics (COMSOL AB, Sweden) and numerical simulation analyses were conducted based on: mass and momentum conservation, turbulent kinetic energy, turbulent dissipation rate equation and energy equation (Kim et al., 2001). In many mass transfer studies, molecular diffusion is always the ultimate mechanism achieving mixing. Its expression is given by Fick's law:

$$j = -D\nabla C$$

With D the molecular diffusion coefficient and C the scalar field, we assumed that there is no volumetric chemical reaction rate. Thus the concentration transport equation considering in the present work can be written at any point as (Miller et al., 2009):

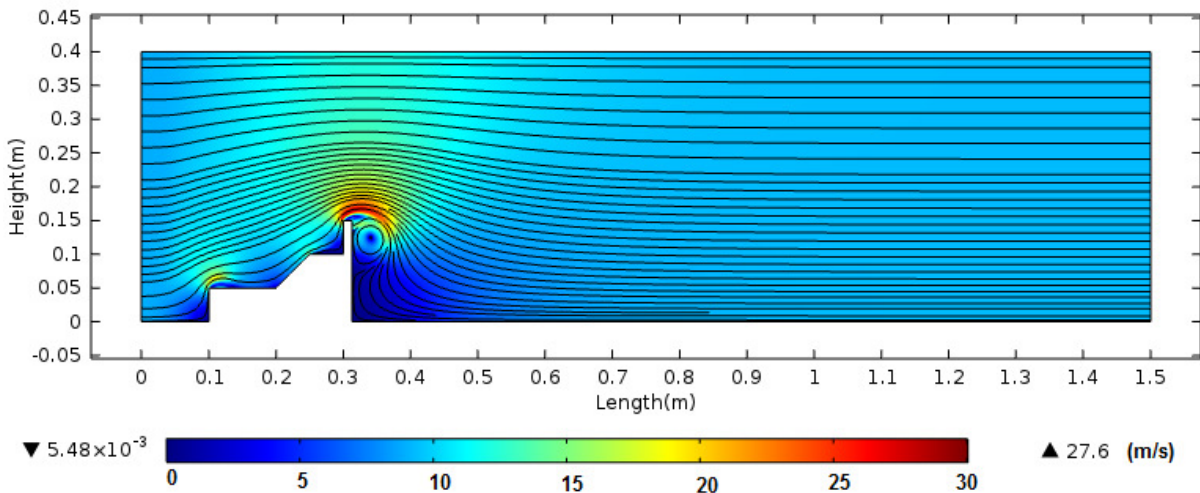
$$\frac{\partial C}{\partial t} + U\nabla C = -\nabla j$$

With U the two dimensional velocity field.

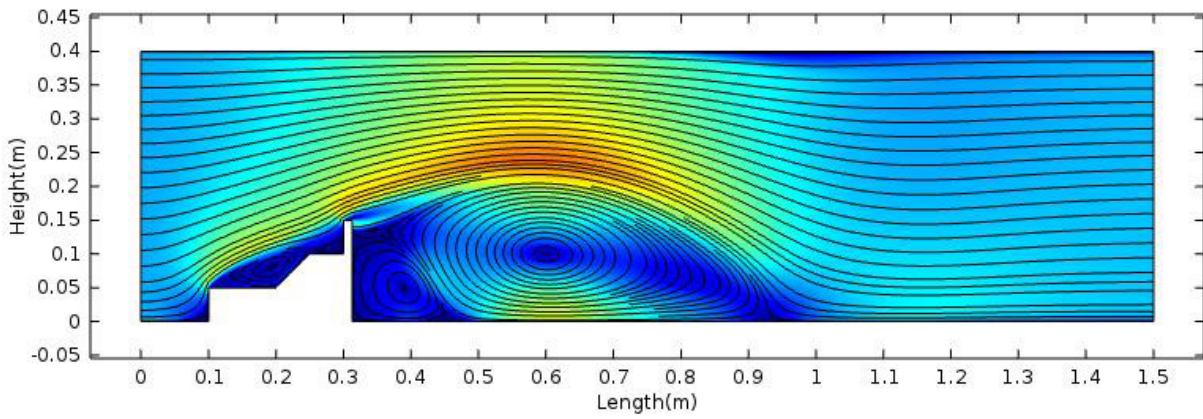
2. Results and discussion

The section starts with a non-exhaustive analysis of the flow structure downstream of heavy duty truck. The aim of this part is to correlate the topology of the flow with the dispersion of the gaseous pollutant. In the second part, we compare the two configurations presented in the previous section, it is unfortunately not possible at this stage of the study to make a fine comparison with the works of Littera et al., (2017) our study configurations aren't strictly the same. But as comparison of numerical study and experimental study being very important for validation, this will be the dealt of the future work.

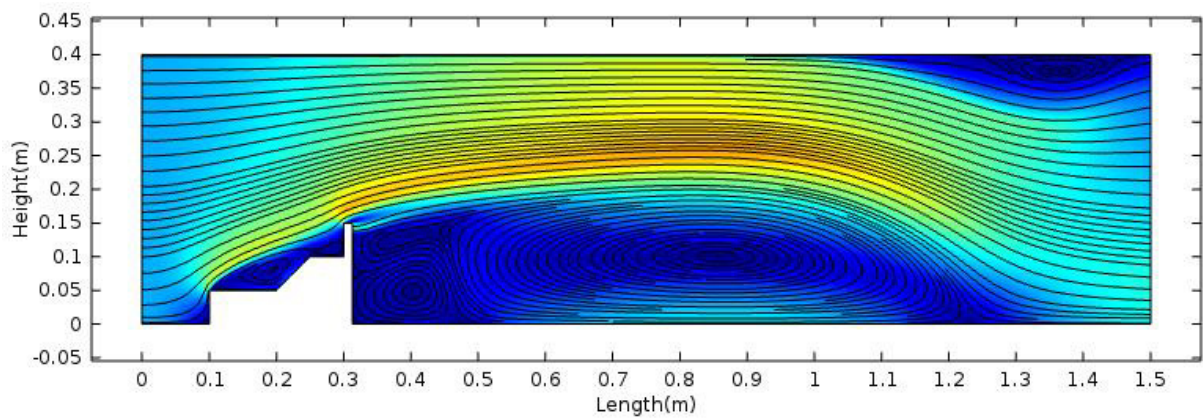
Velocity fields



(a)



(b)

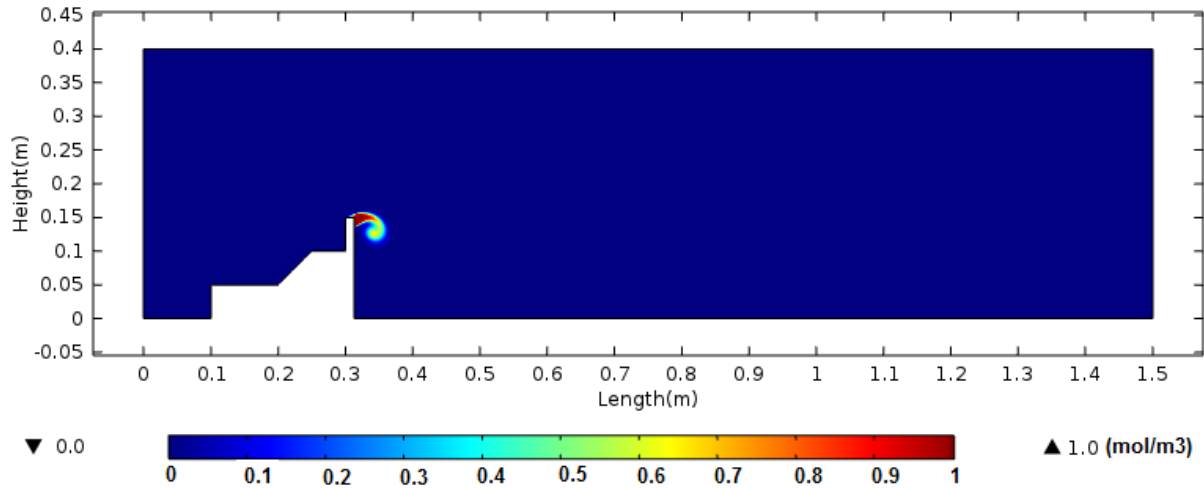


(c)

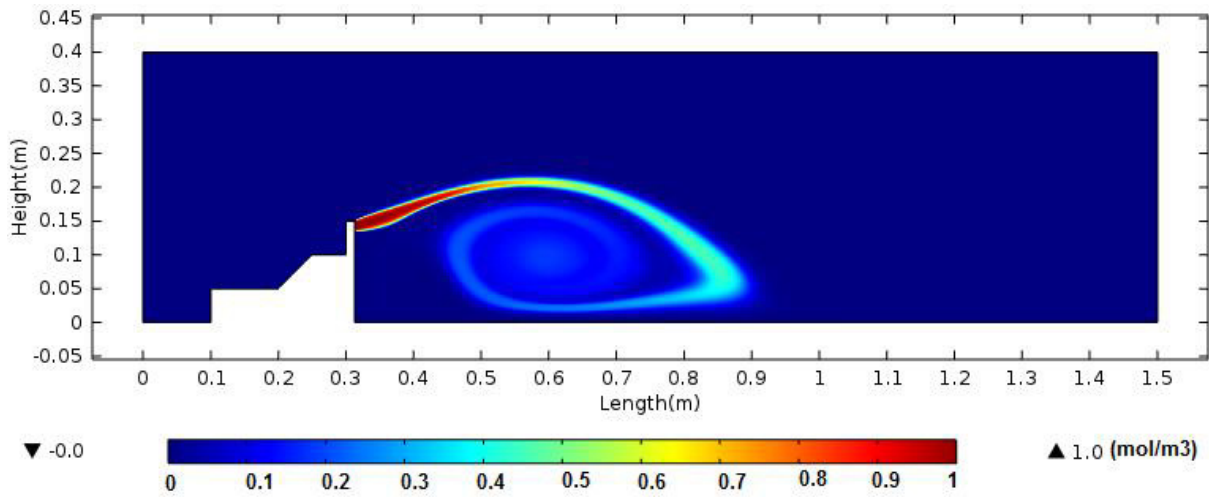
Figure 2 Streamlines and maps of velocity field in the case of configuration 1 (exhaust gas and upstream velocity being parallel). Time steps = 0.005s (a), 0.1s (b) and 0.2s (c)

Figures 2(a) to 2(c) show 2D maps of the dimensional velocity fields superimposed with the streamlines (black lines on the figures). Here we will only focus on the three time steps: 0.005 s, 0.1 s, 0.2 s (beyond 0.2 s, the topology of the flow does not change very fast). Noted that only the first configuration (Figure 1(a)) is considered. Through these maps one can see that flow accelerates at the front of the truck pulling tractor, with peaks of speed up to twice the upstream speed. The minimum streamwise velocity ($U = \sqrt{u^2 + v^2} \sim 10^{-3} \text{ m/s}$) being found at very near-wake region. The results also depict two different flow regions downstream. A homogeneous flow zone, with the highest average speed intensities. This homogeneous zone starts from a height of 0.15 m and extends to the maximum height of the domain (ie: 0.4 m). Below the height of 0.15 m, a more confined zone is observed where two counter-rotating vortices are developed; the flow recirculation is clearly appearing in the vicinity of the truck model (Figure 2(a)) and it is not limited to the region close the truck model. The largest and the most energetic of the two vortices is about 3.5 times the width of the tractor pulling while the smallest one does not exceed 1 times the width of the tractor pulling. Note that the largest vortex grows up by feeding on the smallest vortex as shown in Figure 2(c). The structure and the dynamic of the flow in this confined region are of great importance and will have significant influence on the dispersion of the gaseous pollutant as it will be seen in the next subsection.

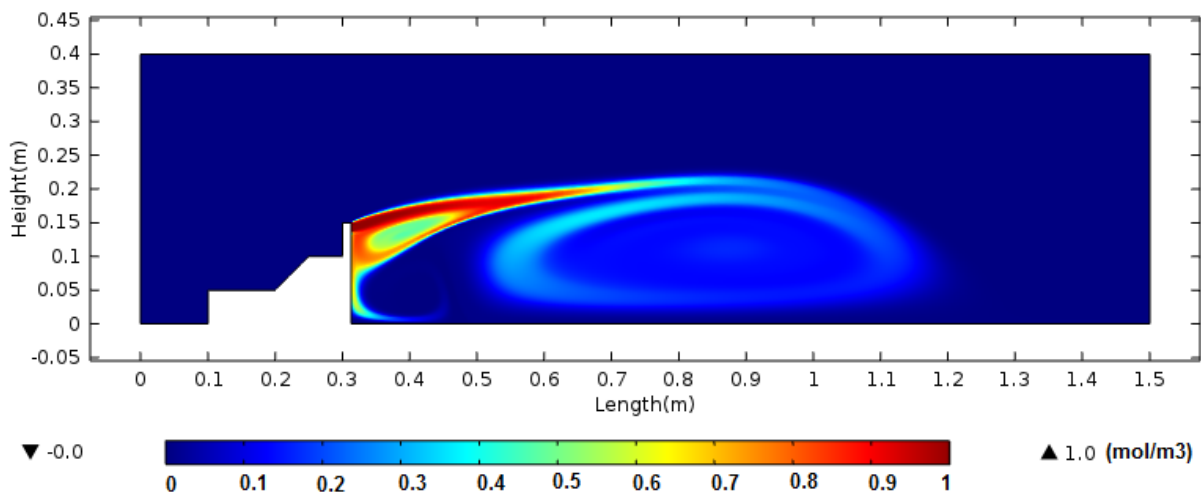
Passive scalar concentration



(a)



(b)

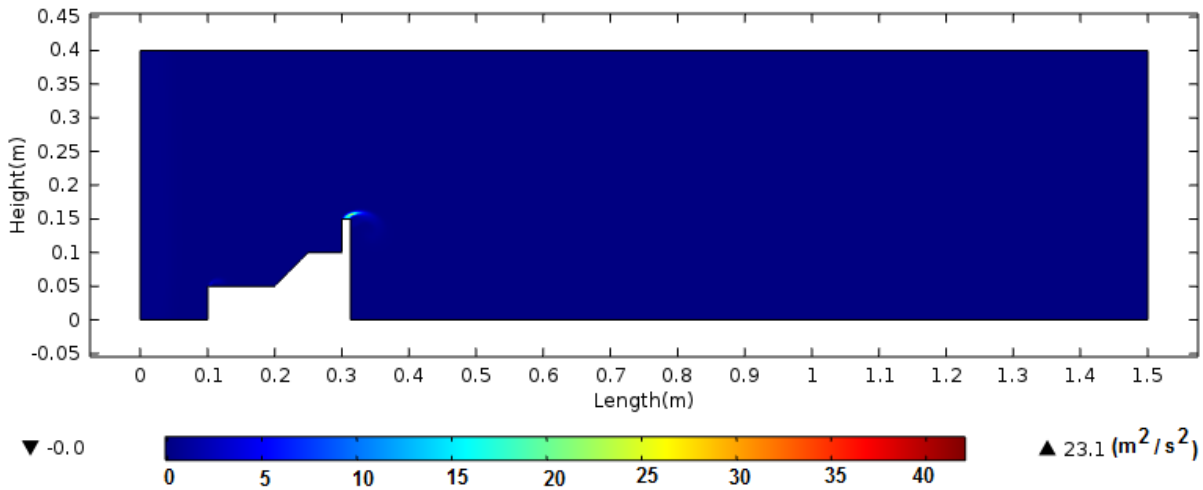


(c)

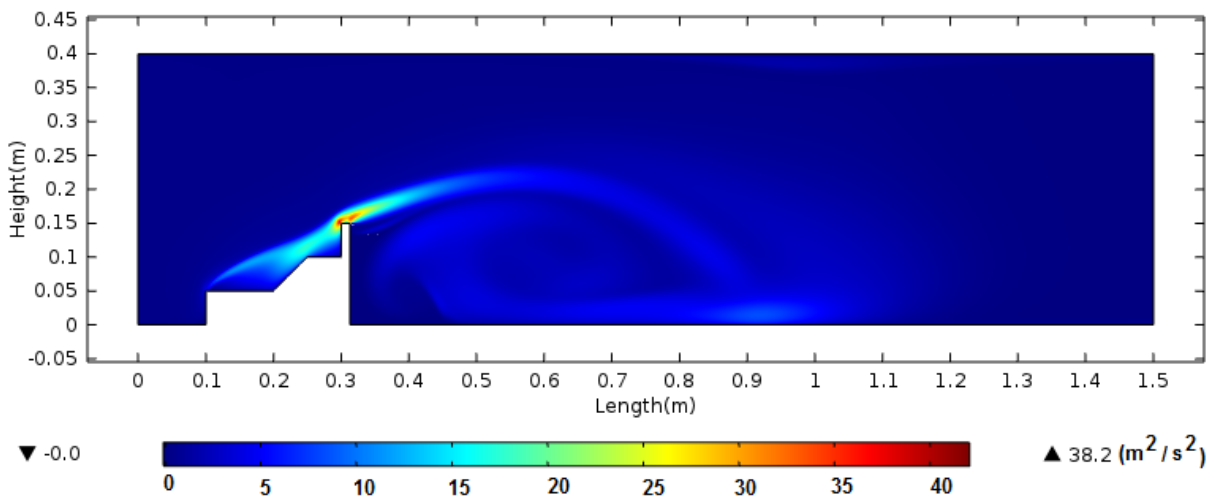
Figure 3 Maps of exhaust gas concentration in the case of configuration 1 (exhaust gas and upstream velocity being parallel). Time steps = 0.005s (a), 0.1s (b) and 0.2s (c)

These figures illustrate a strong influence of the vehicle wake on a scattering of the exhaust gas as mentioned by Mehel and Murzyn (2015). They especially show an important gap between the homogeneous region and the confined one in terms of dispersion of the exhaust gas which, is spread from the end of the chimney to the downstream of the truck model, with a concentration peak in the immediate vicinity of the chimney. In homogeneous region, the concentration of the exhaust gas is practically null. However, in the confined area in which vortex structures are developed, we observe a preferential entrapment of the exhaust gas by the most energetic and biggest vortex. This leading to a strong accumulation of the gas pollutant within the largest vortex.

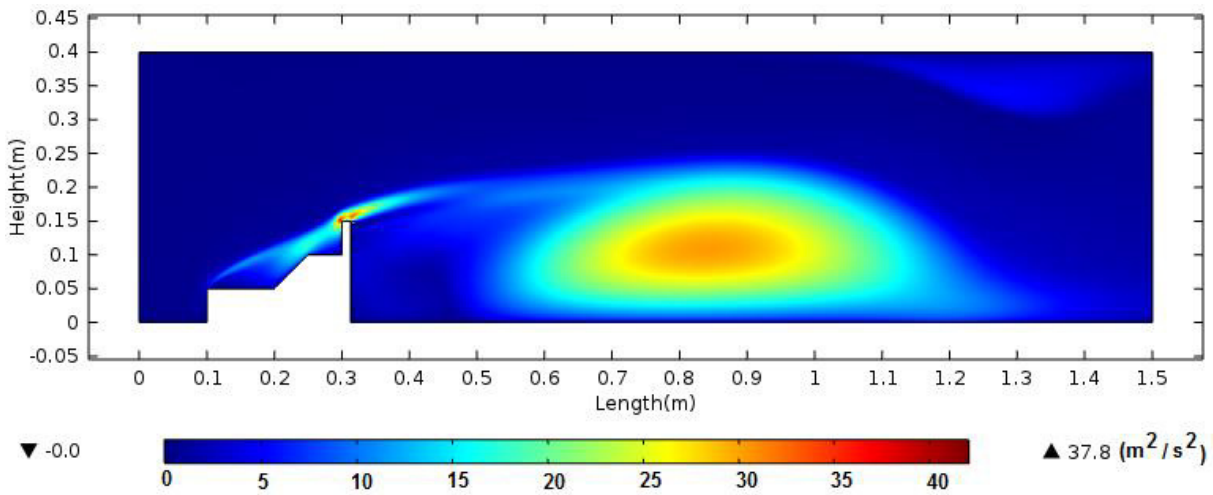
Turbulent intensity



(a)



(b)

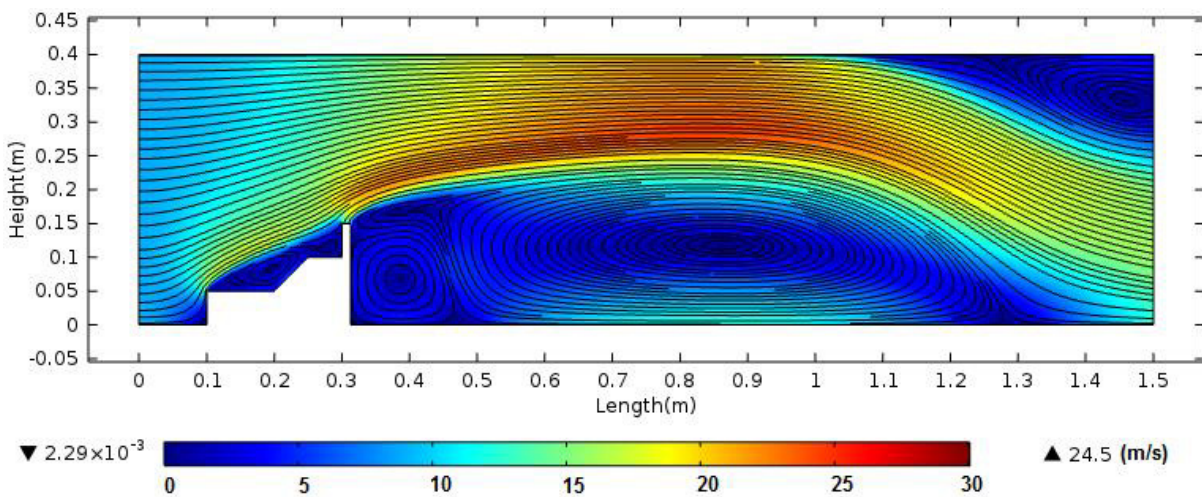


(c)

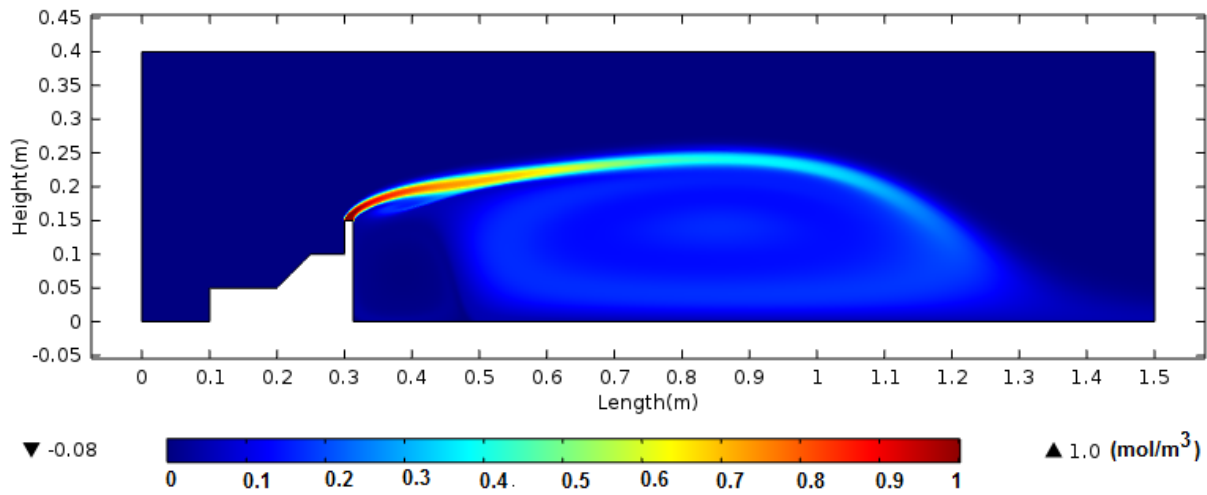
Figure 4 Maps of flow turbulent intensity in the case of configuration 1 (exhaust gas and upstream velocity being parallel).
Time steps = 0.005s (a), 0.1s (b) and 0.2s (c)

Figures 4(a) to 4(c) show the evolution of the average turbulent intensity over time. As expected, the maximum of turbulent intensity is located in the confined area within the biggest vortex. Considering only the Figure 4(c) which shows the most marked values, it can be seen that any longitudinal or vertical profile in the core of the cell will fit a Gaussian profile. The maximum of this Gaussian would be in the heart of the cell. This result is in agreement with the observations of Figure 2 which shows that the largest vortex is also the most energetic one. By comparing the concentration maps with the turbulent intensity maps, it is clear that the parameter that controls the dispersion of the exhaust gases is turbulence.

Comparison of the two configurations of the study



(a)



(b)

Figure 5 Streamlines and map of velocity field (a) and map of exhaust gas concentration (b) in the case of configuration 2 (exhaust gas and upstream velocity being perpendicular). Time steps = 0.2s

Figures 5(a) and 5(b) show the mappings of concentration and flow velocity field for the configuration 2 (Figure 1(b)). Only the results corresponding to the time step 0.2 s are presented and compared. We observe that the flow topology is the same between the two configurations, only the magnitudes of velocity are different, the highest speeds being observed in configuration 2. Note also that the largest vortex is much wider in configuration 2 than in configuration 1. The Comparison between Figures 2 (c) and 5 (b) reveals that the dispersion of the exhaust gas is more homogeneous thus, the gaseous pollutant is better distributed in the cell in configuration 2.

In order to study the extent of the exhaust gas dispersion downstream, we have presented in Figure 7 the horizontal and vertical profiles of concentration. The profiles being extracted as it is shown in Figure 6.

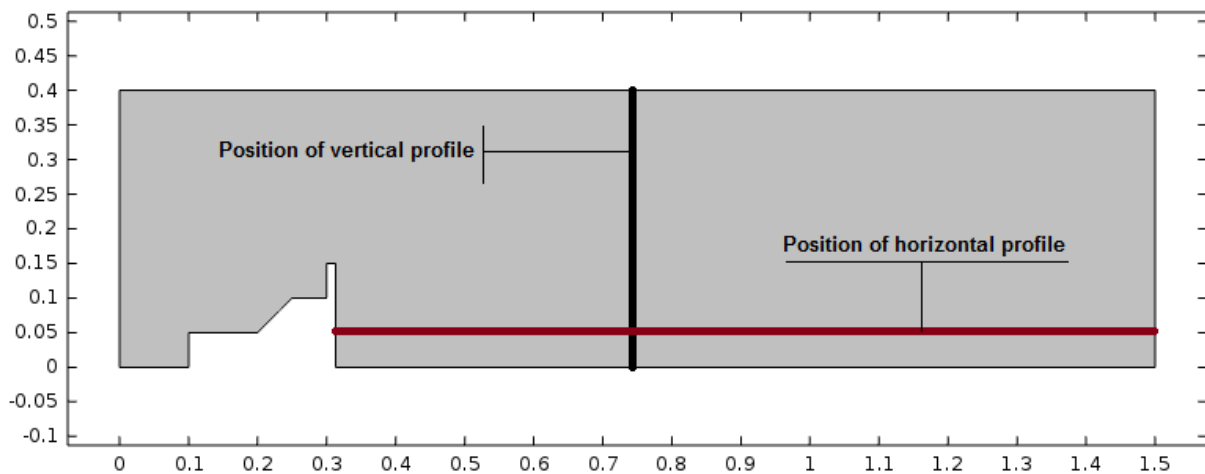
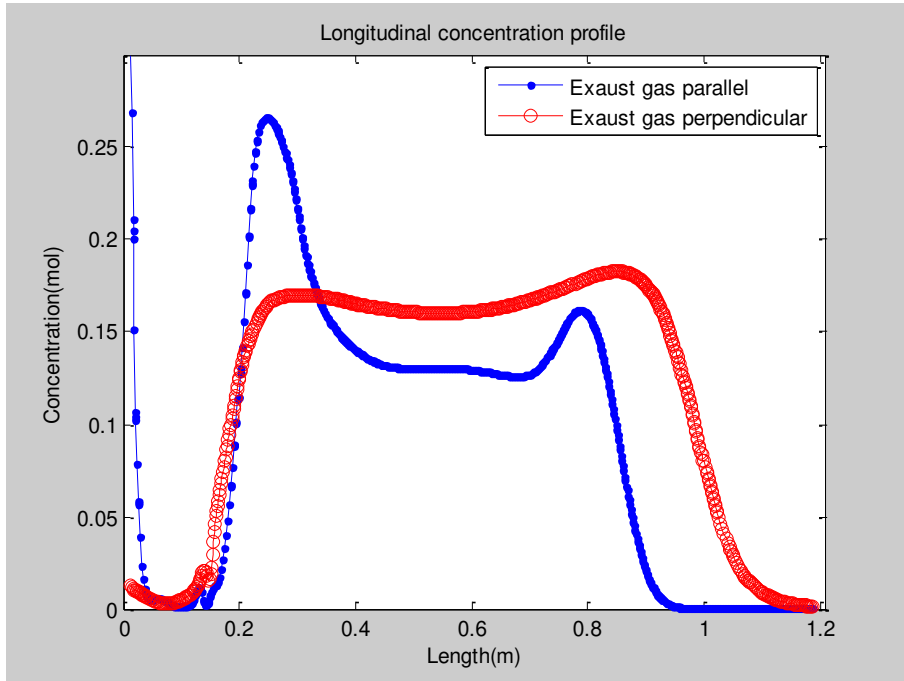


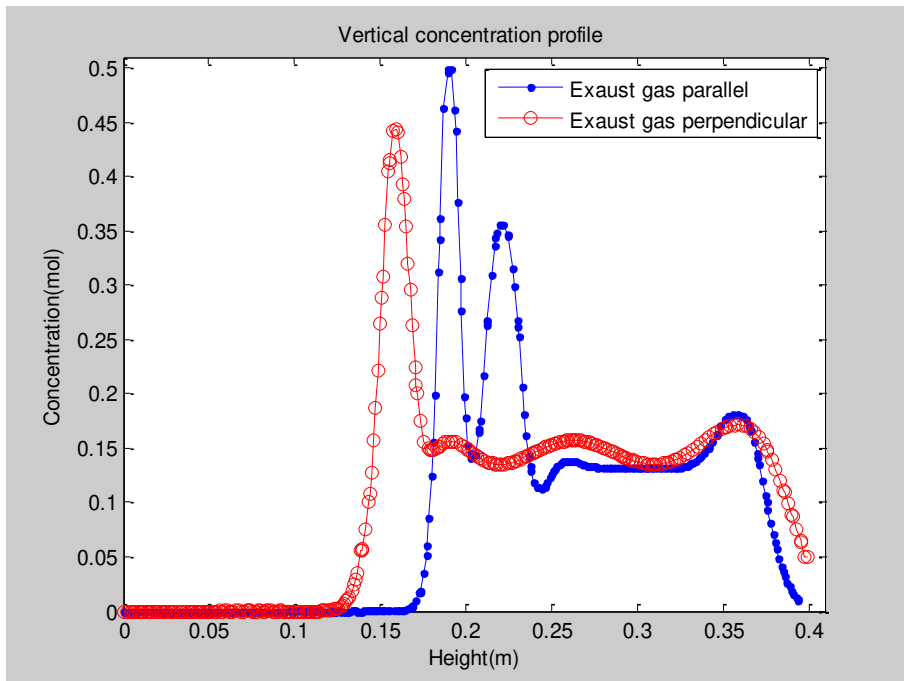
Figure 6 Positions of exhaust gas concentration profiles in vertical and horizontal directions

Figures 6a and 6b illustrate very well all the preceding observations ie: a preferential accumulation of the exhaust gas by the most energetic vortex, a more homogeneous distribution of the pollutant in the configuration 2 (profiles of the configuration 2 are globally more uniform than the profiles of the configuration 1). These figures also show that the vortices are limited in the vertical direction by the height of the truck model, while they can horizontally reach up to 3.5 and 4 times the width of the

truck model respectively in configurations 1 and 2. We also observe that in the immediate vicinity of the truck model, the concentration levels are extremely low, about 10 times lower than in the core of the most energetic vortex.



(a)



(b)

Figure 7 Horizontal (a) and vertical (b) profiles of the exhaust gas concentration

Conclusion

In the present work 2D FEM simulations were used to reproduce the dispersion of a passive tracer by coherent structures downstream of heavy-duty truck. In this modeling passive tracer was representing the exhaust gas concentration. This study helped to characterize the development of flow recirculation in the wake of the truck model and the influence of these flow structures to the dispersion of the exhaust gas. Two configurations of study depending on the orientation of the exhaust gas were investigated. Our main findings are as follows:

- There exist two different flow regions downstream: homogeneous zone above the height of 0.15m and the confined one below, where vortex structures are developed. A recirculating flow starting at the vicinity of the truck model;
- We have observed two counter-rotating vortices, their size being limited by the height of the truck model in the vertical direction, while this size can reach 4 times the width of the truck model in horizontal direction;
- Among the two vortices, the furthest from the truck is the largest and also the most energetic. its energy being at least 10 times greater than that of the small one;
- Results highlight strong interaction between coherent structures and exhaust gas dispersion with a preferential accumulation the exhaust gas in the largest vortex
- Study also evidence turbulence as the parameter that controls the dispersion of the exhaust gas;
- Comparison of the two configurations of the study has shown no difference in terms of flow structures but a disparity in terms of exhaust gas dispersion;

These preliminary results contributed to get a better understanding of a passive scalar dispersion downstream of heavy-duty truck model. But the study felt to reproduce the experimental work of Littera et al., 2017. One of the reasons may be due to the fact that the study configurations are not rigorously the same. Future 3D investigations involving a full truck coupled to its trailer and taking into account the wheels could improve the results.

References

- Chan, T. L., Luo, D. D., Cheung, C. S. and Chan, C. K. (2008). Large eddy simulation of flow structures and pollutant dispersion in the near-wake region of the studied ground vehicle for different driving conditions. *Atmospheric Environment*, vol. 42, no. 21, pp. 5317–5339.
- Delfino, R.J.; Sioutas, C. and Malik, S. (2005) Potential role of ultrafine particles in association between airborne particle mass and cardiovascular health, *Environmental Health Perspectives*, 113, pp 934-946.
- Dong, G., and Chan, T. L. (2006). Large eddy simulation of flow structures and pollutant dispersion in the near-wake region of a light-duty diesel vehicle. *Atmospheric Environment*, vol. 40, no. 6, pp. 1104–1116.
- Gautam, M.; Clark, N.N.; Mehta, S.; Boyce, J.A.; Roger, F. and Gertler, A. (2003) Concentrations and Size Distributions of Particulate Matter Emissions from a Class-8 Heavy-duty Diesel Truck Tested in a Wind Tunnel. SAE Technical paper 2003-01-1894.
- Gidhagen, L., Johansson, C., Langner, J. and L. Foltescu, V. (2005). Urban scale modeling of particle number concentration in Stockholm. *Atmospheric Environment*, vol. 39, no. 9, pp. 1711–1725.
- Hudda, N.; Eckel, S.P.; Knibbs, L.D.; Sioutas, C.; Delfino, R.J. and Fruin, S.A. (2012) Linking in-vehicle ultrafine particle exposures to on-road concentrations, *Atmospheric Environment*, 59, pp 578-586.
- Isella, L., Giechaskiel, B. and Drossinos, Y. (2008). Diesel-exhaust aerosol dynamics from the tailpipe to the dilution tunnel. *Journal of Aerosol Science*, vol. 39, no. 9, pp. 737–758.

Kim, D. H., Gautam, M. and Gera, D. (2001). On the prediction of concentration variations in a dispersing heavy-duty truck exhaust plume using k-epsilon turbulent closure. *Atmospheric Environment*, vol. 35, no. 31, pp. 5267-5275.

Littera, D.; Cozzolini, A.; Besch, M.; Carder, D. and Gautam, M. (2017) Effect of turbulence intensity on PM emission of heavy duty diesel trucks: Wind Tunnel studies, *Atmospheric Environment*, in press.

Mehel, A., & Murzyn, F. (2015). Effect of air velocity on nanoparticles dispersion in the wake of a vehicle model: Wind tunnel experiments. *Atmospheric Pollution Research*, 6(4), 612-617.

Miller, F.P., Vandome, A.F. and McBrewster, J. (2009). *Fik's Law of Diffusion*. VDM Publishing, ISBN: 6130095031, 9786130095031.

Ning, Z., Cheung, C. S., Lu, Y., Liu, M.A., and Hung, W. T. (2005). Experimental and numerical study of the dispersion of motor vehicle pollutants under idle condition. *Atmospheric Environment*, vol. 39, no. 40, pp. 7880–7893.

Uhrner, U., von Löwis, S., Vehkamäki, H. (2007). Dilution and aerosol dynamics within a diesel car exhaust plume—CFD simulations of on-road measurement conditions. *Atmospheric Environment*, vol. 41, no. 35, pp. 7440–7461.

Warhaft, Z., (2000). Passive scalars in turbulent flow. *Annu. Rev. Fluid Mech.* (32) 203-240.

World Bank and Institute for Health Metrics and Evaluation (2016) *The cost of air pollution: strengthening the economic case for action*, Washington DC: World bank. Licence: Creative commons attribution CC BY3.0 IGO.

Using an iterative Markov Chain process to develop driving cycles based on large-scale GPS data: a case study in Beijing

Ruoyun Ma¹, Xiaoyi He¹, Ye Wu^{1,2*}

¹ School of Environment, and State Key Joint Laboratory of Environment Simulation and Pollution Control, Tsinghua University, Beijing 100084, China

² State Environmental Protection Key Laboratory of Sources and Control of Air Pollution Complex, Beijing 100084, China

Abstract

Researches have shown that inadequate representativeness of testing cycles could lead to significant discrepancy in vehicle energy and emission assessment between on-road performance. On-board measurement has been used in past researches to collect vehicle activity data but the amount of data is usually insufficient, and the statistical coverage of various road/traffic types could not be guaranteed. Using “big data” mining techniques, this study examines second-by-second GPS data of 459 private passenger cars in Beijing, covering over 170,000 sampling days to characterize vehicle speed profiles under various traffic condition and road types. We then applied the Markov Chain method to generate sub-cycles and corresponding weighting factors that have similar properties as real-world driving. The resulting cycles (i.e., Beijing Cycle, Off-peak Cycle, Peak Cycle) are combination of sub-cycles representing different road types. A significant test was further conducted to confirm the cycle representativeness. The annual variations of driving profiles were minor, indicating rather consistent driving patterns over the years. Vehicle fuel consumption simulation results show that Beijing cycle leads to 15%-30% higher fuel consumption than regulation test cycles (i.e., NEDC, WLTC). This study proposes a practical method to construct driving cycle from massive GPS data and highlights the importance for developing a representative driving cycles for legislation fuel consumption and emission test.

Introduction

China is a developing country with the world's largest auto market since 2009, and Beijing is the city with the largest vehicle population (i.e., 5.7 million vehicles by 2016) within China. According to the announcement by China Ministry of Environmental Protection, mobile sources emission accounted for 31.1% of local PM_{2.5} emissions, being the largest source. In addition, the automotive industry cannot be neglected in the issue of the world's oil resources consumption. To facilitate the vehicle fuel consumption and emission control legislation, several standard driving cycles were developed worldwide for the purpose of vehicle performance evaluation.

Driving Cycles refer to the typical states of the vehicles running in the transport network, usually presented as speed-time curves. Standard driving cycles can be used to estimate vehicle emissions and fuel consumption as well as environmental impacts, which are widely regarded as the international authoritative method for a complete assessment of exhaust emissions. Additionally, the development of driving cycles is the basis of deriving corresponding emission factors and simulating fuel consumption. Therefore, the accuracy and representation of driving cycles have determined the reliability of emission inventory and fuel consumption analysis.

New European Driving Cycle (NEDC) has now been adopted for the national regulation of vehicle exhaust test in China, which however has been proved significant deviation between the test and the actual results. According to the EU Joint Research Center, the real world emissions including CO₂, CO, NO_x have shown 10% to 10 times higher than those under NEDC. Meanwhile, test results of real word emission and fuel consumption vary with different road types and traffic conditions. Limited data sources and volume has become the restraining factor in previous researches. Additionally, a common consensus exists among researchers that driving characteristics of each city is unique because of different vehicle fleet composition, driving behaviour and road network topography. Therefore, it is of great significance to develop a robust and representative driving cycles corresponding with the characteristic of the specific city.

The aim of this research is to develop typical driving cycles of light-duty vehicles in Beijing, as well as to provide a more scientific method and perspective for the development of driving cycles. The core contents have been listed as follows:

- (1) Data collection and segmentation.
- (2) Generating vehicle driving cycles using an iterative Markov Chain process.
- (3) Spatial and temporal analysis.
- (4) Model validation and representativeness.
- (5) Model application on fuel consumption simulation.

Theory and Method

Markov chain process has usually been applied to engineering problem analysis with stochastic process, but not been extensively used in the field of vehicle driving cycle development yet. Compared with traditional methods above, the Markov method functions based on original velocity-time series, developing driving cycles according to the law of speed change and driving patterns. The research combined the Markov method and large-scale real-world GPS data, applied to the development of light-duty vehicle driving cycles in Beijing.

In a stochastic process, if there are finite values E_0, E_1, E_2, \dots , mark E_0, E_1, E_2, \dots as $\{0,1,2, \dots\}$, then define $\{0,1,2, \dots\}$ and the subsets as state space, denoted as S . For arbitrary $n \geq 0$ and states $i, j, i_0, i_1, \dots, i_{n-1}$, there is

$$P\{X_{n+1} = j | X_0 = i_0, X_1 = i_1, X_2 = i_2, \dots, X_{n-1} = i_{n-1}, X_n = i\} = P\{X_{n+1} = j | X_n = i\}$$

then define stochastic process $\{X_n, n = 0,1,2, \dots\}$ as Markov chain, and conditional probability $P\{X_{n+1} = j | X_n = i\}$ as one-step transition probability matrix of the Markov chain, referred to as transition matrix. If the transition matrix $P\{X_{n+1} = j | X_n = i\}$ is only related to state i, j rather than n , define the Markov chain as time homogenous Markov chain, and denote $p_{ij} = P\{X_{n+1} = j | X_n = i\}$ ($n \geq 0$).

Arrange p_{ij} ($i, j \in S$) as a matrix, assign

$$P = (p_{ij}) = \begin{pmatrix} p_{00} & p_{01} & p_{02} & p_{03} & \cdots \\ p_{10} & p_{11} & p_{12} & p_{13} & \cdots \\ p_{20} & p_{21} & p_{22} & p_{23} & \cdots \\ p_{30} & p_{31} & p_{32} & p_{33} & \cdots \\ \vdots & \vdots & \vdots & \vdots & \ddots \end{pmatrix}$$

then define P as transition probability matrix, referred to as transition matrix. Evidently, the characteristics of p_{ij} ($i, j \in S$) list as follows,

- (1) $p_{ij} \geq 0, i, j \in S$
- (2) $\sum_{j \in S} p_{ij} = 1, \forall i \in S$

The variation of vehicle driving states can be regarded as a random Markovian process. The driving state of the next moment depends on the present moment instead of the last moment. Therefore, the velocity variation of driving records is regarded as homogeneous Markov chain.

Data collection and segmentation. Our previous work (He, 2016) investigated the vehicle activity data of 459 actual personal-owned vehicles using on-board GPS. The original data includes second-by-second speed profiles and location information. A segmentation process further divided these profiles into trips with stop period longer than 5 minutes, which were used as the base elements for driving cycle development.

Driving cycle generation. We first defined four driving modes (i.e., acceleration, deceleration, cruise, and idle) based on instantaneous speed and acceleration. The second-by-second speed profiles were divided into segments according to the driving modes. These segments were further clustered into seven states based their average velocity ranging from 0 km/h to over 60 km/h at interval of 10 km/h. Note that every segment corresponds to only one state, and the all seven states constitute the state space of the Markov chains. Count the number of segments that transfer from state i to state j , denoted as N_{ij} . According to the properties of transition matrix $\sum_{j \in S} p_{ij} = 1$ ($\forall i \in S$), the transition probability equation is obtained.

Table 1: Transition matrix of the whole sample

Transition probability	State 1	State 2	State 3	State 4	State 5	State 6	State 7
State 1	0.830	0.152	0.013	0.003	0.001	0.000	0.000
State 2	0.175	0.642	0.168	0.013	0.001	0.000	0.000
State 3	0.033	0.165	0.629	0.161	0.011	0.001	0.000
State 4	0.012	0.021	0.158	0.656	0.145	0.006	0.001
State 5	0.003	0.003	0.024	0.143	0.691	0.131	0.004
State 6	0.001	0.000	0.004	0.017	0.140	0.721	0.117
State 7	0.000	0.000	0.000	0.003	0.007	0.075	0.915

A trip is defined as velocity-time records from the start to the complete stop (parking over 300 seconds). We consider the average duration of trips, 1398 seconds (i.e., 23 minutes and 18 seconds) as total length of the typical driving cycle of light-duty vehicles in Beijing.

A candidate driving cycle is constituted of three sub-cycles, i.e., highway & freeway, arterial road and residential road, with proportional duration shares to the total sample. A series of candidate driving cycles were developed starting from a random segment with initial velocity of zero, and continuously generating the next moment of velocity profile according to the transition matrix between states and merging with randomly selected segments within the state. This iterative process continues until the driving cycle duration meets the total length (1398 seconds). The derived driving cycles with the lowest relative error of several critical parameters (i.e., velocity, mode ratio) was screened as the standard driving cycle ultimately.

Spatial and temporal analysis

Spatial Analysis.

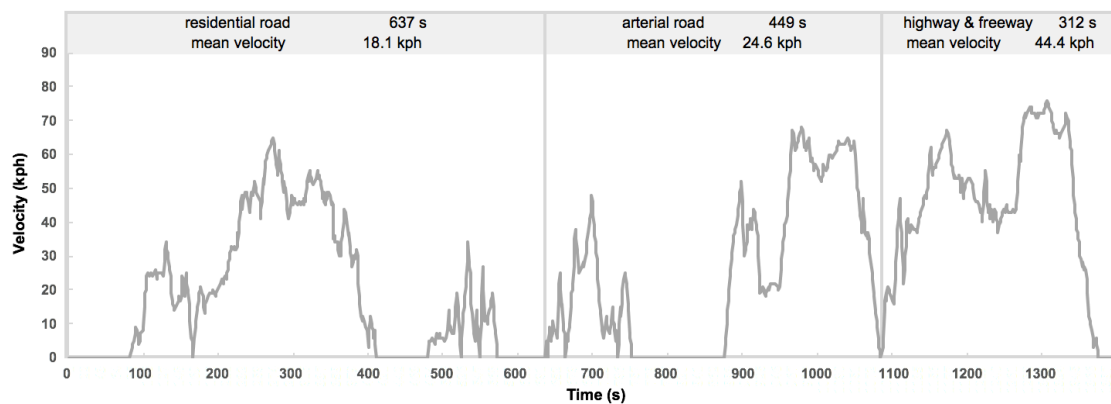


Figure 1: the standard driving cycle of light-duty vehicles in Beijing (Beijing Cycle)

Figure 1 shows significant differences exists among three sub-cycles. From residential road, to arterial road, to highway & freeway, the average velocity and running velocity increase, as the absolute value of average acceleration/deceleration tends to decrease. Meanwhile, the ratio of

idle mode falls sharply from 32.58% to 6.64%, as driving on highway & freeway is less likely to pause at traffic lights. Spatial analysis is able to reveal these discrepancies in the overall driving cycle contributing to accuracy improvement.

Temporal analysis. Travel time was distinguished by peak hour and off-peak hour, on the basis of which standard driving cycles for different traffic period individually, as shown in Figure 2 (Peak Cycle) and Figure 3 (Off-peak Cycle).

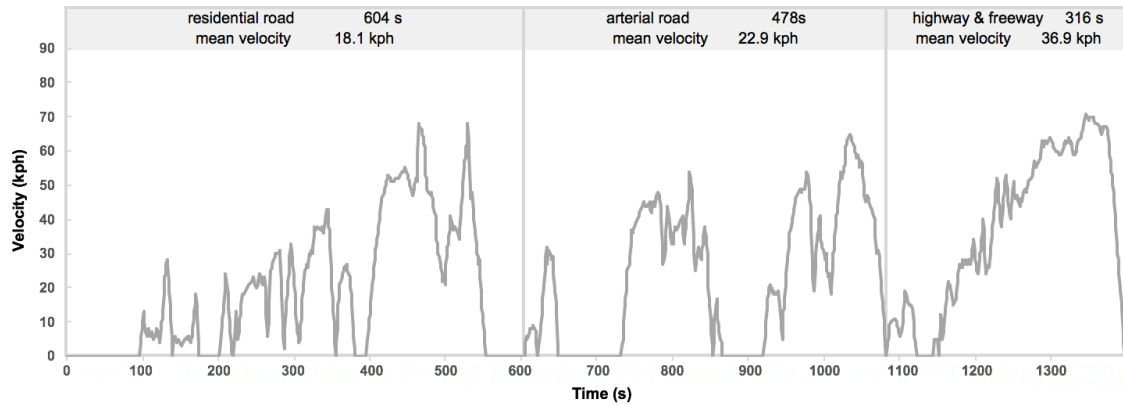


Figure 2: the standard driving cycle of light-duty vehicles during peak hour (Peak Cycle)

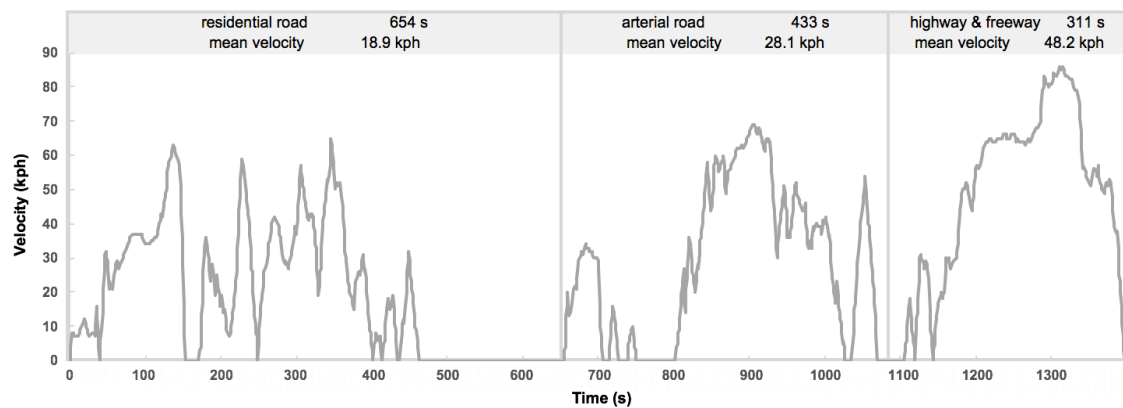


Figure 3: the standard driving cycle of light-duty vehicles during off-peak hour (Off-peak Cycle)

Regardless of road types, the average velocity and running velocity (average velocity except idling) during peak hour are lower than those during off-peak hour, while there exist few discrepancies in average acceleration/deceleration and the ratio of four driving modes (i.e., acceleration, deceleration, cruise, and idle). Highway & freeway sub-cycles show the most significant distinctions between peak hour and off-peak hour, compared with the other two sub-cycles. Consequently, the following research in correlation with driving cycles from the temporal perspective should emphasize the discrepancy under highway & freeway type.

Model validation and representativeness

We conducted model validation by the significance test. The test is based on transition matrix for the correlation analysis of velocity variation between the standard driving cycles and the whole sample. The result of Z values for Beijing Cycle, Peak Cycle and Off-peak Cycle were 10.55, 22.91 and 9.76 (18 degrees of freedom), lower than $\chi^2(\alpha) = 28.87$ (assigning $\alpha = 0.05$), which indicates that it cannot be rejected that the transition matrixes of developed cycles have identical distribution with those of the whole sample. Therefore, we conclude that the three developed driving cycles above are consistent with the total sample characteristics.

We also compared our results with regional statistics released by the Beijing Transport Institute (TRC), from year 2013 to 2015. The average velocity of our sample during morning/evening peak

in 2013-2015 was slightly lower than statistics of TRC (relative error < 10%). The error may come from differences in sample size and range. Both datasets show minor annual variation of average velocity during morning/evening peak in 2013-2015 (relative difference < 5%). Therefore, the obtained driving cycles are representative in the current.

Model application on fuel consumption simulation

Based on the derived driving cycles, we simulated the fuel consumption of two vehicle models (GAC-Toyota Camry and Chevrolet Cruze) based on the VSP method (Zhang, et al., 2014), and compared results with regulation cycles (i.e., NEDC and WLTC). As shown in Figure 4 and Figure 5, fuel consumption under real-world driving are 15%-30% higher than NEDC and WLTC. This is in consistent with previous studies and also implies current regulation cycle in China (i.e., NEDC) lack representative for Beijing vehicle travelling features and could lead to bias in fuel economy estimation.

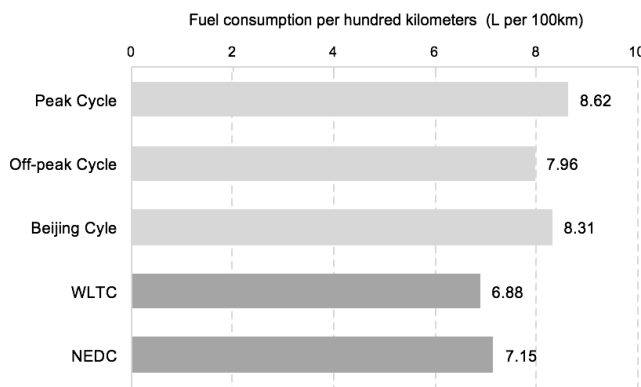


Figure 4: Fuel consumption simulation of Toyota Camry under three real-world driving cycles in Beijing and two regulation driving cycles.

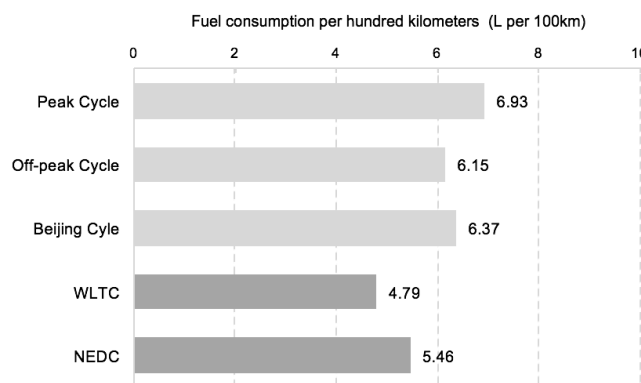


Figure 5: Fuel consumption simulation of Chevrolet Cruze under three real-world driving cycles in Beijing and two regulation driving cycles.

Fuel consumption simulation results during peak period have been about 10% higher than off-peak period. Based on the proportion of segments during peak and off-peak hour, we calculate weighted average of Peak Cycle and Off-peak Cycle fuel consumption simulation values to be 8.15 and 6.37 L/100km for Camry and Cruze respectively. The relative error between weighted average values and results under Beijing Cycle is 1.9% and < 0.1%, which is highly self-consistent.

References

Beijing Transport Institute (2014-2016), *Beijing Transport Annual Report*, Beijing. [in Chinese]
 Chen, X. (2009), *Probability Theory and Mathematical Statistics*, Press of University of Science and Technology of China, Hefei. [in Chinese]

- CJJ37-2012, *Code for design of urban road engineering*, China Architecture & Building Press, Beijing. [in Chinese]
- He, X., et al. (2016), Individual trip chain distributions for passenger cars: Implications for market acceptance of battery electric vehicles and energy consumption by plug-in hybrid electric vehicles, *Applied Energy*, 180, 650-660.
- Jiang, P. (2011), Investigation of the driving cycle construction of mixed roads in the city [D], Hefei University of Technology. [in Chinese]
- Justin D.K. Bishop (2012), A robust, data-driven methodology for real-world driving cycle development, *Transportation Research Part D*, 17, 389-397.
- Lin, H., Yu, Q., Zhang, X. (2014), A review of research on vehicle's driving cycle in urban roads, *Mechanical Science and Technology for Aerospace Engineering*, 33(2), 282-288. [in Chinese]
- Lin, J. (2002), A Markov progress approach to driving cycle development [D], California University.
- Lin, J., et al (2002), An exploratory analysis comparing a stochastic driving cycle to California's regulatory cycle, *Atmospheric Environment*, 36, 5759-5770.
- Monica Tutuianu, Pierre Bonnel (2015), Development of the World-wide harmonized Light duty Test Cycle (WLTC) and a possible pathway for its introduction in the European legislation, *Transportation Research Part D*, 40, 61-75.
- Q, Gong., S. Midlam-Mohler, V. Marano, and G. Rizzoni (2011), An iterative Markov chain approach for generating vehicle driving cycles, *SAE Int. J. Engines*, 4(1), 1035 – 1045.
- Zhang, B., Zhang, J. (2004), *Applied Stochastic Processes*, Tsinghua University Press, Beijing. [in Chinese]
- Zhang, R. (2009), Construction and research of vehicle driving cycle of city road [D], Hefei University of Technology. [in Chinese]
- Zhang, S., et al. (2014), Real-world fuel consumption and CO₂ (carbon dioxide) emissions by driving conditions for light-duty passenger vehicles in China, *Energy*, 69, 247-257.

Global Sensitivity Analysis in the Simulation of Road Traffic Emissions at Metropolitan Scale

Authors, R. Chen^{1*}, V. Mallet², V. Aguiléra³, F. Cohn⁴, D. Poulet⁴ and F. Brocheton⁴

¹ CEREAs, Joint Laboratory of École des Ponts ParisTech - EDF R&D, Université Paris-Est, 77455 Marne-la-Vallée, France. Ruiwei.Chen@enpc.fr

² INRIA, 75012 Paris, France

³ LVMT, Joint Laboratory of École des Ponts ParisTech - IFSTTAR, Université Paris-Est, 77455 Marne-la-Vallée, France

⁴ NUMTECH, 63170 Aubière, France

Abstract

The objective of this paper is applied to analyze the global sensitivity at street resolution of on-road traffic emissions, which depend on both traffic flow and emission factors. At metropolitan scale, traffic flow can be obtained by traffic assignment (TA) models, and emission factors can be computed by COPERT IV formulas. In this work, global sensitivity analysis (GSA) is carried out on this simulation chain, combining (i) a TA model called Meta-LCF and (ii) COPERT IV model, with respect to the inputs of both models, on a case study in the agglomeration of Clermont-Ferrand (France). The Sobol' method was used for GSA. The Meta-LCF model is a surrogate of a TA model called LADTA applied in Clermont-Ferrand. In fact, the GSA requires large-size simulation samples which lead to intractable computations. Consequently, we made use of a meta-model that preserves the main behaviors of the complete TA model but with very low computational cost. The Sobol' first-order and total-effect indices show that the NO_x (hot) emissions of on-road traffic are very sensitive to the traffic demands. They are also sensitive to gasoline car share in passenger cars, and the proportion of heavy duty vehicles. Furthermore, spatial differences are found among sensitivity indices throughout the metropolitan area. For example, on streets without Heavy Duty Vehicles (HDVs), the most influential factor that affect the computed NO_x (hot) emissions is the share of gasoline vehicles, while on streets with HDVs, the share of HDVs is the most influential factor.

Keywords: Global sensitivity analysis (GSA), Sobol' index, dynamic traffic assignment (DTA), on-road traffic emission, meta-model, COPERT

1. Introduction

In recent years, there has been a growing interest for the numerical simulation of air quality at urban (or metropolitan) scale. The reliability of air quality simulations is becoming an important issue since they are subject to various uncertainties. One of the biggest uncertainty sources to urban air pollution is the on-road traffic emissions (Smit et al., 2010; Franco et al., 2013). The on-road traffic emissions are often modeled as the product of (i) the number of vehicles and (ii) the emission factors (EF, in g/km), for different pollutants, vehicle technologies, etc. In metropolitan areas, the former can be estimated by traffic assignment (TA) models, and the latter are often modeled by empirical functional relations between pollutant emissions and characteristics of on-road traffic. The COPERT model is among the most used emission factor models, where EFs are a function of the mean traveling speed. Sensitivity analysis helps us to find the uncertainty source with respect to model inputs.

The main purpose of this paper is to carry out the global sensitivity analysis (GSA) of the simulation chain from traffic assignment model to emission estimation, at street resolution for a metropolitan area. Section 2 presents a brief introduction of the variance-based GSA method and the Sobol' indices. In Section 3, the traffic assignment model called LADTA and the Meta-LCF model are presented. In Section 4, the simulation chain coupling LADTA and the COPERT IV EF model is built. At last, Section 5 presents the GSA results concerning the traffic assignment meta-model, and the complete simulation chain of on-road traffic estimation, at street resolution. Both the first-order effect and the total effect are studied. The spatial distributions of the sensitivity with respect to different input factors are also presented.

2. Global Sensitivity Analysis: Sobol' method and its extension

Sobol' method is one of the variance-based methods for global sensitivity analysis (GSA) (Saltelli et al., 2004, 2008). A model is denoted by $y = g(p_1, p_2, \dots, p_K)$, where K is the dimension of inputs. The Sobol' decomposition can be applied to expectations and the variances of the model output y . The first-order effect expresses what would happen to the uncertainty of y if we could fix a factor $p_i = p_i^*$, where p_i^* is a particular value. The first-order sensitivity index of y with respect to p_i is written as:

$$S_i = \frac{\text{Var}_{p_{\sim i}}(E_{p_i}(y|p_i = p_i^*))}{\text{Var}(y)}, \quad (1)$$

where $p_{\sim i}$ is all other input element in \mathbf{p} except p_i . A high value of S_i implies that p_i is an influential factor. The condition total-effect index $S_{Ti} = 0$ is necessary and sufficient for p_i to be a non-influential factor (Saltelli et al., 2008). This means that the uncertainty of p_i would not significantly affect the output variance $\text{Var}(y)$. In order to estimate S_{Ti} of p_i , we can fix all $p_{\sim i}$ as a particular value $p_{\sim i}^*$. The total effect index is:

$$S_i = \frac{E_{p_{\sim i}}(\text{Var}_{p_i}(y|p_{\sim i} = p_{\sim i}^*))}{\text{Var}(y)} = 1 - \frac{\text{Var}_{p_{\sim i}}(E_{p_i}(y|p_{\sim i} = p_{\sim i}^*))}{\text{Var}(y)}, \quad (2)$$

For computing S_i and S_{Ti} , Saltelli (2002) proposes an efficient strategy by using Monte Carlo estimates. The sample size used for the Monte Carlo estimate is N , and there are K uncertain inputs. Saltelli et al. (2008) recommends that for carrying out GSA with Sobol' method, it is better to have a lower dimension model in inputs and outputs. The recommended CPU time per run of the model should be less than 1 minute. However, for simulating traffic flows and emissions of an urban area at street level, the computational cost is much higher than recommended. Also, the inputs of classic traffic assignment models are of very high dimension (see later in Section 3.1). To reach similar conditions as recommended, we firstly built a meta-model of the traffic assignment model (see later in Section 3), and then carried out the GSA with Sobol' method.

3. Dynamic traffic assignment model and the Meta-model

At the metropolitan scale, traffic assignment (TA) models are used to predict the traffic flows at street level. The inputs of TA models are traffic demand and a modeled network. The network is modeled with origins/destinations, nodes and links. The link capacity constraints and speed limits are given at street level. In the following parts, a "link" represents a modeled "street" or "road" of a city road network. The traffic demand is represented by an Origin-Destination matrix (O-D matrix), summarizing the traffic flow from each origin zone to each destination zone during a certain period. A pair of Origin-Destination zones is referred to an O-D pair. The most commonly used TA models are based on the Wardrop User Equilibrium (UE) principle (Wardrop, 1952), stating that users choose the least cost path to travel through the network from an origin to a destination. There are static TA models and dynamic TA models. In this paper, we used a dynamic TA model in order to take into account time-dependent inputs. The model used here called LADTA (Leurent, 2003; Aguiléra and Leurent, 2009). It is applicable to large-size network (Aguiléra and Leurent, 2009) and can be coupled with emission model for estimating on-road emissions (Chen et al., 2017). LADTA model is computationally costly. A meta-modeling approach was therefore applied to LADTA model in the agglomeration of Clermont-Ferrand. The outputs of the resulting meta-model are very close to those of the complete model, yet the computation time is significantly decreased. Then GSA studies are carried out on this meta-model instead of the complete model.

3.1 Inputs and outputs of LADTA simulation for the agglomeration of Clermont-Ferrand

In our case study, LADTA is applied in the agglomeration of Clermont-Ferrand. The definitions and notation of inputs and outputs are listed here.

3.1.1 Inputs

$\mathcal{G} = (\mathcal{N}, \mathcal{A})$: the nodes ($\in \mathcal{N}$) and links ($\in \mathcal{A}$) of the oriented graph \mathcal{G} modeled for the network of the Clermont-Ferrand. $d = \text{card}(\mathcal{A}) = 19628$. D is the number of links.

$Z_o, Z_D \subset \mathcal{N}$: the set of nodes representing the Origin-Destination zones. $z = \text{card}(Z_o) = \text{card}(Z_D) = 124$.

\mathcal{H} : the simulation period of LADTA.

$\mathbf{C} = [C_a]_{a \in \mathcal{A}}, \mathbf{L} = [L_a]_{a \in \mathcal{A}}, \mathbf{V}_0 = [V_{0a}]_{a \in \mathcal{A}}, \mathbf{T}_0 = [T_{0a}]_{a \in \mathcal{A}}$: the vector of link capacities, link lengths, speed limits and free-flow travel times. $\mathbf{C}, \mathbf{L}, \mathbf{V}_0, \mathbf{T}_0 \in \mathbb{R}^d$.

In order to represent the uncertainty of the network parameters, links are regrouped according to link capacities and speed limits.

$\mathbf{V}_0^{low} = [V_{0a}]_{a \in \mathcal{A}_{low}}$: the vector of low speed limits ($V_0 \leq 50 \text{ km/h}$), with \mathcal{A}_{low} as the set of links with $V_0 \leq 50 \text{ km/h}$.

$\mathbf{V}_0^{high} = [V_{0a}]_{a \in \mathcal{A}_{high}}$ with $\mathcal{A}_{high} = \mathcal{A} \setminus \mathcal{A}_{low}$: the vector of high speed limits.

$\mathbf{C}^{small} = [C_a]_{a \in \mathcal{A}_{small}}$: the vector small link capacities ($C_a \leq 900 \text{ veh/h}$), with \mathcal{A}_{small} as the set of links with $C_a \leq 900 \text{ veh/h}$.

$\mathbf{C}^{big} = [C_a]_{a \in \mathcal{A}_{big}}$ with $\mathcal{A}_{big} = \mathcal{A} \setminus \mathcal{A}_{small}$: the vector of big link capacities.

$\mathbf{Q}(h) = (q_{o,d}(h))_{(o,d) \in Z_o \times Z_D}, h \in \mathcal{H}$: the time-varying O-D matrix, and $q_{o,d}(h)$ is the time-varying traffic demand (in veh) for time h of the O-D pair (o, d) .

$\mathbf{Q}^{peak}(h) = (q_{o,d}^{peak}(h))_{(o,d) \in Z_o \times Z_D}, h \in \mathcal{H}$: O-D matrix of the agglomeration of Clermont-Ferrand during the evening peak hour 17:00 – 18:00, where $(q_{o,d}^{peak}(h))_{(o,d)}$ is the average traffic demand during the evening peak of the O-D pair (o, d) .

3.1.2 Outputs

$\mathbf{X}(h) = [X_a(h)]_{a \in \mathcal{A}, h \in \mathcal{H}}$: the vector of computed traffic volumes at time h .

$\Delta h = 0.25 \text{ hour}$: the time step of simulation in our case study.

$\mathbf{y}(h) = \mathbf{X}(h + \Delta h) - \mathbf{X}(h)$: a vector of average traffic flow during $[h, h + \Delta h]$. It is the final output of the LADTA model.

3.2 LCF model: LADTA applied in Clermont-Ferrand

The LADTA model takes into account the influence of the time-varying traffic demand to compute time-dependent $\mathbf{X}(h)$. The computed $\mathbf{y}(h_{simu})$ at time h_{simu} is assumed to be not affected by traffic demands before 2.25 hours and after 1.0 hour of h_{simu} . We define an *atomic* LADTA simulation for the agglomeration of Clermont-Ferrand as LCF model (for *LADTA applied in Clermont-Ferrand*). With a traffic demand during 3.25 hours to take into account the temporal variation of $\mathbf{Q}(h)$, LCF model computes the traffic flow $\mathbf{y}(h_{simu})$ during $[h_{simu}, \dots, h_{simu} + \Delta h]$. $\mathbf{Q}(h)$ is assumed to be piecewise constant during $[h, h + \Delta h]$. We denote the set $\{h_{simu} - 2.25, h_{simu} - 2.0, \dots, h_{simu} - 0.25, h_{simu}, \dots, h_{simu} + 0.75\}$ as \mathcal{H}_{atomic} . Therefore, the time-varying traffic demand can be represented by 13 O-D matrices $\{\mathbf{Q}(h), h \in \mathcal{H}_{atomic}\}$. With $\mathbf{Q}^{peak}(h)$ given in our case study, the required 13 O-D matrices can be obtained by $\mathbf{Q}(h), h \in \mathcal{H}_{atomic} = P(h) \cdot \mathbf{Q}^{peak}(h)$ where $P(h)$ are *temporal variation coefficients* representing the ratio between (i) traffic demand during $[h, h + \Delta h]$ and (ii) during the evening peak hour. It is assumed that the temporal variation of the demand is independent of the spatial distribution of O-D pairs: at the same time h , $P(h)$ is the same for all $(q_{o,d}(h))_{(o,d) \in Z_o \times Z_D}, h \in \mathcal{H}$.

The O-D pairs are categorized into five groups according to their distance between Origin-Destination zones: 0 km , $0 - 5 \text{ km}$, $5 - 10 \text{ km}$, $10 - 15 \text{ km}$ and $> 15 \text{ km}$. The matrix $\mathbf{Q}^{peak}(h)$ can be divided by 5 submatrices: $\mathbf{Q}_0^{peak}(h)$, $\mathbf{Q}_{0-5}^{peak}(h)$, $\mathbf{Q}_{5-10}^{peak}(h)$, $\mathbf{Q}_{10-15}^{peak}(h)$ and $\mathbf{Q}_{>15}^{peak}(h)$. It is needed to decrease the input dimension for carrying out meta-modeling and GSA. It is assumed that for the given agglomeration, the default values of $\mathbf{Q}^{peak}(h)$, \mathbf{V}_0 and \mathbf{C} remain unchanged. With all the inputs mentioned in Section 3.1.1, the dynamic matrices and uncertainty coefficients, the LCF model can then be represented as:

$$\begin{aligned} \mathbf{y}(h_{simu}) &= \mathcal{F}(\mathbf{Q}(h)_{h \in \mathcal{H}_{atomic}}, \mathbf{V}_0, \mathbf{C}) \\ &= \mathcal{F}(P(h)_{h \in \mathcal{H}_{atomic}}, \delta_0 \mathbf{Q}_0^{peak}(h), \delta_{0-5} \mathbf{Q}_{0-5}^{peak}(h), \delta_{5-10} \mathbf{Q}_{5-10}^{peak}(h), \delta_{10-15} \mathbf{Q}_{10-15}^{peak}(h) \\ &\quad \delta_{>15} \mathbf{Q}_{>15}^{peak}(h), \mu_{low} \mathbf{V}_0^{low}, \mu_{high} \mathbf{V}_0^{high}, \lambda_{small} \mathbf{C}^{small}, \lambda_{big} \mathbf{C}^{big}) \end{aligned} \quad (3)$$

In Equation (3), $P(h)$ can represent not only the temporal variation but also the uncertainty of the traffic demand. $\delta_0, \delta_{0-5}, \delta_{5-10}, \delta_{10-15}, \delta_{>15}$ are five *evening peak coefficients* to represent spatial uncertainty of the demand. $\mu_{low}, \mu_{high}, \lambda_{small}$ and λ_{big} are four coefficients applied to link capacities and speed limits. With the assumption that the default values of traffic demand and network parameters remain unchanged, the LCF model represented by uncertain inputs can be written as:

$$\mathbf{y}(h_{simu}) = \mathcal{M}(P(h)_{h \in \mathcal{H}_{atomic}}, \delta_0, \delta_{0-5}, \delta_{5-10}, \delta_{10-15}, \delta_{>15}, \mu_{low}, \mu_{high}, \lambda_{small}, \lambda_{big}) \quad (4)$$

where $\mathbf{p} \in \mathbb{R}^K$ is the input vector of the LCF model and its dimension is $K = 22$. With the same input at the same time h , $\mathbf{y}(h)$ computed by LCF model and the complete LADTA model are nearly the same. One *atomic* simulation with LCF model takes about 2 hours. A meta-model named Meta-LCF is built for LCF model. With the same input vector \mathbf{p} , the Meta-LCF model also computes traffic flows at street level. The outputs of Meta-LCF are very close to those of the LCF model, but the computational time for each run of the Meta-LCF model was decreased to 0.022~second.

3.3 Meta-LCF model

Firstly, the dimension of $\mathbf{y}(h)$ is reduced by projecting it onto the subspace spanned by the reduced basis $\psi_{j=1,2,\dots,N}, N \ll d$. The reduced basis is obtain by principal component analysis (PCA) computed from a training set. The training set is generated with m input vectors $\mathbf{p}^{(i)}, i = 1, 2, \dots, m$: $\mathbf{y}_i = \mathcal{M}(\mathbf{p}^{(i)})$. The input vectors are generated by Latin Hypercube Sampling (LHS) with certain interval of variations. The mean of the m samples is $\bar{\mathbf{y}}$. The projection of \mathbf{y} is $\mathbf{y} \simeq \bar{\mathbf{y}} + \sum_{j=1}^N \alpha_j \psi_j$, where $\alpha_j = (\mathbf{y} - \bar{\mathbf{y}}) \psi_j$ is the projection coefficient on the j^{th} principal component. The reduced model is then written as: $\mathbf{y} \simeq \bar{\mathbf{y}} + \Psi \Psi^T (\mathcal{M}(\mathbf{p}) - \bar{\mathbf{y}})$, where Ψ is the matrix of the N principal components: $\Psi = [\psi_1 \dots \psi_j \dots \psi_N]$.

Secondly, the relations between \mathbf{p} and α_j are emulated. Emulation techniques are used here to replace $\alpha = \mathbf{f}(\mathbf{p}) = \Psi^T \mathcal{M}(\mathbf{p})$ with a faster $\hat{\mathbf{f}}$ so that $\hat{\mathbf{f}} \simeq \mathbf{f}(\mathbf{p})$. One emulator for each component f_j is built. The training set, previously used for the PCA, is used again here. The proposed emulator consists of (i) a linear regression and (ii) an interpolation between the regression residuals at $\mathbf{p}^{(i)}$, based on Radial Basis Function (RBF). The j^{th} emulator reads $\hat{f}_j(\mathbf{p}) = \sum_{k=1}^K \beta_{j,k} p_k + \sum_{i=1}^m \omega_{j,i} \phi(d_j(\cdot, \cdot))$, where $\gamma_{j,i}$ are weights that depend on the residuals and $d_j(\cdot, \cdot)$ is the Euclidean distance between two input vectors. $\omega_{j,i}$ is obtained by ensuring that the emulator is exact at every $\mathbf{p}^{(i)}$.

Finally, \mathbf{y} of \mathcal{M} can be approximated as $\mathbf{y} \simeq \hat{\mathbf{y}} = \bar{\mathbf{y}} + \Psi(\hat{\mathbf{f}}(\mathbf{p}) - \Psi^T \bar{\mathbf{y}})$, with $\hat{\mathbf{f}}(\mathbf{p}) = [f_1 \dots f_j \dots f_N]$. With the same input vector \mathbf{p} , the output $\hat{\mathbf{y}}$ of the Meta-LCF is also the average traffic flows during $[h_{simu}, h_{simu} + \Delta h]$ at street level.

4. Road traffic emission model

For computing on-road traffic emissions, the method used is the Tier 3 method of the EMEP CORINAIR emission inventory guidebook of European Environment Agency (EEA, 2016). The total exhaust emissions of on-road traffic are calculated as the sum of hot emissions and cold-start emissions. In this study, only hot emissions are considered. The hot emissions can be estimated by the following formulation:

$$E_{hot,i,j}(g) = e_{hot,i,j}(g \text{ km}^{-1}) \times N_j(veh) \times M_j(km \text{ veh}^{-1}), \quad (5)$$

where $E_{hot,i,j}$ and $e_{hot,i,j}$ are the hot emission and hot emission factor (HEF) of pollutant i , for vehicle of technology j , respectively. N_j is the number of vehicles of technology j . M_j is the mileage of vehicle of technology j . The emissions at street level can be computed by combining the HEF with traffic flows at street level. Then the Equation(5) is applied on each road of the studied area and we get:

$$E_{hot,i,j,a}(g) = e_{hot,i,j,a}(g \text{ km}^{-1}) \times N_{j,a}(veh) \times L_a(km \text{ veh}^{-1}), \quad (6)$$

where $E_{hot,i,j,a}$ and $e_{hot,i,j,a}$ are the hot emissions and the HEFs of the road a for pollutant i for vehicle of technology j . $N_{j,a}$ is the number of vehicles on the road a , which is obtained by Meta-LCF model for Clermont-Ferrand. M_j in Equation(5) is considered as the road length of a , i.e, L_a in Equation(6). The emission factors can be modeled by COPERT IV formulas in EMEP inventory standards (EEA, 2016).

4.1 Emission factor model: COPERT IV

The formula used in EMEP guide book (EEA, 2016) is COPERT IV method (Gkatzoflias et al., 2007). According to COPERT IV, $e_{hot,i,j,a}$ is a function of the vehicle average speed v , for a given pollutant i and a given class of vehicle technology j . The HEFs depend on the following factors according to COPERT IV model: (i) vehicle category (passenger car, heavy duty vehicle, etc.), (ii) emission standard technology (pre-Euro, Euro 1, Euro 2, etc.), (iii) engine type (gasoline, diesel, etc.), (iv) engine capacity ($< 1.4 L, 1.4 - 2.0 L, > 2.0L$, etc.), (v) pollutant type and (vi) vehicle average speed. The first four factors are often categorized as *vehicle fleet* inputs. Meta-LCF model gives traffic information (number of vehicles and average speeds) at street level, and hot emissions can then be computed at street level if vehicle fleet inputs are provided at the same level. The computation of emissions at street level combining with traffic information are coded and published by the authors as an open-source program *Pollemission* (Chen and Mallet, 2016).

4.2 Traffic emission simulations in the agglomeration of Clermont-Ferrand

In our case study, it was assumed that the vehicle fleet inputs were the same on all the streets of the network. Meta-LCF model computes the number of vehicles, of which the share of the different categories, technologies, engine types and engine capacities are the same on all links. Five scalar coefficients are used to represent the vehicle fleet inputs. (i) θ_{gaso} is the proportion of gasoline PCs. (ii) $\gamma_{gaso_1.4}$ is the share of gasoline PCs with engine capacity less than $1.4 L$, among all gasoline PCs. (iii) $\epsilon_{diesel_2.0}$ is the proportion of diesel PCs with engine capacity less than $2.0 L$, among all diesel PCs. (iv) ζ_{gaso_euro4} is the proportion of gasoline PCs with emission standard of Euro 4 and higher. (v) ϕ_{diesel_euro4} is the proportion of diesel PCs with emission standard of Euro 4 and higher. For the agglomeration of Clermont-Ferrand, the default vehicle fleet data for PCs is that of France, provided in André et al., (2013) and used in Table 3 and Table 4 of Chen et al., (2017).

With traffic counts collected by detectors, the temporal variation of on-road traffic in Clermont-Ferrand can be obtained for all kinds of days during any periods. A whole-year simulation with Meta-LCF was carried out. The computed traffic flows and average speeds at street level were then entered in COPERT IV model. Together with the default vehicle fleet data, a whole-year hot emissions for PCs were estimated. Figure 1 presents the temporal variation of the daily vehicle counts, total daily on-road traffic (hot) emissions for PCs of NOx and CO during 2014.

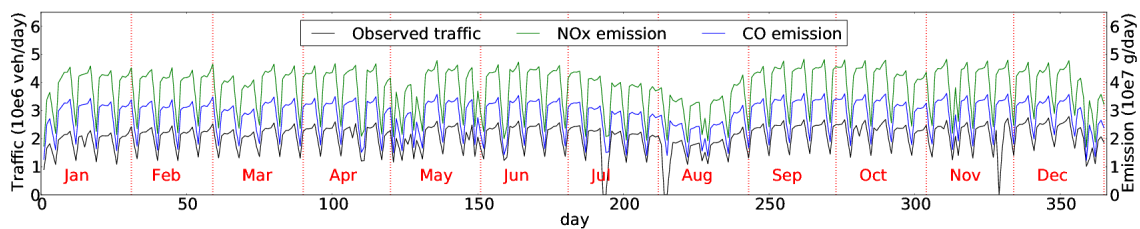


Figure 1: Daily observed on-road traffic (black, in 10^6 veh/day), total daily NOx (green) and CO (blue) emissions (in 10^7 g/day) for PCs estimated by Meta-LCF-COPERT IV, during 2014. (For each day, the traffic data is the sum of observed vehicle counts of all detectors. The value reaches zero when no data was collected. On these days, it was assumed that the values of emissions were the same as those of the same weekday in the previous week, except that if the day in the previous week is a public holiday, and then the value of the same weekday of the next week was taken).

Figure 1 showed that there is a nearly perfect correlation between the traffic volume and computed emissions. According to Equation (5), the number of vehicles, the average speeds and vehicle fleet data can all affect the hot emissions computed by the simulation chain. The following Section 5 presents GSA carried out for the whole emission simulation chain, with respect to inputs of both Meta-LCF and COPERT IV models.

5. Global sensitivity analysis for the simulation chain Meta-LCF-COPERT IV

We focus not only on inputs of COPERT IV model, but also the 22 traffic assignment (TA) inputs in order to analyze the propagation of uncertainty from the traffic model inputs to the computed emissions of the simulation chain. In total, 28 inputs for the whole simulation chain are studied, including the five inputs presented in Section 4.2, and an additional input concerning HDVs (see later). The first-order and total-effect sensitivity indices ($S_{i,a}$ and $S_{T_{i,a}}$) for traffic flows, speeds and emissions are computed for all links a . The variation intervals of Meta-LCF model and COPERT IV model are presented in Table 1 and Table 2.

Table 1: The inputs of LCF model and their variations for training sets

Input	Temporal profile	Capacity	Speed limit	Demand in O-D matrix
Symbol	$P(h)_{h \in \mathcal{H}_{atomic}}$	$\lambda_{big}, \lambda_{small}$	μ_{low} μ_{high}	$\delta_0, \delta_{0-5}, \delta_{5-10}, \delta_{10-15}, \delta_{>15}$
Number	13	2	2	5
Variation	[0.00, 1.50]	[0.70, 1.30]	[0.80, 1.20] [0.70, 1.10]	[0.25, 1.50]

Table 2: The inputs for COPERT IV model and their variations for training sets of our case study

Input	θ_{gaso}	$\gamma_{gaso_1.4}$	$\epsilon_{diesel_2.0}$	ζ_{gaso_euro4}	ϕ_{diesel_euro4}	σ_{HDV}
Variation(%)	[10, 100]	[10, 100]	[10, 100]	[10, 100]	[10, 100]	[0, 30]

Besides the five parameters defined in Section 4.2, we added in Table 2 an input to represent the share of HDVs on a group of roads passing through Clermont-Ferrand and near the industrial logistic center (shown in Figure 2). σ_{HDV} is the ratio between HDVs/PCs. In COPERT-IV model, there are many parameters for computing HEFs of HDVs. In our case study, only one type of HDV was added on given links: 100% charged articulated diesel truck of 28 – 32 t, with emission standard of Euro IV. The slope is assumed to be 0% over all roads. The outputs of the simulation chain are the emissions of NOx at link level of the whole agglomeration, during the time interval of $[h_{simu}, h_{simu} + \Delta h]$.

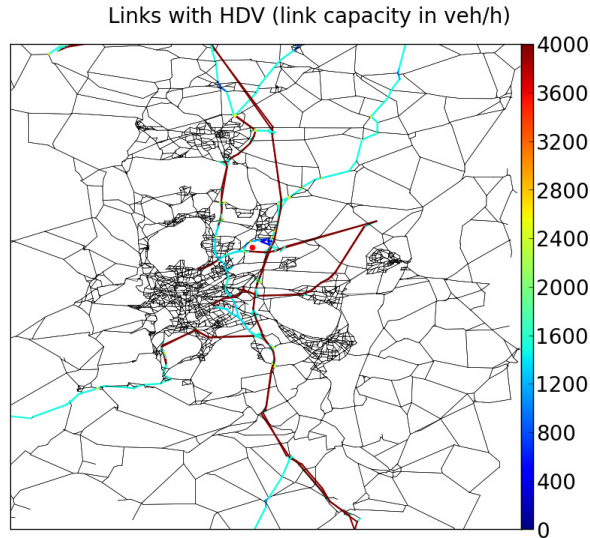


Figure 2: Map of links with HDVs, and link capacity map of the whole agglomeration of Clermont-Ferrand. The red point in the map is a big industrial logistic center.

5.2 GSA results

According to a GSA study of the Meta-LCF model alone Chen et al., (2017), it is found that the computed flows are sensitive to (i) the traffic demand during the previous 30 minutes until h_{simu} , especially during the previous 15 minutes and (ii) traffic demands of the O-D pairs whose inter-distance is between 0 km and 5 km. The traffic demands before 30 minutes and after h_{simu} are not influential to the output traffic flows on any road. The contribution of link capacities and speed limits to the output variance throughout the whole network is limited.

For the whole simulation chain from Meta-LCF model to final emission estimations, the GSA results are shown in Figure 3, where $S_{i,a}$ and $S_{T,i,a}$ are the first-order and total-effect sensitivity indices of computed NOx emissions at all links (in g), with respect to the total 28 input factors in Table 1 and Table 2 of simulation chain Meta-LCF-COPERT-IV.

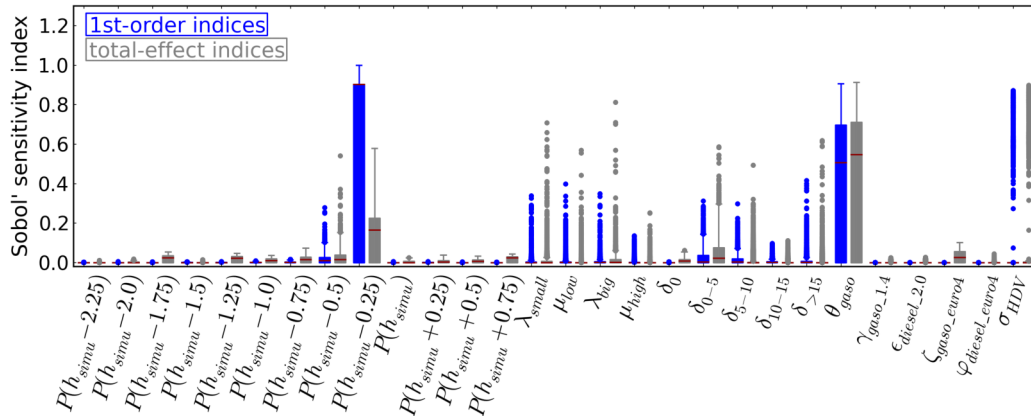


Figure 3: First-order and total-effect Sobol' sensitivity indices of the 28 inputs of the simulation chain Meta-LCF-COPERT IV for the computed NOx emissions

Figure 3 shows that the computed NOx emissions are sensitive to all the factors that are influential to the computed traffic flows. The uncertainty on speed limits does not contribute much to the variance of NOx emissions on most of the streets. The NOx emissions are not very sensitive to the emission standard technology either. However, Figure 3 shows that the NOx emissions are very sensitive to the proportion of gasoline cars (θ_{gasso}), and to the HDV share (σ_{HDV}). The uncertainties of θ_{gasso} and σ_{HDV} are main contributors to the variance of output NOx emissions computed by Meta-LCF-COPERT-IV. On links with HDVs, the computed emissions are still significantly more sensitive to the variation of HDVs than other vehicle fleet inputs of the simulation chain. The spatial distribution of first-order sensitivity index is presented in Figure 4.

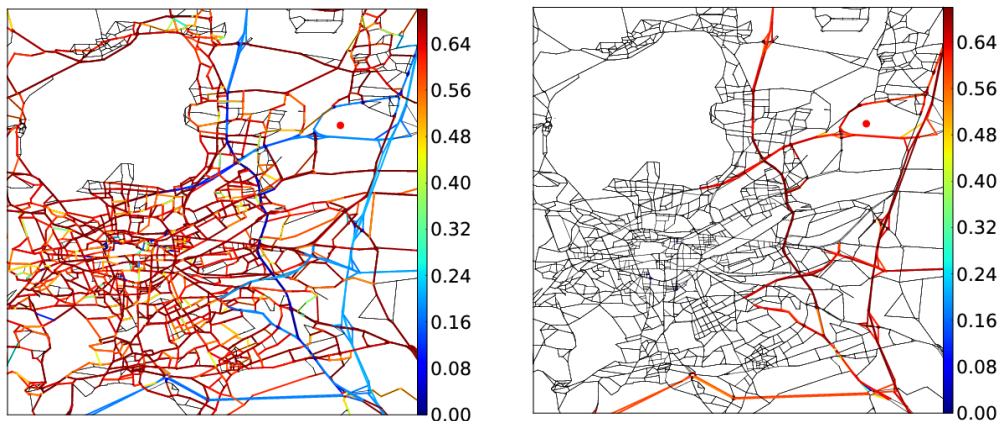


Figure 4: Spatial distribution of the first-order sensitivity indices ($S_{i,a}$) of the computed NOx emissions with respect to θ_{gasso} (left) and σ_{HDV} (right). The red point in the map represents a big industrial logistic center.

Conclusions

With the meta-modeling approach and Sobol' method, a global sensitivity analysis was carried out for the whole simulation chain from traffic assignment (TA) to emission estimation via COPERT IV model, in the agglomeration of Clermont-Ferrand. The main contribution of this paper is the quantification of input sensitivity to the whole emission simulation chain, which allows us to propagate the uncertainty from the inputs of the TA model to the final emission estimation.

Concerning traffic assignment modelling, a TA model called LADTA is applied to the whole agglomeration. An *atomic* simulation with LADTA in Clermont-Ferrand (the LCF model) was built. The LCF model has so high computational cost that cannot be directly used for GSA studies. Therefore, a meta-model (Meta-LCF) is built for it. With the same inputs, the outputs of Meta-LCF and the original model are traffic flows at all links during a simulation interval of 15 minutes. The results from the two models are very close to each other. The computational cost of Meta-LCF is very low: 0.022 s, while the cost of an *atomic* simulation with the original LCF is about 2 hours.

Concerning the global sensitivity analysis (GSA), the Sobol' method was used for GSA studies. The GSA is to the simulation chain Meta-LCF-COPERT IV for computing hot emissions of NO_x due to on-road traffics. The results of GSA show that the computed NO_x emissions are sensitive to all the inputs that influence the traffic flows: (i) the traffic demand during the previous 30 minutes until h_{simu} , especially during the previous 15 minutes and (ii) traffic demands of the O-D pairs whose inter-distance is between 0 km and 5 km. The speed limits do not have significant influence to the NO_x emissions computed by Meta-LCF-COPERT. In addition, computed NO_x emissions are very sensitive to some of the vehicle fleet parameters: the share of HDVs and the percentage of gasoline cars on road. Other fleet parameters such as the emission standards and engine capacities, are non-influential factors to the on-road NO_x emissions simulation.

Acknowledgment

This research is supported by the French National Research Agency (ANR, the *Agence Nationale de la Recherche*), project ANR-13-MONU-0001, ESTIMAIR (<https://project.inria.fr/anr-estimair/>). The City of Clermont-Ferrand provided the traffic flow measurements data. SMTC (*Syndicat Mixte des Transports en Commun de l'agglomération clermontoise*) provided the modeled network for the agglomeration of Clermont-Ferrand and the static O-D matrix.

References

- Aguiléra, V., Leurent, F., (2009). Large problems of dynamic network assignment and traffic equilibrium: Computational principles and application to Paris road network. *Transportation Research Record, Journal of the Transportation Research Board* 2132, 122-132.
- André, M., Roche, A., Bourcier, L., (2013). Statistiques de parcs et trafic pour le calcul des émissions transports routiers en France, *Report IFSTTAR-LTE*. Technical Report.
- Chen, R., Aguiléra, V., Mallet, V., Cohn, F., Poulet, D., Brocheton, F., (2017). A sensitivity study of road transportation emissions at metropolitan scale. *Journal of Earth Sciences & Geotechnical Engineering*, 7, 151-173.
- Chen, R., Mallet, V., 2016. Pollemission software computing traffic emissions of atmospheric pollutants with copert-4 formulations. <https://github.com/pollemission>.
- Chen, R., Mallet, V., Aguiléra, V., Cohn, F., Poulet, D., Brocheton, F., (2017). Meta-modeling of a dynamic traffic assignment model at metropolitan scale for global sensitivity analysis. submitted, *Transportation Research Record, Journal of the Transportation Research Board*.
- EEA, (2016). *EMEP/EEA air pollutant emission inventory guidebook – 2016*. European Environment Agency.
- Franco, V., Kousoulidou, M., Muntean, M., Ntziachristos, L., Hausberger, S., Dilara, P., (2013). Road vehicle emission factors development: A review. *Atmospheric Environment*, 70, 84-97.
- Gkatzoias, D., Kouridis, C., Ntziachristos, L., Samaras, Z., (2007). Copert 4: Computer programme to calculate emissions from road transport. European Environment Agency.

Leurent, F., (2003). On network assignment and supply-demand equilibrium: An analysis framework and a simple dynamic model, in: *European Transport Conference Proceedings*.

Saltelli, A., (2002). Making best use of model evaluations to compute sensitivity indices. *Computer Physics Communications* 145, 280-287.

Saltelli, A., Chan, K., Scott, E.M., et al., (2000). *Sensitivity analysis*. Wiley New York.

Saltelli, A., Ratto, M., Andres, T., Campolongo, F., Cariboni, J., Gatelli, D., Saisana, M., Tarantola, S., (2008). *Global sensitivity analysis: The primer*. John Wiley & Sons.

Saltelli, A., Tarantola, S., Campolongo, F., Ratto, M., (2004). *Sensitivity analysis in practice: a guide to assessing scientific models*. John Wiley & Sons.

Smit, R., Ntziachristos, L., Boulter, P., (2010). Validation of road vehicle and traffic emission models: a review and meta-analysis. *Atmospheric environment*. 44, 2843-2853.

Wardrop, J.G., (1952). Some theoretical aspects of road traffic research., in: *ICE Proceedings: engineering divisions*. Thomas Telford. pp. 325-362.

The Role of Changing Costs in Uptake of Hybrid and Electric Vehicles: A UK Case Study Comparing Diffusion Projection Methodologies

Kate PALMER*, James E. TATE**, Zia WADUD*** & John NELLTHORP**

*School of Chemical and Process Engineering, University of Leeds, Leeds, LS9 2JT, UK
Email: pmkhp@leeds.ac.uk

**Institute of Transport Studies, University of Leeds, Leeds, LS9 2JT, UK

Abstract

With the potential to reduce air pollution and greenhouse gas emissions, adoption of hybrid and electric vehicles is of interest to policymakers across the world. Many studies have projected the future car parc using a range of methods but diffusion modelling has the advantage of a simple approach that takes social interactions and visibility of new technologies into account. This paper compares the Bass, Logistic, and Gompertz diffusion models and their generalised forms (extended to include vehicle ownership costs). For the hybrid mid-sized vehicle segment, the Generalised Logistic method was found to project with lowest error. Using this method, hybrid and electric vehicles car parc share was projected by vehicle segment to 2040, the year that the UK government has banned the sale of conventional petrol and diesel vehicles.

This study concludes that together Battery Electric Vehicles, Plugin Hybrid Electric Vehicles and Hybrid Electric Vehicles is forecast for between 22% and 61% of the car parc by 2040, reducing annual CO₂ emissions by as much as 24.7% and NO_x emissions by up to 27%. Sensitivity analysis revealed that the rate of battery price reduction is critical for Electric Vehicle Uptake. Lower battery prices increases the proportion of battery electric vehicles significantly more than plugin/non-plugin hybrid electric vehicles whereas changing fuel cost affects adoption of hybrid/electric vehicles equally. The continuation of the plugin vehicle grant could incentivise an additional 16% of electric vehicles by 2040. The UK vehicle size split and hybrid/electric vehicle share is similar to many other vehicle markets in Europe therefore the policy outcomes of this study are pertinent to legislators across Europe.

Keywords: *Electric vehicle, Total Cost of Ownership, Bass Diffusion model, Future fleet projections*

Introduction

Electric vehicles such as Battery Electric Vehicles (BEVs), Plugin Hybrid Electric Vehicles (PHEVs) and Hybrid Electric Vehicles (HEVs) offer a low-carbon low-pollution alternative to conventional petrol and diesel technology (Bonilla et al. 2014). The UK government announced in July 2017 that sales of conventional petrol and diesel vehicles will be banned by 2040 (Swinford 2017). For these reasons, the increasing market-share of these vehicle types is interesting to policymakers.

Many studies have projected the future car parc using a range of methods, such as agent-based models (e.g. Eppstein et al. (2011)), consumer choice models (e.g. Cui et al. (2010)), and diffusion rate/time series models (e.g. McManus and Senter (2009)). Diffusion modelling has the advantage over other modelling approaches that it uses a simple approach to modelling durable consumer goods such that social interactions and visibility of new technologies are accounted for by the model diffusion parameters (Bass 1999). There is also the possibility of extending the standard diffusion modelling approach to take other pertinent phenomena into account such as changing vehicle cost (Lamberson 2011). There is no need for consumer surveys, instead models are calibrated either using past data or assuming adoption will follow the same pathway as other technologies.

This paper aims to examine future hybrid and electric vehicle adoption based on up to date historic data and accurate ownership costs, examining the pathway to total market share of hybrid and electric vehicles by 2040. This paper projects BEV, PHEV and HEV adoption for different vehicle size segments giving a more accurate representation of the future car parc than previous studies. For the

first time, six different diffusion models are compared: the Bass, Logistic and Gompertz diffusion models along with their generalised forms. These generalised models include a comprehensive monthly vehicle ownership cost model for 2000 to 2040. Using the model with the lowest prediction error - Generalised Logistic model - the effect of different financial incentives on hybrid and electric vehicle adoption is investigated. In addition, this paper includes a historic market share analysis of UK hybrid and electric vehicles adoption, analysing past adoption by vehicle size and purchase type, a useful summary for researchers and policymakers alike. This study illustrates how a relatively simple method, easily adapted and updated, can be used by legislators to model the effect of different financial incentives on the rate of adoption of hybrid and electric vehicles.

Literature Review

The Bass model was one of the first diffusion models and still features prominently in the literature (Bass 1999). The Bass model accounts for two adoption factors: imitation and innovation. This method builds mathematically on the notion of Roger's classical diffusion theory where adoption follows an S-shaped curve. The first portion of adopters are labelled innovators, the later the individual adopts the greater they are said to imitate others following external factors rather than innovating according to internal attributes (Rogers 2004). Other diffusion models such as the Gompertz and Logistic are similar to the Bass model in that they are a variant on the S-shaped curve. The Gompertz model is generally more appropriate for new technology which does not show any clear advantage over older technology (Muraleedharakurup et al. 2010). These methods generally are less widely used in the literature for projecting adoption of consumer durable goods.

Most studies use the Bass model although several studies extend the basic model to include other pertinent factors. Cao (2004) for example extends the standard version to include lagged fuel price and projected changing awareness. Lamberson (2011) extends the Bass model to include initial and running costs, however, it is unclear how costs are sourced and predicted. Fewer diffusion projections use other models such as the Logistic or Gompertz model. McManus and Senter (2009) project PHEV sales in the USA by comparing the Bass, Generalised Bass, Logistic and Gompertz model. This study finds that the inclusion of cost increase PHEV purchase rate. Finally, Lamberson (2011) compare both the Bass and Gompertz model using endogenous estimates of the saturation point, finding that the Gompertz model was a better predictor. Neither of these studies investigated the effect of changing financial incentives on rate of adoption of hybrid or electric vehicles.

Methodology

This paper projects adoption of BEVs, PHEVs and HEVs by vehicle size using different diffusion models to 2040. Vehicle segments are combined into four groups mini/supermini (A/B), lower medium/upper medium (C/D), executive/luxury (E/F) and, dual purpose/multipurpose (H/I). The sports vehicle segment (G) was not included in this analysis because of the small market share (approx. 1.5%) and difficulty to define a representative sports model.

The diffusion models investigated are the Bass, Logistic and Gompertz and their generalised forms, these are described in Table 1. The generalised models include a comprehensive vehicle cost model of historic and future monthly vehicle ownership costs. Regression analysis on historic data found that running cost and vehicle cost are both correlated with hybrid vehicle sales (see Palmer et al. (2017)), therefore it is reasonable to hypothesise that including these two factors will reduce forecast error.

The initial cost I is taken as the minimum vehicle model Manufacturer Suggested Retail Price for historic data. The vehicle running costs are calculated using the following formula,

$$R = f_t * m * e + a_t + n_t + x_t$$

where t = time, f = fuel price (£/l), m = mileage (miles), e = vehicle efficiency (litre/mile), a = annual maintenance inclusive of vehicle testing, n = annual insurance, x = annual tax. The details of these inputs and their sources are given in Appendix A. For historic TCO analysis for BEVs, PHEVs and HEVs see Palmer et al. (2017).

The saturation point is specified by a constant in each model (exogenous). The exogenous saturation point is calculated for each vehicle type and size segment separately based on vehicle total cost of ownership. For example to calculate the saturation point for the vehicle type HEV in the mid-sized (C/D) segment,

Table 1: Details of equation methods (basic equations sourced from [22], generalisations derived)

Diffusion Method	Differential Equation	Standard equation	Definitions
Bass	$\frac{dA}{dt} = \left(p + q \frac{A(t)}{M} \right) (M - A(t))$	$A(t) = M \left(\frac{1 - e^{-t(p+q)}}{1 + \frac{p}{q} e^{-t(p+q)}} \right)$	<i>A</i> : cumulative sales <i>t</i> : time (months) <i>p</i> : innovation constant <i>q</i> : imitation constant <i>M</i> : saturation point
Generalised Bass	$\frac{dA}{dt} = \left(p + q \frac{A(t)}{M} \right) (M - A(t)) x(t)$ where $x(t) = 1 + \beta_1 \left(\frac{P(t) - P(t-1)}{P(t)} \right) + \beta_2 \left(\frac{G(t) - G(t-1)}{G(t)} \right)$	$A(t) = M \left(\frac{1 - e^{-(p+q)(t+\beta_1 \ln(P)+\beta_2 \ln(G))}}{1 + \frac{p}{q} e^{-(p+q)(t+\beta_1 \ln(P)+\beta_2 \ln(G))}} \right)$ where $P(t) = \frac{I_{EV}}{I_{ICE}} \text{ and } G(t) = \frac{R_{ICE}}{R_{EV}}$	<i>I</i> : Initial vehicle cost <i>R</i> : Running cost per mile β_1 : Initial cost coefficient β_2 : Running cost coefficient
Logistic	$\frac{dA}{dt} = \frac{L_2}{L_1} A(t)^2$	$A(t) = \frac{L_1}{1 + e^{-L_2(t-L_3)}}$	<i>A</i> : cumulative sales <i>t</i> : time (months) <i>L</i> ₁ : Saturation point
Generalised Logistic	$\frac{dA}{dt} = \frac{L_2}{L_1} A(t)^2 x(t)$ where $x(t) = 1 + \beta_1 \left(\frac{P(t) - P(t-1)}{P(t)} \right) + \beta_2 \left(\frac{G(t) - G(t-1)}{G(t)} \right)$	$A(t) = \frac{L_1}{1 + e^{-L_2(t+\beta_1 \ln(P(t))+\beta_2 \ln(G(t))-L_3)}}$ where $P(t) = \frac{I_{EV}}{I_{ICE}} \text{ and } G(t) = \frac{R_{ICE}}{R_{EV}}$	<i>L</i> ₂ : slope parameter <i>L</i> ₃ : time to peak sales <i>I</i> : Initial vehicle cost <i>R</i> : Running cost per mile β_1 : Initial cost coefficient β_2 : Running cost coefficient
Gompertz	$\frac{dA}{dt} = G_2 A(t) e^{-G_2(t-G_3)}$	$A(t) = G_1 e^{-e^{-G_2(t-G_3)}}$	<i>A</i> : cumulative sales <i>t</i> : time (months)
Generalised Gompertz	$\frac{dA}{dt} = G_2 A(t) e^{-G_2(t-G_3)} x(t)$ where $x(t) = 1 + \beta_1 \left(\frac{P(t) - P(t-1)}{P(t)} \right) + \beta_2 \left(\frac{G(t) - G(t-1)}{G(t)} \right)$	$A(t) = G_1 e^{-e^{-G_2(t+\beta_1 \ln(P(t))+\beta_2 \ln(G(t))-G_3)}}$ where $P(t) = \frac{I_{EV}}{I_{ICE}} \text{ and } G(t) = \frac{R_{ICE}}{R_{EV}}$	<i>G</i> ₁ : saturation point <i>G</i> ₂ : slope parameter <i>G</i> ₃ : time to peak sales <i>I</i> : Initial vehicle cost <i>R</i> : Running cost per mile β_1 : Initial cost coefficient β_2 : Running cost coefficient

$$M_{HEV} = \frac{\frac{1}{TCO_{HEV}}}{\frac{1}{TCO_{Petrol}} + \frac{1}{TCO_{Diesel}} + \frac{1}{TCO_{HEV}} + \frac{1}{TCO_{PHEV}} + \frac{1}{TCO_{BEV}}} * F * S$$

where F is the estimated number of cars in the car parc, S is the estimated percentage of cars in the chosen size segment, and TCO_i is the Total Cost of Ownership of vehicle i in the chosen size segment.

At present vehicles have been found to be optimised for the emissions test cycle and therefore emit up to 30% more CO₂ when driven on the road (Mock et al. 2014). However, Real Driving Emissions legislation has been passed to reduce this gap. For new vehicles to meet these stricter limits, emissions control technology is fitted to the vehicle leading to increased initial vehicle costs. Vehicle costs are assumed to increase over the projected time period in line with figures from Hill et al. (2014) to take these factors into account. A battery learning rate of 6% is assumed (Propfe & Redelbach 2012; International Energy Agency (IEA) 2016; Nykvist & Nilsson 2015). The manufacturing cost of the BEV and PHEV vehicle was assumed to fall at a rate of 4% annually as vehicle technology matures and market share grows (Propfe & Redelbach 2012; Rempel et al. 2013; International Energy Agency (IEA) 2016).

Results

Error Analysis

The best model is chosen based on the lowest values of the three error metrics: MAE, RMSE and Bias (for definitions see Armstrong and Collopy (1992)). The MAE and RMSE errors were found to be on the same magnitude for all models. The RMSE and MAE was found to be the smallest for the Logistic models and the largest for the Gompertz models. Generalising the Logistic and Gompertz models was found to reduce MAE by 0.64% and 0.34% and RMSE by 0.57% and 0.32% respectively. However, generalising the Bass model had the opposite effect and increased MAE by 0.18% and RMSE by 0.16%. Therefore the model which performs best under these three error metrics is the Generalised Logistic.

Parameter and Sensitivity Analysis

The results of the diffusion modelling scenarios in this paper illustrate the high potential of HEVs, PHEVs and BEVs across the vehicle size segments (see Figure 1). If all segments follow a slower rate of diffusion (using model parameters from the mid-sized HEV segment), it is estimated that hybrid/electric vehicles will constitute 22% of the UK car parc by 2040, whereas by using fitted parameters this figure rises to 56%. Because the historic rates of adoption of other vehicles types and segments are greater than the mid-sized HEV segment, it is reasonable to assume that the estimate using the mid-sized HEV segment parameters is a lower bound for future estimates. Conversely, projections based on parameters estimated from historic data from the segment/vehicle type in question provide a more optimistic adoption rate.

The logistic parameter (L2) determines the rate of adoption of the technology; the greater this parameter the shorter the time to peak sales (see Appendix B for table of results). The logistic parameter for the HEV C/D segment is estimated at 0.205, this indicates that this segment has had a slow historic adoption rate. This parameter ranges from a minimum of 0.200 for the HEV H/I segment to 0.950 for the PHEV H/I segment.

The initial cost and running cost parameters (β_1 and β_2 respectively) vary significantly over different projections. Certain segments such as HEV A/B have very high estimated values of β_2 , this causes the projection to be very sensitive to changing costs.

A high saturation point coupled with a short time span of historic sales data leads to a large logistic parameter. Massiani et al. (2015) investigated a similar phenomenon, where the saturation point in the Bass model was tested for the effect on fitted model parameters. Massiani et al. (2015) found that increasing the saturation point decreased the model parameters linearly. This study found a similar result for the generalised logistic model; for large increases in the saturation point the logistic parameter increased, but the inclusion of the cost parameter resulted in a non-linear relationship between the variables. Sensitivity analysis of the saturation point found that there is a complex relationship between the saturation point (L1), the logistic parameter (L2) and the time to peak sales (L3). The cost

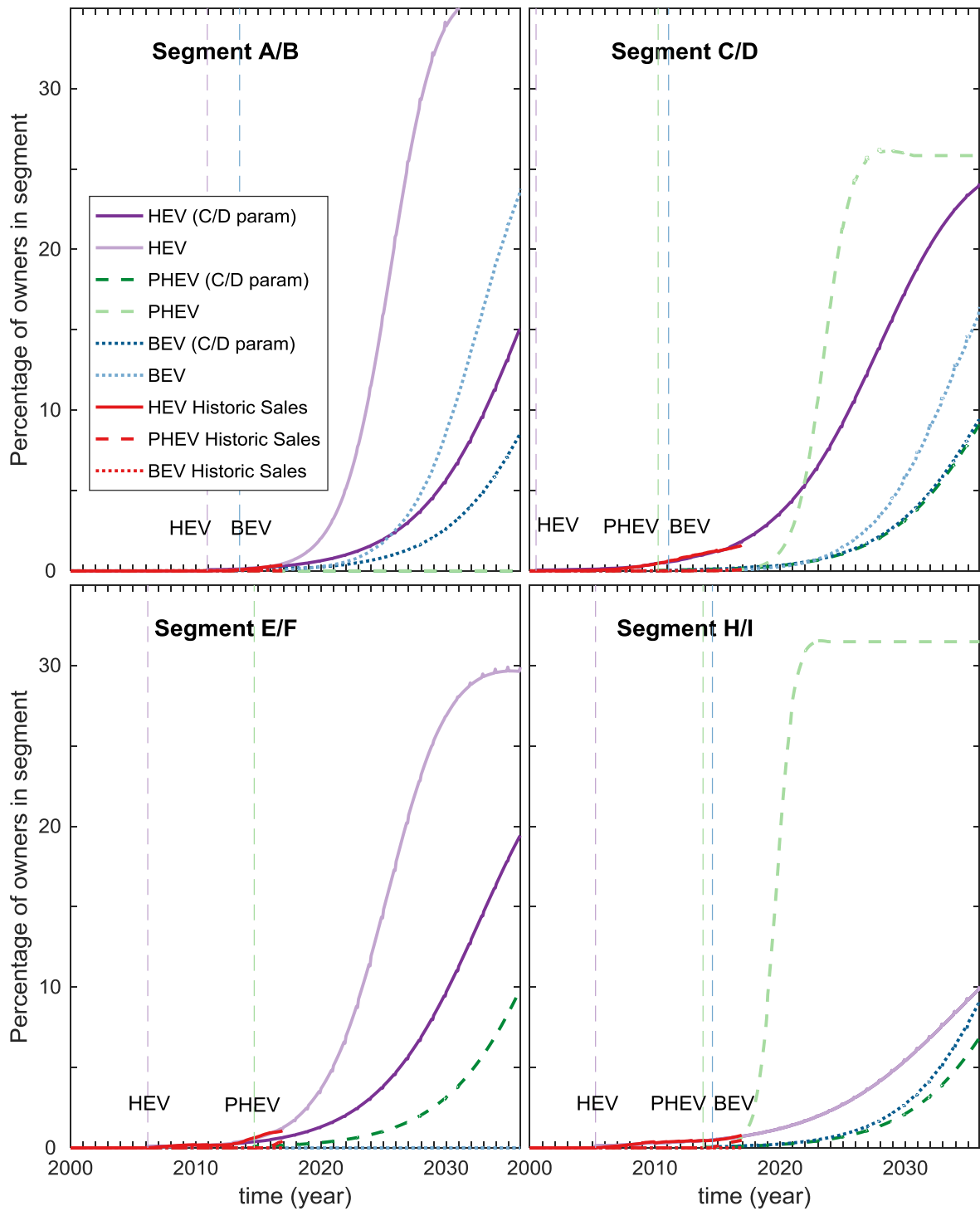


Figure 1: Generalised Logistic diffusion projections for BEVs, PHEV and HEV for all segments. (Vertical line indicates start date of vehicle type, note that HEV C/D parameters have been used for BEV HI and PHEV EF therefore fitted curves are not displayed).

parameters and time to peak sales variable are most sensitive to changes in the saturation point. For example, increasing L1 by 10% results in the time to peak sales increasing by 22%.

The annual reduction in battery costs is estimated using a battery Learning Rate (LR). This LR is defined as the percentage reduction in cost per doubling of production. With a large proportion of the initial cost of BEVs originating from the oversized battery, a higher LR will reduce the initial cost significantly. A sensitivity analysis of LR tested the effect of a number of LRs from 2% to 20%. The sensitivity analysis found that an increase for the high LR scenario, this resulted in an increase of 4% more Electric Vehicles in the car parc. It also appears that under a high LR a number of consumers would choose BEVs or PHEVs over HEVs, and therefore the number of HEVs falls with an increasing battery learning rate (evidenced in the 3% lower saturation point for HEVs in the high LR scenario).

DISCUSSION

Applying the model to financial policies

Financial subsidies have been used to stimulate adoption of low-emission in countries across Europe. Such vehicle incentives fall into two main categories: an initial grant (e.g. plugin vehicle grant in the UK, bonus malus scheme in France, or exemption from registration fees in Norway) or an annual subsidy (e.g. annual tax reduction/exemption in Japan) (Zhang et al. 2014). In the UK, the government offers an initial subsidy in the form of the plugin vehicle grant where £4500 or £2500 is available off the price of a new BEV or PHEV respectively (GOV.UK 2015). At present it is unknown when the plugin vehicle grant will be phased out, however, this could be early as 2018. Two such scenarios are explored using the generalised logistic diffusion model: the plugin vehicle grant withdrawn in December 2018 and the grant continued to 2040. Running the model under the two scenarios leads to the conclusion that the continuation of grant to 2040 leads to a 16% increase in BEV adoption by 2040. This is mainly attributed to small BEVs, as the grant is the greatest percentage cost reduction compared to other size BEVs and PHEVs. However, with the cost of BEV and PHEV ownership considerably lower, this impacts on the number of HEVs adopted over the time period, leading to a reduction of 14%.

Projections Emissions Effects

Diesel vehicles contribute significantly to urban air pollution as a result of high NO_x emissions during stop-start driving. The dieselisation of the car parc is a recent European phenomenon resulting from an initiative to reduce CO₂ emissions. As a consequence, diesel market share in the non-private market has increased from around 20% in 2000 to approximately 60% in 2011. HEVs, and especially PHEVs have been popular in the non-private market (see Section 4.1), therefore, assuming these vehicles have replaced petrol and diesel vehicles proportionally from the same segment, in the last 15 years hybrid/electric vehicles have displaced the purchase of more than 113 000 diesel vehicles.

A shift to greater numbers of hybrid and electric vehicles as projected in this study would result in annual car NO_x emissions to be cut by 27% and CO₂ emissions by 24.7% this translates to CO₂ savings of 14.6 million tonnes annually. This assumes the petrol to diesel ratio remains constant to 2040 (National Atmospheric Emissions Inventory 2013), the Euro standard split of petrol and diesels changes in line with NAEI projections Vehicle fleet composition projections (National Atmospheric Emissions Inventory 2013).

Projection Comparison

The Bass diffusion model is still the most common diffusion methodology for hybrid/electric vehicles (see Section 2). To date, no publications utilising the Generalised Logistic model exist, for this reason no direct comparison of model parameters is available. However, there are several projections of the UK and European car parc using other modelling methods. In this section the projections from these studies (see Figure 2 for summary) are contrasted and compared.

The projections in this study using the diffusion method yields comparable results for the market share of HEVs, PHEVs and BEVs to other projections (see Figure 2). Other predictions have used other methods such as consumer choice models, systems dynamics models or expert panel interviews. Unsurprisingly, different methods yield different forecasts (see Figure 2). Generally other projections predict that HEV market share will peak before BEV and PHEV market share (for example see Ricardo AEA D), although the projection detailed in this paper predicts that PHEV market share will reach

saturation point by 2030 before HEVs. PHEVs are often considered an intermediate technology as

- × This study
- McKinsey 2012 Conventional
- McKinsey 2012 EV dominated
- McKinsey 2012 FCEV dominated
- Ricardo AEA 2013 Reference
- Ricardo AEA 2013 Tech 1
- Ricardo AEA 2013 Tech 2
- Ricardo AEA 2013 Tech 3
- Ricardo AEA 2012 A
- Ricardo AEA 2012 B
- Ricardo AEA 2012 C
- Ricardo AEA 2012 D
- Oeko Institut 2011 Optimised ICE
- Oeko Institut 2011 Mixed Tech
- Oeko Institut 2011 Hybrid and Elt
- UK CCC 2008 Current Ambition
- UK CCC 2008 Extended Ambition
- UK CCC 2008 Stretch
- AEA 2009 Severe Protracted Recession
- AEA 2009 Green Recovery
- AEA 2009 Green Recovery + Upfront Price Support
- JRC 2010 Batt 1 F1
- JRC 2010 Batt 1 F2
- JRC 2010 Batt 2 F1
- JRC 2010 Batt 2 F2
- Ricardo AEA 2014 Low
- Ricardo AEA 2014 Medium
- Ricardo AEA 2014 High
- NAEI 2013 (estimates from fleet share)
- European Commission 2011 Reference
- European Commission 2011 Dominant electricity-battery success
- EcoDriver Policy Freeze
- EcoDriver Green Future
- EcoDriver Challenging Future

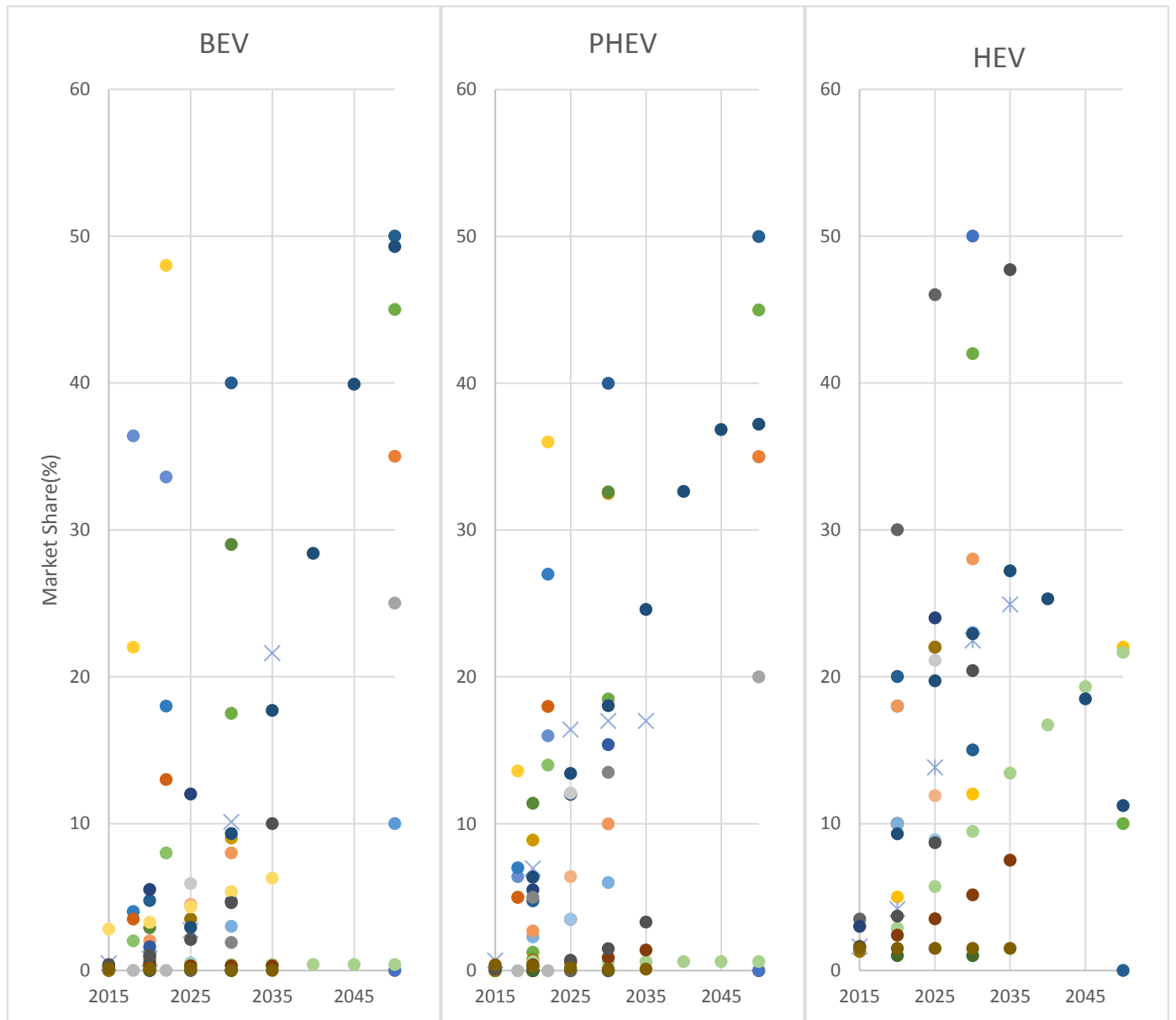


Figure 2: BEV, PHEV and HEV projections (Sourced from McKinsey [2], Ricardo AEA 2013 [3], Ricardo AEA 2012 [4], Oeko Institut [5], UK CCC [6], AEA 2009 [7], JRC 2010 [8], Ricardo AEA 2014 [9], NAEI [10], European Commission 2011 [11], EcoDriver [12])

batteries improve and BEV range increases. The diversity of projections is larger for BEVs than HEVs, this clearly indicates that there are uncertainties about future battery costs (a parameter which is explored in Section 4.3).

In the UK, the projections from the National Emissions Inventory are the leading authoritative source on the future UK car parc (National Atmospheric Emissions Inventory 2013). Market share has been estimated from car parc projections figures. It is clear that the diffusion model estimates are more optimistic at roughly three times that of the NAEI estimates (see Figure 2).

The projections from other studies (summarised in Figure 2) are generally complex models with dozens of sub-models and numerous hidden assumptions. Such models take years to build and are difficult to update. With market share of BEVs, PHEVs and HEVs increasing rapidly (see Section 4.1), many of these models cannot be updated or re-run to accommodate for changing conditions. The diffusion projection detailed in this paper has the advantage that it uses a transparent methodology, inputting up-to-date market share data with clear model assumptions. The generalised logistic model has not previously been used to model HEV, PHEV or BEV adoption and therefore this study illustrates how a relatively simple low-cost method can easily be used and adapted to test the effect of different financial scenarios on hybrid and electric vehicle adoption.

Conclusions

With climate change posing a significant threat to the habitats across the world, the need to reduce greenhouse gas emissions from all sources is pressing. As a result of greater fuel efficiency of BEVs, PHEVs and HEVs; hybrid and electric vehicles have the potential to reduce carbon dioxide emissions from the road network. Another advantage of these vehicle types is the comparably low NO_x emissions which lead to lower air pollution levels, a problem which leads to millions of deaths annually (World Health Organisation 2014). Although measures need to be taken to curb demand and incentivise travel on public transport, if hybrid and electric vehicles reach the numbers projected in this paper, NO_x emissions from cars will be cut by 27% and CO₂ emissions by up to 24.7% this translates to CO₂ savings of 14.6 million tonnes annually.

Estimating the potential number of hybrid and electric vehicles on the roads and resultant vehicle emissions reduction can inform and direct low-carbon transport policy. This paper highlights how a low-cost, easily updatable, relatively simple to execute projection method can be used to test the effect of different financial policies on the car parc.

Many countries in Europe have a vehicle market with a comparable split of petrol to diesel vehicles across car segments to the UK. Similar to the UK, many other European vehicle markets are experiencing lagging electric vehicle sales. For this reason, the conclusions of this paper are applicable to many different markets and demonstrate that the number of Electric Vehicles in the fleet could increase significantly over the coming decades.

Acknowledgements

Funding: this project was fully funded by the UK Engineering and Physical Sciences Research Council (EPSRC) (grant number EP/G036608/1).

References

- Armstrong, J.S. & Collopy, F., 1992. Error measures for generalizing about forecasting methods : Empirical comparisons *. , 8, pp.69–80.
- Bass, F., 1999. A New Product Growth for Model Consumer Durables. *Management Science* , 16(5), pp.1825–1832. Available at: <http://web.b.ebscohost.com/ehost/pdfviewer/pdfviewer?sid=d1b895dd-e9b7-4b0c-82b7-0eb2fdb7bba8%2540sessionmgr104&vid=1&hid=118>.
- Bonilla, D. et al., 2014. Innovation, the diesel engine and vehicle markets: Evidence from OECD engine patents. *Transportation Research Part D: Transport and Environment*, 27, pp.51–58.
- Cao, X., 2004. the Future Demand for Alternative Fuel Passenger Vehicles : a Diffusion of Innovation Approach. *Scenario*, 94274(31), pp.1–117. Available at: <http://aqp.engr.ucdavis.edu>.
- Cui, X. et al., 2010. A Multi Agent-Based Framework for Simulating Household PHEV Distribution and Electric Distribution Network Impact. In *Proceedings of the transportation research board 90th annual meeting, Washington, DC, Paper 11–2036*.
- Eppstein, M.J. et al., 2011. An agent-based model to study market penetration of plug-in hybrid electric vehicles. *Energy Policy*, 39(6), pp.3789–3802. Available at: <http://dx.doi.org/10.1016/j.enpol.2011.04.007>.
- GOV.UK, 2015. Plug-in car and van grants. *Driving and transport*. Available at: <https://www.gov.uk/plug-in-car-van-grants/overview> [Accessed October 14, 2015].
- Hill, N. et al., 2014. *Environmental Support to the Development of a London Low Emission Vehicle Road Map*, London, UK.
- International Energy Agency (IEA), 2016. *Global EV Outlook 2016 Electric Vehicles Initiative*,
- Lamberson, P.J., 2011. *Future Research Directions in Future Research Directions in Sustainable Mobility and Accessibility*, Available at: http://www.um-smart.org/project_research/Future_directions.pdf.
- Massiani, J. & Gohs, A., 2015. The choice of Bass model coefficients to forecast diffusion for innovative products: An empirical investigation for new automotive technologies. *Research in Transportation Economics*, 50, pp.17–28. Available at: <http://www.sciencedirect.com/science/article/pii/S0739885915000220>.
- Mcmanus, W. & Senter, R., 2009. Market Models for Predicting PHEV Adoption and Diffusion. *University of Michigan Transportation Research Institut*, (46827).
- Mock, P. et al., 2014. *From Laboratory to Road*, London, UK. Available at: http://www.theicct.org/sites/default/files/publications/ICCT_LaboratoryToRoad_2014_Report_English.pdf.
- Muraleedharakurup, G. et al., 2010. Building a better business case: the use of non-linear growth models for predicting the market for hybrid vehicles in the UK. In *Ecological Vehicles and Renewable Energies*. Monaco.
- National Atmospheric Emissions Inventory, 2013. Vehicle fleet composition projections (Base 2013). Available at: naei.beis.gov.uk/resources/rtp_fleet_projection_Base2013_v3.0_final.xlsx [Accessed July 27, 2017].
- Nykqvist, B. & Nilsson, M., 2015. Rapidly falling costs of battery packs for electric vehicles. *Nature Climate Change*, 5(4), pp.329–332.
- Palmer, K. et al., 2017. Total Cost of Ownership of Electric Vehicles: Global Comparisons and UK projections. In *Transportation Research Board*. Washington DC.
- Propfe, B. & Redelbach, M., 2012. Cost analysis of plug-in hybrid electric vehicles including maintenance & repair costs and resale values. *Proceedings of Electric ...*, pp.1–10. Available at: http://elib.dlr.de/75697/1/EVS26_Propfe_final.pdf [Accessed May 14, 2015].
- Rempel, J., Barnett, B. & Hyung, Y., 2013. PHEV Battery Cost Assessment. , pp.1–26.
- Rogers, E.M., 2004. A prospective and retrospective look at the diffusion model. *Journal of health communication*, 9 Suppl 1(July 2015), pp.13–19.

Swinford, S., 2017. Diesel and petrol car ban: Plan for 2040 unravels as 10 new power stations needed to cope with electric revolution. *The Telegraph*. Available at: <http://www.telegraph.co.uk/news/2017/07/25/new-diesel-petrol-cars-banned-uk-roads-2040-government-unveils/>.

World Health Organisation, 2014. 7 million premature deaths annually linked to air pollution. *Media Centre*. Available at: <http://www.who.int/mediacentre/news/releases/2014/air-pollution/en/> [Accessed July 25, 2016].

Zhang, X. et al., 2014. Policy incentives for the adoption of electric vehicles across countries. *Sustainability (Switzerland)*, 6(11), pp.8056–8078.

Appendix A: Vehicle Ownership Cost Summary table

Component	Details	Source
Past Initial Vehicle Cost	<ul style="list-style-type: none"> Minimum vehicle model Manufacturer Suggested Retail Price. 	Parkers [23]
Projected Initial Vehicle Cost	<ul style="list-style-type: none"> Petrol and Diesel costs assumed to increase to account for more stringent emissions legislation BEV/PHEV/HEV vehicle learning rate of 4% Battery learning rate of 6% 	Department for Transport [25] [26–34] [26–35]
Past Fuel Price	<ul style="list-style-type: none"> Monthly historic 	DECC [36]
Projected Fuel Price	<ul style="list-style-type: none"> Annual projected (linearly interpolated) 	DECC [36]
Annual Mileage	<ul style="list-style-type: none"> Assumed as 10 400 miles 	Department for Transport [37]
Past Vehicle fuel efficiency	<ul style="list-style-type: none"> Real world fuel efficiency 	Spritmonitor [24]
Projected Vehicle fuel efficiency	<ul style="list-style-type: none"> Projected fuel efficiency for conventional petrol and diesel vehicles from 2016-2035 HEV fuel efficiency trends extrapolated Fuel efficiency increases from battery weight reductions calculated from first principles. 	Department for Transport [38]
Past Maintenance	<ul style="list-style-type: none"> Costs were found to be cheaper for hybrid and electric vehicles due to less wear on the brakes and fewer moving parts 	CAPP automotive consulting [39]
Projected Maintenance	<ul style="list-style-type: none"> Assumed 2015 maintenance insurance costs rise with inflation 	
Past Tax	<ul style="list-style-type: none"> Vehicle Excise Duty: Jan 2000 to Mar 2001: Annual rate based on Engine power Apr 2001-Dec 2016: Annual rate based on NEDC rated CO₂ emissions 	Department for Transport [40,41]
Projected Tax	<ul style="list-style-type: none"> Vehicle Excise Duty: Jan 2017 - Mar 2017: Annual rate based on NEDC rated CO₂ emissions Apr 2017- : Annual flat rate for all vehicles (BEVs exempt) with an initial CO₂ dependent charge 	Department for Transport [40,41]
Past Insurance	<ul style="list-style-type: none"> British Insurance index, with an additional vehicle factor calculated based on current quotes [42] 	AA [43]
Projected Insurance	<ul style="list-style-type: none"> Assumed 2015 insurance costs rise with inflation. 	

Appendix B: Results of Generalised Logistic model using exogenous saturation point (Note that not all vehicle segments have reached saturation point by 2035 – see Fig 5).

Vehicle type/segment	Logistic parameter: L_2	Initial vehicle cost parameter: β_1	Running cost parameter: β_2	Saturation point: L_1	Peak sales year (L_3)
HEV A/B	0.523	33.1	-10.8	4.96×10^6 (13.3% 2035 fleet)	2025
HEV C/D	0.205	-584	-29.4	3.92×10^6 (10.5% 2035 fleet)	2029
HEV E/F	0.320	-554	-345	5.86×10^5 (1.57% 2035 fleet)	2026
HEV H/I	0.200	195	-122	1.28×10^6 (3.44% 2035 fleet)	2034
PHEV C/D	0.879	-0.278	-0.176	3.44×10^6 (9.23% 2035 fleet)	2023
PHEV E/F	0.205	-584	-29.4	3.93×10^6 (10.5% 2035 fleet)	2043
PHEV H/I	1.28	19.2	-1130	1.97×10^6 (5.29% 2035 fleet)	2019
BEV A/B	0.361	-51.0	-598	4.41×10^6 (11.8% 2035 fleet)	2019
BEV C/D	0.368	378	-727	3.49×10^6 (9.35% 2035 fleet)	2028
BEV H/I	205	-584	-29.4	3.93×10^6 (10.5% 2035 fleet)	2043

Developing a high-resolution traffic emission inventory for the metropolitan area of Nanjing, China

Shaojun Zhang^{1*}, Tianlin Niu² and Ye Wu²

¹ Sibley School of Mechanical and Aerospace Engineering, Cornell University, Ithaca, New York 14853, USA, sz262@cornell.edu

² School of Environment, Tsinghua University, Beijing, China

Background

The rapid development of road transportation system has brought benefits by connecting people, business, and goods together to an unprecedented degree. However, it has also created substantial challenges including congestion, carbon emissions, air pollution, and land use issues. To manage environmental impacts, road transport emission inventories have been established by governmental stakeholders and researchers to track historical emissions abatement progress and examine potential benefits from future emission mitigation strategies (Wu et al., 2017; Air Quality Expert Group, 2015). The growing awareness of urban sustainability challenges has increased the need for dynamically managing the road transportation systems within the cities and communities across the world.

High-resolution traffic profiles, such street-level traffic volume, speed and mix data, are essential to developing high-resolution road emission inventories (Zhang et al., 2016; GLA, 2016; Gately et al., 2015; McDonald et al., 2014). It is worth noting that intelligent transportation systems (ITS) have been deployed in many cities during the past decade, which contain a wide spectrum of elements such as smart traffic infrastructure, vehicle connectivity, real-time information service and big data analytics. The Municipality of Nanjing, a populous metropolitan area in East China (6,600 km²), offers an opportunity to develop a high-resolution emission inventory based on multiple ITS technologies, where RFID detectors, traffic camera, inter-city highway traffic monitoring system, and floating cars have been deployed extensively (see Figure 1). Based on real-world CO₂ emission factors developed for vehicle fleets in Nanjing, we demonstrate the development of a state-of-the-art and data-driven road emission inventory on the metropolitan level.

Method and Data

Nanjing is the capital city of Jiangsu Province and is an important metropolis within China's most prosperous region (the *Yangtze River Delta* region). The Municipality of Nanjing consists of 11 districts and has a population of more than 8 million people. The total vehicle population in Nanjing had climbed to 2.39 million by 2016, representing an ownership density of approximately 290 vehicles per thousand people (NJSB, 2015). The urban area is defined as four districts (Gulou, Xuanwu, Qinhuai, and Jianye) covering a total land area of 259 km². More than 80% of established RFID detectors are located within these four urban districts.

The main objective of the present work was to establish a high-resolution CO₂ emission inventory for the entire road networking in Nanjing and comprised three steps (see Figure 2). First, high-resolution traffic profiles were generated based on hybrid ITS datasets and other supplemented methods providing traffic count, vehicle speed and fleet configuration meshed in link-level and hourly levels. Second, real-world CO₂ emission factors of all vehicle categories were developed based on user-reported and on-road measured fuel consumption data, and these emission factors were associated with traffic dynamics (e.g., speed, fleet configurations) (Zhang et al., 2014a and 2014b; Wu et al., 2015; Yang et al., 2016). Third, a high-resolution CO₂ emission inventory was established for all road links, which could elucidate on-road emission patterns with respect to real-world traffic characteristics.

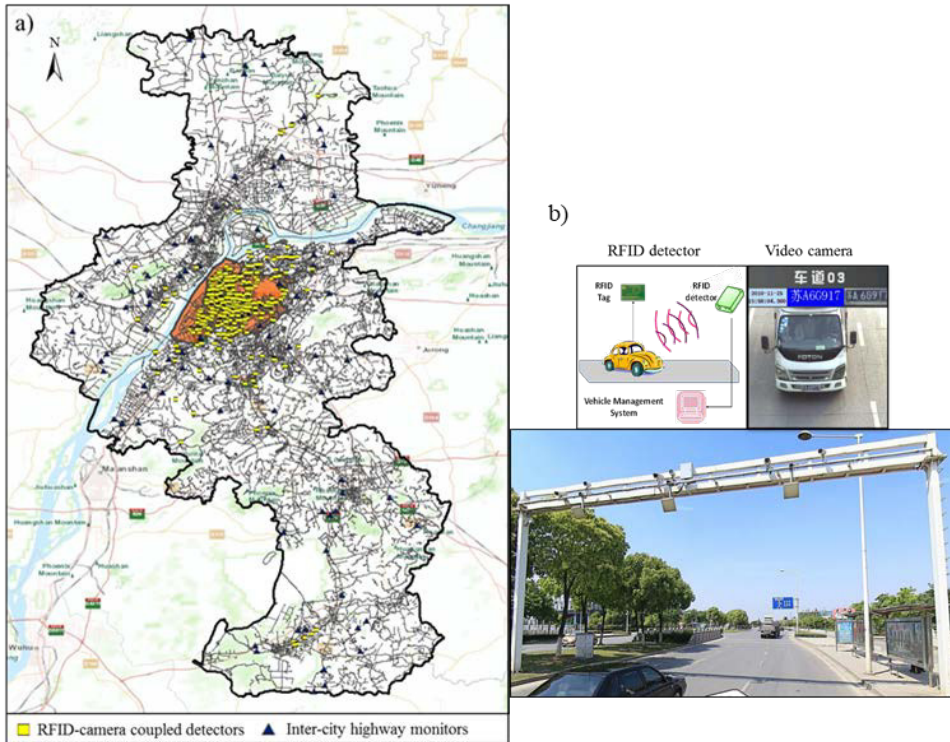


Figure 1: (a) Map of RFID and camera coupled detectors and inter-city highway monitoring sites in Nanjing and (b) one example of the RFID and camera coupled detection. The urban area of Nanjing consists of four districts and is marked as the orange domain.

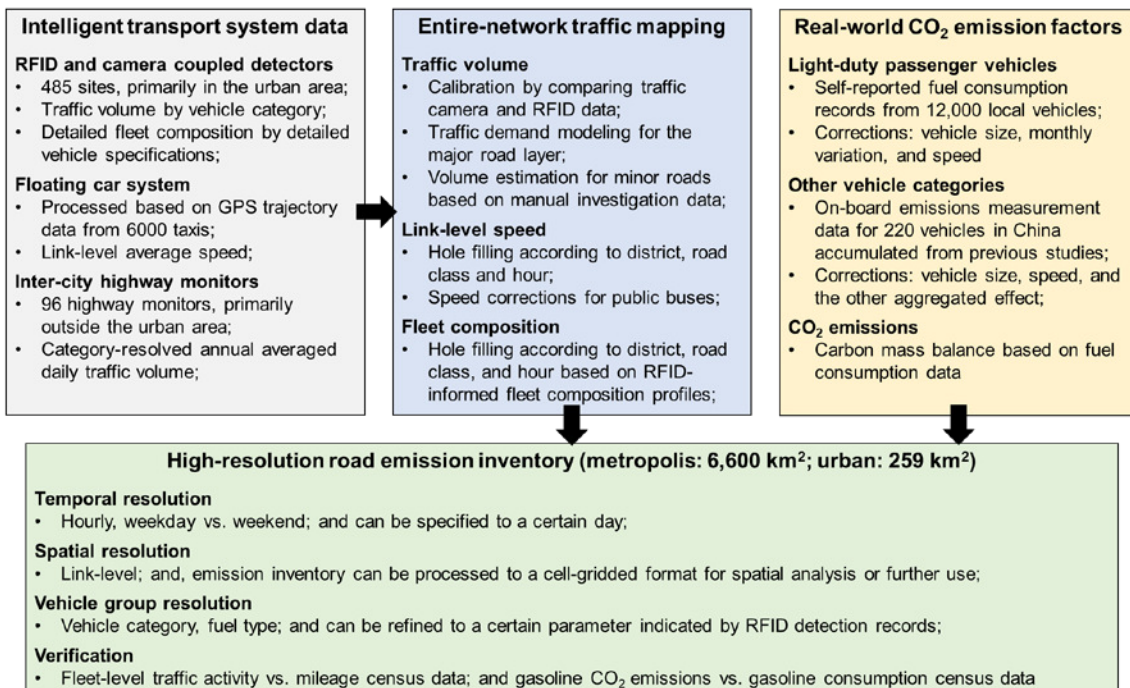


Figure 2: Overview of intelligent transportation system (ITS) data sources, generating traffic profile, developing localized CO₂ emission factors, and constructing a high-resolution road transportation emission inventory.

Results and Discussion

Using August 2013 as a case study period, average total daily CO₂ emissions from vehicles in the entire metropolis were 21.3 thousand tons (kt) and 17.6 kt during weekdays and weekends, respectively. Figure 3 illustrates the estimated 24-h vehicle emissions in the research domain by hour and vehicle category or fuel type. The combined emissions from light-duty passenger vehicles and taxis are responsible for 58% and 59% of total daily CO₂ emissions during weekdays and weekends, respectively, followed by heavy-duty passenger vehicles (HDPVs, 14%-15%), heavy-duty trucks (HDTs, 7%-8%), public buses (7%) and light-duty trucks (LDTs, 5%). The total daily CO₂ emissions on weekends were approximately 17% less than on weekdays because of lower traffic activity by 10% and higher vehicle speed by 5%. The hourly CO₂ emission rates during the peak traffic hours on a weekday (e.g., 8 am and 5 pm) could be higher by approximately 80% than the daily average level. This reflects increased traffic activity, particularly for LDPVs, and increased traffic congestion.

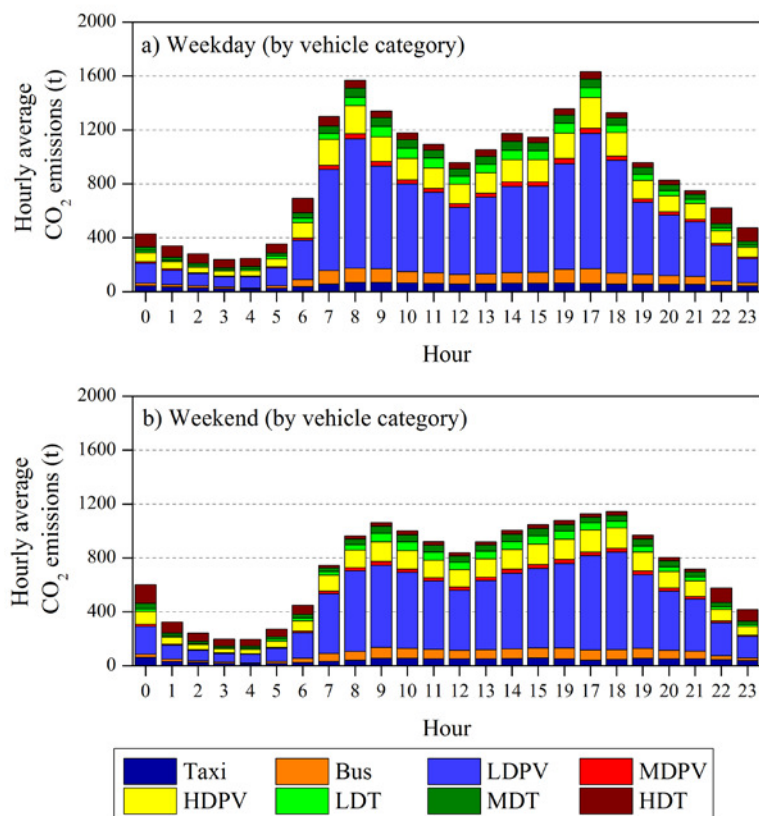


Figure 3: Estimated hourly CO₂ emissions from on-road vehicles in the entire municipality according to vehicle category during an average (a) weekday and (b) weekend.

The high-resolution emission inventory was constructed on the link-level basis for entire road networking in the municipality, and can further converted to a cell-gridded form (see Figure 4 as an example for weekdays). As seen from the red and orange cells in Figure 4 the CO₂ emission intensity was significantly higher in the urban area and along the major traffic corridors, which was consistent with the road network topology. For the entire metropolis, the 10% busiest traffic cells contributed approximately 30% of the total 24-h CO₂ emissions during both weekdays and weekends, 39% of which were located in the urban area. Table 1 shows the emission intensity results for the four major districts and the entire research domain. *Gulou* is the most densely populated district within the city and has the highest CO₂ emission densities during both weekdays and weekends.

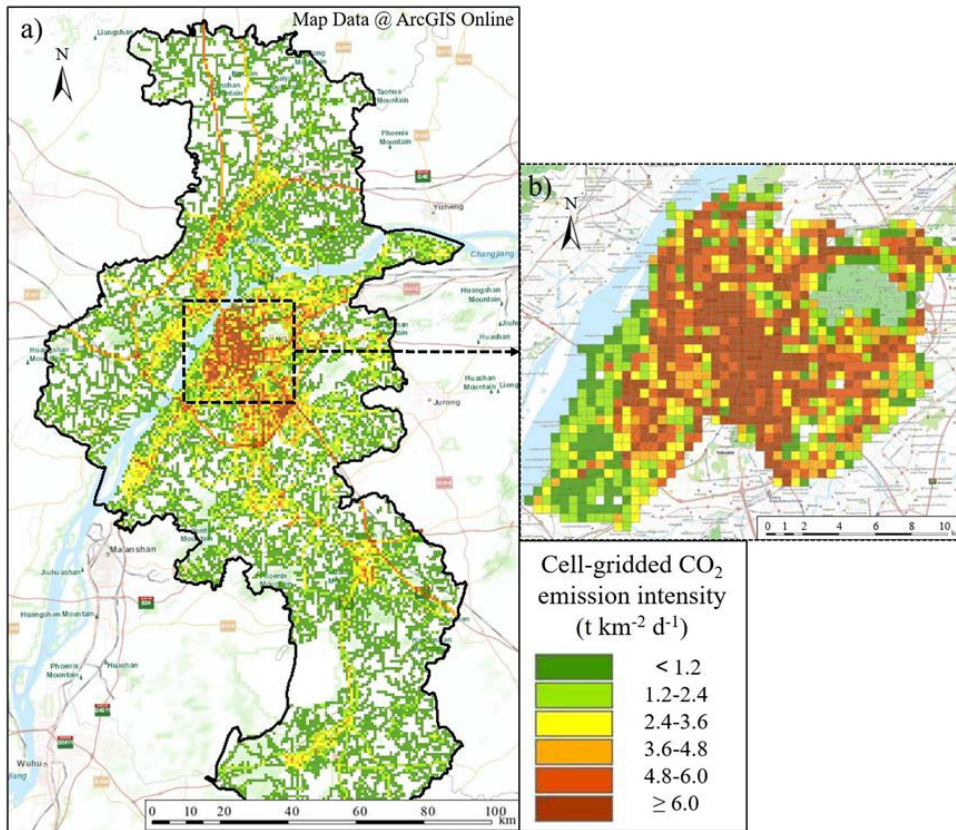


Figure 4: Cell-gridded daily CO₂ emission intensity from on-road vehicles in (a) the entire municipality and (b) the urban area, respectively, on an average weekday.

Table 1: Summary of CO₂ emission intensity (unit in t km⁻² h⁻¹) from on-road vehicles by region

Region	Weekday		Weekend	
	Median (P10–P90)		Median (P10–P90)	
	24h-average	8 am ^a	24h-average	9 am ^a
Entire municipality	0.73 (0.08–8.81)	1.08 (0.42–12.24)	0.64 (0.07–7.56)	1.01 (0.28–11.33)
Urban area	1.81 (0.38–4.71)	2.72 (0.52–7.24)	1.47 (0.32–3.52)	2.10 (0.48–4.89)
<i>Gulou District</i>	2.59 (0.62–5.16)	3.86 (0.90–8.34)	1.98 (0.43–3.65)	2.72 (0.61–4.97)
<i>Xuanwu District</i>	1.80 (0.40–4.40)	2.87 (0.66–6.86)	1.52 (0.36–3.56)	2.02 (0.39–4.66)
<i>Qinhuai District</i>	2.50 (0.70–5.35)	3.72 (1.06–8.25)	1.87 (0.61–3.99)	2.80 (0.88–5.75)
<i>Jianye District</i>	0.97 (0.32–3.17)	1.31 (0.40–4.51)	0.80 (0.26–2.32)	1.24 (0.40–3.46)

Note: ^a 8 am and 9 am were two typical rush hours with the highest traffic activity on the weekdays and weekends, respectively.

According to unpublished statistics provided by the Nanjing Environmental Protection Bureau, the annual consumption of gasoline and diesel fuels in the Municipality of Nanjing was 1.34 million ton (Mt) and 2.75 Mt, respectively, during 2013. In China, diesel fuels are considerably consumed by non-road sources (e.g., agriculture, industrial and construction machinery, and vessels), and therefore it is difficult to obtain census data of diesel consumption explicitly by on-

road vehicles. For gasoline consumption, on-road vehicles dominate the total use among all sectors in Nanjing except for minor consumption volumes by motorcycles (0.02 Mt estimated) and industrial plants (0.03 Mt reported) (NJSB, 2015). According to the estimated daily CO₂ emissions from gasoline vehicles, our study suggests the total gasoline consumption in the entire municipality was 1.30 Mt, very close to the statistical data. As a result, both mileage and gasoline consumption statistics can provide sufficient verifications to guarantee the accuracy of traffic activity and gasoline CO₂ emissions on the municipality level.

References

- Air Quality Expert Group. Linking emission inventories and ambient measurements. 2015 (accessed on Sep 12, 2016). Available at https://uk-air.defra.gov.uk/library/reports.php?report_id=828
- Gately, C.K., Hutyra, L.R. and Wing, I.S. Cities, traffic, and CO₂: A multidecadal assessment of trends, drivers, and scaling relationships. *Proceedings of the National Academy of Sciences of the United States of America*, **2015**, 112(16), 4999-5004.
- Greater London Authority (GLA). London Atmospheric Emissions Inventory 2013. 2016 (accessed on Sep 13, 2016). Available at: <http://data.london.gov.uk/dataset/london-atmospheric-emissions-inventory-2013>
- McDonald, B.C., McBride, Z.C., Martin, E.W. and Harley, R.A.. High-resolution mapping of motor vehicle carbon dioxide emissions. *Journal of Geophysical Research: Atmospheres*, **2014**, 119(9), 5283-5298.
- Nanjing Statistic Bureau (NJSB). Statistical Yearbook of Nanjing 2014. 2015 (in Chinese).
- Wu, X., Zhang, S., Wu, Y., Li, Z., Zhou, Y., Fu, L., Hao, J. Real-world emissions and fuel consumption of diesel buses and trucks in Macao: From on-road measurement to policy implications. *Atmospheric Environment*, **2015**, 120, 393-403.
- Wu, Y., Zhang, S., Hao, J., Liu, H., Wu, X., Hu, J., Walsh, M.P., Wallington, T.J., Zhang, K.M., Stevanovic, S. On-road vehicle emissions and their control in China: A review and outlook. *Science of the Total Environment*, **2017**, 574, 332-349.
- Yang, L., Zhang, S., Wu, Y., Chen, Q., Niu, T., Huang, X., Zhang, S., Zhang, L., Zhou, Y., Hao, J. Evaluating real-world CO₂ and NO_x emissions for public transit buses using a remote wireless on-board diagnostic (OBD) approach. *Environmental Pollution*, **2016**, 218, 453-462.
- Zhang, S., Wu, Y., Liu, H., Huang, R., Un, P., Zhou, Y., Fu, L., Hao, J. Real-world fuel consumption and CO₂ (carbon dioxide) emissions by driving conditions for light-duty passenger vehicles in China. *Energy*, **2014a**, 113, 1645-1655.
- Zhang, S., Wu, Y., Liu, H., Huang, R., Yang, L., Li, Z., Fu, L., Hao, J. Real-world fuel consumption and CO₂ emissions of urban public buses in Beijing. *Applied Energy*, **2014b**, 113, 1645-1655.
- Zhang, S., Wu, Y., Huang, R., Wang, J., Yan, H., Zheng, Y., Hao, J. High-resolution simulation of link-level vehicle emissions and concentrations for air pollutants in a traffic-populated eastern Asian city. *Atmospheric Chemistry and Physics*, **2016**, 16(15), 9965-9981.

Particulate emissions of Light Duty Vehicles in the future

Authors, G. Kadijk¹*, N.E. Ligterink¹, R.P. Verbeek¹ and R.J. Vermeulen¹.

¹ Research Group Sustainable Transport and Logistics, TNO, PO Box 96800, 2509 JE Den Haag, the Netherlands, gerrit.kadijk@tno.nl

Abstract

Particulate emissions of modern diesel vehicles with a proper working particulate filter (DPF) are very low. Also petrol vehicles have low particulate emission. During the lifetimes of these vehicles the real-world PM emissions may increase substantially because engine technologies may wear or fail or particulate filters are removed. This might contribute to a 25 to 100 fold increase in PM and PN emission in case of diesel engines.

This paper evaluates how In Service Conformity (ISC) and Periodic Technical Inspection (PTI) contribute to securing low particulate emissions during the life time of the vehicle and how this can be improved. Also measurement and type approval results are presented.

Better monitoring of PM and PN emissions of diesel and also petrol vehicles seems necessary.

It is recommended to extend the ISC emissions durability period above the current 100,000 km for both diesel and petrol vehicles. It is also concluded that the standard PTI smoke opacity test is not suitable at all for the evaluation of PM levels for diesel vehicles. A new PTI PN test procedure for diesel vehicles is proposed which is suitable for this purpose, namely to detect removed or broken DPFs. The risks of elevated PM and PN emissions of petrol vehicles are judged much lower than for diesel vehicles. These could be monitored in improved ISC test programmes.

Keys-words: *Particulate emissions, Light Duty Vehicles, DPF, GPF, ISC, PTI, PM, PN, EC, RDE.*

Introduction

On a global scale the number of metropolitan areas increases and urban traffic as well. One of the main pollutants of road traffic is Particulate Matter (PM) which is divided in several micrometer based size classes: PM_{0.1}, PM_{2.5} and PM₁₀. The annual yearly average concentration of PM₁₀ in Europe is limited to 40 µg/m³ and the World Health Organization (WHO) air quality guidelines for PM₁₀ is 20 µg/m³ and the hourly maximum 10 µg/m³. For smaller sized particulates; PM_{2.5} the WHO has annual and hourly average maxima of 25 µg/m³ and 10 µg/m³ respectively. There is no European official limit value for the PM_{2.5} concentration in ambient air but these are more directly correlated to PM emissions of petrol and diesel engines, their sizes typically range from 23 to 200 nm, than PM₁₀. Apart from particle size, the composition of PM may differ and one of the main future challenges is to find a relationship between specific components of PM and human health.

As a result of the Euro emission standards, see Table 1, the (laboratory) pollutant emissions of light-duty vehicles as observed in type approval tests have been reduced significantly over the past decade. However, under real driving conditions some emissions substantially deviate from their type approval equivalents. The real driving nitrogen oxides, or NO_x, emissions of diesel vehicles are currently the largest issue with regard to pollutant emissions and PM emissions are of great concern because DPFs are removed in certain cases. In the Netherlands, the ambient PM₁₀ concentration still exceeds European limits at numerous road-side locations and the levels have decreased in the last years.

Table 1: The different emission limits for PM and PN associated with the different Euro-classes for passenger cars with diesel and GDI engines (Gasoline Direct Injection).

	introduction dates		PM [mg/km]		PN [# /km]	
	new models	all models	diesel	GDI	diesel	GDI
Euro-4	1-Jan-2005	1-Jan-2006	25	-	-	-
Euro-5a	1-Sep-2009	1-Sep-2010	5	5	-	-
Euro-5b	1-Sep-2011	1-Sep-2012	4.5	4.5	6.0E+11	-
Euro-6	1-Sep-2014	1-Sep-2015	4.5	4.5	6.0E+11	6.0E+12
Euro-6c	1-Sep-2017	1-Sep-2018	4.5	4.5	6.0E+11	6.0E+11

Road traffic is one of the main contributors to air pollution. Modern diesel and petrol vehicles should have low PM emissions (see Figure 1) but during their life time these PM emissions may increase for several reasons. Especially the introduction of specific technologies such as particulate filters (DPF or GPF) or direct fuel injection (GDI) substantially influence the real world PM emissions. Furthermore their technical status may deteriorate and this could increase the PM emissions of these vehicles.

PM emissions of vehicles are strongly dependent on the applied technology. In Figure 1 the Exhaust particulate emissions (EC and non-EC) from Dutch diesel and gasoline passenger cars in urban traffic with standard traffic flow are shown. Petrol vehicles with direct fuel injection have little PM emissions, but these emissions are somewhat higher than the typical PM emission of diesel vehicles with a particulate filter. Wall flow diesel particulate filters (DPFs) are a very effective way to reduce emissions of soot particles in the exhaust gases. DPF's reduce the real-world PM emissions of light-duty vehicles with diesel engines strongly to an average of 1-2 mg/km, including the emissions associated with regeneration events. It is however known that DPFs are quite frequently removed if there are problems with DPF regeneration. Removal and tampering or manipulation of the engine software is more economical than a DPF replacement. The actual PM emission of such vehicles increase with a factor 25 to 100. Currently, there are no reasonable accurate tests to assess the presence or functionality of DPFs during periodic technical inspections. The current test that is used for periodic inspection of vehicles with diesel engines, the free acceleration smoke emission test, has a lack of sensitivity and it does not correlate with real world PM or PN emissions (Kadijk 2016b, 2017). Furthermore, the limit values used for diesel smoke, can even be met without a particulate filter.

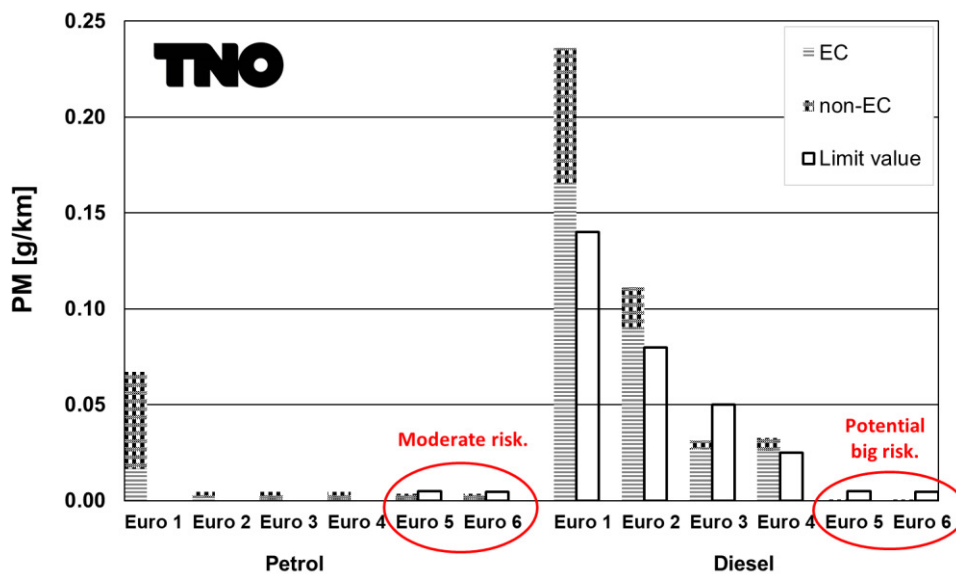


Figure 1: Exhaust particulate emissions (EC and non-EC) from diesel and petrol passenger cars in urban traffic with standard traffic flow (no congestion). Due to technical failures or manipulation the PM emission of Euro 5&6 vehicles may be higher.

Commissioned by the Dutch Ministry of Infrastructure and the Environment, since 1987 TNO regularly performs test programs to determine real-world emission performance of vehicles in the Netherlands. From 2012 onwards, special attention was paid to PM/PN emissions (Kadijk 2013, 2015, 2016a,b, 2017), (Ligterink 2016). The main goal of the programs is to gain insight into trends in real-world emissions of light-duty vehicles under conditions relevant for the Dutch and European situations. These test data are the basis for the emission factors of Dutch road traffic.

What are the legislative procedures to control (PM) emissions of road vehicles?

On different moments in a lifetime of a vehicle (type), emission tests must be performed and the actual emission levels are measured. These moments are:

- Type approval (TA) of a new vehicle type carried by type approval authorities. The type-approval includes:
 - Chassis dynamometer emission tests & Real Driving Emission tests on a pre-model,
 - Durability tests of emission control devices, prior to type-approval.
 - Conformity of production (CoP) tests of new vehicles, sampling the factory output,
 - Smoke emission test on a single engine
- In Service Conformity (ISC) of a limited number of in-use vehicles with a maximum mileage of 100,000 km. Chassis dynamometer tests as well as Real Driving Emission (RDE) tests on the road are to be carried out for new vehicle models from September 2017.
- Dutch national Periodic Technical Inspections (PTI) for all vehicles, mostly every two years starting at the vehicle age of 4 years carried out by PTI service stations/shops.
- Road Side Inspections (RSI) at random times carried out by national authorities.

Diesel PM/PN and smoke emissions in TA, ISC and PTI tests:

In type approval and ISC tests the PM & PN emission of each vehicle type is measured on a chassis dynamometer. The smoke emissions of an engine are determined in full load and free acceleration type approval tests. This free acceleration smoke test is also applied in PTIs. Unfortunately, the operating conditions of a free acceleration test are not representative for real world operation and the smoke emission limit values for vehicles with a DPF are relatively high (Kadijk 2017), which could result in false positives.

In Figure 2, a picture of the ISC and PTI test regime is shown. Although the ISC PN limit values are quite strict, they are only applicable up to 100,000 km. Mostly at a vehicle age of 4 years the PTI test regime starts. The PTI smoke emission limit values are not strict ($> 0.7 \text{ m}^{-1}$) and not well related to real world PM emissions; Consequently the real-world emissions of older vehicles can be substantial.

In the future monitoring programs and PTI may not have the same function as the current legislation. If high emission are observed for a vehicle, or vehicle model, in monitoring programs it might not be a priori clear if it is a road-worthiness issue, tampering, or has to be taken up in the in-service conformity.

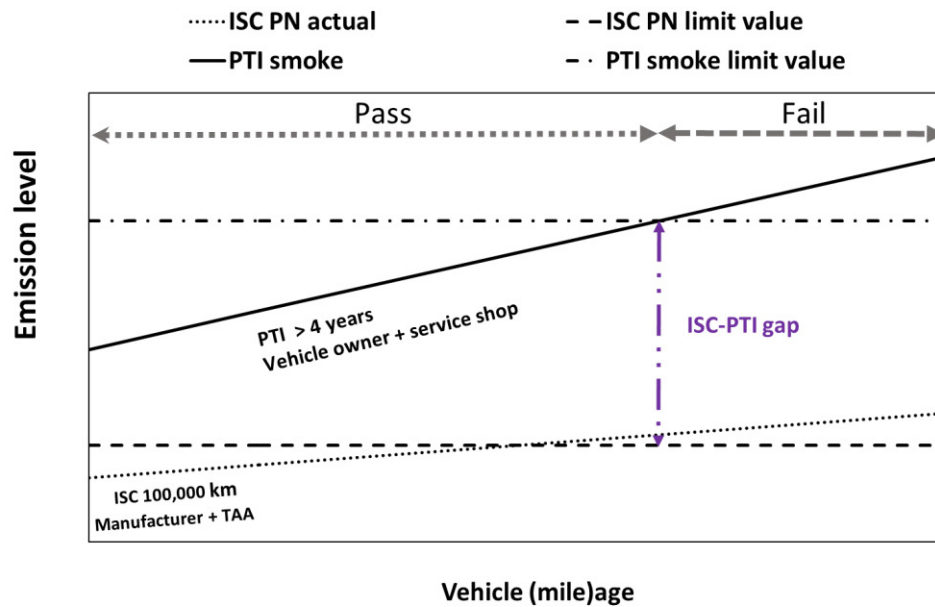


Figure 2: Example of the life time emission behavior of a diesel vehicle and different legislative instruments. The ISC-PTI gap may result in relative high average real world PM emissions of older vehicles.

Objective

The objective of the investigation reported here is to:

- present information on the real-world PM and PN emissions of modern diesel and petrol vehicles,
- assess the risks for an increase of these emissions over their lifetime and
- present possible pathways to reduce these risks.

Method

To be able to determine the trends of real world particulate emissions and to assess for possible risks on elevated emissions during the useful life of a vehicle, data was collected of several studies that were performed between 2013 and 2017 (Kadijk 2013, 2015, 2016a,b, 2017), (Ligterink 2016) for which the particulate emissions of more than 500 diesel and petrol passenger cars and light-duty vehicles were tested. The data comes from several types of PM emission tests.

The following tests were performed:

- Chassis dynamometer emission tests according to UNECE R83.
- The EC fractions of the PM of the GDI vehicles were chemically analyzed.
- Smoke emission test for diesel engines according to UNECE R24 of 1958 & 72/306/EEC.
- Free acceleration and PN emission tests at idle speeds for Periodic Technical Inspection (PTI). PN tests were done (also with cracked DPFs) with different (handheld) PN-testers which were correlated with the PMP-PN test protocol.

Results

The risks of elevated PM & PN emissions of diesel and petrol vehicles primarily depend on what engine and aftertreatment technology is used. The main issues and risks of petrol and diesel vehicles are described in the next sections and in separate text boxes.

Vehicles with Gasoline Direct Injection (GDI) engines:

In the past vehicles with GDI engines were a small group among all petrol vehicles sold. With the introduction of European CO₂ targets, GDI technology became one of the ways to increase the efficiency

of a conventional petrol engine. Hence, in the last few years vehicles with GDI engines were sold in larger numbers. In 2010, the GDI's were only 1% of the total petrol vehicle fleet. In summer 2016, 9% of the petrol fleet in the Netherlands has a GDI engine. In the last two years GDI's even make up 44% of the total sales. In particular, vehicles with a small GDI engine (0.9-1.2 litres) with a relatively high power output of 60–100 kW are sold in large numbers.

In type-approval GDI's clearly have higher particulate number emissions than diesel vehicles (see Figure 3). Moreover, there is some correlation between the particulate number and the particulate mass emissions on the type-approval test. Lagging three years behind the initial date of the introduction of Euro-6, with Euro-6c the particulate mass and number emissions of GDI's should satisfy, in all aspects, since the same stringent limits and standards as those of diesel vehicles apply. This also means that the RDE procedures should incorporate a particulate number test with appropriate limit for PN.

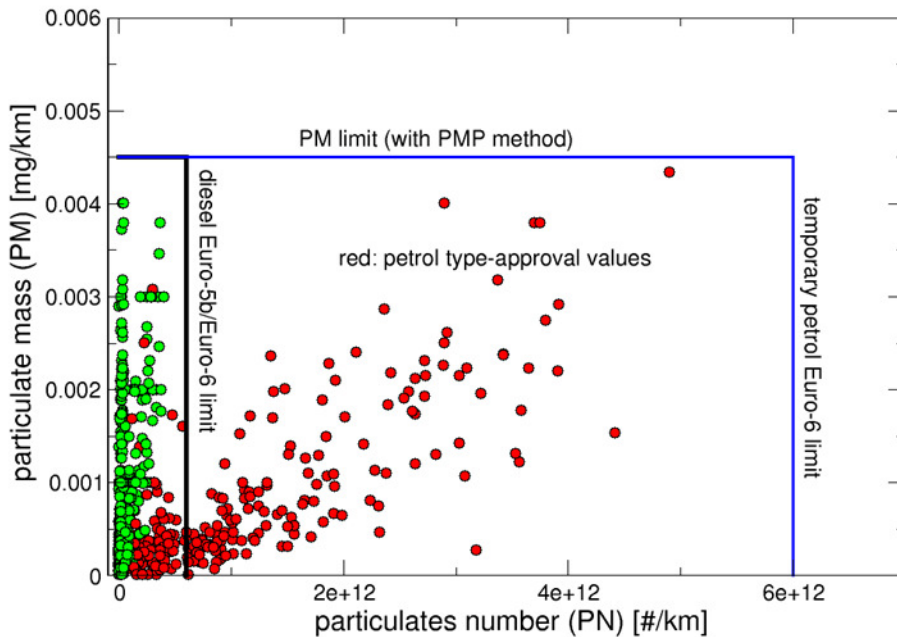


Figure 3: The particulate mass and particulate number measurement results in the NEDC type approval test of diesel vehicle models (green) and GDI's (red) which are sold in 2015 and 2016 in The Netherlands. The particulate number limit of GDI's is $6 \cdot 10^{12}$ #/km, while the diesel vehicles have a limit of $6 \cdot 10^{11}$ #/km.

In a dedicated real-world emission test program on the chassis dynamometer (2016c) three main stream GDI vehicles (see Table 2) were tested over CADC¹ test cycles with a maximum motorway speed of 150 km/h.

Table 2: Three main stream Euro 6 GDI vehicles

Trade Mark	Type	Power [kW]	Registration date	Vehicle test mass [kg]	Odometer [km]
Ford	Focus	74	17-03-15	1,176	11,628
Peugeot	308	81	11-12-15	1,450	14,268
Volkswagen	Golf	77	03-12-14	1,450	32,331

In Table 3 the average emission results the three GDI vehicles (average of 3 CADC tests per vehicle) are shown. In all cases, the NOx emissions exceeded the NEDC emission limits, but taking into account that the tests were performed with high load settings of the chassis dynamometer and a normal though demanding cycle and that the separate urban test had a short distance of only 4.8 km,

¹ Common Artemis Driving Cycle: this is a more dynamic and realistic drive cycle than the NEDC test required for the type approval.

the measured emissions do not raise special concern. In the case of an NEDC type-approval test the additional emission due to a cold start would have been spread over double the distance, yielding lower g/km results for the urban part of the test.

Table 3: Chassis dynamometer CADC average test results of the three Euro 6 GDI vehicles, based on equal weighing of vehicles and tests.

	THC	CO	CO ₂	NO _x	NMHC	CH ₄	PN	FC	PM (sum)
Averages	[mg/km]	[mg/km]	[g/km]	[mg/km]	[mg/km]	[mg/km]	[/km]	[l/100km]	[mg/km]
Urban	80	706	227.6	180	72	9	4.6E+12	9.90	2.8
Rural	9	134	129.0	90	8	1	9.1E+11	5.59	0.3
Motorway	11	396	168.8	70	9	2	1.8E+12	7.33	1.2
Total	33	412	175.1	115	30	4	2.4E+12	7.61	1.4

To obtain sufficient accuracy, for this programme the PM mass emissions were sampled over three consecutive tests (Ligterink 2016). This was done because generally the PM concentrations of GDI engines are very low and over three tests more PM mass could be collected so to increase the accuracy.

All vehicles with GDI engines have higher particulate number emissions than comparable diesel vehicles equipped with a DPF (Diesel Particulates Filter) which have emissions below 6×10^{11} #/km. Especially, over the cold start urban test a high number of particulates is emitted. In terms of emissions level, however, is of minor concern, given the fact that a Euro-4 diesel vehicle without DPF produces typically 10^{13} to 10^{14} #/km. This is a factor 10 to 100 higher than the particulate number emissions of these GDI's.

For the GDI engines also the particulate mass emission is low. Current emission factors for all petrol vehicles are about 5 mg/km. The measured values, despite the demanding tests, are below this current estimate of 5 mg/km. Hence, in terms of absolute emission levels GDI's are of little concern. Moreover, the differences between the vehicles may appear large, but current levels are below the emission limits. A cause for the large variations may be found at the measurement itself, as PM concentrations are generally rather low.

For the determination of the elemental (EC) and organic carbon(OC) fraction quartz filters were used and analysed in a chemical laboratory. The elemental carbon and the organic carbon together make up the total carbon in PM10 emissions. Generally, only a small mass fraction from other elements and the majority of the total mass is elemental carbon. The SUNSET method used is considered to be best suited to determine EC fractions. In Table 4 the EC fraction range is reported per type of road. Surprisingly, the fractions of EC in particulate matter are constant across the tested vehicles for a given road type, but vary widely between the road types. The EC fraction is higher than for petrol vehicles without direct injection, which are generally estimated at 30% and less, depending on technology and driving behaviour.

Although the fraction of elemental carbon is substantial, especially for an urban tests with cold start, the absolute levels are very low, ranging from 0.3 to 3 mg/km. Consequently, GDI's have a limited contribution to the total EC emissions of traffic. Only by the time that the large majority of diesel vehicles is equipped with well-functioning diesel particulate filters, the EC emissions of GDI's will become a significant remainder.

Table 4: The EC fraction range of three GDI vehicles per road type, as opposed to the fraction of carbon as part of organic compounds

CADC road type	Elemental Carbon Fraction [%]
Urban	81 – 90
Rural	28 – 38
Motorway	54 – 60

Potential risk of increased PM emissions of GDI vehicles: The emission performance of older GDI vehicles (> 100.000 km) is unknown. Analogue to diesel fuel injection technology, deterioration of fuel injectors as well as increased lubricant consumption may lead to elevated PM emission. It is expected that the PM emission of older GDI vehicles may increase up to 10-15 mg/km.

Unfortunately the current ISC or PTI test protocols do not offer a test regime to check the real world PM emissions of older GDI vehicles (100.000 to 300.000 km). An improved definition of ISC or a robust PM or PN test in the PTI in combination with good enforcement are needed to improve the PM emission of the total GDI vehicle fleet.

Increased PM/PN emissions of GDI vehicles: With low ambient temperatures and/or sportive driving styles PM/PN emissions of GDI vehicle are relatively higher. The new RDE test regime which can be carried out at low ambient temperatures (just above 0 °C, and an extended region to -7 °C) and the new PN limit value of 6.0 E¹¹ #/km are steps forward and this is expected to result in lower average real world PM emissions. A point of concern is the quality of trade fuel, with heavier HC-fractions the PM/PN emission increases. If the quality of PEMS PN analysers (especially at the lower ambient temperatures of -7 °C) can be improved the real world emissions may be further decreased. Currently European legislators pay a lot of attention to improve the vehicle emission legislation in which they also study the relevance of smaller particles (< 23 nm).

Diesel vehicles with DPF:

In Figure 1 and Figure 2 a potential big risk of high PM emission of Euro 5/6 diesel vehicles is shown. Diesel Particulate Filters in good condition have a PM filtration efficiency of more than 95% but in case of a big failure or DPF filter removal (as result of manipulation) the PM emission may increase very severely from approximately 1 to 25 - 100 mg/km.

Manipulation of DPFs is carried out by some service shops because users are faced with technical failures of the DPF. Failures happen during normal use of the vehicle, when the DPF cannot be (sufficiently) regenerated. This may be due to elevated engine out PM emissions (due to fuel injection system wear or higher oil consumption) or due to relatively slow driving during which yields too low exhaust temperatures to regenerate the soot. Consequently, the DPF gets clogged and due to the high back pressure in the exhaust the engine fails. Instead of a root-cause analysis and repair of the engine or a different user profile, one decides to remove the DPF. The manipulation consists of removal of the DPF and modification of the OBD-system which will need to be reprogrammed in order to mask the absence of the DPF. These manipulated vehicles can pass the PTI test because the OBD system does not yield an emission related failure code for the DPF and the smoke emission in the free acceleration test is below the PTI limit.

Manipulation of diesel vehicles (removal of DPF) is a real thread for air quality:

Diesel Particulate Filters are extremely effective and the PM/PN emissions of an engine are often typically reduced with more than 98%. Unfortunately this success is a threat because in case of failures of the relative sensitive DPF system, the DPF can be removed and consequently the PM/PN emissions of such a vehicle increase dramatically. It is known that some diesel vehicles in certain applications (rental fleets) meet severe problems with DPFs because the user driving profile is too soft. In order to avoid downtimes risks of certain vehicles (i.e. rental fleets), DPFs of new vehicles are removed. Currently removal of the DPF cannot be detected with a legal (PTI) test procedure. In order to be able to detect manipulation (DPF removal) at road side inspections dedicated test procedures must be developed.

The current PTI free acceleration smoke emission tests is not suitable to test for assessment the possible removal of a DPF in the PTI. A lack of sensitivity, the poor definition of the test procedure and the very weak relationship with PM and PN emissions are the most important reasons (2017).

PTI free acceleration smoke emission test for diesel vehicles is outdated.

The current PTI free acceleration smoke emission test was developed in the fifties of the previous century; The smoke emission is measured with an opacimeter. Meanwhile the smoke emissions of modern diesel vehicles with DPF became extremely low (near 0.00 m^{-1}). A modern diesel engine without DPF has a PTI smoke emission of 0.2 to 0.5 m^{-1} which is lower than the current PTI smoke emission limit value of 0.7 m^{-1} . Consequently a modern diesel engine can even pass the PTI test without a particulate filter. For these vehicles a new PTI emission test procedure must be developed which suits to the current emission levels and is able to detect somewhat larger DPF leakages.

Dedicated research of PTI emission tests of diesel vehicles with DPF (2013), (2015), (2016a), (2016b) (2016d) and (2017) has led to the development of an alternative PTI emission test procedure. This procedure contains three elements:

1. An emission test at low idle speed, suitable for the PTI test.
2. A PN concentration limit value that is expressed in particles per cm^3 ($\#/\text{cm}^3$)
3. A definition of a dedicated PTI PN-tester.

An example of a PTI PN emission test at low idle speed with a hot DPF is shown in Figure 4. At first four different PTI PN testers measured PN emissions (3.000 to $40.000 \#/\text{cm}^3$) of ambient air and after installation of all sample probes in the tail pipe (@ 460 s) of a warm vehicle with DPF within ten seconds all PN emissions decreased below $500 \#/\text{cm}^3$. This very low PN emission at low idle speed enables to detect very small DPF leakages which cannot be detected by smoke measurements in a free acceleration test. This simple PTI emission test at low idle speed only takes 10-20 seconds.

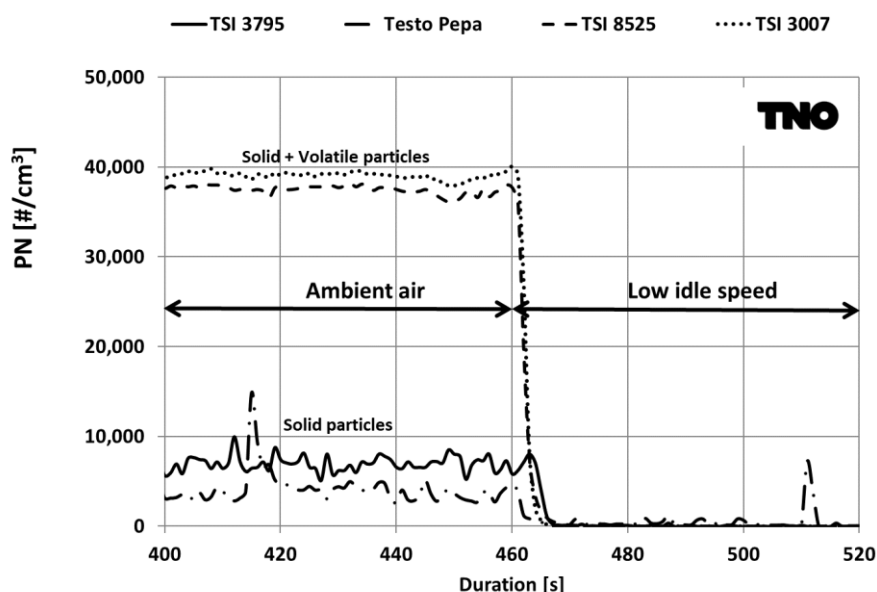


Figure 4: PN emissions measured with four different mobile PN-testers of ambient air and at low idle speed of a Peugeot 308 diesel Euro 6b with DPF @ 104,755 km.

Effectiveness of the current In Service Conformity protocol:

The current ISC protocol is not very effective in solving a problem with a substantial rate of faulty vehicles. The procedure is designed to fail a vehicle model if 40% or more develop problems. The malfunctioning should appear within 100,000 km and despite good maintenance and moderate use. If, for example only a 25% of the vehicles develop problems, there is virtually no need for improvement of maintenance procedure, or the replacement of a defective part from the perspective of the ISC protocol. Such problems have been observed with inferior DPFs.

The relationship of smoke emissions in PTI free acceleration tests and PN emissions at low idle speed was investigated; In Figure 5 the test results of more than 200 ex-lease diesel vehicles with DPF are depicted which clearly show a relative high sensitivity for the PN emission at low idle speed. Most vehicles with a hot DPF in good condition have a PN emission at low idle speed around 100 particles/cm³ (#/cm³) which is below the PN concentration of Dutch urban ambient air which is around 5000 #/cm³.

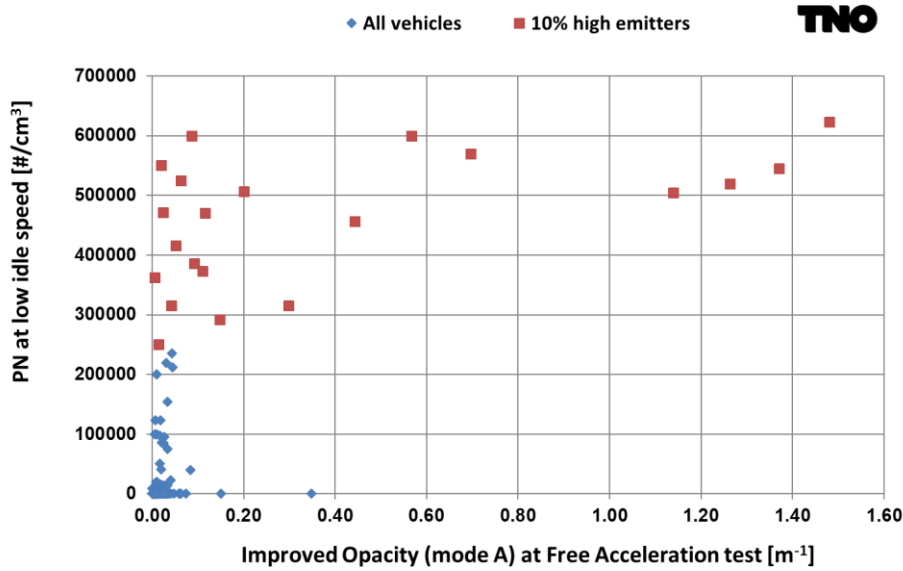


Figure 5: Relation between improved opacity (Mode A) in free acceleration tests and PN emission at low idle speed of 213 diesel vehicles with DPF.

To obtain a better understanding of the correlation of PTI-PN emissions and regulated PM&PN emissions, chassis dynamometer tests and PTI tests were carried out at three different vehicles with simulated DPF failures. The PTI PN-emission was determined with a TSI NPET, which measures solid particles in the particle size range of 23 to 1000 nm. In Figure 6 the relationship of PN emissions at low idle speed and PM/PN emissions in NEDC tests is shown; The PN emission at low idle speed correlates well with the PN emission in an NEDC test on the chassis dynamometer. Additional dedicated test programs with other vehicles with cracked DPF's in combination with prototypes of new PTI-PN testers are needed to develop a final PTI-PN test procedure.

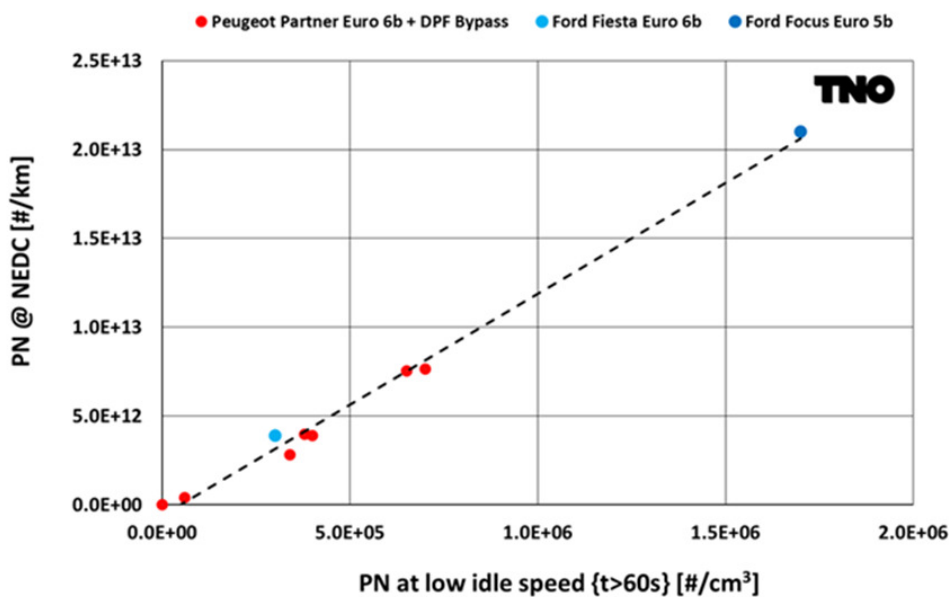


Figure 6: PN emissions at low idle speed and NEDC tests of 3 different diesel vehicles with (cracked) DPF or variable bypass.

Discussion

PM10 and EC fractions in ambient air and exhaust gas:

The ambient air contains particles from many different emission sources, including sand, dust, and sea salt. The particulates from vehicle exhaust are only a small fraction in the total particulate matter below a size of 10 micron (PM10), and a somewhat larger fraction of the PM2.5. Zooming in on the ambient concentration of specific components of PM10, in particular, EC or black carbon, a substantially higher fraction is directly related to tailpipe emissions from vehicles. For most diesel vehicle categories specific EC emissions have been determined in previous test programmes. Based on that, the relative contribution of particular vehicle categories to the ambient EC concentration could be established. The intention is that a complete picture for EC emissions of all road vehicles will be available for Dutch air-quality assessments. By adding specific information on EC emissions of GDI's, these GDI test results fills an important gap in the current understanding needed for the full assessment.

PM/PN emission risk assessment of vehicles:

In Table 5 the results of the assessment of the risks of increased PM emissions of road vehicles in different emission tests is summarized. From these results it is clear that PM emissions are well secured up to the in service conformity (ISC). Beyond the conditions of the in-service conformity test (> 100.000 km) there is a fair risk on elevated emissions and the (PTI) test procedures have insufficient performance to detect high emitters. Consequently, adequate test procedures are needed to secure the emission performance of in-use vehicles with modern aftertreatment systems with particulate filtration efficiencies of more than 90%. For PTI a relative simple test is needed, but in order to be able to prove manipulation (as a basis for legal procedures) a reasonably accurate test procedure must be developed. Currently, there is not a good view on the real-world performance of DPFs of trucks.

A draft PTI test procedure was developed for the detection of removed or broken DPF in a rather simple test procedure which constitutes of an idle test at which particle number concentrations are measured. The procedure is described in this paper and is meant to check for problems that concern (highly) elevated PM/PN emissions. However, the procedure doesn't cover the performance of the NOx aftertreatment systems (LNT or SCR). Due to the very specific NOx reduction technologies a dedicated PTI test procedure would be needed which can preferably also be performed at low idle speed. The potential increase of PM emissions of older petrol vehicles with GDI engines is expected to be moderate and can be well monitored in improved ISC test programmes. In case of GDI vehicles with a particulate filter (GPF) a dedicated PTI-PN test might be an option. For this specific PTI test of petrol vehicles the development of a dedicated PTI-PN tester which can handle exhaust gas with higher water concentrations seems to be needed.

Table 5: PM/PN emissions and risk of increased PM/PN emissions

Field	Emission level		Risk	
	Petrol	Petrol	Diesel	Diesel
Type approval	++	++	++	++
In Service Conformity	++	++	++	++
Real world emissions (RDE)	+	-	+	-
Durability	+/-	-	-	--
Periodic Technical Inspection	n.a.	n.a.	-	--
Road side inspections	n.a.	n.a.	-	-
Manipulation	-	+/-	--	--

++ very low risk, + low risk, +/- some risk, - reasonable risk, -- high risk

Currently there is still not a good view on the relationship of the specific toxic elements of PM and PN emissions of vehicles and human health. Specific ultrafine particulate emissions, often suggested to be the most toxic, could agglomerate quickly once emitted and could very well be not particularly harmful. From the available parameters such as particles sizes, PM10, PM2.5, PM0.1, particle concentrations, organic carbon (OC), elemental carbon (EC), polycyclic aromatic hydrocarbons, metals, and black smoke, the impact on specific diseases is basically unknown. In order to improve this research the specific relationships of specific elements/actors and human health should be investigated.

Conclusions

Particulate emissions of diesel vehicles

- According to the type approval tests PM and PN emissions of Euro 6 diesel vehicles, all equipped with wall flow DPF, are very low. PM emissions are similar to petrol vehicles. PN emissions of diesel engines are about tenfold lower than those of petrol vehicles which reflects the tenfold lower PN emission limit for diesel engines: 6×10^{11} #/km versus the (temporarily) limit of 6×10^{12} #/km for petrol vehicles.
- With diesel engines there appears to be a large risk of PM and PN increase during the life time of the vehicle due to DPF removal and failures. This might contribute to a 25 to 100 fold increase in PM and PN emission.

Particulate emissions of GDI petrol vehicles:

Three tested Euro 5/6 GDI's, which are common makes and models with odometer readings from 10,000 to 32,000 km, showed the following particulate emissions:

- Fairly low PM₁₀ emissions in the range of 0.1 to 6.1 mg/km. The total average PM emission of the three vehicles is 1.4 mg/km and this can be split in urban (2.8 mg/km), rural (0.3 mg/km) and motorway (1.2 mg/km) parts. In general the emissions are consistent with the type approval emission limits of 5.0 mg/km. Deviations can be explained by the more severe test conditions in this test programme, compared to the type-approval test, and multiple inclusion of cold starts.
- Particulate Number (PN) emissions are close to the current emission limit value of 6×10^{12} #/km. When the type-approval limit for GDI vehicles will be lowered to 6×10^{11} #/km – as of 1 September 2017 for new models – it is expected that the real-world particulate number emissions will decrease accordingly. Only if GPF particulate filters will be the common technology for GDI's, real-world particulate number emissions might be substantially lower than the limit values, as is already the case for diesel vehicles equipped with particulate filters.
- The fraction of elemental carbon (EC) in the PM₁₀ emissions of GDI vehicles is higher than for other petrol vehicles. Given the low absolute PM₁₀ emission levels, combined with upcoming RDE legislation and the change of the PN emission limit from 6×10^{12} to 6×10^{11} #/km in the type-approval tests there is no specific concern regarding EC emissions of GDI's.

The risks of elevated PM&PN emissions of petrol vehicles are judged much lower than for diesel vehicles. Possible elevated particulate emissions are mainly related to the fuel injection and the combustion of the engine as well as increased lubricant consumption. Given the growing group of vehicles with GDI, specific attention for the emissions of these vehicles is justified. There are suggestions that some of these vehicles have significantly higher PM and PN emissions in normal use than other petrol vehicles.

Monitoring of vehicle PM&PN emissions over their lifetime:

Better monitoring of PM and PN emissions of diesel and possibly also petrol vehicles seems necessary. This would need to include the following elements:

- Increase of the In Service Conformity (ISC) requirements above the current 100,000 km. A life time of up to 250,000 km seems more appropriate, especially for diesel engines.
- Introduction of a sufficiently accurate but simple test for the Period Technical Inspection (PTI), especially for diesel cars.

The combination of these elements is essential in addressing the different responsibilities in securing reasonable emissions during the life time of vehicles.

Improved PTI test procedure for diesel vehicles with DPF:

The current PTI smoke emission test procedure for diesel vehicles is outdated because the sensitivity of the opacimeter is too low; small and normal DPF failures and even a removed DPF cannot be detected. An improved PTI test procedure with relatively simple PN-test test equipment was investigated in cooperation with equipment manufacturers. A simple test performed at low idle speed with an appropriate PN limit value (i.e. 250.000 #/cm³) seems to be a good candidate to detect removed or broken DPFs. The PN emission at low idle speed has a good correlation with the regulated PN emissions in NEDC tests, although more tests are recommended to support this.

Current mobile PN-testers are accurate but too expensive for PTI workshops. A new draft specification for a simplified low cost PTI-PN-tester for diesel vehicles is proposed (Kadijk, 2017). After standardization of this new PTI-PN-tester a final PTI test procedure can be built and implemented in UNECE R83 or WLTP regulations.

Acknowledgments

This work is part of the in-use compliance program of light-duty vehicles, which is financed since 1987 by the Dutch Ministry of Infrastructure and The Environment (I&M).

References

- Kadijk G. (2013), Roadworthiness Test Investigations of Diesel Particulate Filters, *TNO report 2013 R10160 v3 (30p)*.
- Kadijk G., Spreen J.S. (2015), Roadworthiness Test Investigations of Diesel Particulate Filters on vehicles, *TNO report 2015 R10307 v2 (23p)*.
- Kadijk G., Spreen J.S., van der Mark P.J. (2016a), Investigation into a Periodic Technical Inspection test method to check for presence and proper functioning of Diesel Particulate Filters in light-duty diesel vehicles, *TNO report 2016 R10735v2 (60 p)*.
- Kadijk G., Spreen J.S., van der Mark P.J. (2016b), Diesel Particulate Filters for light-duty diesel vehicles: Operation, Maintenance, Repair and Inspection, *TNO report 2016 R10958 (19 p)*.
- Kadijk G., Elstgeest M., Ligterink N.E., van der Mark P.J. (2017), Investigation into a Periodic Technical Inspection test method to check for presence and proper functioning of Diesel Particulate Filters in light-duty diesel vehicles-part 2, *TNO report TNO 2017 R10530 (85 p)*.
- Ligterink N.E. (2016), Emissions of three common GDI vehicles, *TNO report 2016 R11247 (17 p)*.
- Spreen J.S., Kadijk G., Vermeulen R.J., Heijne V.A.M., Ligterink N.E., Stelwagen U., Smokers R.T.M., van der Mark P.J., Geilenkirchen G. (PBL) (2016), Assessment of road vehicle emissions: methodology of the Dutch in-service testing programme, *TNO report 2016 R11178 (86 p)*.

Emission of PM10 and coarse particles from “silent” asphalt

M. Norman^{1*} and C. Johansson^{1,2}

¹Environment and Health Administration, SLB, Stockholm, Sweden, michael.norman@slb.nu

²Department of Environmental Science and Analytical Chemistry, Stockholm University, Stockholm, Sweden

Introduction

Particle emissions from road traffic has since long been connected to adverse health effects (WHO, 2005). However most regulations and measures has been associated with the tail-pipe emissions. Non-exhaust emissions of particulate matter (PM) from road traffic are in addition a significant air pollution problem (van der Gon et al., 2013; Amato et al., 2014). In many areas, and especially in Scandinavian countries, are the non-exhaust particles more important to PM pollution in terms of particle mass (Norman and Johansson 2006). A large part of the non-exhaust PM emissions in Scandinavian countries are associated with road wear from studded winter tyres or winter sanding (Gustafsson et al., 2009). Direct emissions from the interaction between tyre and road occurs during dry road conditions, but some parts are also accumulated during the wet winter season and are then later suspended into the air in spring when the road surface get dry (Denby et al., 2013). This road dust has also been connected to adverse negative health effects in Stockholm (Meister et al., 2012).

Several measures in order to reduce the production and emission of road dust have been tested in Scandinavian cities including studded tyre ban and speed regulation (Norman et al., 2016), intensive cleaning activities (Gustafsson et al., 2017) and dust binding (Denby et al., 2017).

Road traffic is also the cause for high noise levels close to major roads and highways, especially close to high speed roads (Morley et al., 2015). In Scandinavia are usually hard pavements used in order to resist the wear from the studded winter tyres. These pavements are contributing to higher noise levels than softer pavements. One measure to reduce the noise levels is therefore to change the pavement type. Tests have shown a significant reduction in noise levels when changing the pavements. However any change in the pavement characteristic might also change the emission of particles as has been shown in laboratory tests (Gustafsson et al., 2009). It is therefore important to test how any change to silent asphalt might affect the particle emissions from roads in real world conditions.

Measurements

The highway E4 north of Stockholm is the major road between Stockholm and Arlanda airport and Uppsala. It is one of Sweden’s most busy road and is almost straight in north-south direction. A “silent” asphalt called ABD11 was placed along a 1.4 km long stretch of the highway E4 in summer of 2014 (Figure 1). A reference asphalt ABD16 is used along other parts of E4. There was observed a significant decrease with 7 db in the noise level at the silent asphalt when it was new (Jacobson and Göransson 2017). After two years the noise reduction was still 6 db.

A measurement station called Rotsunda was placed along the silent asphalt including PM10, PM2.5 (GRIMM EDM 180), NOx (PALGO Environment AC32M) and meteorology. At the same time was another measurement station (Häggvik) placed along a reference asphalt stretch. Both stations were placed on the eastern side of the road and 4 m from the edge of the road. Road surface conditions (VAISALA DSC111) were also measuring on E4 but at another location closer to Stockholm. All three sites are shown in figure 1. Measurements were performed during Feb-May (4 months) in 2015, 2016 and 2017. The measurements will continue until 2019 (total 5 spring seasons of measurements). The period during the year was chosen because during those months are the highest levels of PM10 measured in the Stockholm area (Norman and Johansson 2006; Norman et al., 2016).

Detailed traffic information was available nearby both air quality sites.

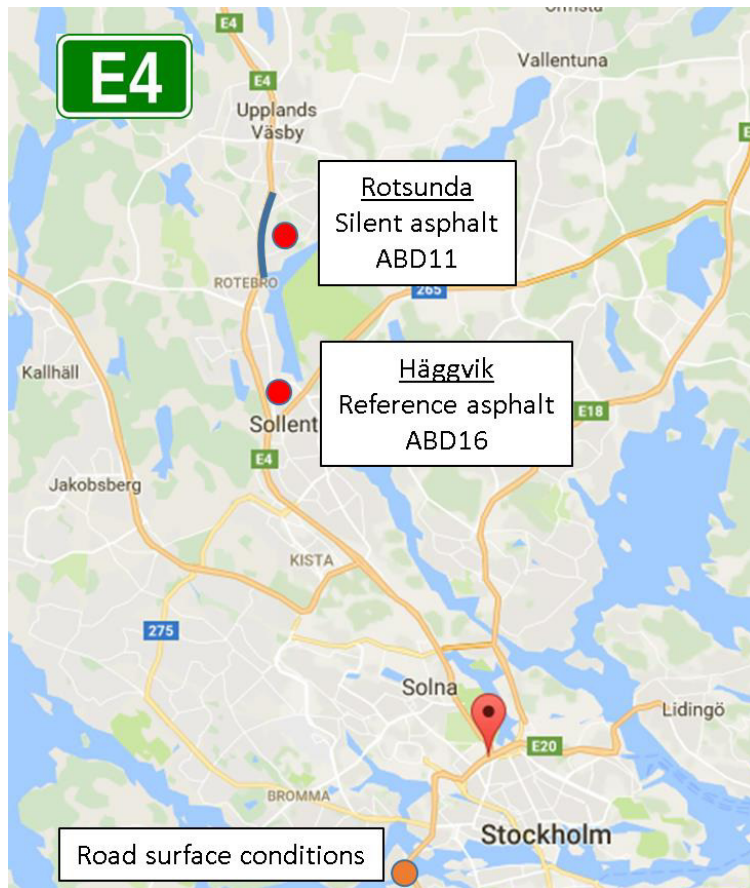


Figure 1: Map showing the location of the stretch with silent asphalt, location of the two air quality stations and the road surface sensor. Map from Google.

Traffic

Results from the traffic measurements are shown in table 1 for 2016 and 2017. No traffic counts were done in 2015. The difference between the two sites (higher at the reference asphalt) is explained by a relatively large road that is situated between the stations diverting traffic towards the west. The signed speed is 110 km/h at the silent asphalt (Rotsunda) and 90 km/h at the reference asphalt (Häggvik) from Feb until middle of April and then 110 km/h. Both the traffic number and the heavy duty vehicle (HDV) share increased slightly from 2016 to 2017 at both sites.

Table 1: Traffic measurements during Feb-May 2016 and 2017.

		Vehicles /day	Vehicles /day (weekdays)	Speed km/h	HDV share
2016	Silent asphalt (Rotsunda)	86400	96000	108	4.3 %
2016	Refernce asphalt (Häggvik)	90000	100000	102	3.1 %
2017	Silent asphalt (Rotsunda)	90100	97800	107	4.6 %
2017	Refernce asphalt (Häggvik)	92900	101200	102	3.9 %

NO_x emission factors

Emission factors for NO_x were calculated for both sites based on HBEFA 3.2 (<http://www.hbefa.net/e/index.html>). The emission factors were based on vehicle speed and vehicle composition. They were also adjusted for the 2% slope on the highway E4 at the Rotsunda site.

Table 2: Calculated NO_x emission factors using HBEFA 3.2.

NO _x EF g / (veh km)	2016	2017
Silent asphalt (Rotsunda)	0,61	0,61
Reference asphalt (Häggvik)	0,50	0,52

The major reason for the difference in NO_x emission factor between the two sites is the 2% slope at the Rotsunda site. The difference in HDV share also contributed while the differences in speed had very little influence.

Influence from wind direction

The influence from the wind direction on the observed NO_x levels at the Rotsunda site was analysed and are presented in figure 2. Since we are interested in the changes in the emissions from the road we only use data for wind directions between 200 and 340 degrees.

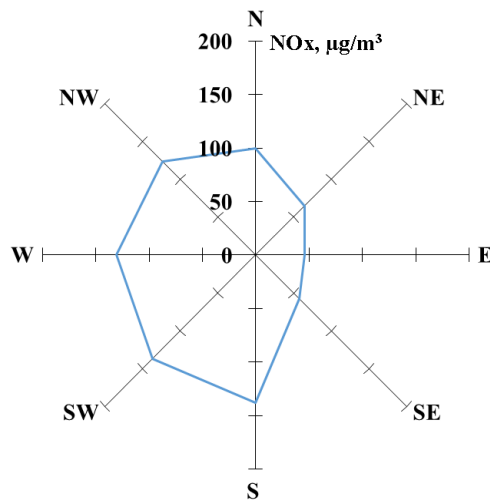


Figure 2: The average NO_x concentration for different wind directions at the Rotsunda site. Only daytime (07:00 – 19:00) is included in the analysis.

Results

Road surface conditions

The emission of road dust from road wear is strongly dependent on the road surface wetness and especially in Scandinavia where the road dust contribution to PM₁₀ might be very large (Norman and Johansson 2006; Denby et al., 2013). The measured road surface condition at E4 is presented in figure 3 for Feb-May 2017. During February and beginning of March the road was mostly wet or moist. A snowfall around the 7th of March created a longer period with wet and snowy surface. From 11th of March was the road more or less dry until the end of May, but moist condition occurred periodically.

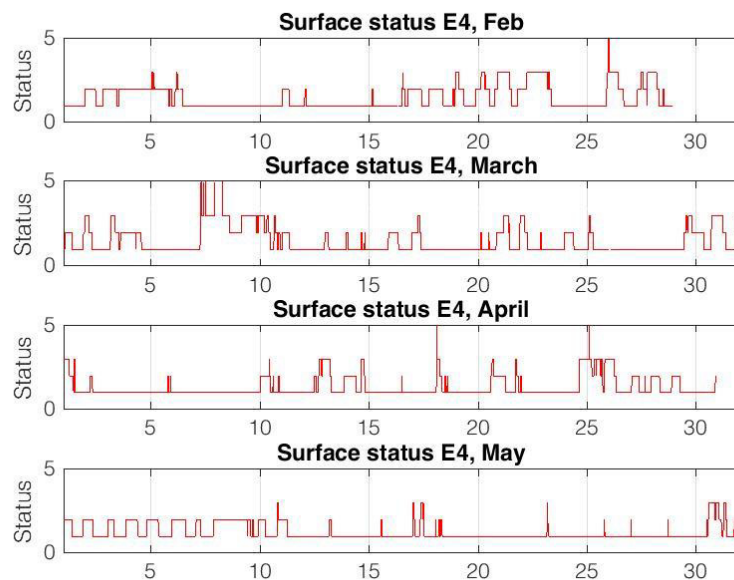


Figure 3: Measured road surface conditions at E4 during Feb-May 2017. 1=dry, 2=moist, 3=wet, 5= snow.

Results

Air quality

PM10, PM2.5 and NO_x concentrations for 2017 are presented in figures 4, 5 and 6, respectively. The concentrations exhibit large variations, but with close correlations between the two sites. The PM10 is largely influenced by the road conditions (figure 3) and high PM10 concentration occur only during periods with dry road surface. This is in line with several previous studies in Stockholm (Norman and Johansson 2006; Denby et al., 2013; Norman et al., 2016). During dry periods were the PM10 concentration in general slightly higher at the silent asphalt compared to the reference site.

The PM2.5 concentrations (figure 5) show much less variation in concentration but also less difference between the two sites (table 2). Observed PM2.5 is to a large extent connected to long range transported particles in Scandinavia. A small part of the road dust emissions is also included in PM2.5 which can be observed with slightly higher PM2.5 concentrations during periods with dry road surface (figure 3), which in turn occurs at the same time as high PM10 concentrations (figure 4).

The observed NO_x concentrations (figure 6) is not affected by the road surface conditions and show a smaller variation than for PM10. The concentrations at the two sites are closely correlated but often concentrations are higher at the silent asphalt compared to the reference site, table 2. The 2% slope on the road at the silent asphalt has large influence on the NO_x emissions and is probably the major reason for the observed difference.

Table 3: Average concentrations 18th Feb – 30 May 2017 at the two sites.

Average concentration µg/m³	PM10	PM2.5	NO_x
Silent asphalt (Rotsunda)	31.6	6.5	90.4
Reference asphalt (Häggvik)	23.6	5.2	65.8

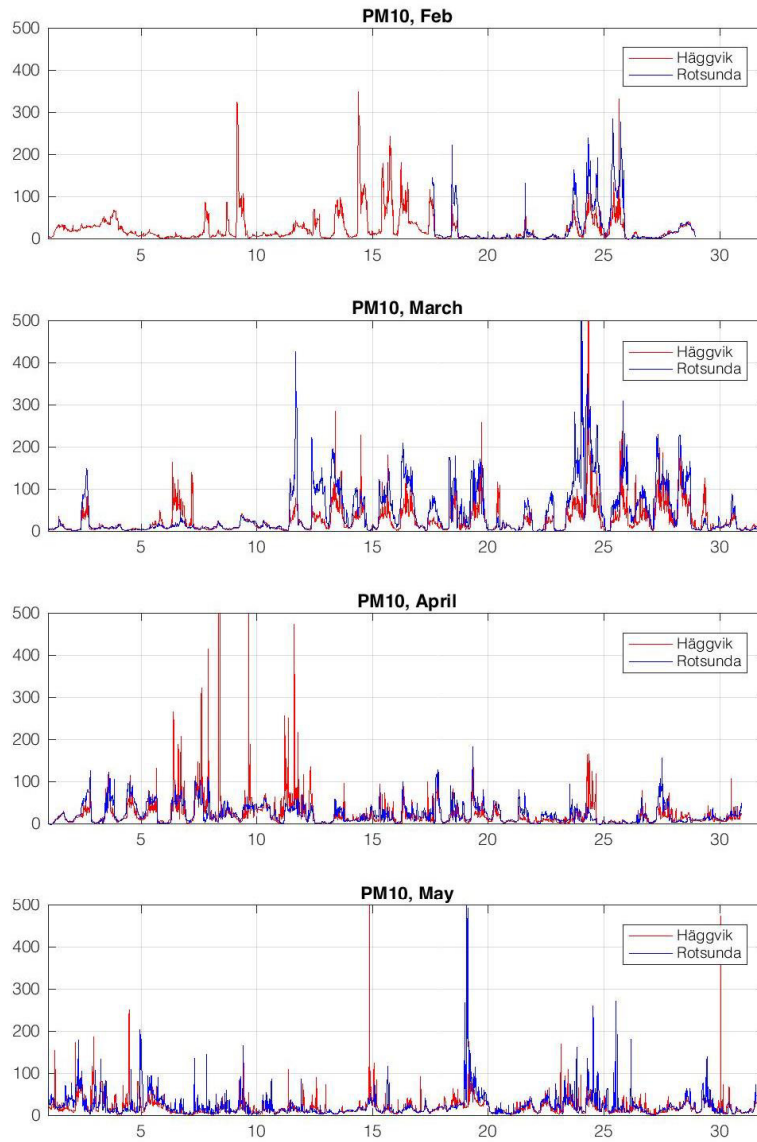


Figure 4: Measured PM10 concentrations during Feb to May 2017. The silent asphalt was placed at Rotsunda and the reference asphalt at Häggvik.

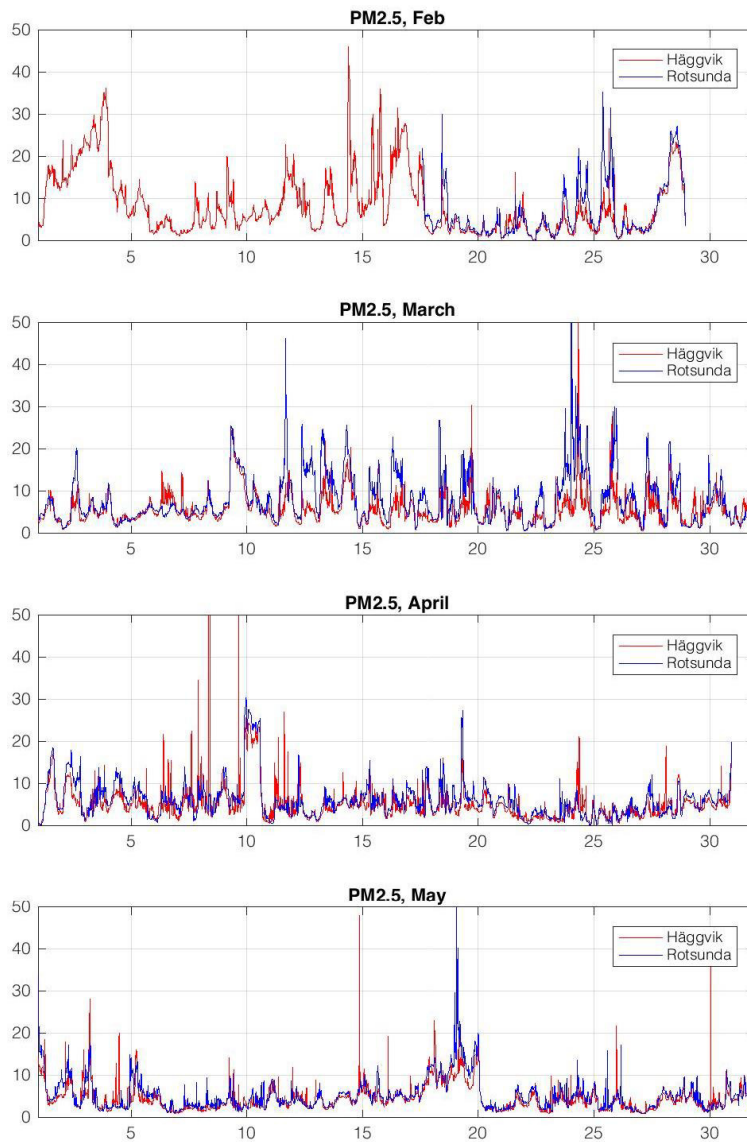


Figure 5: Measured PM2.5 concentrations during Feb to May 2017. The silent asphalt was placed at Rotsunda and the reference asphalt at Häggvik.

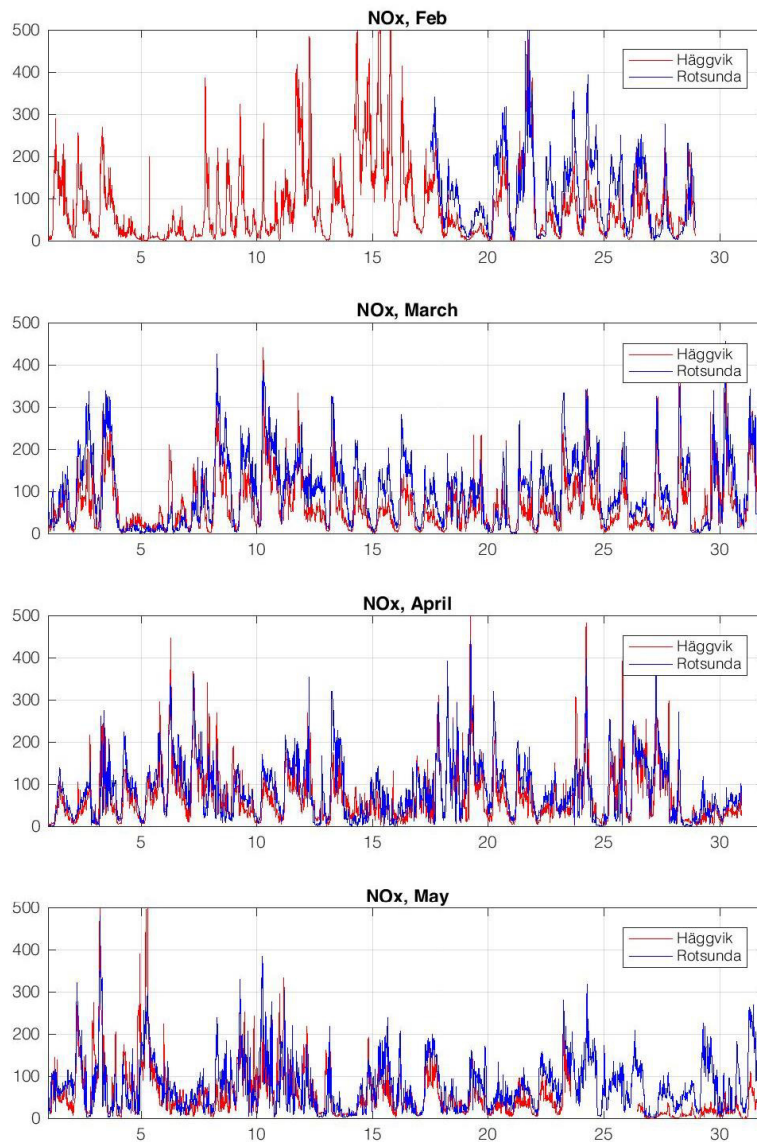


Figure 6: Measured NO_x concentrations during Feb to May 2017. The silent asphalt was placed at Rotsunda and the reference asphalt at Häggvik.

Emission of coarse particles from different asphalts

As expected, highest coarse particle concentrations occurred during daytime (figure 4) with wind direction from the road (figure 2) and during dry road conditions (figure 3 and figure 4). Therefore the analysis included only data between 07:00 and 19:00, only periods with wind directions between 200 and 340 degrees and dry road surface conditions.

Comparison of the emission of coarse particles (PM₁₀-PM_{2.5}) from the asphalt were done by comparing the PM_{coarse}/NO_x ratio between the two sites. The measured NO_x levels were adjusted according to differences in emission factor between the sites based on the emission factors presented in table 2 and also adjusted for the difference in traffic flow between the two sites, table 1. Identical calculation were performed on the measured data from 2015, 2016 and 2017 respectively. The analysis were further done by comparing the ratio between the silent asphalt (Rotsunda) and the reference asphalt (Häggvik). By measuring NO_x and compare it with the emissions of NO_x we get information about the dilution of the pollutant from the road to the measurement site. This is based on a theory how to determine PM emission factors used in mays studies, but for example presented in Ketznel et al. (2007). Shortly the particle emission factor at a site can be calculated using equation (1).

$$\text{Eq (1)} \quad EF_{PM_{coarse}} = EF_{NOx} \frac{PM_{coarse}}{NOx}$$

If we are interested in the ratio between the emissions between the test and the reference site we instead use equation (2).

$$\text{Eq (2)} \quad \frac{EF_{PM_{coarse}}(\text{silent})}{EF_{PM_{coarse}}(\text{reference})} = EF_{NOx} \frac{PM_{coarse}}{NOx}(\text{silent}) / EF_{NOx} \frac{PM_{coarse}}{NOx}(\text{reference})$$

Equation 2 will then give the ratio between the emissions of coarse particles at the two sites.

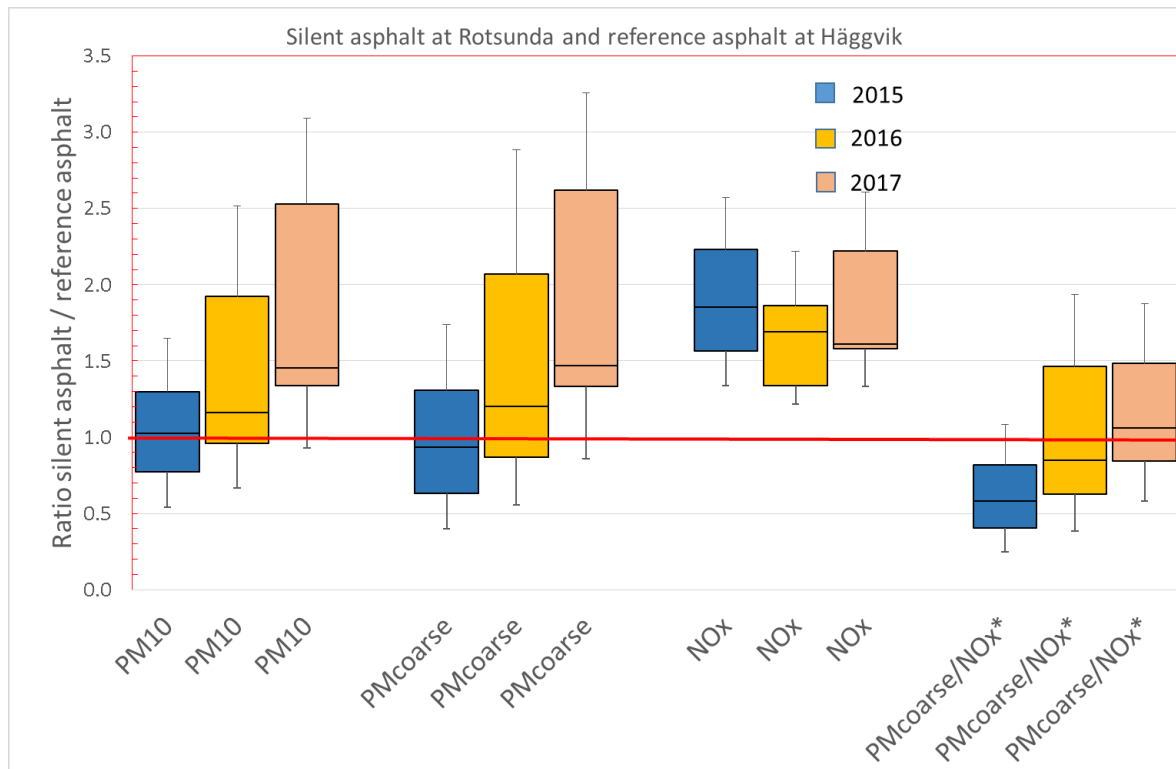


Figure 7. The ratio between measured pollutant at the silent asphalt and the reference site. The black line is the median, the coloured box the 25th and 75th percentile and the vertical bars the 10th and 90th percentile. The NOx* concentrations are adjusted according different NOx emission factors at the two sites.

During the first season (spring 2015) was the PM10 levels (and PMcoarse) about equal at the two sites while the NOx levels were higher at the silent asphalt site (figure 7). The PMcoarse/NOx ratio between the sites indicate that the emission of coarse particles were about 40 % lower at the silent asphalt compared to the reference.

During both the second and the third season (spring 2016 and 2017) was the PM10 levels (and PMcoarse) higher at the silent asphalt site compared to the reference site. At the same time was the NOx levels still higher at the silent asphalt site, but the median ratio was slightly smaller than for the first season. This means that in comparison to the reference site higher PM10 (and PMcoarse) but almost the same NOx levels was measured at the silent asphalt during the second and third season, although the traffic was almost constant between the years. The estimated emissions of coarse particles (eq. 2) were about 15 % lower at the silent asphalt compared to the reference asphalt during 2016, but about 5 % higher during 2017.

This indicates that the emission of coarse particles from the silent asphalt increased significantly from the first to the second season and third season.

Discussion

This study showed that the emission of coarse particles at the silent asphalt was about 40 % lower compared to the reference site the first season. However for both the following seasons has the emission of coarse particles from the silent asphalt increased. During the third season, the emission was even about 5 % higher at the silent asphalt compared to the reference site.

This study uses theoretical emission factors from HBEFA 3.2 for NO_x. There is known to be a discrepancy between the real world emissions factors for NO_x and the ones found in HBEFA. But since the use of HBEFA is the same for all three seasons the increasing trend should be reliable.

A study in Copenhagen by Nordstroem et al., (2010) showed a 15 % decrease in PM₁₀ concentration when a new asphalt was in place although it was the same type as before. The results in this study cannot explicitly tell if the lower emission during the first year was due to the fact that the pavement is new or due to the different characteristics of the silent asphalt compared to the reference.

There exist some potential causes for the increase in emissions in the second and third seasons. The pavement structure in the silent asphalt contains more pores than the reference asphalt. One reason could be that the cleaning has been insufficient and that the surface therefore has collected more particles that in spring are available for resuspension. Another potential cause is that the surface structure of the silent asphalt has changed due to the traffic (worn and compacted), which might have increased the particle emissions.

The continuation of the project for two more seasons will tell if the emissions of non-exhaust particles will continue to increase from the silent asphalt. This information will be important for further use of silent pavements in Sweden.

Conclusions

On a 1.4 km long stretch on the highway E4 north of Stockholm was silent asphalt of type ABD11 placed in 2014. A measuring campaign has been ongoing close to this stretch for three spring seasons (Feb – May) in 2015, 2016 and 2016, and during the same period measurements were made alongside a reference pavement with ABS16. Detailed traffic counts were performed at both sites. Only small differences in traffic were observed between the years.

The concentrations at the two sites showed very high correlations indicating that both stations are similarly affected by particle emissions from the roads when the wind direction blows from the road. The sites were well suited for the experiment.

It was found that the emission of coarse particles from the silent asphalt was about 40 % lower than the reference asphalt the first year. During the second season the emission of coarse particles from the silent asphalt was about 15 % lower than the reference and during the third season it was around 5 % higher than the reference site. The results strongly indicate that emission of coarse particles from the silent asphalt has increased significantly during the three measured seasons.

The continuation of the project for two more seasons will tell if the emissions of non-exhaust particles will continue to increase from the silent asphalt.

Aknowledgements

This work was supported by the Swedish Road administration (Trafikverket, Region Stockholm).

References

- Amato F, Cassee FR, Denier van der Gon HAC, Gehrig R, Gustafsson M, Hafner W, Harrison RM, Jozwicka M, Kelly FJ, Moreno T, Prevot ASH, Schaap M, Sunyer J, Querol X. (2014). Urban air quality: The challenge of traffic non-exhaust emissions. *Journal of Hazardous Materials*; 275: 31-36
- Denby, B.R., Sundvor, I., Johansson, C., Pirjola, L., Ketzel, M., Norman, M., Kupiainen, K., Gustafsson, M., Blomqvist, G., Kauhaniemi, M. and Omstedt, G. (2013). A coupled road dust and surface moisture model to predict non-exhaust road traffic induced particle emissions (NORTRIP). Part 2: surface moisture and salt impact modelling. *Atmos. Environ.*, 81, 485-503. DOI: <http://dx.doi.org/10.1016/j.atmosenv.2013.09.003>
- van der Gon, Denier, H.; Gerlofs-Nijland, M.E.; Gehrig, R., Gustafsson, M.; Janssen, N.; Harrison, R.M.; Hulskotte, J.; Johansson, C.; Jozwicka, M.; Keuken, M.; Krijgsheld, K.; Ntziachristos, L.; Riediker, M.; Cassee, F.R., (2013). The Policy Relevance of Wear Emissions from Road Transport, Now and in the Future - An International Workshop Report and Consensus Statement. *J Air Waste Manag Assoc.*, 63, 136-149, 2013.
- Gustafsson, M., Blomqvist, G., Gudmundsson, A., Dahl, A., Jonsson, P., Swietlicki, E., (2008). Factors affecting PM10 emissions from road pavement wear. *Atmos. Environ.*, 43, 4699-4702
- Gustafsson, M., G. Blomqvist, S. Janhäll, C. Johansson and M. Norman (2014). Operational measures against PM10 pollution in Stockholm – evaluation of winter season 2015–2016. *VTI report 928* (In Swedish). <https://www.diva-portal.org/smash/get/diva2:1111887/FULLTEXT01.pdf>
- Jacobsson, T., and Göransson, N-G., (2017). Pavement for noise reduction. E4, Rotebro – Bredden, 2014-2017. (In Swedish), TRV Dnr: 2014/44543, VTI Dnr: 2014/0431
- Meister, K., Forsberg, B., and Johansson, C., (2012). Estimated short time effects of coarse particles on daily mortality in Stockholm Sweden. *Environmental health Perspectives*, 120, No 3, pp 431-436.
- Morley, D.W., de Hoogh, K., Fehcht, D., Fabbri, F., Bell, M., Goodman, P.S., Elliott, P., Hodgson, S., Hansell, A., Gulliver, J., (2015). International scale implementation of the CNOSSOS-EU road traffic noise prediction model for epidemiological studies. *Environmental Pollution*, 206, 332-341.
- Nordstroem, C., Ellermann, T., and Ketzel, M., (2010). The effect on PM10 of a new road pavement on a heavily trafficked road, H.C.A. Boulevard (HCAB), Copenhagen, Denmark. Poster at the Road dust – Health effects and abatement strategies, Stockholm 2010. <http://gpc.slb.nu/register/wp-content/uploads/2010/10/PosterPM10newroadpavement.pdf>
- Norman, M., I. Sundvor, B.R. Denby, C. Johansson, M. Gustafsson, G. Blomqvist, S. Janhäll, (2016) Modelling road dust emission abatement measures using the NORTRIP model: Vehicle speed and studded tyre reduction, *Atmos. Environ.*, Volume 134, June 2016, Pages 96-108, ISSN 1352-2310, <http://dx.doi.org/10.1016/j.atmosenv.2016.03.035>.
- Norman M., Johansson C. (2006). Studies of some measures to reduce road dust emissions from paved roads in Scandinavia. *Atmos. Environ.*, 40, 6154-6164.
- WHO, (2005). Health effects of transport-related air pollution. Edited by Michal Krzyzanowski, Birgit Kuna-Dibbert and Jürgen Schneider. WHO Regional Office for Europe. ISBN 92 890 1373 7.
- Ketzel, M., Omstedt, G., Johansson, C., Düring, I., Pohojola, M., Oettl, D., Gidhagen, L., Wählin, P., Lohmeyer, A., Haakana, M., Berkowicz, R. 2007. Estimation and validation of PM2.5/PM10 exhaust and non-exhaust emission factors for practical street pollution modelling. *Atmos. Environ.* 41 9370-9385.

Algebraic and geometric aspects of traffic control models on complex networks

A.P. Buslaev^{1}, Kuchelev D.A.² and M.V. Yashina²*

¹Department of Mathematics, Moscow Automobile and Road State Technical University, Moscow, 125319, Russia, apal2006@yandex.ru

²Department of Mathematical Cybernetics and IT, Moscow Technical University of Communications and Informatics, 111024, Russia

1. Introduction. Traffic and air pollution problems in Moscow megacity

Most of environmental problems are largely related to the road network structure and the critical traffic functioning in saturated mode. In megacities, (Lukanin et al, Part I and II, 2003). At the same time, technological achievements in road construction engineering and automotive industry make it possible to expand and develop the road infrastructure and, simultaneously, increase the load on street - road network.

The problem is how to predict the behaviour of saturated flows on complex networks? How to take into account the cumulative effects of local traffic difficulties on network in whole? How to control traffic flows on the network in general? At current moment the traffic flow theory can't answer all of these questions.

2. Big Data and problems of adequate models development

Modern natural-scientific studies are with revolutionary changes in information and communication technologies (ICT). So, it provides a higher level of actual tests and experimental data. Therefore, most of relevant modern applied natural-scientific researchers have access to a qualitatively different level of full-scale tests and experimental data.

A large number of observable information – BigData - makes it possible to assume higher standards for information processing and quality of developing models. The amount of data, as a rule, grows exponentially depending on the dimension. It is necessary to be able to find basic parameters that determine a system dynamics.

The relevance of traffic models creation is not exclusive. Problems of flows modelling on complex networks are also widely used in other areas of study, such as material science for design of new materials, (Kotani and Ikeda, 2016), study of biological processes (metabolism), (Wagner and Fell, 2004),, medicine for the study of new drugs, in computing (supercomputers), quantum computers, etc. In traffic modelling the traditional infinitesimal approach in the form of hydrodynamic models on networks leads to numerical schemes and simulations calculations. But it does not allow to have a priori analysis of system behaviour, to evaluate the quality of projects and to obtain a behaviour forecast.

3. Dynamical systems on networks, cellular automata and traffic modeling

We consider a discrete graph consisting of cells and connections between neighbors and agents (particles) moving on this graph according to a given plan and according to a discrete chronometer. The characteristic properties of the dynamical system are

- a) rules for moving in accordance with the standard classification of cellular automata, (Wolfram, 1983);
- b) the principle of a small-sized cell; the discretization is such that there are not more than one particle in one cell;
- c) special rules for the movement of particle flows at nodes when competition takes place.

The behaviour of such systems has been poorly studied. Exact a priori results are available only for simple contours (Blank, 2000, Gray and Griffeth, 2001). Most of the papers in this area have experimental results presenting the model formulation and exclusive calculating. As

network models have large dimension, and it necessary needs exponential number of computation, but it is impossible next future.

In our work we consider *networks from contours with arbitrary links*. The subject of the study are *traffic delays depending on the network load, traffic rules on the contours and rules for competition resolving at nodes*.

We considere as deterministic rules of competition resolution, as the probability rules. In the case of deterministic rules the priorities of particles participating in the competition are one-to-one correspondent identified. An example of a probability rule is a *fair rule*, in accordance with which all the particles win the competition with equally probability.

Thus, *depending on system architecture, we initially have either a dynamical system with totally deterministic rules, or a Markov process*. Stationary states of the systems are studied, in particular, *steady fields of competitions, the reachability of free movement, self-organization and stop of the system*.

4. Qualitative properties of dynamical traffic-systems

4.1. The spectrum of nonlinear systems

In the paper (Biham et al., 1992), *a cellular automaton on Manhattan grid spanned by a torus* has been considered. There are two types of particles in the model. Particles of the first type move along the meridians, the second type particles move along the parallels of the torus. For this model, *for the first time, the self-organization effect of the system is obtained*, and as well as the conditions have been found when the system can reach the stop state. Thus, the authors of (Biham et al., 1992) *laid down the foundation of the spectral theory for considered systems*.

4.2. Regular networks

We develop flow models on more general periodic symmetric structures, (Kozlov et al., 2015).. The constructions of dynamical systems - *Necklace, Honeycombs, Chainmail*, etc., have been introduced. The class of dynamical systems with *isolated movement* has been determined and investigated. In these system, each particle of flows moves in a certain direction with fixed probability and in accordance with given rules. The ratio between the number of particles and the number cells of the network is called *system density (load)*. The qualitative behaviour of dynamical system is described by *state function, i.e. the dependence of average system velocity on density*.

4.3. Abstract dial as a model of complete graph

A variant of the general algebraic formulation of the problem for the complete graph on an *N-dial* is considered. Plans for moving particles on such a graph are given by representation of a real number in *N-ary* positional system. The results characterizing the qualitative behaviour of the system are obtained. Approaches for estimating the velocity of plan implementation for moving particles and the intensity of the flow have been found. Various generalizations of the considered posed problems are formulated. Interconnections of given logistical problems of flows on networks with classical directions of mathematics have been obtained, in particular, with *diophantine equations*, (Buslaev et al, 2015).

4.4. Local flows on regular networks

Suppose that at the nodes of connecting contours the control is organized by fair rule of competition resolution. The computer simulation calculations present the following results.

Then it is hold that if the particle flow density (the ratio of the number of particles to the number of cells) is less than $1/k$, where k is the number of contour neighbours, then self-organization of a wide class of the system happens in a finite time and at some point the system has free movement.

The effect of *phase transition* has been found and the boundary of the phase transition is studied. For a density $\rho = 1/k$, the velocity of particles in a steady state depends on the initial state of the system, and in the case of a stochastic rule of competition resolution, the movement velocity can obtain different values with positive probabilities.

4.4. A posteriori results of computer experiments

Computer simulations have been executed on 10000 experiments on dynamical systems on closed Necklace with different values on counters numbers. Following typical properties of the considered systems are obtained.

(1) The behaviour of a deterministic-stochastic system becomes completely determined after a time interval with a finite mathematical expectation, although the time to reach the transition point in the deterministic behaviour can be arbitrarily large with a positive probability.

2) The considered dynamical system is a Markov chain, the set of states of which in the general case is divided into classes of communicating essential states and the set of nonessential states. The velocity of the particles depends on *in which class of essential states the Markov chain is located or is in initial position. States of collapse correspond to absorbing states of Markov chain.*

5. Traffic-model of a phase transition on a closed chain: Following-the-Leader model (FL), clusters and phase transitions

5.1. Nonlinear system of ODE

The generalized FL-model describes the cars movement in one direction way and one after another (the chain) without overtaking. This model reduces to the study of a nonlinear system of ordinary differential equations (ODE) of the following type

$$x_{n+1} - x_n = f(\dot{x}_n), \quad (1)$$

where $x_n(t)$ is the coordinate of n -th vehicle, the function $f(x)$ is monotonically increasing and $f(0) > 0$, with phase constraints on velocities and coordinates

$$x_n(t) < x_{n+1}(t), n = 1, 2, \dots \quad (2)$$

If flow satisfies the conditions (1) - (2), then it is called totally connected movement.

The basic concept in the FL model is *dynamic dimension*, i.e. the distance from the bumper of the i -th car to the bumper of behind driving $(i-1)$ -th car.

In (Buslaev, 2014), it is proved that *under very broad assumptions the velocity of the chain is stable with respect to leader behavior and becomes uniformly $v = C$ after a certain time lag, if the leader moves uniformly.* The steady-state mode of the car chain

$$x_1 < x_2 < \dots < x_n$$

is equivalent of uniformly movement of *cluster* with velocity $v = f^{-1}(C)$ and with density $\rho = C^{-1}$.

5.2. Cluster model of incompressible flows

In (Bugaev et al, 2011), there was proposed an approach to modeling of flows on networks as

cluster model, which synthesizes the main concepts of the traffic flows theory such that wave model (Lighthill, Whitham, 1955), cellular automata (Nagel, Schreckenberg, 1992) and model *Follow-the-Leader Model (FL-model)* (Greenshilds, 1933).

We consider a model of vehicles flow on a highway corresponding a coordinate straight line or a circle divided into segments. On each segment (platoon of cars) the particles (cars) are located uniformly, i.e. the flow density is constant, and the particle velocity is the same. A function describing the dependence of the flow velocity on density is given. *Rectangles with base correspondent to segments with constant density and heights correspondent to values of flow densities, are called the geometric image of clusters* (Buslaev et al, 2012).

A dynamic system is defined by a system of ordinary differential equations describing the interaction of clusters that is a change of boundary coordinates of cluster bases or cluster height depending on the scenario.

Clusters, depending on mode of properties change at the interaction, are classified as follows. *Compressed cluster* is a cluster whose length and speed change when interacting with other clusters or obstacles. It is assumed that clusters interact under conditions of total-connected behavior. *Incompressible cluster* is a cluster having one value of velocity corresponds to train-transport. Incompressible cluster is an extreme variant of a compressible cluster with less variable parameters, which makes it possible to simplify the qualitative and computer research of its behavior on complex networks.

To study the behavior of incompressible clusters on complex networks, *the application "MultiClock"* is created which allows modeling networks consisting of contour blocks and conjugate at given points-nodes, as well as simulating the motion of clusters and removing limiting characteristics.

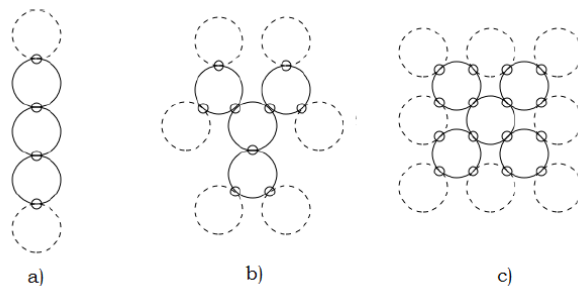


Figure 1. a) Necklace 2-network, b) Honeycombs 3-network and c) Chainmail 4-network

5.3. Contour k - network

Urban transport networks have more complex structures. Therefore, for their modeling, contour k -network, where the parameter k is equal to the number of neighboring contours and corresponding to the number of nodes on each contour. In Figure 1 it is shown Necklace 2-network (a), Honeycombs 3-network (b) and Chainmail 4-network (c).

5.4. Numerical experiments at cluster model

Let us consider a network consisting of contours of local motion, having one common point between each pair of neighboring contours. The contour length are normalized. We assume that their length is equal to one, on each contour we choose the initial point, the movement direction and the positions of points on the contour are given by angular coordinates, Fig. 2, a).

Let $2n$ be the number of contours, x be the length of the cluster. Simulation fixes the average speed over all contours, to which the dynamic system comes to the limit. Then the dependence of the average velocity on the length of the cluster $F(x, 0.5, n)$ is called a function of the state of the system.

If the system changes its characteristics dramatically when a certain parameter is changed,

then there is a *phase transition*. Computer simulation shows that for a large set of initial conditions the symmetric Necklace state function has a phase transition point equal to half the length of the contour, Fig. 2, b).

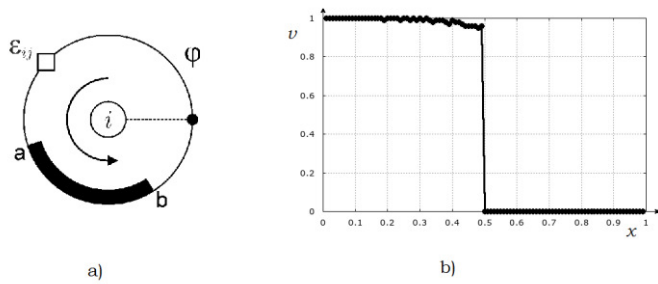


Figure 2. a) Movement rules on contour, b) State function $F(x, 0.5, 8)$

Also we have investigated the load point $1/2$. It is hold that *condition for load being less than $1/2$ is only necessary but not sufficient condition*. There exists an example of initial condition of cluster with length less than $1/2$ and system behavior with not self-organization.

5.5. Numerical experiments at variation of 2-network with “papa-mama” nodes

We consider a variation of symmetrical 2-network Necklace that has 2 nodes located in symmetrical point with distance equal to 180 degrees. Let y be a parameter indicated a distance between nodes in degrees, $0 < y < 180$. We call this system as Necklace with “mama-papa” nodes, Fig. 3 a).

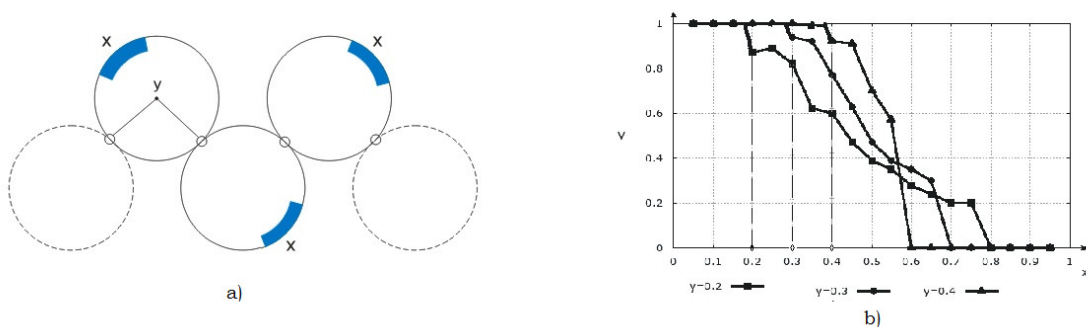


Figure 3: a) “Papa-mama” Necklace, b) State function $F(x, 0.2, 8)$, $F(x, 0.3, 8)$ and $F(x, 0.4, 8)$

Computer simulation was carried out for 10 000 experiments at different values of the distance between nodes. Results of simulation are shown in Fig.3 b). The point of phase transition for system with parameter y is equal to $x=y$.

6. Information model of network traffic with node buffering

Computer and computer networks are the basis of modern technological revolution the end of the last century and the beginning of the present. Such technical implementations of communication networks are *computer networks, telephone networks, cellular networks, cable television networks, etc.*

The *data network* is understood as a system of physical communication channels and *commutators* (nodes of the network), implementing this or that *protocol* of data transmission, i.e. *topology with rules for moving packets*.

Information processing in the network node is performed using the *router*, which generates a route for the packet that came to the node. Rules for traffic on the network are defined by the *protocol* (or logical interface), which means rules set defined the logic of messages exchanging and a set of information messages of a specific format exchanged between two nodes. *Cluster model of information traffic* takes into account these features. Network node becomes complex, including the possibility of buffering.

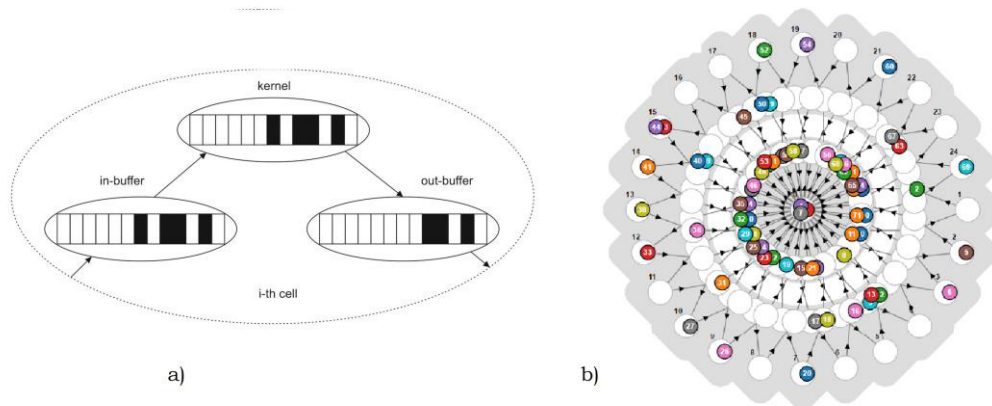


Figure 4: a) Structure of i -th cell, b) Example of topology of information model

The cell consists of one kernel and in-out buffers, Fig. 4 a). The number of the buffer depends on the multiplicity of t cell as the graph vertex; i.e. the number of incident communication channels. At each point in time the kernel and buffers can contain given number of particles (*capacity*).

For *road traffic* we will assume that the traffic between nodes occurs with velocities, significantly exceeding the passage of nodes. If the next node is occupied the follow particles forms a queue for the exit and entry into the node. Thus, the information model can be applied to traffic.

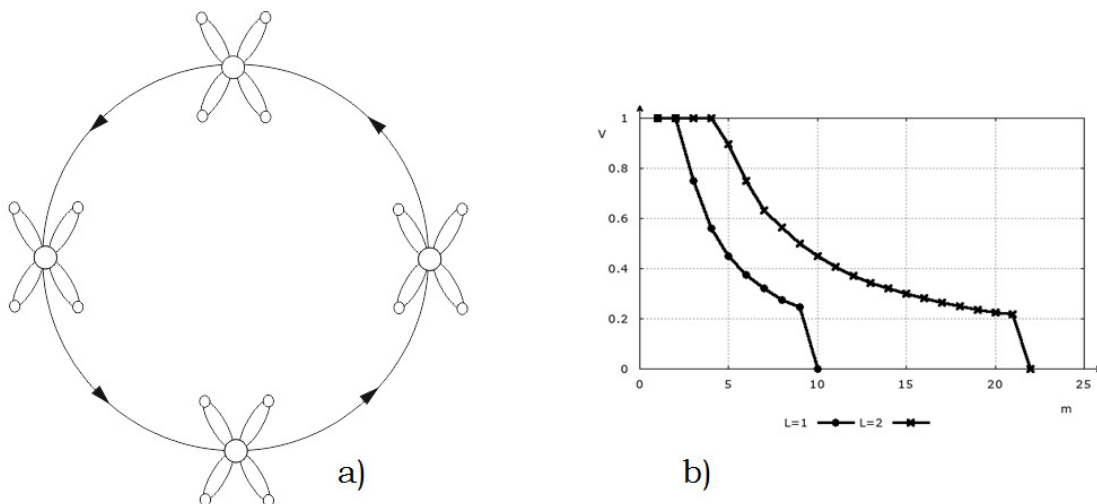


Figure 5: a) Experiment on information model with topology, b) its state function

In Fig. 5 it is shown topology of dynamical system and its state function.

7. Flow control models and perspectives

Flow control on the network in a broad sense implies the availability and technology of implementing the rules of the movement of each agent, depending on the current configuration

and other factors. Thus, *unlike rule 184*, (Wolfram, 1983) determined solution of local information and leads in certain situations to partial or full stop, for example, behaviour can be selected "move " or "stand " depending on "material motion", i.e. the number of clusters of agent particles in the area under consideration.

In

Fig.

6

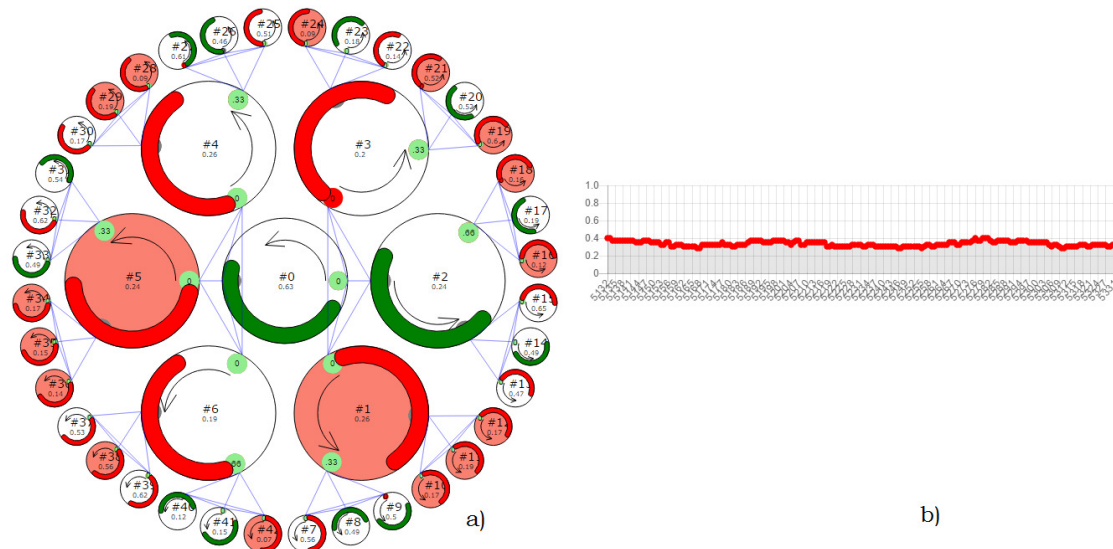


Figure 6: a) Cluster model on networks with complex topology, b) dependence velocity on time in steady mode

A software has been developed that makes it possible to carry out numerical experiments on the tasks of control. In the future it is supposed to develop algorithms for assessing the negative impact of flows depending on the geometry of the network. In Fig. 6 it is shown the model of a three-level contour network of cells with velocity separation and buffering. There is a periodic function of system velocity in the Fig. 6 b). The fluctuations are about 0.4 point for this dynamical system.

The developed software allows to have numerical experiments on control problems on complex regular network. In the future, it is supposed to develop algorithms for evaluate the negative impact of traffic flows depending on the geometry of network.

References

Lukanin V.N., A.P. Buslaev, A.V. Novikov and M.V. Yashina (2003), Traffic flows modeling and the evaluation of energy-ecological parameters.Part I, *Int. J. of Vehicle Design*, 33(4), 381-399.

Lukanin V.N., A.P. Buslaev, A.V. Novikov and M.V. Yashina(2003), Traffic flows modeling and the evaluation of energy-ecological parameters. Part II, *Int.J. of Vehicle Design*, 33(4), 400-421.

Kotani M., S. Ikeda (2016), Materials inspired by mathematics. *Science and Technology of advanced Material S*, 17(1), 253-259.

Wagner A., D.A. Fell (2001), The small world inside large metabolic networks. *Proceedings of the Royal Society of London B: Biological Sciences*, 268(1478), 1803-1810.

Wolfram S. (1983), Statistical mechanics of cellular automata, *Rev. Mod. Phys*, 55, 601-644.

Blank M.L. (2000), Exact analysis of dynamical systems arising in models of traffic flow, *Russian Mathematical Surveys*, 55(3), 167-168.

- Gray L., D. Griffeath (2001), The ergodic theory of traffic jams, *Journal of Statistical Physics*, 105(3), 413-452.
- Biham O., A. Middleton, D. Levine (1992), Self-organization and dynamical transitions in traffic-flow models, *Physical Review A*, 46, N 10.
- Kozlov V.V., A.P. Buslaev, A.G. Tatashev (2015), A dynamical communication system on a network, *Journal of Computational and Applied Mathematics*, 275, 247-261.
- Bugaev A.S., A.P. Buslaev, V.V. Kozlov, M.V. Yashina (2011), Distributed Problems of Monitoring and Modern Approaches to Traffic Modeling, *14th International IEEE Conference on Intelligent Transportation Systems*, 477-481.
- Buslav A.P., V.V. Kozlov (2014), On a system of nonlinear differential equations for the model of totally connected traffic, *J. Concr. Appl. Math.*, 12(1-2), 86-93.
- Buslaev A.P., M.V.Yashina (2012), Cluster model of total-connected flow with local information, *Proc. of Int. Conf. CMMSE-2012*, 1, 225-232.
- Buslaev A.P., A.G. Tatashev, M.V. Yashina (2013) Cluster flow models and properties of appropriate dynamic systems, *Journal of Applied Functional Analysis, Eudoxus Press*, 8(1), 54-76.
- Buslaev A.P., P.M.Strusinskiy (2014), On qualitative properties of incompressible cluster flow model on the ring network. *AASRI Conference on Sports Engineering and Computer Science (SECS 2014), AASRI Procedia*, 9, 114-122.
- Buslaev A.P, A.G Tatashev and M. V.Yashina, (2015) On Irrational Oscillations of a Bependulum, *Theory and Engineering of Complex Systems and Dependability of the series Advances in Intelligent Systems and Computing*, 365, 57-63.

SmartAQnet – spatial/temporal high-resolution detection of air quality by new data products

M. Budde¹, K. Schäfer^{2}, J. Cyrus³, S. Emeis⁴, T. Gracza⁵, H. Grimm⁶, M. Hank⁷, S. Hinterreiter⁶, E. Petersen⁸, A. Philipp⁸, J. Redelstein⁸, T. Riedel¹, J. Riesterer¹, J. Schnelle-Kreis⁹, D. Young⁴, V. Ziegler⁷, M. Beigl¹*

¹ Karlsruhe Institute of Technology, Institute of Telematics, Chair for Pervasive Computing Systems / TECO, 76131 Karlsruhe, Germany

² Atmospheric Physics Consultant, 82467 Garmisch-Partenkirchen, Germany, schaefer@atmosphericphysics.de

³ German Research Center for Environmental Health - Helmholtz Zentrum München GmbH, Institute of Epidemiology II, 85764 Neuherberg, Germany

⁴ Karlsruhe Institute of Technology, Institute of Meteorology and Climate Research, Department Atmospheric Environmental Research, 82467 Garmisch-Partenkirchen, Germany

⁵ Stadt Augsburg, Umweltamt, 86152 Augsburg, Germany

⁶ Aerosol Akademie e.V., 83404 Ainring, Germany

⁷ GRIMM Aerosol Technik Ainring GmbH & Co. KG, 83404 Ainring, Germany

⁸ University of Augsburg, Institute of Geography, Chair for Physical Geography and Quantitative Methods, 86159 Augsburg, Germany

⁹ German Research Center for Environmental Health - Helmholtz Zentrum München GmbH, Cooperation Group of Comprehensive Molecular Analytics, 81379 München, Germany

Abstract

Although air quality is an important topic of health risks in our time, it is very difficult for many cities to take measures to guarantee a clean air that we breath, because a consistent data base with fine-granular data and information on causal chains is missing. This has the potential to change, as today, both large-scale basic data as well as new promising measuring approaches are becoming available. The project “SmartAQnet”, funded by the German Federal Ministry of Transport and Digital Infrastructure (BMVI) within mFund, is based on a pragmatic, data driven approach, which for the first time combines existing data sets with a networked mobile measurement strategy. By connecting open data, such as weather data or development plans, remote sensing of influencing factors, and new mobile measurement approaches, such as participatory sensing with low-cost sensor technology, “scientific scouts” (autonomous, mobile smart dust measurement device that is auto-calibrated to a high-quality reference instrument within an intelligent monitoring network) and demand-oriented measurements by light-weight unmanned aerial vehicles (UAVs), a novel measuring and analysis concept is created within the model region of Augsburg. In addition to novel analytics, a prototypical technology stack is planned which, through modern analytics methods and Big Data and IoT technologies, enables application in a scalable way.

Introduction

The spatial and temporal distribution of air pollutants is very variable in urban areas because it depends on influences which are caused by emissions (spatial location, temporal activity) as well as meteorological conditions, cultivation and chemical processes. Currently, air pollutants are measured by a measurement network of rare spread dedicated instruments corresponding to EC guidelines. So, the responsible agencies only are able to collect and provide data of high quality. This incomplete data basis does not allow to study and simulate all cause-and-effect chains between quality of air, which we breath, and the built and natural environment.

The trend is toward distributed measurements with large spatial resolution (Budde et al., 2013; Budde et al., 2014; Kumar et al., 2015; Gao et al., 2015; Hüglin et al., 2015; Gozzi et al., 2016; Castell et al., 2017) as well as small-scale numerical simulation of pollutant distributions. This allows assessing and predicting the spatial and temporal variability of these pollutants, as well as to fuse collections of relevant data and enable their real-time analysis in a common context. Finally, evaluation of these numerical simulations and predictions is possible on a higher level of completeness.

The project “Smart Air Quality Network” (Acronym: “SmartAQnet”, <http://www.smartaq.net/>), funded by the German Federal Ministry of Transport and Digital Infrastructure (BMVI) within the

financial assistance program mFund and presented here, is based on a pragmatic, data driven approach, which for the first time combines existing data sets with a networked mobile measurement strategy. It started on April this year and is running for three years (see also Budde et al., 2017a).

Project goals

SmartAQnet gives priority to data of many different observations over simulation based data of few precise measurements. Thus, the core component of the system is a data storage and processing architecture, which allows data to be easily imported, analysed and made available to different applications at different levels of abstraction. The network will be designed to ensure that the data can be provided and widely used in the future for science, public authorities and citizens alike, compatible for scientific purposes as well as for user-oriented service development.

SmartAQnet employs a multi-layered heterogeneous network of sensors for the small-scale detection of air quality parameters in the model region Augsburg. Research questions include novel algorithms, e.g. for distributed calibration, verification of data sources or the protection of the privacy of the citizens involved in the measurements (Markert et al., 2016) who are to be tested under realistic conditions. Based on the obtained data of the developed platform and historical data, prototypical exemplary applications and services, e.g. on smartphones such as an application for air quality-related navigation, will be implemented and made accessible, in order to also demonstrate third-party exploitation possibilities.

Data architecture

Figure 1 shows the data architecture of the project, which implements a complete Internet of Things Stack using the latest Smart Data technologies. The underlying software architecture is a so-called kappa architecture, in which live data as well as historical data can be integrated continuously from constantly growing data sources. One important aspect of this architecture is that all incoming raw data is recorded as a log file before processing, which allows the reproduction of the results at any given time. This is important as calibrated and fused measurement will never be independent of each other and any changes made to a single part of the processing might require “replaying” of the whole analysis chain.

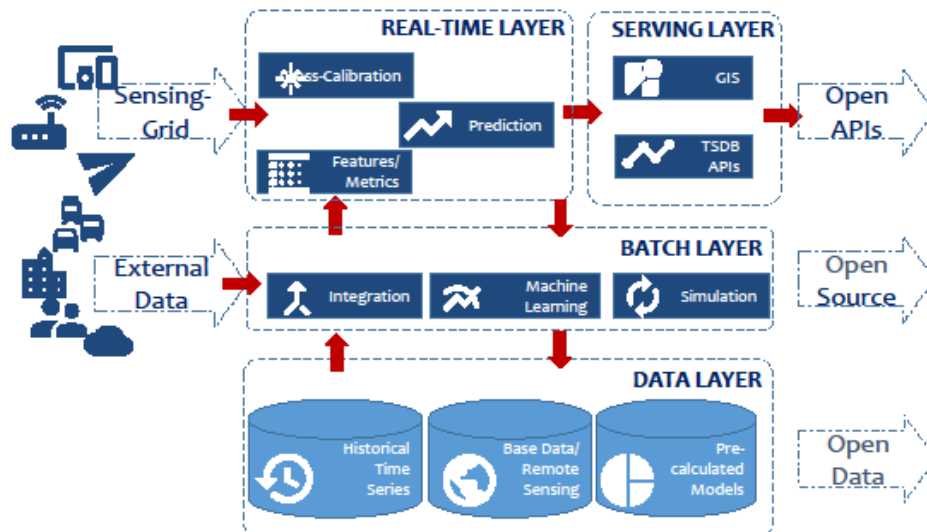


Figure 1: Data architecture of the project, which implements a complete Internet of Things Stack using the latest Smart Data technologies. Red arrows show data flow in processing chain.

A real-time view on the data is made possible by the fact that raw data (possibly anonymous) is processed directly and stored simultaneously as a historical time series. In a data flow oriented processing chain (red arrows), it is then merged with historical results using pre-calculated simulative and predictive models and made available almost real-time in services and

applications. Thanks to the use of scaling technologies, this processing chain can easily be transferred to several larger (or smaller) regions.

The SmartAQnet Internet of Things (IoT) platform allows everyone to simply load measured environmental data into the system. The integration of various existing data sets (weather, traffic, topography, etc.) and data of stationary and mobile measuring devices of different quality, as well as the provision of useful metrics calculated using Big Data methods is another central aspect.

Mobile sensor network

To simultaneously increase the measurement density and the measurement quality, not only existing data are integrated, but also intensive measurements are carried out in the Augsburg model region. This also includes the development and testing of new mobile measuring instruments in order to minimize or close adaptively existing gaps of static measurement networks. The measurements should be carried out at fixed representative places, mobile platforms, by citizens or if necessary by unmanned aerial vehicles (UAVs). One important aspect of the project is that any "measurement" devices are included that provide observation which potentially decrease the uncertainty of a hypothesis in contrast to perfectly controlled measurement processes.

The challenges in the development of new sensor systems include low investment costs (to achieve a high density), while maintaining sufficient accuracy and precision at a high temporal resolution (to globally decrease the uncertainty of a given model). For long-term research and sustainable operation, reliability of measurements and a high tolerance to environmental influences (load, temperature, pressure and humidity) is critical. Further aspects, such as network capability and smartphone connection (for integration into modern telematics systems or building monitoring systems), long-term stability and low maintenance must be viewed and weighed against each other and with other system parameters (for example, algorithms for compensating lower precision). Methods have to be defined in order to ensure uniform time standardization (time stamp) and temporal resolution of all sensors in the network.

The development / manufacturing of stand-alone Scientific Scouts (autonomous, mobile smart dust measurement device that is auto-calibrated to a high-quality reference instrument within an intelligent monitoring network) for mobile and stationary use within the project (e.g. on public urban transport platforms, road lighting, etc.) involves the exploration of two different types of measuring instruments. These are, on the one hand, measuring instruments which primarily measure particulate mass concentrations (PM values) and, on the other hand, particle measuring devices which place their measuring focus on the particle number concentration and particle size distribution in order to obtain important information on the cause analysis of the exposure to fine particles (source identification). In doing so, it is important that the self-diagnostic tools are maintained, e.g. pollutant levels and the associated measured value drift. Depending on the measuring focus, the measuring principle is based on optical sum (nephelometry) and / or individual particle analysis (optical particle counting). Optimally, both should be covered by an inexpensive nephelometer. A major challenge lies in an extremely fast and intelligent signal evaluation, which has to be developed through extensive comparison measurements to reference devices. Such devices generally have a low signal-to-noise ratio, which can additionally be significantly altered by environmental influences. The aim of the project is to build up the test network in the model region consisting of 50 scouts + 5 reference meters.

Part of the sustainability of the platform is an open and participatory approach, which requires awareness and active participation (Burke et al., 2006). In contrast to existing air quality information, the citizen (initially in the model region) should be able to record measurement data and to feed it into the platform, e.g. via smartphones, which in turn provides him with more accurate air quality information for his location or movement route (see also Budde et al., 2015). The (commercial) exploitation strategy is based both on these data-based applications and services as well as on the new technologies for the detection. This is also to ensure the long-term recording and provision of the data. The data, as well as the technology for integration and analysis, should be freely made available (as long as no rights of third parties are affected).

The project work includes the cooperation with schools, school children and volunteers who can notify at the project home page. They will perform not only such measurements by the new sensor techniques and submit the data to the demonstration network but also test the new services

provided on their smartphones. Routine bicycle-based measurements by students on selected routes are planned also.

Conclusions

The SmartAQnet research initiative focuses on the subject of data access and data-based applications. Central to this is the development and utilization of partial, already existing (but not yet combined) data on the one hand and the collection and integration of relevant missing data on the other hand. This includes the integration of third-party sources and the development of novel measuring devices, as well as an improvement of the overall data quality and the identification and implementation of meaningful interfaces between devices, databases and the end user.

On the data, new applications will be implemented. For this entire data-driven software chain, also new methods are explored. Specifically, these are big data analyses for quality improvement and model validation, as well as novel algorithms, e.g. for distributed calibration, verification of data sources or the protection of privacy of the measuring individuals. The project involves substantial novelty in several of the eligible categories: the core is a feasibility study aimed at investigating the potential of wide-spread distributed aerosol measurements with intelligent measurement networks of heterogeneous sensors in urban area. In particular, the possibilities and dangers of bringing experts together with laypersons will also be investigated (see (Budde et al., 2017b) for first results).

Finally, the project is also intended to promote industrial research. In recent years, it has become clear that air quality monitoring will change fundamentally in the future (Snyder et al., 2013). If this new generation of air quality monitoring is to be consistently pursued, in Germany, too, the expensive costly stations, which are now around 800, will not be supplemented with other high-price stations but with a spatially high resolved, heterogeneous network of distributed and possibly also mobile measuring instruments. This provides information for end users with consumer measurement technology and access to personified air quality data.

Acknowledgements

Project SmartAQnet is funded by the German Federal Ministry of Transport and Digital Infrastructure - Bundesministerium für Verkehr und digitale Infrastruktur (BMVI) under grant no. 19F2003B.

References

- Budde, M., P. Barbera, R. El Masri, T. Riedel and M. Beigl (2013), Retrofitting smartphones to be used as particulate matter dosimeters, *International Symposium on Wearable Computers (ISWC'13)*, ACM, 139–140.
- Budde, M., L. Zhang and M. Beigl (2014), Distributed, low-cost particulate matter sensing: Scenarios, challenges, approaches, *ProScience*, 1, 230–236.
- Budde, M., M. Köpke and M. Beigl (2015), Robust in-situ data reconstruction from poisson noise for low-cost, mobile, nonexpert environmental sensing, *International Symposium on Wearable Computers (ISWC'15)*, ACM, 179–182.
- Budde, M., T. Riedel, M. Beigl, K. Schäfer, S. Emeis, J. Cyrus, J. Schnelle-Kreis, A. Philipp, V. Ziegler, H. Grimm and T. Gratzka (2017a), SmartAQnet – Remote and In-Situ Sensing of Urban Air Quality, *Proceedings of SPIE, SPIE, Bellingham, WA, USA*, 10424, 104240C-1 – 104240C-8.
- Budde, M., A. Schankin, J. Hoffmann, M. Danz, T. Riedel and M. Beigl (2017b), Participatory Sensing or Participatory Nonsense? – Mitigating the Effect of Human Error on Data Quality in Citizen Science, *Proceedings of the ACM on Interactive, Mobile, Wearable and Ubiquitous Technologies (IMWUT)*, 1.
- Burke, J.A., D. Estrin, M. Hansen, A. Parker, N. Ramanathan, S. Reddy and M.B. Srivastava (2006), Participatory sensing, *Workshop on World-Sensor-Web (WSW'06): Mobile Device Centric Sensor Networks and Applications*, 117–134.
- Castell, N., F.R. Dauge, P. Schneider, M. Vogt, U. Lerner, B. Fishbain, D. Broday and A. Bartonova (2017), Can commercial low-cost sensor platforms contribute to air quality monitoring and exposure estimates? *Environment International*, 99, 293–302.

- Gao, M., J. Cao and E. Seto (2015), A distributed network of low-cost continuous reading sensors to measure spatiotemporal variations of PM_{2.5} in Xi'an, China, *Environmental Pollution*, 199, 56-65.
- Gozzi, F., G. Della Ventura and A. Marcelli (2016), Mobile monitoring of particulate matter: State of art and perspectives, *Atmospheric Pollution Research*, 7, 228-234.
- Hüglin, C., P. Graf, M. Müller, B. Schwarzenbach and L. Emmenegger (2015), Sensortechnologien für die Messung von Luftschadstoffen. Einschätzung der Möglichkeiten und Grenzen von kostengünstigen Sensoren, *Empa, Abt. Luftfremdstoffe/Umwelttechnik. CH-8600 Dübendorf*, www.empa.ch/nabel.
- Kumar, P., L. Morawska, C. Martani, G. Biskos, M. Neophytou, S. Di Sabatino, M. Bell, L. Norford and R. Britter (2015), The rise of low-cost sensing for managing air pollution in cities, *Environment International*, 75, 199–205.
- Markert, J.F., M. Budde, G. Schindler, M. Klug and M. Beigl (2016), Private rendezvous-based calibration of low-cost sensors for participatory environmental sensing, *2nd International Conference on IoT in Urban Space (Urb-IoT'16)*, ACM, 82–85.
- Snyder, E.G., T.H. Watkins, P.A. Solomon, E.D. Thoma, R.W. Williams, G.S. Hagler, D. Shelow, D.A. Hindin, V.J. Kilaru and P.W. Preuss (2013), The changing paradigm of air pollution monitoring, *Environmental Science & Technology*, 47, 11369–11377.

Particle Dispersion from Railway Rolling Stock: Preliminary Results from Wind Tunnel Experiments and CFD

A. DURAND¹, A. MEHEL^{2*}, F. MURZYN³, G. FOKOUA² and S. PUECH¹

¹ Rolling Stock Engineering Centre (CIM), SNCF, 72100 Le Mans, France

² Department of Composite Materials Mechanics and Environment, ESTACA, 78180, Montigny-Le-Bretonneux, France Fax +33 01 76 52 11 43 - email: amine.mehel@estaca.fr

³ Department of Composite Materials Mechanics and Environment, ESTACA, 53061, Laval, France

Abstract

The exposure to particle pollution has become a major issue since it is responsible for the general enhancement of adverse health effects. In the last decades, regulation of outdoor air pollution became stricter. However, regulation in underground railways is still at early stages despite the fact that, ultrafine particles (UFP) are generated and emitted from train brakes. Thus, commuters and workers could be exposed to these particles while standing on platforms and inside rolling stock where outer particles can infiltrate through leakages, windows or ventilation systems. In the present paper, we are interested in investigating UFP dispersion from train braking systems in correlation with the flow topology. Having that in mind, two approaches are considered. In the first one, wind tunnel experiments are conducted using a 3D-printed train model at 1/87 scale and a 2D-LDV system. The second approach deals with numerical simulations to investigate the flow topology and to assess the particle dispersion. Results show a high correlation between ultrafine particle dispersion and turbulent vortices generated in the train wake. The confrontation of experimental to numerical results show differences in the flow structure, this is mainly due to the 2D-flow simulations that could be different from a real 3D case.

Keywords: wind tunnel, airborne ultrafine particle, particle dispersion, railways, brake, train aerodynamics, CFD.

Introduction

Transit mode significantly contributes to the total daily exposure of the commuter (Knibbs et al., 2010). Commuters who use underground railway transportation mode are exposed to particle pollution as trains generate several metallic UFP pollutants during braking stage (Railway Test Agency known as AEF, 2010-2015). Furthermore, some of deposited ultrafine particles (UFP) on the ground may be lifted by trains entering into a station. It is worthwhile to note that UFP concentration in mass in underground train stations, where ventilation may not be sufficient and confinement effect is important, can reach high level (Fortain, 2008; Airparif, 2016).

For a long time, particle pollution was not regulated in underground railways. Since 2000, some regulations have been defined in European countries such as Norway or Finland where several limits values of PM_{2.5} and PM₁₀ concentration are defined depending of environmental conditions (French Agency for Food, Environmental and Occupational Health & Safety known as ANSES, 2009). Studies, conducted by ANSES, are ongoing to set limit values for underground train stations in France.

Many studies have shown the toxicity of UFP. It was shown that, at the same mass concentration with similar compositions, smaller particles are more toxic than larger ones (Oberdörster, 2001). Indeed, for a given mass concentration smaller particles are more numerous than larger ones. Furthermore, the smaller particles are, the higher is their ability to infiltrate deeply respiratory system. Smallest particles are able to reach pulmonary alveoli where they can penetrate blood system (Oberdörster et al., 2004). Toxicological studies showed that UFP enhance respiratory diseases, cardiovascular diseases and cancer risks. Metallic dusts can also scar lung tissue by oxidizing while they are inhaled (Buzea et al., 2007). Some studies showed that significant improvement of particle pollution has a great benefit on public health, lessening the number of consultations for respiratory troubles such as asthma and the number of death by cardiovascular or respiratory disease (Henschel et al., 2013; Duchesne et al., 2016). Moreover, health troubles caused by UFP can lead to economical loss. For example, in France,

the concrete mean cost, of a sick leave day is close to \$55 and the daily cost linked to chronic diseases such as cancer is even higher (Rafenberg et al., 2015).

This quick overview shows the interest to increase our knowledge about the dynamics of UFP issued from rail transportation. In the present paper, we investigate UFP dispersion in an enclosed environment such as underground station in interaction with the flow topology. To date, little is known about the aerodynamics of a train during the braking stage, in particular in enclosed environment. To reach this goal, wind tunnel experiments and numerical simulation were conducted. The main goal of wind tunnel experiments was to assess the slipstream of a commuter train when entering a station at 45 km/h. While 2D numerical simulations were conducted at longitudinal cross-section plane of the braking discs. In the following parts, we first present the experimental method. Then, the numerical method is exposed followed by the results. A conclusion ends this paper and some future works are suggested.

1. Experimental method

Experiments were conducted in a 1000 mm length, 300 mm width and 300 mm height wind tunnel located at ESTACA Laval. Sidewalls are made of transparent altuglass allowing flow visualizations and the use of optical devices. The upstream air velocity is set at $U_\infty = 12.5$ m/s with a 1% margin of error for each experiment. Velocity fields were measured using a 2D Laser Doppler Velocimetry (LDV) system provided by DANTEC Dynamics. The train model was a 1/87 scaled model of a Z20500, which is one of the rolling stocks used in Paris underground railways. The train model has a length of $L_m=572$ mm, a width of $W_m=32.41$ mm and a height of $H_m=49.66$ mm. The track model has a length of 1000 mm, a top width of 35 mm, a bottom width of 64 mm and a height of 12.41 mm (Fig 1). In these conditions, blockage ratio is lower than 5% (no correction was considered regarding wall effects). The turbulent intensity of the incoming flow is below 1%. The Reynolds number based on train height ($Re_m = U_\infty \cdot H_m / \nu$) is $Re_m=4.10^4$. For all measurements, we acknowledge steady conditions and no heat flux from outside is considered.

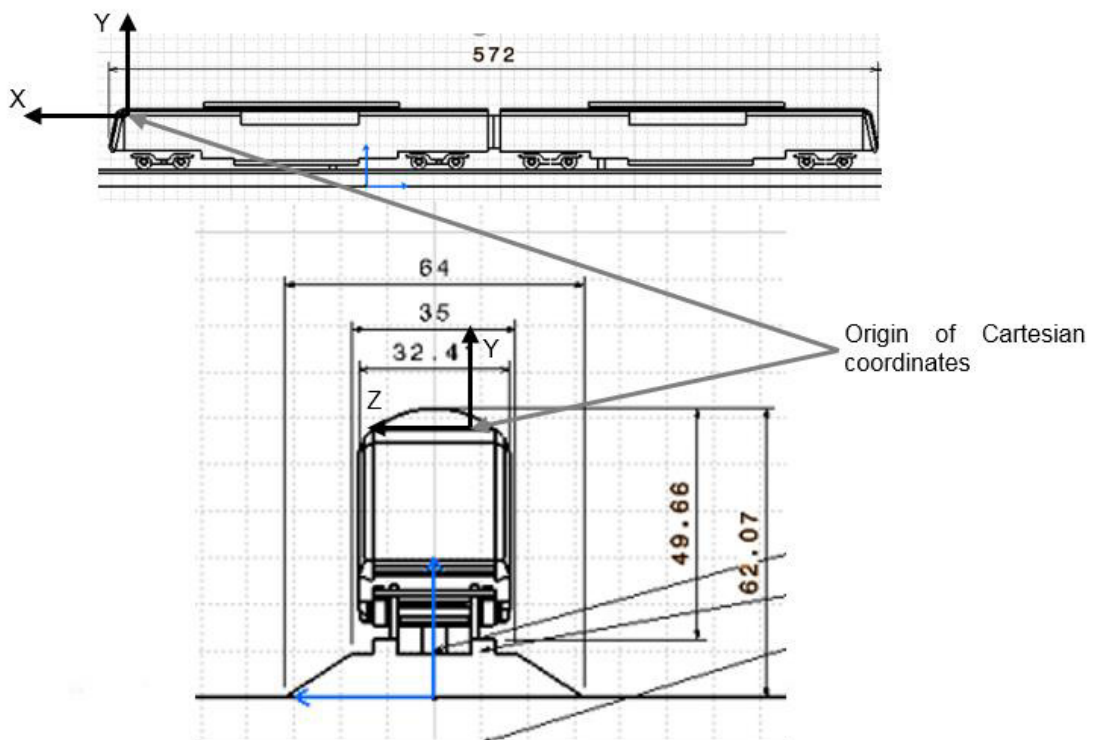


Figure 1: Model blueprint, dimensions are displayed in mm.

The model is made up of two motor cars instead of two trailer cars surrounded by two motor cars in order to fit with wind tunnel length. Model was made using a plastic Selective Laser Sintering (SLS) 3D printer, and 1/87 scaled model of the track was made with aluminum. All

parts are painted in black in order to minimize light reflection allowing optimum use of 2D LDV system. Parts are also sanded to avoid surface roughness. A complete motor car is shown in Fig. 2.

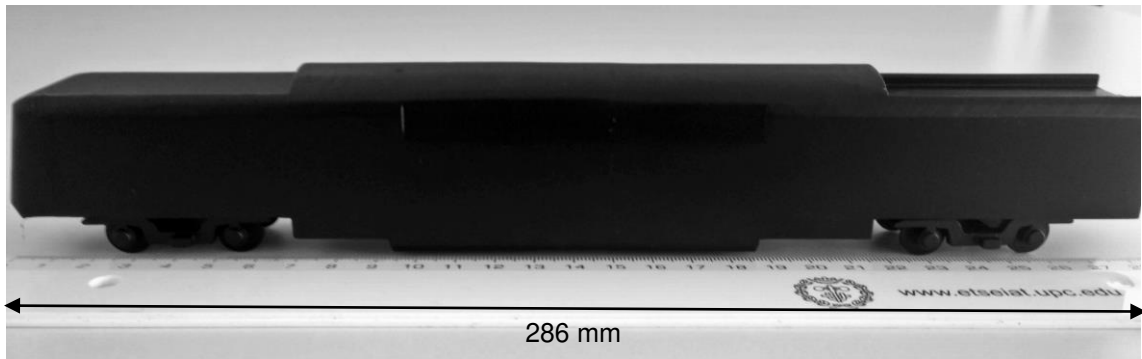


Figure 2: Complete motor car.

Velocity fields were measured using a 2D LDV system mounted on a 3D displacement table. Both streamwise (U) and vertical (V) components of the velocity are recorded at 735 different locations in the wake of the train. In this paper, x , y and z correspond to the horizontal, vertical and transversal directions, respectively. Investigated area spreads such as $0.2H_m < x < 0.8H_m$ and $-0.6H_m < y < 0.2H_m$ on five (xy) section planes which corresponds to both sides of the train ($z/H_m = -0.1$ and $z/H_m = 0.3$), both internal side of the rails ($z/H_m = 0$ and $z/H_m = -0.2$) and the center of the model ($z/H_m = 0.1$). Measurement origin was set, for the x -axis at the level of the beginning of the rear hull, for the y -axis at the level of the top of the train at the rear hull, which is at $0.85 H_m$ from the track, and z -axis falls into line with the rail. On the x -axis, the step between two points is $0.1 H_m$, on the y -axis, the step between two points is $0.04H_m$. Data acquisition lasts 90 seconds and mean data rate is above 10Hz, however some data rates are about 5Hz but it only concerns a very few points. It was caused by some seeding troubles.

2. Numerical method

The study is based on a full-scale SNCF Z20500, which is a representative French commuting train external shape. Computer-Aided Design (CAD) was achieved with the help of SNCF blueprints and partial CAD. Train length is $L_t = 98760$ mm, train width is $W_t = 2846$ mm and train height is $H_t = 4320$ mm. The numerical analysis is based on a slightly simplified geometry which as the same dimensions. Although the model is simplified (details such as HVAC units or accessibility equipments are not considered), the main geometry is kept such as external shape, bogies or carriage gaps. 3D CAD model is detailed in Fig.3. The train is located on a single-track ballast and rail. Two numerical configurations were conducted, the first where the tunnel height is $1.3H_t$ to fit real operating conditions. And the second one where it is equal to $6.1H_t$ to fit wind tunnel conditions.

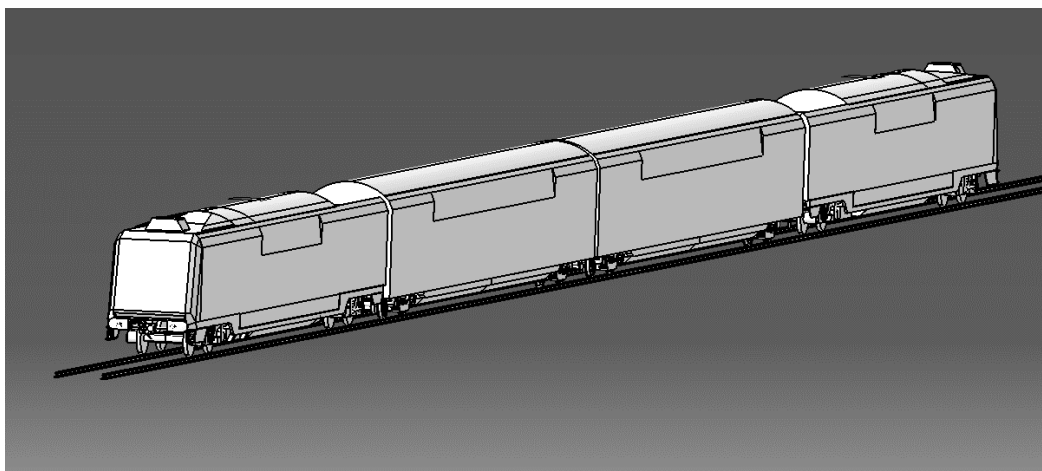


Figure 3: CAD model.

Simulations consist of 2D-flow analysis in the longitudinal cross-section plane at braking discs. It corresponds to the section plane where the particles are injected. The origin of coordinate system is located at the rear point of the train on the x-axis and at the level of the ground on the y-axis. As a first approach, in this study a constant upstream velocity is set at 12.5 m/s, which is the mean speed between the beginning and the end of mechanical braking. In this part, the Reynolds number based on train height is $3 \cdot 10^6$ ($Re = U_\infty \cdot H_t / \nu$), and turbulent intensity is 2%. The atmospheric pressure is considered at the outlet boundary. To avoid the development of spurious boundary layer, moving wall conditions are applied to tunnel walls. In the wind tunnel conditions simulation, and since our wind tunnel has no rotating belt, the stationary wall conditions were applied.

Our meshing strategy is based on a $0.023H_t$ unstructured mesh with two refinement zones. The former covers the train and the near-wake with a $0.005H_t$ refinement while the latter covers trailer bogies with a $0.001H_t$. Thus, there are three zones with different meshing parameters, coarse (corresponding to general meshing settings), medium (train and its near-wake) and fine (bogies where particles are injected). The meshing parameters are summarized in the table 1.

Mesh	Coarse	Medium	Fine
Cell size	$0.023H_t$	$0.005H_t$	$0.001H_t$
Transition between zones	20%	20%	20%
First inflation layer	0.0001 mm	0.0001 mm	0.0001 mm
Inflation rate	30%	30%	30%
No. of inflation layers	-	10	21
Train wall y^+ ($y^+ \equiv \frac{u_* y}{\nu}$)	-	3-10	1-5

Table 1. Meshing parameters. Dimensionless wall distance (y^+) is defined as the ratio of the friction velocity (u_*) times the distance to the nearest wall (y) over local kinematic viscosity (ν).

CFD simulations were conducted with the commercial code ANSYS Fluent 16.1 software suite. A complete Lagrangian two phase flow simulations are achieved, where the continuous phase were simulated using the RANS-based turbulence models. i.e. the RNG k- ϵ model or the Reynolds Stress Model combined to the Enhanced near-wall treatment model. While the particulate phase was treated using the Lagrangian approach combined to the Eddy Interaction Model (EIM) for particle dispersion by turbulence. The UFP injection position is located at the level of braking discs. Particle size, chemical composition, emission speeds and mass flow rate are based on AEF classified reports (AEF, 2010-2015).

3. Results and discussion

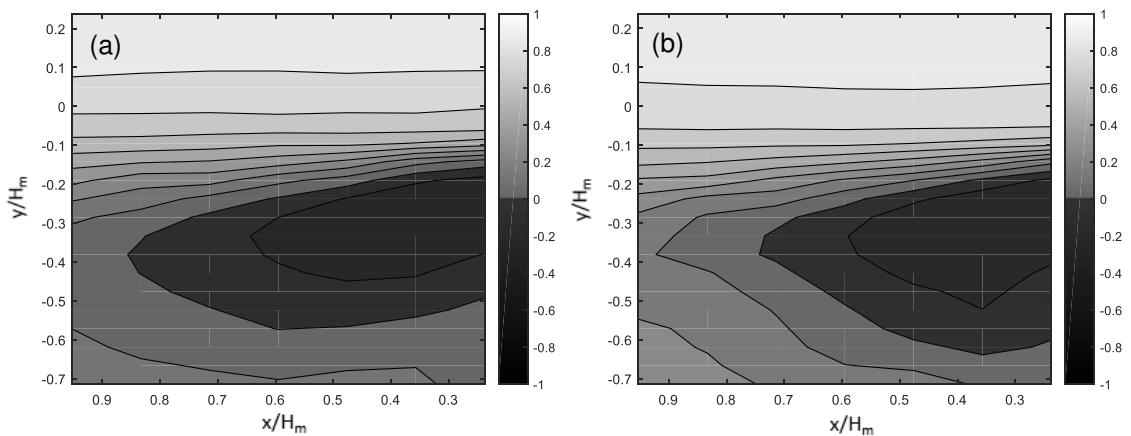


Figure 4: Dimensionless X-velocity in the near-wake region (a) at the centerline of train ($z/H_m=0.1$) (b) at the level of the rail ($z/H_m=0$) (b); flow from right to left.

Figure 4 presents a 2D vertical map (XY) of the dimensionless mean streamwise velocity (U/U_∞), measured at the centerline of the train, $z/H_m=0.1$ (a) and at the level of the rail $z/H_m=0$ (b). On the one hand, our results indicate that negative velocity components are found in the near wake of the train, more precisely, located in the center-bottom region. This zone spreads from $-0.5H_m$ to $-0.15H_m$ on the vertical direction and from 0 to $0.85H_m$ on the horizontal axis on the centerline of the train (Figure 4a). On the other hand, at the level of the track (rail), we noticed that this zone spreads down to $-0.6H_m$ and is shorter ($0.7H_m$) on the longitudinal direction (Figure 4b). These results depict the development of a recirculation region, which might have an influence on the dispersion of UFP. Beyond this very close wake region, positive streamwise velocity are measured with increasing value as the distance from train tail increases. These results are comparable to those found by Ahmed et al. (1984) for an automotive ground car.

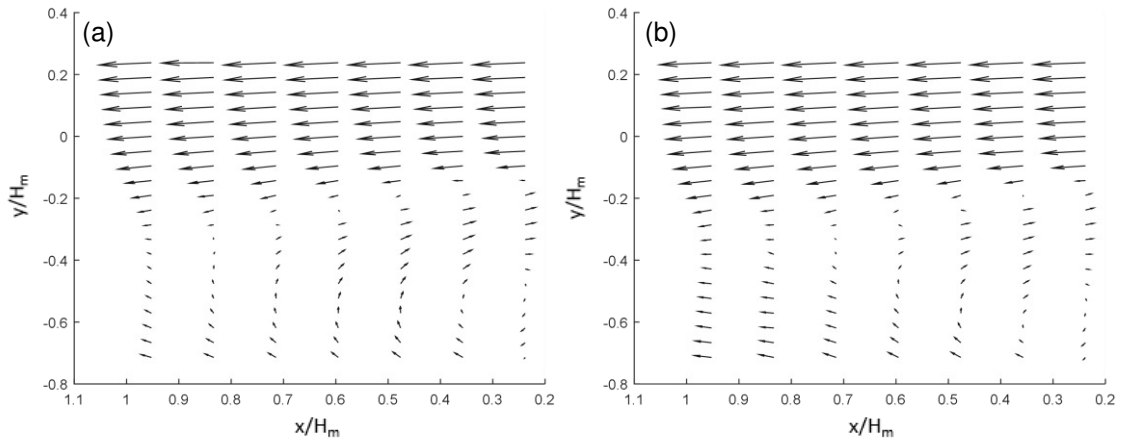


Figure 5: Dimensionless near-wake velocity magnitude vectors at the centerline of train ($z/H_m=0.1$) (a), at the level of the rail ($z/H_m=0$) (b); flow from right to left. The components of the top line vectors are about $U=U_\infty$ and $V=0$.

Figure 5 presents a 2D (xy) vector map of the dimensionless velocity magnitude at the centerline of the train (a) and at the level of the rail (b). For $y/H_m > 0.1$ and for $x/H_m > 1.5$, the vertical component V is close to 0 and U is roughly equal to U_∞ . The maximum of the dimensionless vertical velocity $(V/U_\infty)_{max} \sim 0.2$ is recorded at $x/H_m=0.4$ and $y/H_m=-0.48$ at the centerline of the train (Figure 5a) and at $x/H_m=0.4$ and $y/H_m=-0.56$ with a dimensionless value $(V/U_\infty)_{max} \sim 0.16$ at the level of the rail. The lowest values of the horizontal dimensionless component is recorded at $x/H_m=0.30$ and $y/H_m=-0.24$ $(U/U_\infty)_{max} \sim -0.21$ at the centerline of the train (Figure 5a) and at the same point with a dimensionless value $(U/U_\infty)_{max} \sim -0.18$ at the level of the rail (Figure 5b). Combining all these results, it clearly denotes the apparition of a recirculation zone in the near-wake of a low-speed train. The structure and intensity of the turbulent flow in this zone have a significant impact on particle dynamics. This point will be discussed in the section related to the two-phase flow simulations. Figure 6 present the turbulent intensity in both longitudinal and vertical directions. The turbulent intensity is defined as the ratio of the RMS value of the corresponding velocity component to the upstream velocity U_∞ . Turbulent intensity in longitudinal and vertical directions are named I_x and I_y , respectively. Figures 7 correspond to $z/H_m=0.1$ the centerline of the train with the same scale.

r

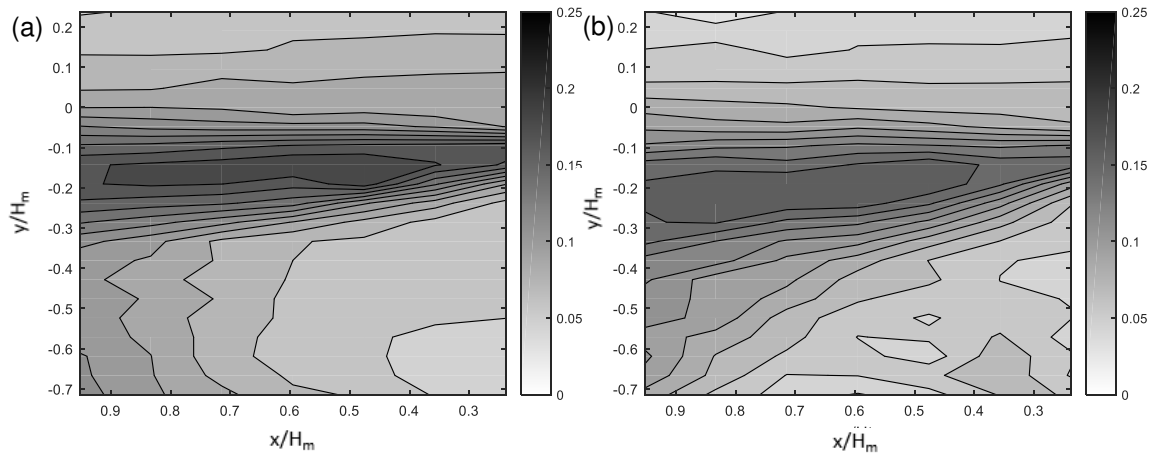


Figure 6: Turbulence intensity I_x (a) and I_y (b) at the center of the train ($z/H_m=0.1$); flow from right to left

Our results show that the turbulence intensity levels are higher between the top part of recirculation area and the top of train hull. The maximum longitudinal turbulence intensity ($I_x \sim 19.2\%$) is recorded at $x/H_m=0.5$ and $y/H_m=-0.12$ and the maximum vertical turbulence intensity ($I_y \sim 16.9\%$) is recorded at $x/H_m=0.4$ and $y/H_m=-0.16$.

Hereafter the CFD simulations results are presented. Even if the flow simulation is considered as 2D, the description of its general topology is required to get a better understanding of the particle trajectory in two-phase flow simulations. A noteworthy difference between 2D-flow analysis and the experimental topology is the occurrence of a third vortex [V3] (it may be caused by the lack of the spanwise z -momentum) in the recirculation area as shown in Figure 7 which would tend to decrease the momentum in the other directions, i.e. the Figure 8 shows that recirculation vortices [V1] and [V2] are stressed by [V3] in 2D-flow numerical analysis leading to an underestimation of about $0.1H_t$ of recirculation length in our case. The recirculation length corresponds to the region length for which the streamwise velocity change its direction and it is representative of the flow topology (vortices distribution)

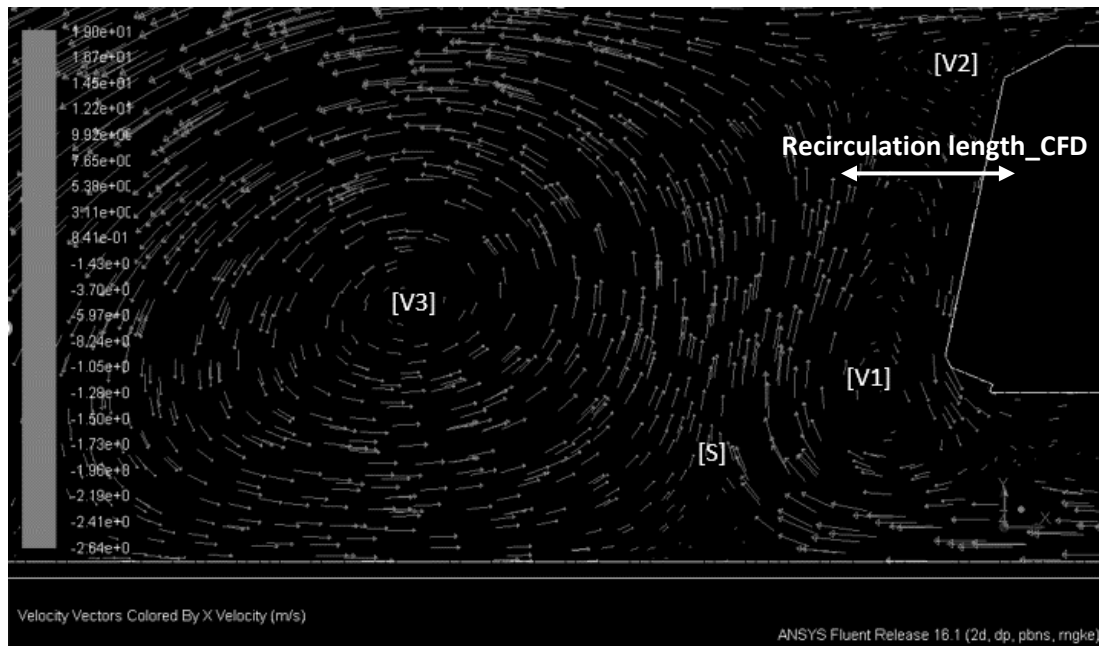


Figure 7: Numerical single-phase flow topology for wind tunnel conditions (smaller tunnel height); flow from right to left

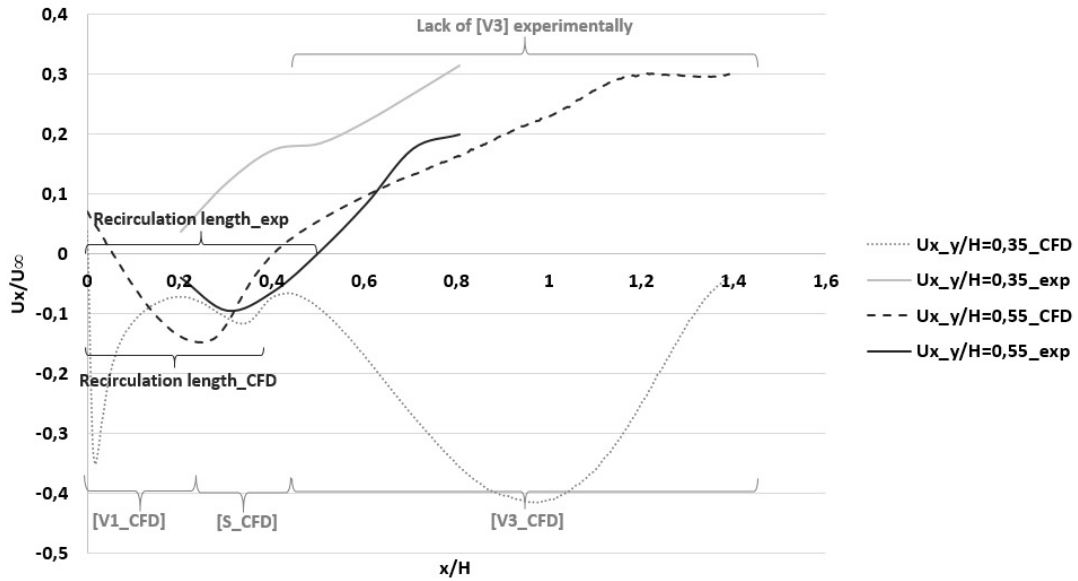


Figure 8: Comparison of the horizontal velocity at $y/H_m=0.35$ (light gray) and $y/H_m=0.55$ (dark gray), experimental values are plotted with solid lines. CFD values in dotted lines

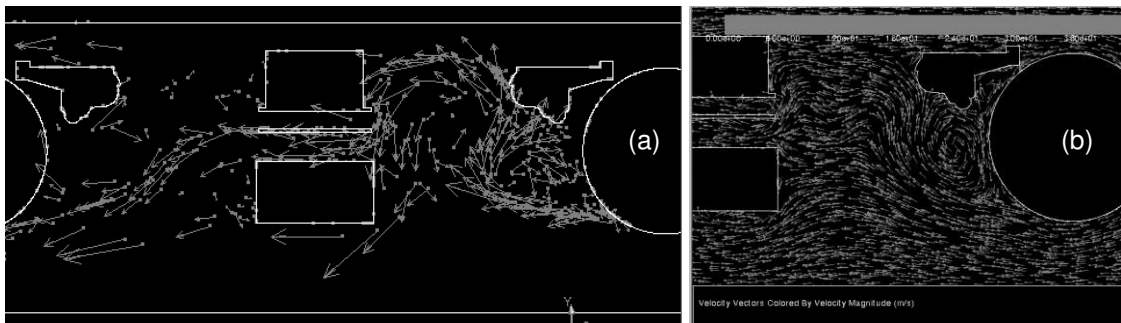
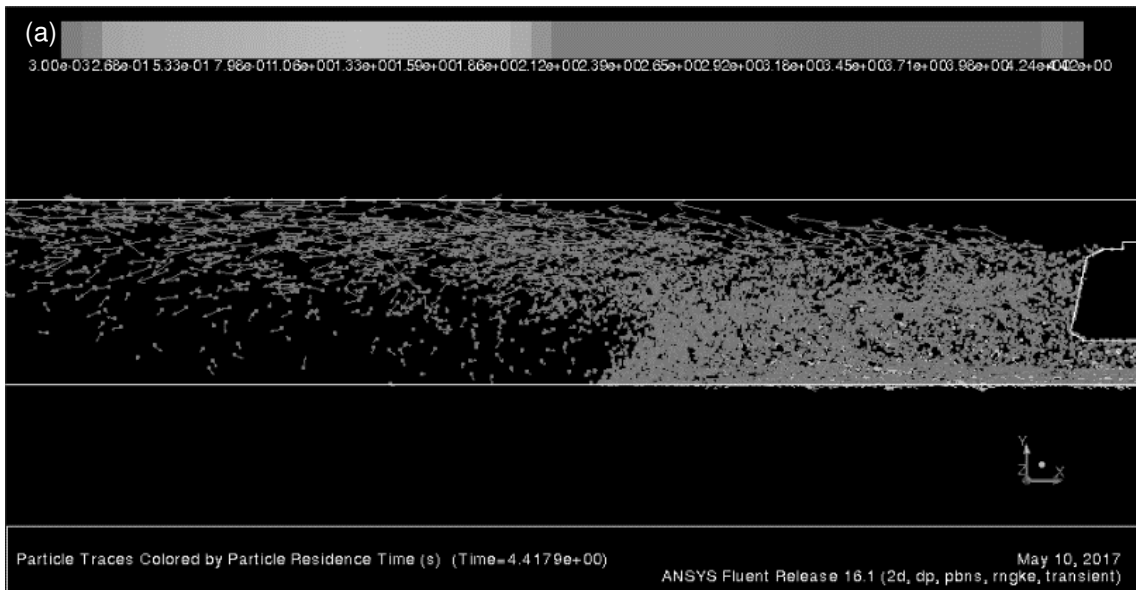


Figure 9: Particle path at braking (a) and velocity magnitude vector field (b) at the level of a trailer bogie in a streamwise braking discs cross-section. Flow from right to left.



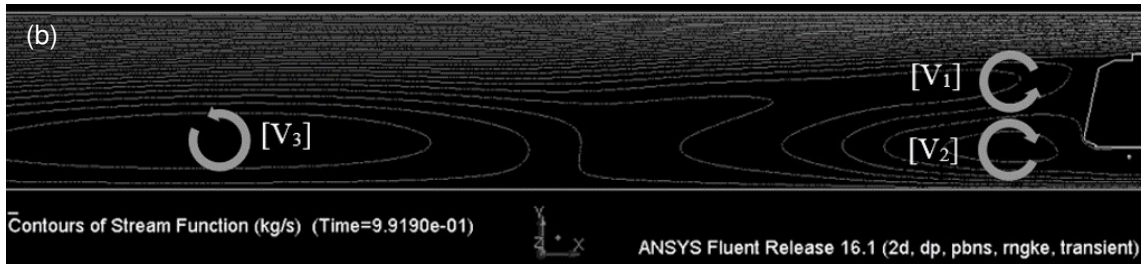


Figure 10: Streamlines (a) and particle dispersion (b) in underground train station configuration in a streamwise braking discs cross-section. Flow from right to left.

Figure 9 and Figure 10 present particle velocity vectors so to understand the dispersion mechanism in the close region of the bogies and in the train near wake flow region respectively. It can be seen that particle dispersion is closely related to the flow topology. Indeed, in the wake of the bogies or the train, the created depression induces the appearance of vortical structures that influence particle dynamics. The particles issued from braking system have speed and direction that are strongly related to the flow speed and direction for a given position. Particles are first dispersed vertically in the bogies region upstream the rail road before their acceleration in the jet flow that develops between the suspension elements (Figure 9). After that, they are sucked by the vortices of the recirculation near wake region. They are caught in recirculation zone at a height between H_t and $1.2H_t$. Then, they disperse vertically and then they are blown by the flow coming from the top of the train at a speed close to $4U_\infty$ (both particle and flow speed). Some particles remain trapped inside vortices, both at the level of bogies and at the level of recirculation area. Other particles follow the flow topology. Once they are released from recirculating region they are dispersed longitudinally which lead particles to move along tunnel roof.

Conclusion

This paper presents a preliminary study of the flow topology and particle dispersion in the wake of a train entering in an underground station. Experimental measurements and numerical simulations were performed. Even if some improvements can be made, our results were helpful to characterize the recirculation region that develops in the close wake of the train. This will be taken into account for future 3D numerical simulations.

Although scale effects may exist, our results provide a general overview of the recirculation length. Our 2D two-phase simulations were able to give a general description of turbulence-particle interaction. Our results depict that, at the level of the bogies and on the near-wake region of the train, UFP paths were very similar to the velocity field. It also shows how recirculation zone can suck particles up and entrap them leading to high UFP vertical dispersion.

From our investigations, our main conclusions highlight that:

- A recirculating flow develops in the near-wake of the train which has the ability to influence particles dynamics;
- Vertical and longitudinal turbulent intensities can reach up to 20%;
- 2D flow simulation can give an overview of vortical structures that develop in the flow. However, it is noticed that it could be the cause of a non-physical vortex (V3) which leads to an underestimation of the real recirculation length;

UFP trajectory is narrowly related to turbulent flow topology. It is expected that these preliminary results will contribute to get a better understanding of the particle dispersion in underground railways stations. The final goal being to provide solutions to improve air quality in this enclosed environment, such as improvements of staff protection equipments; heating, ventilation and air conditioning (HVAC) optimization inside rolling stock and train stations. Future works include 3D numerical investigations, single-phase and two-phase flows experimental measurements combined with in-situ tests campaign. These topics will be investigated in the context of a new PhD research project focusing on the correlation between commuter train braking emissions and particle mass and number concentrations in underground train stations.

Acknowledgments

The authors would like to express their gratitude to the Rolling Stock Engineering Center (SNCF, Le Mans, France) for providing the funds required for this work, the Railway Test Agency (AEF, Vitry-sur-Seine, France) for allowing us to visit their braking emissions test bench and for providing us various data about braking pad emissions.

References

- AEF (2010), Characterization of braking emissions of a TTNG on a typical route using test bench, *Internal Classified Report*, 1-40.
- AEF (2011), Material analysis and braking emissions using test bench, *Internal Classified Report*, 1-36.
- AEF (2012), Characterization of braking emissions of a Regio2N on a typical route using test bench, *Internal Classified Report*, 1-52.
- AEF (2013), Characterization of pollutant braking emissions of composite braking pad using test bench, *Internal Classified Report*, 1-53.
- AEF (2014), Material analysis and characterization of braking emissions of a Regio2N using test bench, *Internal Classified Report*, 1-25.
- AEF (2015), Characterization of braking pad binder, *Internal Classified Report*, 1-14.
- AEF (2015), Material analysis of G36-029 lining and braking emissions using test bench, *Internal Classified Report*, 1-31.
- Ahmed, S., Ramm, G., Fatin G. (1984), Some salient features of the time-averaged ground vehicle wake, *Society of Automotive Engineers, Inc.*, Warrendale, PA.
- Airparif (2016), Indoor air quality for underground Transilien train station, <http://www.airparif.asso.fr/pollution/air-interieur-gare>.
- ANSES (2010), Guide values for indoor air quality – Particles, *Air et agents chimiques Edition scientifique*, 1-73.
- Buzea C., Pacheco I., Robbie K. (2007), Nanomaterials and nanoparticles: sources and toxicity, *Biointerphase*, 2, 4, 17-71
- Duchesne L., Medina S. (2016), Health effects of intervention studies related to air quality, *Santé Publique France*, 1-43.
- Fortain A. (2008), UFP characterization in underground train stations, PhD *Dissertation*, Université de La Rochelle, 1-224.
- Henschel S., Medina S., Goodman P. (2013), Overview of interventions on atmospheric pollution, *Bulletin Epidémiologique Hebdomadaire*, 2, 13-16.
- Knibbs L., Cole-Hunter T., Morawska L. (2011), A review of commuter exposure to ultrafine particles and its health effects, *Atmospheric Environment*, 45, 16, 2611-2622.
- Oberdörster, G. (2001), Pulmonary effects of inhaled ultrafine particles, *International Archives of Occupational and Environment Health*, 74,1,1-8.
- Oberdörster, G., Sharp, Z., Atudorei,V., Elder, A., Gelein, R., Kreyling,W., and Cox, C., 2004. Translocation of inhaled ultrafine particles to the brain, *Inhalation Toxicology*, 16, 437–445.

Computer Vision in Modern Intelligent Transport System

A.P. Buslaev^{1*} and M.V. Yashina²

¹Department of Mathematics, Moscow Automobile and Road State Technical University, Moscow, 125319, Russia, apal2006@yandex.ru

²Department of Mathematical Cybernetics and IT, Moscow Technical University of Communications and Informatics, 111024, Russia

1. Introduction. Population dynamics, urban road networks and level of mobilization in Russia

Population in Russia tends to grow, especially in metropolises. Now population of the Russian Federation is 147 mln inhabitants, population in Moscow is 12.3 mln, population of Saint Petersburg is 5.1 mln and so on. Moreover the population of Moscow increased by 2 million in 5 years. The level of motorization in Russia in comparison with the developed countries is low. In Europe it's 800 vehicles per thousand people, in Russia is only 300. In Russia many regions are classified as highly intensive traffic, mainly in Moscow, which in number of vehicles rating in Russian metropolises is on the fourth place, but the situation with traffic jams is extremely bad.

INRIX Global Traffic Scorecard analyzes and ranks the impact of traffic congestion in 1,064 cities across 38 countries worldwide - the largest ever study of its kind. Los Angeles tops the list of the world's most gridlocked cities, with drivers spending 104 hours in traffic jams in 2016 during peak time periods, followed by Moscow (91 hours), New York (89 hours), San Francisco (83 hours) and Bogota (80 hours). Among the European cities, Moscow tops the list, followed by London, Paris.

Thus, the **urgency of modeling and control of saturated traffic flows on complex urban networks is high**. The problems of saturated flows are caused by limited urban road network. The last decade in many cities of the world an Intelligent Transportation System (ITS) is actively being developing, based on the technological revolution in information technologies, the development of wireless networks, high-resolution network video cameras and software, which development is moving toward artificial intelligence. Moscow is also following these trends. In Fig.1 it is shown a map of traffic police cameras, installed in Moscow and the nearest Moscow suburbs. The development of payment systems allows to minimize the time for paying for public transport, but the saturated flows and traffic jams problem of transport mobility of the population still exist.

2. Development of information and communication tools for traffic monitoring

Moscow government is observing these trends. Now, the exponential pace of technological information and communication technology gets possibilities integrating technical means of traffic flows monitoring on complex networks in a large territory with synchronized data transfer to a single center. These opportunities are used by management structures and business corporations, for example, the Yandex-jams internet service in Russia, and the scientific community for research purposes.

The critical situation with traffic jams in Moscow prompted the Moscow government to allocate colossal funds for creating of Moscow ITS in 2011.

As a result, surveillance cameras were installed, software was installed to fix violations of traffic rules and to impose fines on the population. The Moscow government announced this introduction of imported technologies as "Dynamic transport model of Moscow", which is a monitoring of the state in real time with manual control elements (publications in the media by M. Liksutov, A. Polyakov and others). In Fig.1 a map of traffic police cameras, installed in Moscow and the nearest Moscow suburbs is presented. In Fig.2 it is shown the interface of police cameras with recognition elements.

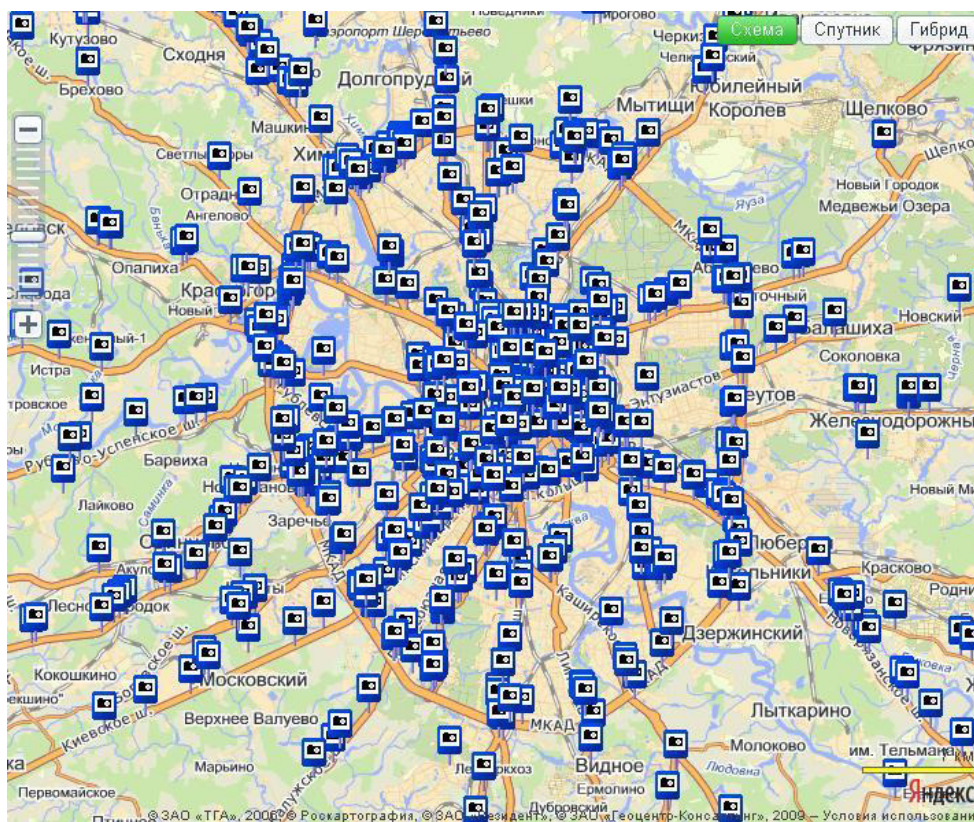
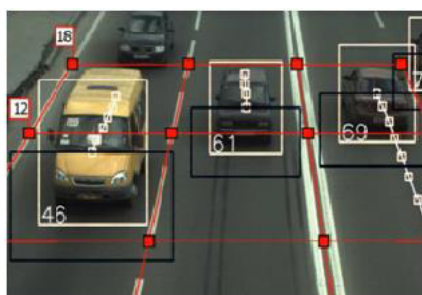


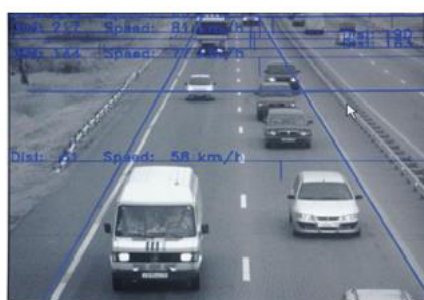
Fig. 1. Moscow scheme of traffic police cameras localization for speed control

The development of payment systems allows to minimize the paying period for public transport, but the saturated flows and traffic jams do not improve the transport mobility of inhabitants. Also a system of paid parking lots is actively being developed, that is also associated with the imposition of fines to inhabitants. As positive results, it can be noted the following:

- 1) Cleaning the main roads from chaotically parked cars, especially in the city centre, where the first lane of central streets was occupied for a long time during the working days,
- 2) Creation of workplaces for manual collection of photo-data in the system of Parcons.



a)



b)

Fig. 2. Monitor interface of police cameras

It must be mention that the main results of Moscow ITS implementation is the financial stream to the city treasury from the fines and the lack of opportunities for the citizens to chargeback in case of the ITS system's mistakes. City officials announce actions of "reducing erroneous fines,"

and the law enforcement agencies open criminal cases of spending money on the creation and operation of ITS Moscow.

Now Big Data in traffic is used in any megalopolises of the Russian Federation. But new situation causes new questions: how to process this information?

Where and what needs to be measured?

What part of the available information is insignificant?

There are no answers to these and similar questions - there is no adequate model for those who are trying to do measurements.

Thus, **robust natural-scientific models of traffic flows on complex networks are relevant.**

For more than a quarter of a century, our department has been working on modeling such systems, as well as methods of pattern recognition in transport.

3. Classification of traffic patterns on complex networks

Analysis of traffic flows theory on networks concludes that **there is no balanced model, describing the traffic on complex networks today.** The classification of developing directions in this area is follows:

Agent models, i.e. short time forecast of movement states: there are too many parameters and rapid accumulation of errors.

Equilibrium models, i.e. averaging over a long period and lack of consideration for the influence of local events in distribution and time.

4. Problems of transport Artificial Intelligence: autonomous car

The development of the technological revolution poses new problems for the scientific community. Intelligent methods are developing in the management of an individual car, computer vision systems are being introduced to ensure safety, dynamic dimensions, and models of automatic driving are developing.

We introduce the following concepts:

CD = Car + Driver,

CR = Car + Robot.

Now the problem of model (replacement) of a separate CD (flow from one car with the driver) to CR is solved in principle.

The scientific problem is **how the saturated CR-flow will behave on the network?** There is no theory!

Even in the case of coherent motion along one band of the CR chain, it is necessary to investigate the properties of a system of nonlinear ODEs (for example, (Buslaev, Kozlov, 2014)).

The model of following the leader of the CR on the network has not been investigated even in this production!

So, whether the saturated CR-flow on the network will be stable? It is not known!

Is it possible to merge CD and CR- flows within the same network?

May be as in the case with **oil and water a mixing of CD-flow and CR-flow is unattainable?** -

5. Spectral analysis of flows on networks

We create a new approach for analyzing traffic on complex metropolitan networks, which allows reducing the number of parameters, introducing a basis in the network space (local and cross-mixing of vehicles), and combining discrete and continual models of coherent flows.

In order to integrate the flow of real data on flow characteristics and the geometry of the road network, our approach is based on the theory of dynamical systems and Markov processes.

The concept of the approach is the following

5.1. The model of the transport network is the contour graph corresponding to the average route assignments-division into local (within contours) and cross-movement (global traffic over the network) (Buslaev et al, 2013)).

5.2. The subject of the movement is the steady cluster - the limiting state of the chain of connected traffic of cars. Clusters represent a compromise between agent and equilibrium models (Buslaev et al, 2016, Bugaev et al, 2011, Kozlov et al 2013).

The developed cluster model of motion allows you to take away the agent models limitations and to explore the qualitative properties of network traffic.

5.3. A system of rules for passing conflict points of contours for clusters is introduced, which reduces either to a dynamical system (Kolmogorov A.N., Arnold V.I.) or the Markov process (Markov A.A.)

5.4. Implementation of IT – researchers are cellular automata by Wolfram, Turing machine for carrying out computational experiments for processing BigData flows using distributed technologies and parallel computations.

5.5. The notion of a flow spectrum is introduced to describe the process of interaction of clusters on regular contour networks in accordance with the theories of Kolmogorov and Markov.

The study of the cluster model of the transport flow on regular networks leads to the concept of the spectrum of a nonlinear system between extreme states: free motion (self-organization) and total stop (collapse).

5.6. The problem of reconstructing the points of the spectrum from the basic data is solved. Technologies are created for automating the restoration of theoretical functions at monitoring measurement points, including using machine vision.

Thus, we obtain an analogue of the Sturm-Liouville theory for traffic flows. Infocommunication technologies and methods of pattern recognition allow on-line capture of information about the sizes and dynamic characteristics of real clusters of cars.

6. Methods of machine vision for the spectral problem of traffic

Our scientific group OMM MADI was formed in the mid-90s of the last century. At this time, Corresponding Member of the Russian Academy of Sciences, the Rector of MADI V.N.Lukanin, a specialist in traffic noise, did formulated the problem of assessing the environmental impact of traffic flows in the case of Moscow. As a result of these studies, methods for describing motor transport flows on complex networks have been developed, and experimental methods for capturing and processing real data on the characteristics of motor transport streams have been developed. The main of these methods are related to image processing and pattern recognition.



Figure 3. Method of virtual detectors

The main characteristics of traffic flows are the density (the number of units of cars per unit length) and the intensity (the number of units of cars per unit of time). These basic characteristics are parameters of the hydrodynamic flow model on networks related to the type of equilibrium models. We developed this model using the example of a transport network in Moscow, so the main one of the first projects for recognizing objects in images was the method of virtual detectors (Buslaev et al, 2005, Buslaev et al, 2010). The interface of the image developed on the basis of this method is shown in Fig. 4. At present, these techniques are implemented in police systems for controlling the speed regime.



Figure 4. Traffic sign recognition

Rules linked to specific points of the road network and to which drivers in streams must obey are installed in the form of road signs. Our scientific group began to develop systems for recognizing road signs from the side of the car in the early 2000s and automatically adding them to the database, Fig. 4. Now such systems have an industrial implementation.



Figure 5. Mobile Laboratory(OTROK) on the base of VWT5 owned by Math.Dept of MADI

For traffic patterns of functional dependencies of intensity and density on time, it is important to have information about flows not at one or several points of the network, but over a sufficiently long distance. To solve such problems, our group is developing a project of the Mobile Traffic Sensor based on the VW T5. Figure 5 shows the mobile laboratory itself, data capture devices installed on the torpeda and students installing optical equipment.

Also we develop the direction of data collection with the help of smartphones. This is the most economical option, it does not require specially equipped cars. A group of research students can simultaneously examine the traffic flow at the points of interest by using mobile applications installed on smartphones with automatic recognition of cars transmitting data to the research server, Fig. 6.



Figure 6. Distributed system with smartphone-client application

To improve the accuracy of video measurements, we develop algorithms for converting signals from virtual sensors, Fig. 7. Thus, a prototype of distributed means for collecting actual data on flows has been created for investigating the spectral properties of the metropolitan traffic network.

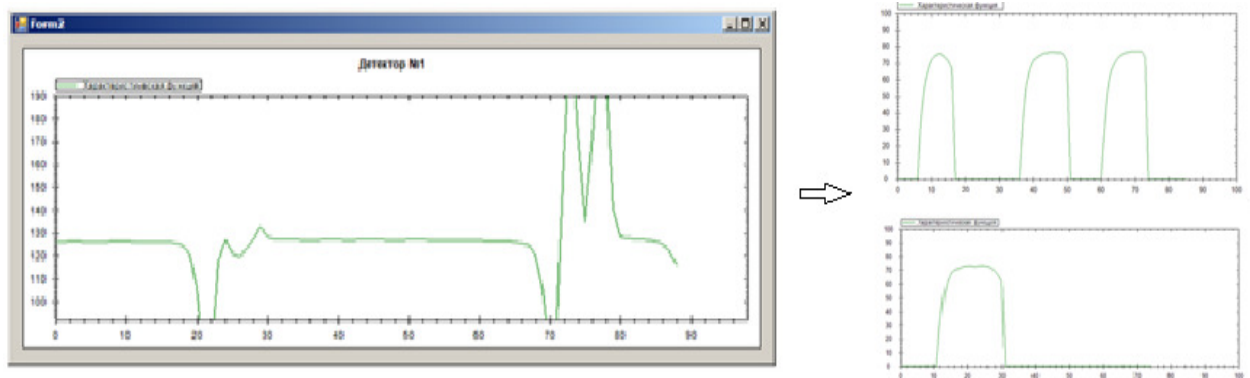


Figure 7. Algorithm of image signal processing for evaluation of traffic intensity

8. Conclusion

The results of studies of cluster models on regular networks have shown that the behavior of such a dynamic system depends not only on the load, but also on the phase.

The problem of finding the points of phase transitions (threshold values) for transport flows on complex urban networks is a priority task of machine vision in ITS systems.

It is established that under a certain load the dynamic system does not enter the self-organization mode. Intellectualization of transport monitoring systems using machine vision should be oriented towards the system's achievement of self-organization regimes and the prevention of states that divert it from this regime.

References

Buslaev A.P, A.G Tatashev, (2016), Bernoulli algebra on common fractions and generalized oscillations, *Journal of Mathematics Research*, 8(3), 82–93.

Buslaev A.P, A.G Tatashev, (2016) On dynamical systems for transport logistic and communications, *Journal of Mathematics Research*, 8(4), 195 – 210.

Bugaev A.S., A.P. Buslaev, V.V. Kozlov, M.V. Yashina (2011), Distributed Problems of Monitoring and Modern Approaches to Traffic Modeling, *14th International IEEE Conference on Intelligent Transportation Systems*, 477-481.

Buslaev A. P., V. V. Kozlov, (2014), On a system of nonlinear differential equations for the model of totally connected traffic, *Journal of Concrete & Applicable Mathematics*, 12.

Kozlov V. V., Buslaev, A. P., Tatashev, A. G. (2013). Monotonic random walks and clusters flows on networks. Models and applications. *Saarbruecken: Lambert Academic Publishing*, 260.

Buslaev A.P., A.G.Tatashev, M.V. Yashina, (2013) Cluster flow models and properties of appropriate dynamic systems, *Journal of Applied Functional Analysis*, 8(1).

Buslaev, A. P., Tatashev, A. G., & Yashina, M. V. (2012) On Properties of the NODE System Connected with Cluster Traffic Model, *Applied Mathematics & Approximation Theory May 17 - 20, 2012–Ankar a–Turkey*, 66

Buslaev , A. P ., Gorodnichev, M. G., Provorov, A. V., & Yashina, M. V. (2016) Quality Properties of Connected Flow Model and Application for Traffic, *International Journal of Applied Mathematics, Electronics and Computers*, 4(4), 136-139.

Buslaev, A. P., Provorov, A. V., & Yashina, M. V. (2013) Infocommunication systems of saturated traffic control in megalopolises. *In Proceedings of the 2013 International Conference on Internet Computing and Big Data (WORLDCOMP13)* 622-625.

Buslaev, A. P., & Yashina, M. V. (2013) On recovery of state parameters of systems via video-images analysis. *Computational and Mathematical Methods in Science and Engineering*.

Buslaev, A., Yashina, M., & Kotovich, I. (2010). On problems of intelligent monitoring for traffic. *Logic Journal of IGPL*, 19(2), 384-394.

A. P. Buslaev, V. V. Dorgan, D. M. Kuzmin, V. M. Prikhodko, V. Ur. Travkin, M. V. Yashina (2005) Image recognition and monitoring of road pavement, traffic flows and movement safety factors. *Vestnik MADI (STU)*, 4, 102–109.

A real-world driving monitoring for 44T Natural Gas & Diesel Heavy Duty Trucks: Equilibre Project first results

F. Baouche¹, B. Schnetzler¹, B. Jeanneret¹, R. Trigui¹, N.-E. El Faouzi¹, Pascal Mégevand²

¹ French Institute of Science and Technology for Transport, Spatial Planning, Development and Networks (IFSTTAR), Lyon, 69500, France

² Mégevand Logictics, Association Equilibre, 01600 Sainte Euphemie, France

Keywords: Natural gas vehicle, heavy Good Vehicles, real driving emissions, fuel consumption.

Abstract

Natural Gas Vehicles (NGV) have received increasing interest in recent years. To anticipate the NGV expansion, a large-scale demonstration project, called Equilibre was launched with the support of the French Environment Agency (ADEME), two gas distribution companies (GrDF & ENGIE) and six Freight Logistics Operators (Equilibre Association).

The main objective of this project is to evaluate the potential benefit of the NGV in real driving conditions. To achieve this, a new approach for the emissions and consumptions analysis is presented.

1. Introduction

The number of in-use projects that are used to hasten the adoption of newer technologies has increased over the last years. The Transnova project studied the energy consumption of a fleet of diesel Heavy Duty Trucks (HDT) in Norway [1]. The study focused on the impact of the drivers' behavior on the energy consumption. In [2], the emissions from seven NGV were measured along major California freight corridors. However, this study measured the pollutants using a full-scale mobile laboratory, which does not correspond to real operating conditions. The Blue corridors project[3] was founded by the European Commission to study the potential benefit of the Liquefied Natural Gas as truck energy. Nonetheless, they were interested in the study of long-haul routes, which represents only 22 % of the actual use of HDT in France[4]. For this purpose, a large scale demonstration project called Equilibre was launched[5]. This project involved the French environment agency (ADEME), the French Institute of Science and Technology for Transport (IFSTTAR), and a gas distribution company GrDF, with the active involvement of six freight logistic operators. This project aims to characterize the in-use emissions and consumption of the newer diesel and Natural Gas Vehicles (NGV).

To achieve this goal emission and consumption of six 44 tons Heavy Duty Trucks (HDT): 3 EURO VI Diesels, two Compressed Natural Gas (CNG) and one Liquefied Natural Gas (LNG) were monitored using Portable Emission Measurement System (PEMS). These trucks were monitored in real-world conditions. In addition to emission and consumption data, operational data (transported load) and context data (e.g. road topology such as altitude, road class...) are collected.

Tableau 1: List of the 44Tons heavy duty trucks

Number	Engine Size	Horse power	Fuel
CNG.1	9L	340 hp	CNG
CNG.2	9L	340 hp	CNG
LNG.1	8L	330 hp	LNG
Diesel.1	13L	500 hp	Diesel
Diesel.2	13L	460 hp	Diesel
Diesel.3	13L	460 hp	Diesel

We assumed that the consumption and CO₂ emission of a HDT mainly depends on three factors: **the frequency of the accelerations**, the total weight and the slope of the road. For this purpose we propose a characterization of the travelled roads based on the cited factors.

This study is based on the assumption that our characterization of the travelled road is a major explanatory factor of consumption and emission. This leads us to construct a road database that covers one third of the French road network. A specific classification of 5 types of **roads sections** has been defined: motorways, country roads, urban expressways, urban crossing and dense urban area.

These categorizations are defined according to the supposed influence of the road characteristics, roadways infrastructure and the mean traffic on **the speed stability** (unstabilized speed involves accelerations and then high fuel consumption). In

the present case, urban planning criteria were used mainly to carry out these categorizations. The relevance of this categorization was confirmed by the results of the experiment.

On the one hand, this classification allows us to study the emissions of the HDT during the rolling phase where we compare CO₂ and NO_x emissions for the six HDTs for different road classes. On the other hand we isolated the maneuvering phases (e.g. customer delivery) where we observed that HDT emissions & consumption are at their highest level.

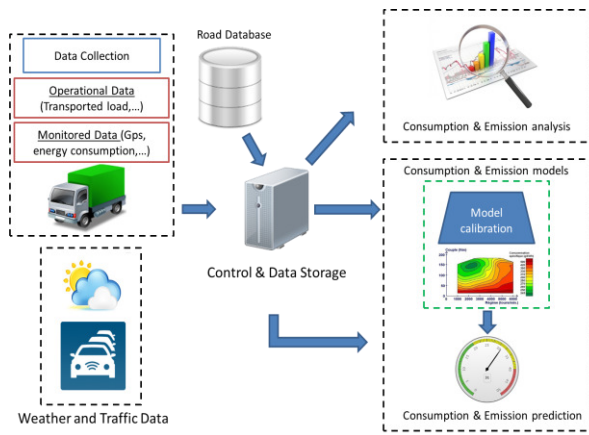


Figure 1: General methodology

In this paper, we aim at investigating the in-use consumption, CO₂ and NO_x emissions of six EURO VI (Diesel and NGV) trucks in order to show the disparities on the fuel consumption and pollutant according to the trucks use and technology.

To that end, a novel approach for the emissions and consumptions analysis is presented in Sec.II. We then target HDT monitoring process in Sec.III. The road database construction is described in Sec.IV. Our results, discussed in Sec.V and Sec. VI summarize the main findings and provide insights about future works.

2. Methodology

2.1. Consumption factors

Many studies have identified various factors influencing energy consumption and pollutant emissions such as: speed (stabilized), accelerations, weather conditions, total laden weight (vehicle weight and transported load), drivers behavior, road type, elevation profile, and traffic conditions [6]–[18]. This paper focuses on the prediction of the mean consumption and pollutant emissions and

therefore on factors which are known several weeks in advance: trip description (roads and elevation profile) and total laden weight.

2.2. Selected factors

In order to identify the consumption and emission influencing factors, we assume that the energy consumption (and pollutant emission) on a mid-length section (the kilometer scale depends on a road section categorization that will be seen below) depends mainly on the speed instability (i.e. high consumption occurs during acceleration phases), the elevation difference and the total laden weight. A preliminary statistical analysis indicated that on such sections the energy consumption is negatively correlated to the *average speed*: figure 2 shows the result of a Principal Component Analysis (PCA) over one year for one vehicle. The PCA is computed on a population set of 125.000 items with 4 variables: *the average speed, the elevation difference, the consumption and the total laden weight*. These variables are computed over road sections with a 4.22 km average length. This negative correlation means that a *low average speed computed on a mid-length section reflects an unstabilized speed*. This is explained by the fact that the average speed of a vehicle accelerating from zero to a 90 km/h (desired) speed is about 45 km/h.

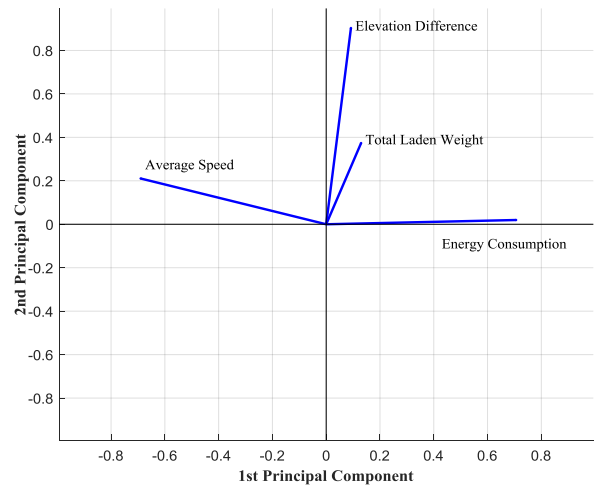


Figure 2: Principal Component Analysis of energy consumption

3. Vehicle data

3.1. On board vehicle instrumentation

As mentioned previously, we collect the on-board data of a fleet of 6 vehicles (3 Diesel and 3 NGV) under actual operating conditions. All trucks are equipped with a PEMS and a GPS device. The collected data include time stamps, GPS position, speed, acceleration, brake use, cruise control use, fuel or gas consumption, CO₂ and NO_x emissions, engine speed, torque, and oil and water temperature. The frequency of the data logger is set to 5 hertz.

Since, the NGV do not have a fuel gauge or a flowmeter, the fuel consumption is calculated from the engine map and the exhaust flow rates.

3.2. Operational data collection

Truck operators provide additional operational data that include transported load, loading and unloading operations, coupling and uncoupling operations, drivers' identifiers and refueling information.

As the gas composition of the NGV varies daily, the chromatographic analyses of the gas stations are provided in order to adjust the energy consumption and emissions. From the data of one year experiment over three gas stations, we observed that the mean value of the lower heating value (LHV) was equal to 47.3 MJ/kg with a standard deviation of 0.36 MJ/kg. Figure 3 shows the methane variation within a month.

The fuel consumption estimation is compared with the refueling information (provided by the transport operators): the accuracy is in order of 1 %.

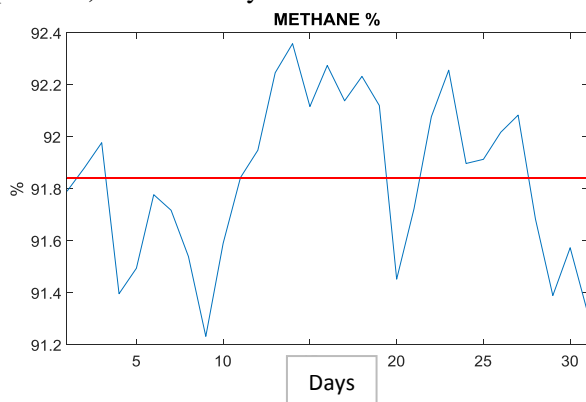


Figure 3: Monthly composition of Methane (January 2016)

4. Road database

4.1. Road data

One of the main contributions of this project is the creation of an enriched road network database that covers one third of the French territory. This database was created using digital maps supplied by the French National Institute of Geographic Information (IGN), which provides a metric precision, and a demographic database from the French National Institute of Statistics and Economic Studies (INSEE) to map each section of the road network to one of the five road classes: motorways, country roads, urban expressways, urban crossing and dense urban area. Although some names are identical, this classification does not match the administrative nomenclature. It is noteworthy that a trip or a road is a sequence of sections of different categories.

The road section categorization is based on the presumed influence on the consumption, which is caused by the presumed speed instability. Figure 4 shows a half-an-hour speed-recording enriched by the road categorization; consumption occurs during accelerations. This instability depends on the road section characteristics but also on the mean traffic flow. These information are deduced from a road network database (topological data and road attributes) and urban data (total population and population density). These categories require some clarification:

- For trucks, a dense urban area does not refer to inner cities (accesses are prohibited) but suburbs of large cities (location of factories and shopping centers) and small towns crossings. A population density criterion was chosen: 1000 inhabitants per km², which yields about 900 French municipalities out of 36,000.
- By definition, an urban crossing zone (very small towns and villages) is delimited by 50 km/h speed limit signs; however, this category is spatially extended before the speed limit sign because the traffic increases when approaching urban areas (in France, this spatial extension can be deduced from urban data).
- The urban expressway definition is based on the same principle as the urban crossing definition. For instance, in France, toll gates, which are located far from the city

borders, provide a discrimination criterion between motorways and urban expressways.

- The country road category is the default value for all the other sections. Therefore, it is quite heterogeneous. For instance, observations show that some country road at the periphery of a large city with a 90 km/h speed limit may have the same consumption characteristics as “urban crossing” with a 50 km/h speed limit. This could be explained by roundabouts crossing, which involve deceleration up to 10 or 20 km/h and have almost the same effect as a stop imposed by a light or a stop sign.

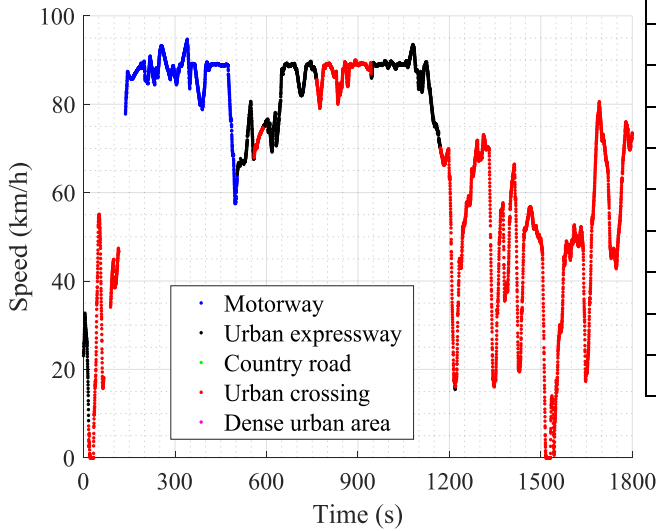


Figure 4: Speed recording

The statistical validity of this road categorization was checked *a posteriori*. Table 2 shows travelled distance, average speed, number of stop & go for a six-month period. The data show that these categories are correlated with the average speed (reflective of the speed instability), the number of ‘stop and go’, and that intraclass variances are low. Note that travelled distances on urban expressways are too low in our database; therefore this class was excluded from the analysis.

Table 2 Statistics according to the road category

Travelled distance (km)				
Vehicle	Motorway	Country road	Urban crossing	Dense urban area
CNG.1	4469	3998	21,398	13
CNG.2	2248	10,444	12,304	79
LNG.1	14,614	1540	1503	1416
Diesel.1	50,513	4620	8503	1875
Diesel.2	18,064	620	3112	19
Diesel.3	36,271	5504	5128	4966
Average speed (km/h)				
CNG.1	80.3	54.3	46.6	33.0
CNG.2	82.1	60.9	40.7	31.6
LNG.1	78.7	53.2	42.1	28.3
Diesel.1	85.3	52.7	44.1	33.5
Diesel.2	80.9	53.6	41.8	35.5
Diesel.3	81.2	53.2	37.7	28.7
Stop & go (number/100km)				
CNG.1	1.0	14.7	31.8	70.2
CNG.2	0.1	3.8	31.1	27.0
LNG.1	0.6	5.1	8.1	75.0
Diesel.1	1.1	15.0	39.1	71.0
Diesel.2	0.8	1.7	33.1	79.6
Diesel.3	0.6	6.9	23.8	79.6

4.2. Topographic data

The elevation profile of a trip has a major impact on the fuel consumption. The IGN Data base provides elevation information for each collected GPS point.

Each section is characterized either by a positive elevation difference ($\Delta Z \geq 0$) or a negative elevation difference ($\Delta Z < 0$). The elevation difference of a trip is expressed by the sum of all positive elevation difference; this criterion takes into account all climbing. Table 3 provides mean values of the elevation difference for each vehicle during the experiment; note that over long distances $\sum \Delta Z_+ + \sum \Delta Z_- = 0$.

TABLE 3: Positive elevation difference ratio per kilometer

Truck	ΔZ +/-100km			
	Motorway	Country road	Urban crossing	Dense urban area
CNG.1	0,56	0,84	1,01	0,85
CNG.2	0,22	0,46	0,46	0,49
LNG.1	0,72	0,58	0,82	0,48
Diesel.1	0,42	0,70	0,84	0,74
Diesel.2	0,68	0,90	1,63	0,77
Diesel.3	0,71	0,51	0,90	0,55

To summarize, given GPS positions, a map-matching algorithm locates a vehicle on a road map. The road map provides the elevation difference. Then the vehicle trip is split in consecutive homogeneous sections: same road category, same sign of the elevation difference and same laden weight. The average length of a section ranges from a few tens of meters in urban area to a few kilometers on motorways.

5. Consumption & emissions analysis

The main contribution of this paper is to highlight the disparities of the fuel consumption and pollutant according to truck use and road type, especially in urban areas. The first part of the analysis focuses on the comparison of the six vehicles according to their fuel and CO₂ emissions. The second part deals with the NO_x emissions.

This comparison allows an overview of the emissions and fuel consumption according to mission types and used routes. However, the journeys made by the six vehicles are far from being representative of all cases on the French national territory.

The vehicles CNG.1 and CNG.2 perform local distribution whereas the others vehicles perform long haul missions. The vehicles CNG.1, LNG.1, Diesel.2 and Diesel.3 run in mountainous area.

In this study, the trucks missions have been described by some observable variables (laden weight, elevation difference and road category) which are the main explanatory factors for the consumption and pollutant emissions. Traffic is also a main explanatory factor, but it is not directly observable and depends on time: the road categorization, which spatially extends the urban crossing and urban expressway categories, takes into account a presumed mean traffic.

Finally, we excluded the urban expressway from the analysis because of the low mileage on this type of section, which is not likely to obtain significant results.

5.1. Fuel consumption and CO₂ emission

The Motorway class represents more than 70% of the use of diesel vehicles of the project. The average consumption varies between 24.4 and 31.7 l / 100km. The high consumption of the Diesel.3 could be explained by the significant elevation difference in the highway part of the route (0.71km / 100km, cf. Table 3). However, the positive elevation difference variable does not fully explain the fuel consumption, as can be seen with the Diesel.2, which has an average value of (0.68 km/100 km), but which shows an average consumption lower than that of Diesel.1 (0.42km/100km). Several factors could explain this result: a slightly higher average PTC (+3 tons), a lower average speed (81 km/h vs 85 km/h), traffic, meteorological factors, or improved fuel efficiency of the engine used on Diesel.2 due to high frequencies of high engine torque uphill.

Table 4 shows three different uses of NGV on motorways with a clear disparity in the average consumption. This example shows the impact of the elevation difference (cf. Table 3), which is one of the main factors influencing the consumption of heavy duty trucks: there is a lower consumption (-24%) between CNG.2 (0.22 km/100km) and LNG.1 (0.72 km/100km). even though the total laden weight is greater for CNG.2 (32.7 tons) than for LNG.1 (28.7 tons).

TABLE 4: Energy consumption according to the road category

Energy consumption (NGV: kg/100km ; Diesel: l/100km)				
Vehicle	Motorway	Country road	Urban crossing	Dense urban area
CNG.1	24.3	29.2	36.1	38.5
CNG.2	21.1	25.2	32.3	39.6
LNG.1	29.4	37.7	-	37.2
Diesel.1	27.3	35.8	39.7	37.9
Diesel.2	24.4	-	33.7	-
Diesel.3	31.7	42.9	39.7	44.7

The country roads account for 40% of the use of the vehicle CNG.2 with a total of 10.444 km. Its average consumption (25.2 kg /100km) is the lowest for this type of road. This can be explained by the low elevation difference in altitude (0.46km / 100km).

The CNG.1 has an average consumption of 15% above the CNG.2, despite a lower PTC (23.8 t compared to 28.0 t). Here again the difference in altitude (0.84km/100km vs 0.46km/100km) could explain this consumption.

There is a large difference in consumption between the Diesel.3 vehicle and Diesel.1 (42.9 l/100km and 35.8 l/100km), which cannot be explained by the altitude difference, the average speed, or by the total laden weight. The same type of overconsumption (37.7 kg/100 km and 29.2 kg/100 km) is observed between the LNG.1 (which travels the same route as the Diesel.3) and the CNG.1. This parallel allowed us to assert that the characteristics of the road borrowed by both LNG.1 and Diesel.3 explained this overconsumption. Factually, a microscopic analysis proved that the overconsumption occurred on roads located at the periphery of large cities (with speed limits up to 90 km/h), particularly after roundabouts.

A roundabout which involves a deceleration up to 10 km/h has the same effect as a traffic light on consumption. This example highlights the existence of large disparities within the “country road” categorization.

Eventually, the greater consumption was observed in the dense urban area (from 37.2 to 39.6 kg/100km for the NGV and from 37.9 to 44.7 l/100km for the diesels).

To conclude, these preliminary results show high consumption variability depending on the vehicle use (roads, elevation profile and laden weight). Moreover some main explanatory factors depending on time (prevalent meteorological conditions, prevalent traffic) are not taken into account. Currently, these dependences on the vehicle use and temporal factors prevent comparisons of technologies or any judgement on the fuel consumption efficiency of a freight logistic operator.

TABLE 5: CO2 Emission Statistics according to the road category

Truck	CO ₂ (kg/100km)			
	Motorway	Country road	Urban crossing	Dense urban area
CNG.1	66.9	80.3	99.3	106.0
CNG.2	60.8	69.4	88.9	108.8
LNG.1	80.9	103.8	-	102.3
Diesel.1	73.6	96.6	107	102.4
Diesel.2	66	-	91.0	-
Diesel.3	85.5	115.9	107.1	120.7

It should be remembered that CO₂ emissions are directly correlated with consumption (cf. Table 5). We observe a slight advantage for the NGV. If we compare the LNG1 and Diesel.3 (which carried out the same missions), the Diesel.3 emits 6.25% more than the LNG.1. However, it should be remembered that the LNG.1 develops 330 hp vs 460 hp for the Diesel.3.

5.2. NO_x Emissions

It is important to stress that the depollution technologies differ for the Diesel vehicles. The Diesel.1 and Diesel.2 are equipped with a selective catalytic reduction and an exhaust gas recirculation system. The Diesel.3 has only a selective catalytic reduction system. The measurements presented below include the cold start phases.

Note that from our measurements, we could check that all vehicles satisfy the Euro 6 norms.

The main conclusions from Table 6 are:

- Lower NO_x emissions for NGV
- Emission levels in urban area are three to nine times higher than emissions levels on motorway.

TABLE 6: NO_x Emission Statistics

NO _x (g/100km)				
Truck	Motorway	Country road	Urban crossing	Dense urban area
CNG.1	8.9	24.8	39.4	53.1
CNG.2	9.7	17.9	40.0	42.4
LNG.1	12.3	56.2	-	109.1
Diesel.1	34.4	80.6	112.5	125.9
Diesel.2	32.5	-	117.0	-
Diesel.3	27,7	45,3	82,7	174,9
NO _x (mg/kWh)				
CNG.1	63.7	146.4	189.4	252.0
CNG.2	73.3	124.6	216.2	198.0
LNG.1	81.6	301.3	-	572.1
Diesel.1	301.8	520.7	629.0	759.8
Diesel.2	326.0	-	734.4	-
Diesel.3	217.5	267.5	470.6	805.5

To conclude: NO_x emissions are very sensitive to accelerations (use of the acceleration pedal) because depollution systems are less effective during transient period. Therefore NO_x emission levels are very high in urban or mountainous areas.

However, NO_x emissions in urban areas have major impact for health reasons. The problem is that norms based on mean values of emissions (the current ponderation is 55 % for motorway) are not representative of emission in urban area.

5.2.1. NO_x emission of the Diesel.3

The initial period of the experiment proves a failure of the depollution system. Then the vehicle has been serviced by the manufacturer and table 6 reports measurements done later.

Table 7 reports emissions during a six-month period before the vehicle review. Emission levels are two to five times higher.

TABLE 7: NO_x Emission Statistics for six month experiment

Diesel.3 NO _x emissions (mg/kwh)				
	Motorway	Country road	Urban crossing	Dense urban area
g/100km	117.7	233.8	278.8	367.1
Mg/kwh	758.4	1233.7	1468.3	1719.3

5.3. Maneuver consumption & emission

The results presented above concern the fuel consumption during the rolling phase. However, the vehicles perform multiple maneuvers such as: coupling and uncoupling the trailer and docking.

The consumption and emissions during maneuver phases are very high: for NGV the mean consumption is around 1kg/km and NO_x emission is in order of 1g/km.

The extra consumption depends on the nature of the mission: long haul mission with few loading operation or local distribution with higher rates of loading operation. (cf. Table 7 and Table 8). However most of these operations are performed in suburban area.

TABLE 7: Number of load and unloading/100km

Number of load/unloading	
CNG.1	3,35
CNG.2	1,73
LNG.1	1,03

TABLE 8: Energy consumption, driving phase vs maneuver phase (in kg)

Consumption (kg)			
Vehicle	During maneuver (kg)	Total consumption (kg)	Consumption during maneuver (%)
CNG.1	906	12262	7,4
CNG.2	1093	9116	11,9
LNG.1	199	6612	3,0

6. Conclusion

This study presents an overview of a recent on-road measurement project that measured the fuel and pollutants emissions of NGV and Diesel heavy duty trucks. Preliminary results of the Equilibre project confirm the expected results: lower NO_x emissions for NGV vehicles than for Diesel vehicles. Others results highlight that consumptions and emissions heavily depend on the vehicle use: roads, elevation profile, laden weight and maneuvers. This proves that mean values are meaningless and that future norms should be based on more realistic cycles.

Moreover, given numerous explanatory factors (most unknown) and a wide range of values, a monitoring of the efficiency (for fuel consumption and emission reduction) is not easily attainable.

Finally, the main explanatory factor is a road categorization which identifies urban zone and near area. Not only fuel consumption and NO_x emissions heavily depend on traffic and roadways infrastructures, in the vicinity of conurbations, but pollutant emissions do not start or end at the speed limit signal delimiting the urban zone. This implies that consumption in urban areas is much higher than an estimate based on average values and on a restrictive definition of an urban area.

Reference

- [1] “Transnova 2012. Transnova for bærekraftig mobilitet. Prosjektrapport etter 3 år.” Trondheim, 2012.
- [2] D. C. Quiros *et al.*, “Real-World Emissions from Modern Heavy-Duty Diesel, Natural Gas, and Hybrid Diesel Trucks Operating Along Major California Freight Corridors,” *Emiss. Control Sci. Technol.*, vol. 2, no. 3, pp. 156–172, Jul. 2016.
- [3] J. Dominguez, F. Mariani, M. Maedge, X. Ribas, and E. Van Gysel, “LNG Blue Corridors position paper,” 2015.
- [4] FNTR, “Les « chiffres blancs » du TRM français - FNTR.” [Online]. Available: <http://www.fntr.fr/espace-documentaire/chiffres-cles/les-chiffres-blancs-du-trm-francais>. [Accessed: 05-Jul-2017].
- [5] “Equilibre Project.” [Online]. Available: <http://www.projetequilibre.fr/>. [Accessed: 05-Jul-2017].
- [6] K. H. Kozawa, S. S. Park, S. L. Mara, and J. D. Herner, “Verifying emission reductions from heavy-duty diesel trucks operating on southern California freeways,” *Environ. Sci. Technol.*, vol. 48, no. 3, pp. 1475–1483, 2014.
- [7] C. Guo, Y. Ma, B. Yang, C. S. Jensen, and M. Kaul, “EcoMark,” *Proc. 20th Int. Conf. Adv. Geogr. Inf. Syst. - SIGSPATIAL '12*, p. 269, 2012.
- [8] H. Rakha and K. Ahn, “Closure to ‘Estimating Vehicle Fuel Consumption and Emissions based on Instantaneous Speed and Acceleration Levels’ by Kyoung Ahn, Hesham Rakha, Antonio Trani, and Michel Van Aerde,” *J. Transp. Eng.*, vol. 129, no. 5, pp. 579–581, 2003.
- [9] S. Pandian, S. Gokhale, and A. K. Ghoshal, “Evaluating effects of traffic and vehicle characteristics on vehicular emissions near traffic intersections,” *Transp. Res. Part D Transp. Environ.*, vol. 14, no. 3, pp. 180–196, May 2009.
- [10] W. Zeng, T. Miwa, and T. Morikawa, “Prediction of vehicle CO₂ emission and its application to eco-routing navigation,” *Transp. Res. Part C Emerg. Technol.*, vol. 68, pp. 194–214, 2016.
- [11] Huanyu Yue, “Mesoscopic fuel consumption and emission modeling,” Faculty of the Virginia Polytechnic Institute and State University, 2008.
- [12] T. J. Laclair and R. Truemner, “Modeling of Fuel Consumption for Heavy-Duty Trucks and the Impact of Tire Rolling Resistance,” *Engineering*, no. 724, 2012.
- [13] W. Dib, A. Chasse, P. Moulin, A. Sciarretta, and G. Corde, “Optimal energy management for an electric vehicle in eco-driving applications,” *Control Eng. Pract.*, vol. 29, pp. 299–307, Aug. 2014.
- [14] W. Dib, A. Chasse, D. Di Domenico, P. Moulin, and A. Sciarretta, “Evaluation of the Energy Efficiency of a Fleet of Electric Vehicle for Eco-Driving Application,” *Oil Gas Sci. Technol. – Rev. d’IFP Energies Nouv.*, vol. 67, no. 4, pp. 589–599, Sep. 2012.
- [15] M. Boujelben, R. Trigui, F. Badin, S. Ardizzone, and D. Escudie, “Modeling and optimization of a plug-in hybrid urban microbus,” in *2008 IEEE Vehicle Power and Propulsion Conference, VPPC 2008*, 2008.
- [16] H. Rakha, K. Ahn, and A. Trani, “Development of VT-Micro model for estimating hot stabilized light duty vehicle and truck emissions,” *Transp. Res. Part D Transp. Environ.*, vol. 9, no. 1, pp. 49–74, 2004.
- [17] K. Chen, R. Trigui, A. Bouscayrol, E. Vinot, W. Lhomme, and A. Berthon, “A common model validation in the case of the Toyota Prius II,” in *2010 IEEE Vehicle Power and Propulsion Conference, VPPC 2010*, 2010.
- [18] E. Vinot, J. Scordia, R. Trigui, B. Jeanneret, and F. Badin, “Model simulation, validation and case study of the 2004 THS of Toyota Prius,” *Int. J. Veh. Syst. Model. Test.*, vol. 3, no. 3, pp. 139–167, 2009.

Effects of Driving Behaviour on Fuel Consumption

V.A.M. Heijne^{1}, N.E. Ligterink¹, U. Stelwagen¹.*

1 Research Group Sustainable Transport and Logistics, TNO, PO Box 96800, 2509 JE Den Haag, the Netherlands, veerle.heijne@tno.nl

Introduction

Deviations in fuel consumption are hotly debated. Car manufacturers give low reference values, drivers may have poor driving styles, congestion will increase the fuel consumption, and different measures, such as traffic smoothing and driver instructions, are presented with large fuel-saving benefits. To disentangle all these aspects and to determine the baseline and bandwidth of personal driving styles on fuel consumption, driving styles have been monitored in a large European project: UDRIVE.

A vehicle's fuel consumption during a specific trip depends on several aspects, such as:

- infrastructure (traffic lights, roundabouts, lane width, road surface, etc.);
- congestion and other road users;
- personal driving style;
- vehicle type and condition (mass, engine size, number of gears, tyre pressure, etc.);
- engine and drivetrain technology;
- fuel type;
- ambient conditions (weather).

Most of these aspects require a change in technology, infrastructure or transport demand to result in lower fuel consumption and therefore lower CO₂ emissions. Partly because it is the only parameter with immediate impact on CO₂ emission reduction, personal driving style is a popular fuel saving measure. However, the potential effect of changes in driving behaviour is hard to determine, mainly because a good description of the distribution of average driving behaviour is lacking. The current paper reports results from recent studies on European driving behaviour and its relation to fuel consumption, such as the eco-driver analysis in the UDRIVE project (Heijne et al., 2017) and a TNO study on driving behaviour in several European countries (Ligterink et al., 2017)

Central to the distinction of personal driving styles is the separation of driving behaviour enforced by the environment on the one hand, and the remaining personal choices and anticipatory behaviour on the other hand. To assess the fuel consumption reduction potential, it is crucial to separate personal driving style from the other factors mentioned above, of which the infrastructure, speed limits, and degree of congestion are the main influences.

A traffic light or a car ahead may require a driver to brake, but in some cases braking is unnecessary or can be avoided by keeping more distance or through better anticipation. Within the UDRIVE project an effort was made to untwine the different aspects that may lead to a higher fuel consumption. If one can successfully do this, the remaining bandwidth of personal driving styles, between the worst and the best performing driver, determines the potential room for fuel saving related to more economic driving behaviour. The three main aspects that are evaluated are braking, gear shifting behaviour and personal speed choice.

The overall objectives of the UDRIVE eco-driver study (Heijne et al., 2017) were firstly to improve the understanding of the variation in driving styles and the contribution of different driving styles to "average" driving behaviour in relation to eco-driving, and secondly to assess the fuel consumption and the CO₂ emission reduction potential associated with adopting an eco-driving style. This should improve insight in the overall net potential for eco-driving at the national and EU level, by studying different parts of the driver population, different road types and traffic situations, and different vehicle applications.

Eco-driving in the context of this study denotes a driving style associated with low fuel consumption. Some practical examples of an eco-driving style are:

- shift gear up as soon as possible, between 2000 and 2500 revolutions per minute;
- anticipate traffic flow (to minimise dynamics and limit braking);
- maintain a steady speed;
- decelerate smoothly by coasting.

Combining the results of the driving style analysis with fuel consumption measured in other studies allows detailed analysis of the impact of different driving styles on fuel consumption and emissions. This analysis provides valuable insight in mechanisms that contribute to the current environmental footprint (CO₂) of the EU transport sector.

Measurements of European driving behaviour

UDRIVE

A monitoring programme with random participants across Europe, UDRIVE, forms the basis for a large dataset that was analysed for eco-driving characteristics in normal vehicle use. Unique to UDRIVE, compared to the generic collection of velocity data of random drivers such as the WLTP (Worldwide harmonised Light vehicles Test Procedure, Marotta et al., 2012) database, is the augmentation of the velocity data with driving circumstances, such as road type, speed limits, headway, and in-vehicle information. This allows for placing the behaviour in context and distinguishing personal driving behaviour from driving behaviour forced by local traffic conditions. Figure 1 for example shows how instantaneous velocity measurements can be categorised into different speed limits.

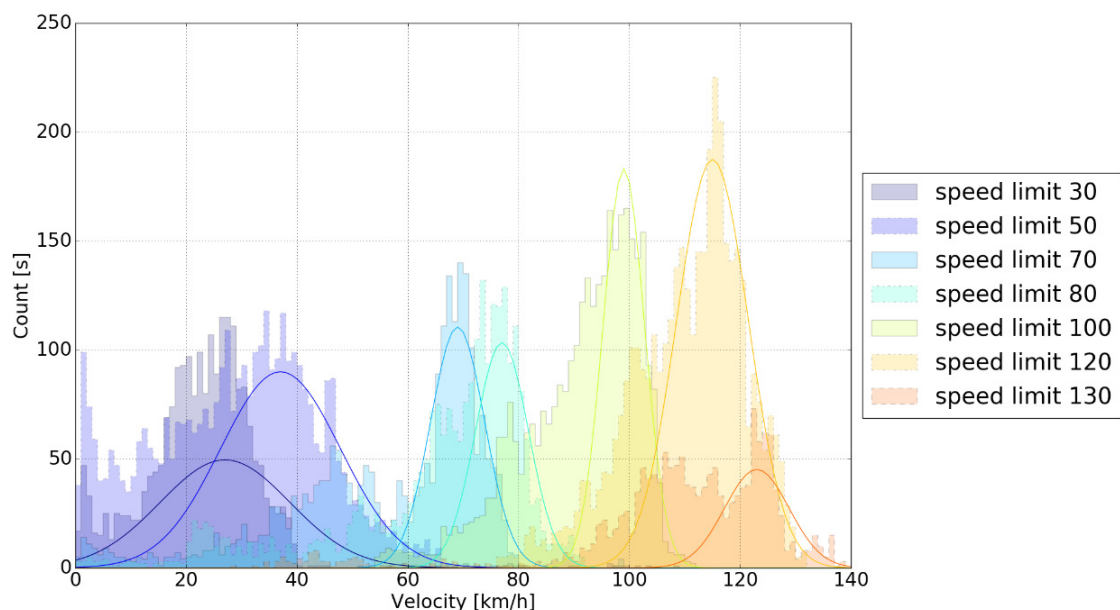


Figure 1: Velocity distribution per speed limit, for one driver in The Netherlands, with fits of the most likely velocity distribution per speed limit (Heijne et al., 2016).

The UDRIVE dataset used for this analysis contains about 13,500 hours of naturalistic, i.e. uninstructed, driving data, distributed over more than 150 drivers. More details about the data set can be found in Table 1. Although the total number of drivers is enough to draw significant conclusions, the statistical noise is expected to become substantial when dividing them in subcategories such as driver nationality or age. The analysis of eco-driving characteristics addresses the average behaviour of the driver, as extracted from the complete time series signals for each driver comprising typically hundreds of hours per driver. The most distinguishing parameters are combined to determine an eco-driving score per driver. Finally, the significance of the deviation of the residuals with respect to average driving behaviour is determined. For a given road type or speed limit, the infrastructure and degree of congestion will be the main

influence on the fuel consumption during a trip. The difficult task is to uncover the remainder, the personal driving style that can be improved by a fuel economic driving style.

The added value of the eco-driving study within the UDRIVE project is substantial, due to the sample of different drivers distributed over different EU regions and the possibility to analyse driving styles in detail for particular driving conditions, using the additional recorded parameters, and relate them to actual vehicle emissions. The availability of large amounts of continuous 1 or even 10 Hz signals allows for better analysis of correlation between variables, and a lower statistical uncertainty than previous studies. This gives more insight in the mechanisms that cause fuel consumption than given by studies performed so far such as the European Eco-driver project (Saint Pierre et al., 2016). Furthermore, the quantity of naturalistic driving data acquired in UDRIVE was never reached in earlier eco-driving studies.

Table 1: Characteristics of the UDRIVE dataset available in April 2017 (Heijne et al., 2016).

country	total time [h]	total distance [km]	number of drivers	v_{avg} per driver [km/h]
United Kingdom	4240	216397	50	56.9
Germany	903	48047	17	60.9
The Netherlands	1035	65945	16	62.0
France	5358	282495	43	63.5
Poland	2128	114284	28	65.5
total	13665	727169	154	61.3

TNO chase car study

A test programme was set up to determine normal driving behaviour by randomly following vehicles across The Netherlands, Germany, France, and Belgium using a high-powered passenger car with automatic transmission (Ligterink et al., 2017 R10436; Ligterink, 2016 R10188). The velocity signal and latitude and longitude information were recorded, along with a radar signal to study potential differences between the velocities of the subject vehicle and the instrumented vehicle. An appropriately large headway distance was used, such that the actions, i.e., braking and acceleration, of the subject vehicle were not enhanced by the car follower. This way, all driving behaviour was determined in the same period, producing a coherent picture across different traffic situations and road types. Each country has data for at least three working days of driving, covering urban, rural and motorway driving. The car was instrumented with a camera to record license plate data in the Netherlands to investigate the dependencies in driving behaviour with the power-to-mass ratio of the vehicles. All trips were driven by the same experienced and well-instructed driver to prevent the introduction of a bias.

These studies have two purposes. First, to determine normal driving on the road for average emissions, such that the emission data from different measurement programmes can be weighted appropriately with the traffic situations as they occur on the road. The second purpose is to establish whether normal driving is sufficiently incorporated in the Real Driving Emissions (RDE) legislation, which prescribes how vehicles are to be tested on-road for the type-approval in Europe. If there is too much deviation between normal driving on the road and normal driving for RDE, the RDE legislation may not be as effective as it should be to avoid high emission risks.

Average driving behaviour

The TNO chase car study revealed that no single average driving style on either EU or national levels exists; a broad range of driving behaviours has been observed. In order to sufficiently cover 'normal' driving behaviour, RDE boundaries should allow for inclusion of this broad range. Driving dynamics vary significantly among countries. The highest dynamics and the widest span in driving behaviour were observed in Belgium. Very likely it is linked to the infrastructure, city planning and congestion levels.

The typical road usage and a few average characteristics retrieved from the UDRIVE data are shown in Table 2. On average, Polish drivers have the highest average velocity, whereas Dutch

drivers drive most of their kilometres on motorways. Again, the spread between individual drivers is very large, resulting in large differences in dynamics as discussed in the next section.

Table 2: Characteristics of driving on different road types within UDRIVE (Heijne et al., 2016).

country	distance urban	distance rural	distance motorway	V_{avg} [km/h] urban	V_{avg} [km/h] rural	V_{avg} [km/h] motorway
United Kingdom	36%	21%	31%	24	52	91
Germany	40%	20%	36%	28	70	91
The Netherlands	22%	11%	59%	25	52	91
France	37%	30%	27%	25	60	97
Poland	51%	16%	17%	26	78	104
total	38%	22%	31%	25	60	95

Variation in driving styles

To define personal driving styles, the UDRIVE eco-driving study looked at the occurrence and necessity of braking, gear shifting behaviour and the amount and the reason why drivers deviate from the speed limit in free-flow situations. Free-flow within UDRIVE is defined as the situation in which there is no vehicle detected in front of the subject car by the camera-measurement of headway. The resolution of the headway signal was not sufficient to accurately measure the velocity of the vehicle in front, or to detect vehicles at a distance over 20 meters.

Since braking translates in a loss of propulsion energy, the fuel consumption will be lower if braking can be safely avoided. The braking energy has a significant contribution to the total energy consumption at low velocities. Clear differences can be seen between different drivers in the amount of braking energy lost. One expects that the more headway a driver keeps, the less he needs to brake because he has time to anticipate the traffic. Indeed, UDRIVE showed that drivers who keep a larger time headway (either due to personal driving style or due to the absence of traffic), tend to lose less energy in braking. Also, the higher the instantaneous velocity, the lower the average time headway and the amount of hard braking. The same conclusion can be drawn when comparing braking and headway averages for all drivers. Drivers lose most energy through braking when driving at low velocities and in urban areas. The bandwidth between drivers is very large, up to 70% from the average, or 120% between the best and worst driver. When selecting only straight road sections without intersections and without a vehicle in front, the braking energy does not decrease with respect to the full data sample, although the difference between individual drivers increases. This indicates a larger difference in personal driving style, independent of driving circumstances.

The difference between better and worse eco-driving behaviour is most easily recognised in a gear shifting analysis. There is a large bandwidth in average engine speed at the gear shifting moment between drivers. The eco-driver advice is to change gear between 2000 and 2500 RPM, but drivers range from 1400 to 3000 RPM, depending somewhat on the vehicle type and the gear, but mostly on the drivers themselves. Table 3 shows the average and extreme values of the engine speed when changing gear, grouped per vehicle type and gear.

Table 3: Average and range of engine speed at the gear shifting moment, for different vehicle categories in the UDRIVE experiment (Heijne et al., 2016).

variable	gear	Clio III	Clio IV	Mégane
average engine speed [RPM]	2	1987	2034	1952
	3	2169	2196	2127
	4	2167	2115	2108
	5	2127	2074	2012
	6	-	-	1964
engine speed range min-max [RPM]	2	1391-2647	1418-2776	1452-2696
	3	1520-2903	1583-3079	1622-2742
	4	1546-2787	1530-2743	1610-2767
	5	1634-2974	1532-2698	1660-2731
	6	-	-	1543-2813

The difference between drivers with respect to the most frequent velocity is up to 20 km/h from the speed limit, both below and above it. Figure 1 gives an example of the velocities at different speed limits for a single driver. The variation in velocity, which causes extra fuel-consuming dynamics, shows an even larger spread, up to 50%. The selection of straight road sections without intersections and without a vehicle in front does not yield significantly different results for dynamics. The question why drivers deviate from the speed limit remains unanswered, since there is no clear correlation with road obstructions or congestion. A more detailed study of driving circumstances, for example by looking at velocity behaviour in very specific traffic situations, could yield more information on the reason for the personal speed choice. A more reliable definition of free-flow (data excluding congestion and infrastructural obstructions) would give a cleaner free-flow velocity distribution that better represents the driver's personal style.

In the TNO car chase study (Ligterink et al., 2017 R10436), the vehicle's velocity was the main signal used to parameterise driving behaviour. In the context of vehicle emission regulation, driving behaviour is commonly characterised in terms of velocity and acceleration: $v^*a_{pos}(95\%)$ is defined as the value of the 95% percentile of the highest values among the positive values of velocity times acceleration. This value is determined separately for three velocity ranges: 0-60 km/h, 60-90 km/h, and above 90 km/h. With an increase of $v^*a_{pos}(95\%)$ the polluting emissions of older vehicles, like Euro-2 and Euro-3, increase dramatically. The 95% percentile is to ensure the result is independent of the length of the trip. The longer the trip, the higher the probability that a high v^*a_{pos} value is encountered, while the 5% highest values remain more or less the same. Only the number of samples that make up this 5% grow with the length of the trip.

Figure 2 to Figure 5, where each point represents one trip of typically 40-50 km, reveal that no average driving exists; a broad range of driving behaviours has been observed over the various trips. Driving dynamics vary significantly among countries. The highest dynamics have been observed in Belgium (Figure 2). A significant number of Belgian trips was well above the $v^*a_{pos}(95\%)$ limit value for the new Real Driving Emission regulation, depicted with a black line. The average speed during urban driving was frequently below the lower limit of 15 km/h, most strikingly demonstrated in the Paris trips. This stop and go traffic is frequently observed in densely populated areas with high traffic density. Higher (or absence of) speed limits in a county are not necessarily reflected in high dynamics, as is the case for Germany (Figure 4).

The results of the UDRIVE eco-driving study can also be expressed in $v^*a_{pos}(95\%)$, see Figure 6. Here, each point represents the average of one driver with at least 10 hours of data. This gives a better indication of the spread between individual drivers than the car chase study. The results of both studies agree that there is a wide spread in driving dynamics.

P95th of V*Apos for Belgium

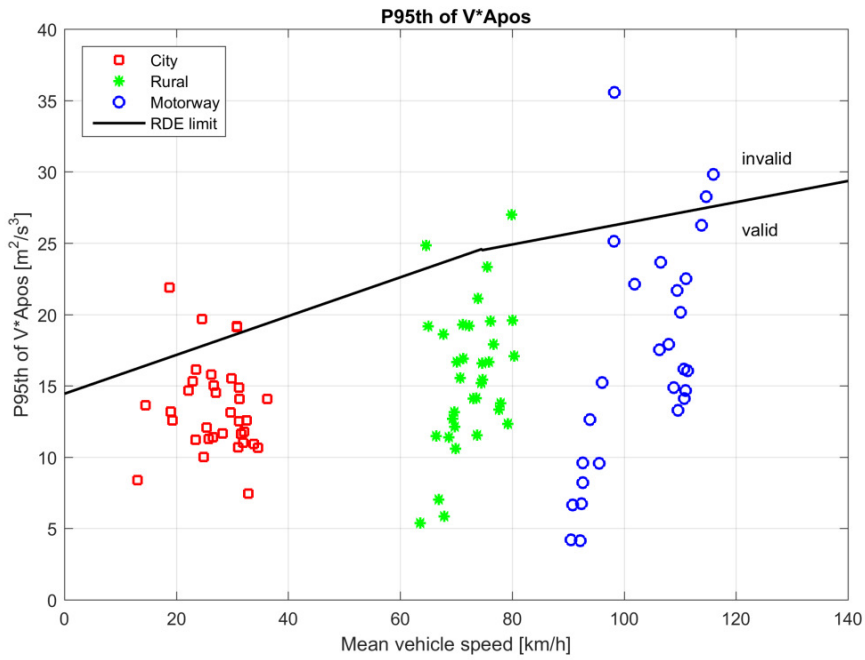


Figure 2: The v*a positive [m²/s³] values per trip of the car chase tests in Belgium (Ligterink et al., 2017 R10436)

P95th of V*Apos for France

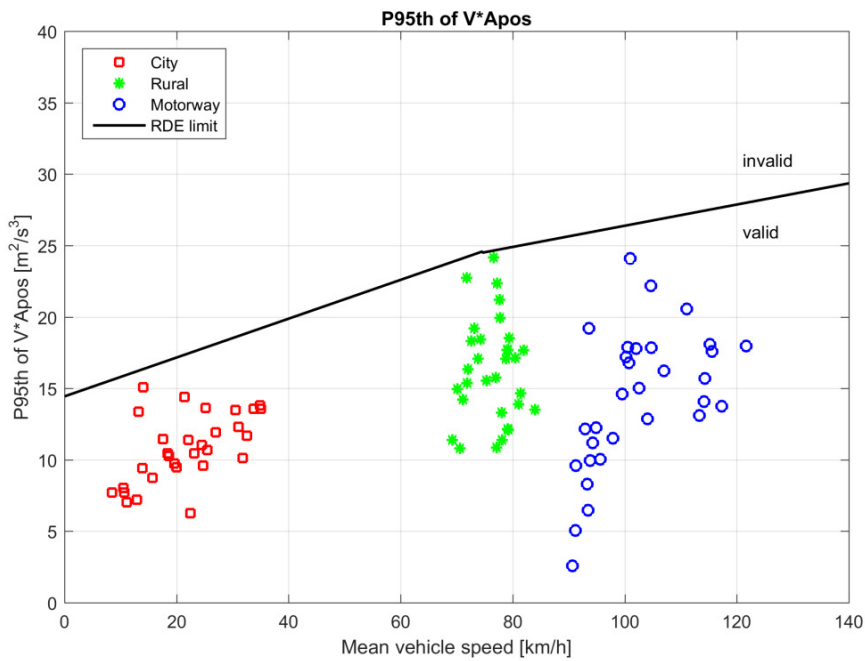


Figure 3: The v*a positive [m²/s³] values per trip of the car chase tests in France (Ligterink et al., 2017 R10436).

P95th of V*Apos for Germany

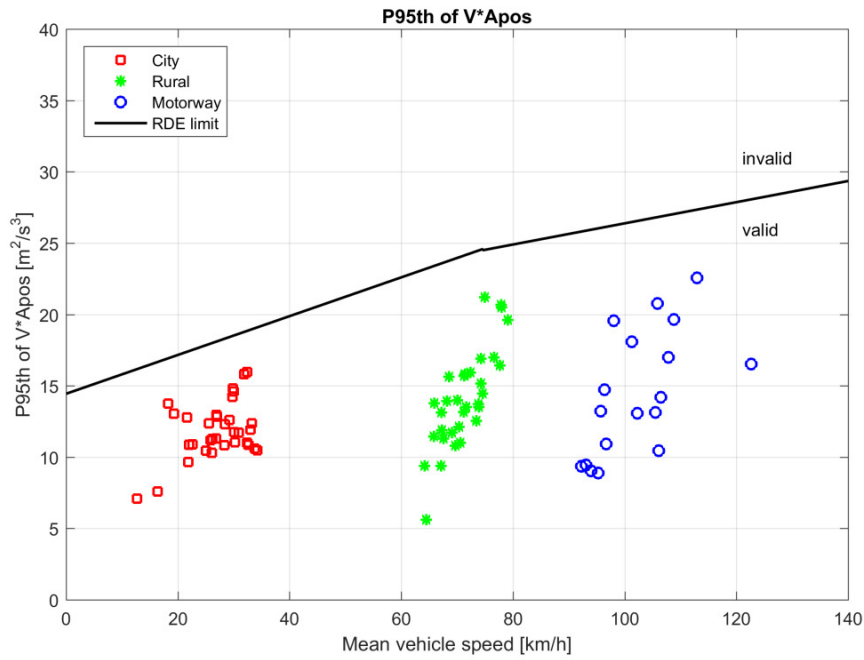


Figure 4: The v*a positive [m²/s³] values per trip of the car chase tests in Germany (Ligterink et al., 2017 R10436).

P95th of V*Apos for Netherlands

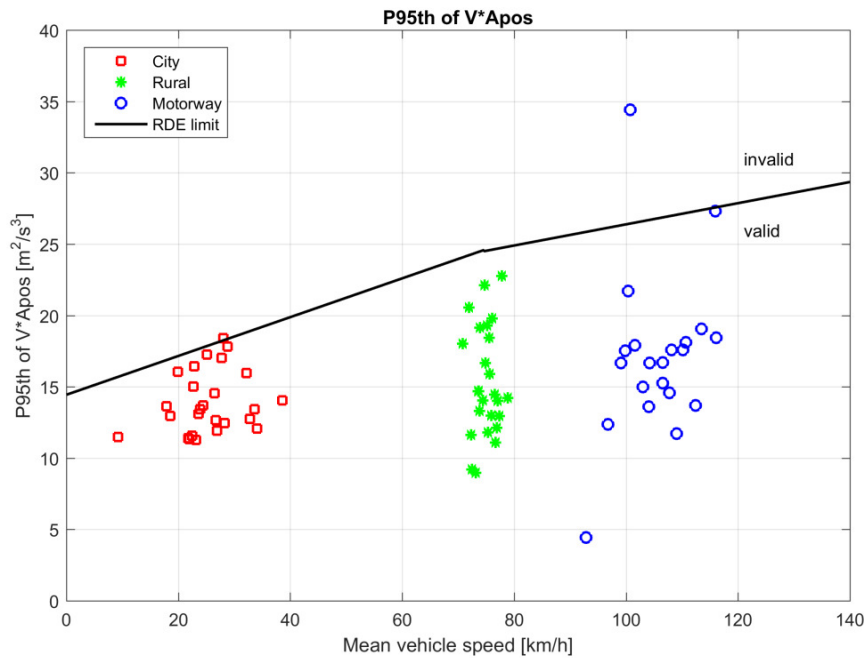


Figure 5: The v*a positive [m²/s³] values per trip of the car chase tests in The Netherlands (Ligterink et al., 2017 R10436).

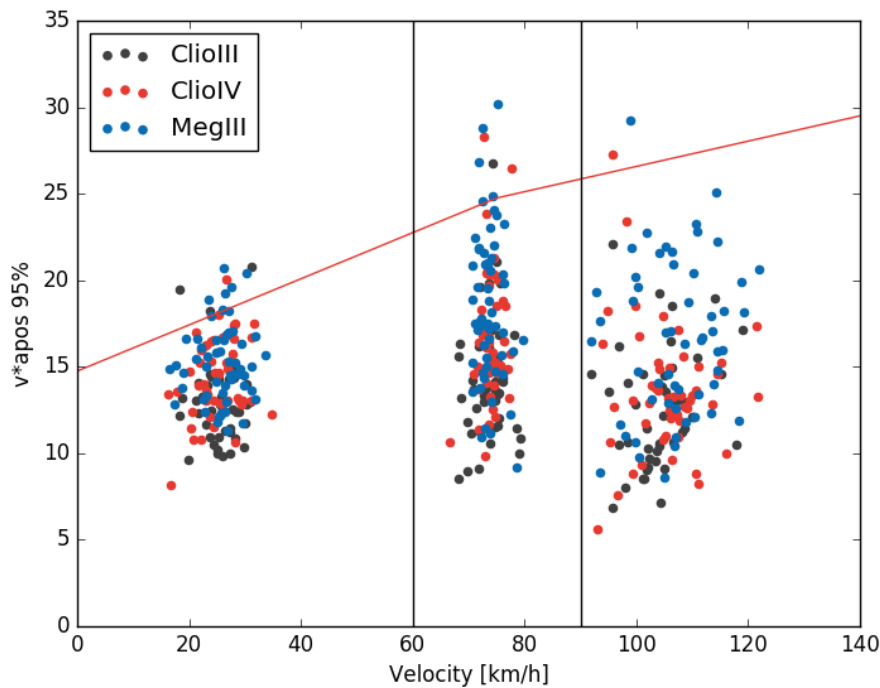


Figure 6: The $v \cdot a$ positive [m^2/s^3] per driver, in three different velocity ranges, coloured per vehicle type. Each point represents the average of one car driver in the UDRIVE experiment. The red line indicates the current upper limit for the Real Driving Emission legislation (Heijne et al., 2016).

Relation between driving behaviour and fuel consumption

The UDRIVE study aims to study driver aspects of fuel efficiency that are unrelated to the vehicle technology. The energy consumption through braking, the additional air-drag forces at high velocities, and the higher engine losses with higher engine speeds are the three main types of energy demand associated with additional fuel consumption for the same mobility demand. The rolling resistance remains invariant for different driving styles. These factors are expected to be independent of the vehicle type whereas other effects on fuel consumption may change with technology. In UDRIVE, fuel consumption was not logged, to prevent a bias in the conclusions due to vehicle technology. Other studies are used to relate driving behaviour to fuel consumption.

TNO performed several test programmes in which the CO_2 emission was logged during real-world driving. The CO_2 emission test results of on-road test trips of ten Euro 5 light commercial vehicles are shown in Figure 7. In real-world tests the CO_2 emissions per kilometre were 7% to 52% higher than the declared CO_2 emissions in the type approval tests (Kadijk et al., 2016). On top of that, the driving behaviour and payload were varied, resulting in significantly different fuel consumption values. An even larger effect due to payload and driving style is observed for Euro 6 light commercial vehicles, as shown in Figure 8 (Kadijk et al., 2017). All the Euro 6 trips were Real Driving Emission trips driven on equal or comparable routes within a few weeks' time, comprising equal amounts of urban, rural and motorway driving. Studies like these indicate that for the same road type and driving conditions, basically the same trip, the fuel consumption can increase by almost 50% depending on the particular usage, including driving style, of the vehicle.

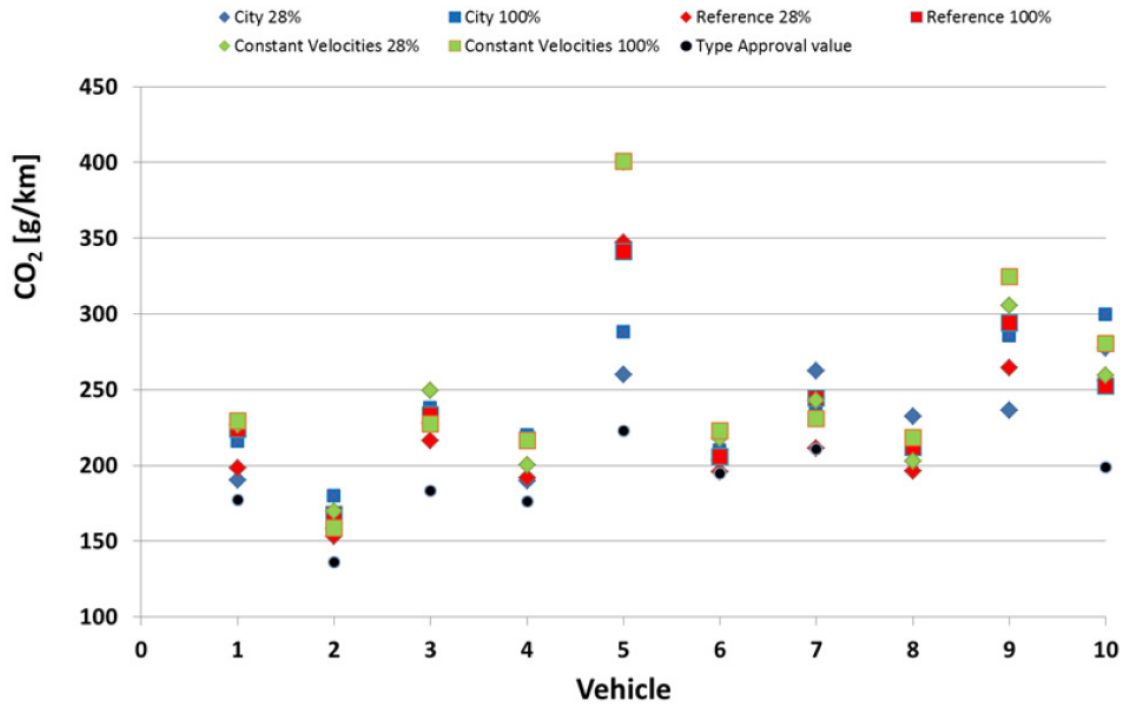


Figure 7: CO₂ emissions per trip for ten Euro 5 light commercial vehicles. Source: (Kadijk et al., 2016)

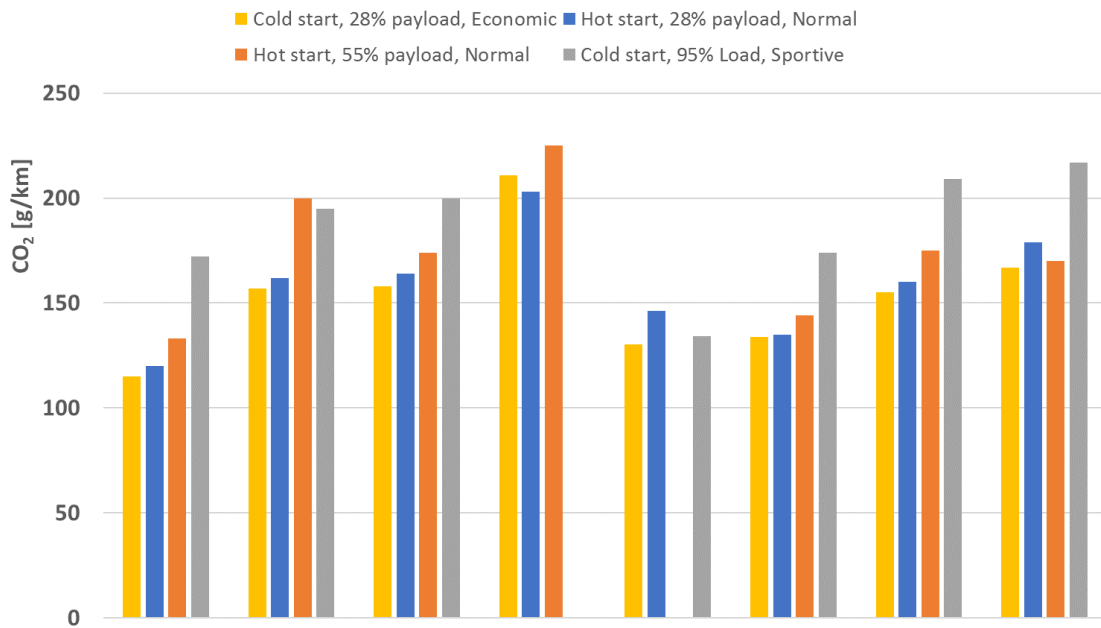


Figure 8: CO₂ emissions of RDE trips with different payloads and driving styles of 8 light commercial vehicles. Source: (Kadijk et al., 2017)

To isolate the effects of driving style from the influence of payload, one vehicle was measured in more detail, using a combination of payloads and driving style instructions. The results are shown in Figure 9. For this vehicle, payload has least influence on the fuel consumption, judging from the emissions with two different payloads under ‘normal’ driving circumstances. There is however a clear dependency on the instructed driving style. The sportive trips on average emit 46% more CO₂ than the eco-trips. Although the driver was instructed to adapt a certain driving style in this test programme, described in (Kadijk et al., 2017), the variation in dynamics corresponds well with the variation in naturalistic driving studies such as UDRIVE. The effects on fuel consumption

might therefore be of a similar magnitude in the real world. Consequently, citing a single number for fuel consumption ignores the many factors on which such a number depends, not only the route.

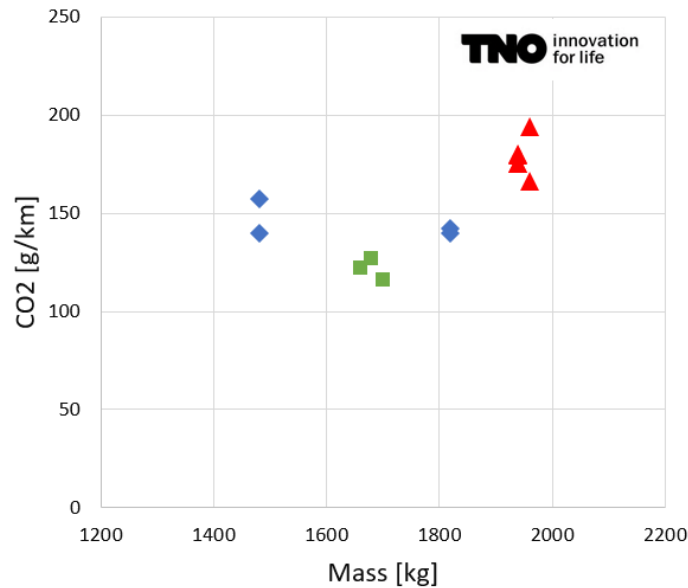


Figure 9: CO₂ emissions per trip for RDE trips with different weights (x-axis) and driving styles: eco (green squares), normal (blue diamonds) and sportive (red triangles). All trips are driven by the same Euro 6 light commercial vehicle.

A way to quantify the driving behaviour in the UDRIVE study is to combine several energy-consumption-related parameters to define an eco-driving score that can be used to make an overall comparison between drivers. This facilitates a translation of the differences in driving style into differences in fuel consumption. The following characteristics are used:

- braking energy at 50-60 km/h;
- engine speed at the gear shifting moment from second to third gear;
- most frequent (peak) velocity at speed limits between 95 and 120 km/h;
- width of the peak around the most frequent velocity at speed limits between 95 and 120 km/h;
- weighted mean of the absolute acceleration at speed limits between 95 and 120 km/h.

The residual percentages with respect to the average of all drivers are averaged to give an eco-score that is negative for better and positive for worse than average eco-drivers. Since it is expected that a correction for driving circumstances has a large influence on driving behaviour, a selection is made on free-flow circumstances (based on headway) excluding trajectories with bends and intersections. Such a grouping of driving style-related parameters can be used to compare individual drivers with the average. The set of 150 drivers can be dissected into different categories, enabling a study of the dependency of eco-driving behaviour on factors such as country, driver age or vehicle type.

Vehicle specifications and technologies may limit the effects of certain driver behaviour. For example, an automatic transmission will remove the driver's influence on engine losses almost completely. A recuperation of braking energy in hybrid vehicles will reduce the braking losses to some extent. High velocities, above 100 km/h, are always associated with additional air drag and fuel consumption, almost independent of the vehicle technology. When grouping the UDRIVE eco-scores by vehicle, Figure 10 is retrieved. The Clio IV shows the 'best' economic driving, and the Mégane the worst. The difference between the vehicles can either be caused by different driving behaviour in those vehicles, or by the larger engine and vehicle size.

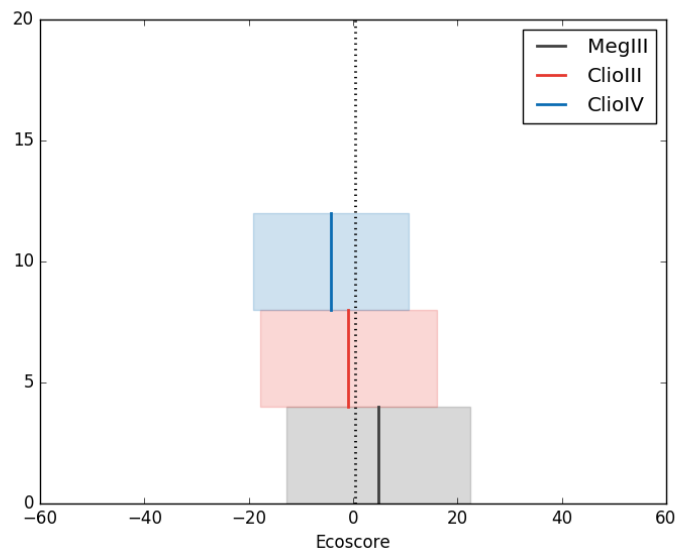


Figure 10: Residual ecoscore with respect to average of all drivers in the UDRIVE project, grouped per vehicle type, for straight sections and freeflow conditions. The shaded area denotes the standard deviation of the underlying ecoscore distribution.

Other studies by TNO investigate these aspects from different angles. The general assumption underlying the Real Driving Emissions legislation is that the power-to-mass ratio does not affect the driving style, and that despite the high v^*a attainable with high powered vehicles, these high values are seldom reached in normal driving. The limits for aggressive driving were set at a fraction of the maximal attainable values for a modern average European car, which have considerable engine power compared to older cars. The 2015 study of driving behaviour in the Netherlands (Ligterink, 2016 R10188) showed different results. Accelerations, in particular accelerations at lower vehicle speeds, turned out to be much higher than assumed based on average driving behaviour derived from the WLTP database.

The study in (Ligterink et al., 2017 R10436) concluded that high powered vehicles show higher dynamics, expressed as v^*a , at higher v^*a values, but less dynamics at lower v^*a values. Between 90% and 95% percentiles of v^*a values, there is a crossover where all vehicle classes, independent of their engine power, show similar dynamics. The limited amount of data, about half an hour each for the three vehicle segments, restricts the conclusions from this test. A minor effect is observed for different power-to-mass vehicles, but it is not significant at the scales under consideration.

Potential reduction effect of eco-driving

The 'eco-score', as defined in UDRIVE and explained above, shows a large spread for the different drivers, as becomes clear from Figure 11. The potential effect of eco-driving can be estimated given the bandwidth in driving styles (or in this study: eco-score) between drivers, after correcting for driving circumstances. The 80% difference between drivers indicates that eco-driving, as defined by this score, is an observable characteristic of certain drivers. It should be noted however, that fuel consumption does not linearly depend on this eco-driving scoring. To get more insight in this dependency, the potential effects on fuel consumption due to the different driving style parameters studied in the UDRIVE project are discussed below.

The braking energy is a significant contribution to the total energy consumption at low velocities. The rolling resistance and air drag ask about 200-300 kJ/km in urban driving for average passenger cars. This means that braking energy, in the order of 300-800 kJ/km, is for most drivers the main energy consumer at the low velocities, larger than rolling resistance and air drag. The difference in lost braking energy between the best and worst driver is in the order of 120%, resulting in a difference in energy consumption of up to 10%.

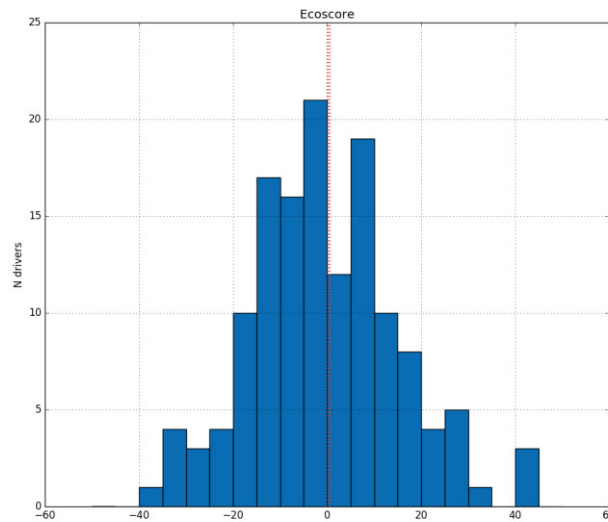


Figure 11: Distribution of eco-driving scores of all drivers, for straight sections and free-flow conditions.

The engine losses are not negligible for passenger cars. Idling in urban areas occurs for 15% of the time, within a bandwidth of 0-50%. The idle CO₂ emission associated with low engine losses is typically 0.3-0.5 g/s. At 36 km/h, these minimal losses are associated with a substantial 30-50 g/km additional emissions, unrelated to the propulsion. When driving at higher engine speeds, above idling at 800-1000 RPM, the engine losses increase. It is expected that losses increase more than proportionally with engine speed, and that a 200 RPM higher engine speed will increase the engine losses with 10%-20%. The relative effect on total fuel consumption depends on the velocity.

Some drivers shift gear much earlier than others, also in the same type of vehicle. The bandwidth of engine speed when changing gear varies between 1400 and 3000 RPM for different drivers. This large bandwidth in gear shifting behaviour means there is quite some room for improvement by better eco-driving behaviour. The estimated difference in fuel consumption due to different engine speeds can be up to 20-25%.

In conclusion, the three aspects braking, gear shifting and the velocity choice on the motorway, all have effects on the fuel consumption of 10% or higher for a traditional vehicle.

Discussion

In this paper, complementary studies on naturalistic driving are brought together to reach a synthesis. The different studies have limitations in the recorded signals and augmentation of the data, such that it is not completely possible to attribute fuel consumption variation to different aspects. However, some major aspects, such as braking and gear shifting are quantified to a certain extent.

Due to the large number of aspects affecting eco-driving, such as velocity, braking, and gear-shifting, and the large number of underlying parameters, such as country, driver, road type, speed limit, and infrastructure, the amount of data in the UDRIVE experiment, by nature of this complexity, is limited for each specific combination. Grouping the results with respect to country, driver age or gender do not yield strong correlations that are with certainty independent of infrastructure, vehicle type and other factors. Due to the limited number of drivers per individual country, the results are not statistically significant. The more general the results, such as the velocity distribution around the speed limits on the motorway, the more data can be combined.

This yields more robust results that can be generalised to the European average with more confidence. The major drawback of these generalisations is the limited traffic information which may cause an unknown bias. The poor quality of the headway signal is the main culprit to the problems to separate different traffic situations that affect driving behaviour.

Generalisability of the UDRIVE results to a European average is possible for generic results. However, there are many correlations and underlying dependencies causing possible biases on driving behaviour, on which there is limited information in the study. Specifically, such a generalisation would assume that the traffic situations are representative for the European average. From other studies (e.g. Marotta et al., 2012; Ligterink et al., 2017), it is also clear there is a substantial variation in driving behaviour from country to country.

For more statistically significant results, in future naturalistic driving data collection one should include more different drivers and more different vehicle types, even if this means that less data is available per driver. Besides that, one must ensure a well-calibrated and continuous headway signal is available, along with other crucial parameters such as road gradient, vehicle payload and road surface. The reliance on video and CAN signals for such a study has many limitations.

Conclusion

The three aspects braking, gear shifting and the velocity choice on the motorway, all have effects on the fuel consumption of 10% or higher for a conventional technology vehicle. The UDRIVE study does not attempt to arrive at a generic number, as it would depend strongly on the vehicle technology. Very likely, in the last twenty years the influence of the driver on the fuel consumption has decreased significantly with technology improvements. It is very likely this trend will continue. On the other hand driver behaviour does not evolve quickly over time, save for changes in the capabilities of the vehicle and in the traffic rules.

References

- Heijne, V.A.M., Ligterink, N.E., Stelwagen, U. (2017), UDRIVE deliverable 45.1 Potential of eco-driving of the EU FP7 Project UDRIVE (www.udrive.eu)
- Heijne, V.A.M., Kadijk, G. et al. (2016), NOx emissions of fifteen Euro 6 diesel cars: Results of the Dutch road vehicle emission testing program 2016. TNO report R11177.
- Kadijk, G., van Mensch, P., Ligterink, N.E., (2016) Variations of real world NOx emissions of diesel Euro 5 and 6 light-duty vehicles. *TAP Lyon conference proceedings*.
- Ligterink, N.E., Cuelenaere, R.F.A, Spreen, J. S. (2017), Chase car study: driving behaviour in the Netherlands, Belgium, France and Germany. TNO report R10436.
- Ligterink, N.E. (2016), On-road determination of average Dutch driving behaviour for vehicle emissions. TNO report R10188.
- Marotta, A., Tutuianu, M., Martini, G. (2012), Task 7 Europe-centric light duty test cycle and differences with respect to the WLTP cycle. JRC technical report.
- Saint Pierre, G., Brouwer, R., et al. (2016), D43.1 Eco driving in the real-world: behavioural, environmental and safety impacts. ecoDriver project.
- Kadijk, G., Heijne, V.A.M., Ligterink, N.E., (2017) Variations of real-world NOx emissions of diesel light commercial vehicles. *TAP Zurich conference proceedings, to be published*.

Research of Emissions with Gas PEMS and PN PEMS

J. Czerwinski¹, P. Comte¹, Y. Zimmerli¹, L. Cachon², E. Remmele³ and G. Huber³

¹University of Applied Sciences, 2500 Biel-Bienne, AFHB^{*}, Switzerland

²Testo SE & CO. KGaA, Titisee – Neustadt, Germany

³TFZ Straubing, Germany

Keywords: PEMS, PN PEMS, RDE, LD-vehicles, flowmeter, slope

Presenting author email: jan.czerwinski@bfh.ch

Abstract

Measuring and controlling of real driving emissions (RDE) of passenger cars with PEMS (portable emission measuring systems) is an actual requirement.

In different projects the Laboratory for Exhaust Emissions Control (AFHB) of the Berne University of Applied Sciences (BFH) performed comparisons on passenger cars with different PEMS's on chassis dynamometer and on road, considering the quality and the correlations of results. A system measuring the particle number (PN PEMS) was also included in the investigations.

This paper presents: the experiences with PN PEMS, the comparisons of Horiba OBS1 with SEMTECH, the correlations of Pitot flowmeter on engine dynamometer and influences of slope on chassis dynamometer.

The most important statements are:

PN PEMS, which is based on DC-classifier (DiSC) indicates higher PN-values, than the stationary CPC, but these results can be validated and adapted by means of WLTC on chassis dynamometer.

The investigated GasPEMS indicate higher values of CO₂, than the stationary installations.

The flowmeters show the biggest dispersion of results in the lowest flow-range, which is typical for idling.

Varying slope has clear influences on emissions and must be considered in the measuring procedures.

The presented works brought further insight in improving the procedures and the quality of results.

Introduction

Measurement of Real Driving Emissions (RDE) becomes since this year (2017) an element of legal homologation procedure for passenger cars WLTP (Worldwide Harmonized Light-Duty Vehicles Test Procedure), [1, 2, 3]. This new procedure will enforce for new cars (introduced to the market since this year), that there will be no discrepancy between the emissions and fuel consumption values obtained in the homologation tests and in real application, [4, 5].

Unlike previous vehicle emission tests, parameters such as engine load and vehicle speed are no longer defined by a fixed pattern, but are largely

determined by the traffic situation, driver behaviour and the course of the route during the RDE test. [6, 7, 8].

There is a change of paradigm for all market players:

First of all, the manufacturers have to adapt their R&D processes to meet with the calibration of engines and of exhaust systems the extreme multitude of operating conditions which may occur. There are efforts and possibilities to use dynamic engine- or chassis test benches, equipped with specific software, to fulfil the requirements of new development tasks, [6, 9, 10, 11].

An important requirement is the continuous improvement and development of measuring technics, both: for laboratory and for on-road testing, [12]. Since 2015, the portable particle number measuring systems (PN PEMS) have been tested and introduced in the activities of development and legislation, [13].

The official testing laboratories and organisations perform intense research activities in order to increase the knowledge, the experience and to adapt the testing capacities to the new requirements, [4, 5, 7, 8, 14].

The RDE legislation is divided into four packages:

The first package of RDE legislation requires an on-the-road test of up to 2 h, including urban, rural and motorway journeys with clearly specified conditions, which will allow effective evaluation of the emissions produced. The second package of the legislation determines the NO_x emission limits using a conformity factor (CF). The third RDE package extends this conformity factor to the particle number (PN) emissions limit and outlines the relevant requirements for measuring technology (PN-PEMS). The legislation package as a whole also covers cold starts, particulate filter regeneration and validation of hybrid vehicles. The fourth and final RDE package defines in-service conformity testing as well as surveillance tests carried out by third parties.

The independent surveillance test procedures, called New Periodical Technical Inspection (NPTI) are actually a subject of research and discussions, [15, 16]. These procedures have to be adapted to the actually used exhaust aftertreatment and OBD technologies.

In this interesting dynamic situation of progress AFHB performs several test & research projects, or working packages. Some of the recent results are presented in this paper.

Test installations

Chassis dynamometer

Parts of the tests were performed on the 4WD-chassis dynamometer of AFHB (Laboratory for Exhaust Emission Control of the Bern University of Applied Sciences, Biel, CH).

The stationary system for regulated exhaust gas emissions is considered as reference. This equipment fulfils the requirements of the Swiss and European exhaust gas legislation.

- regulated gaseous components:
 - exhaust gas measuring system Horiba MEXA-7200 CO, CO₂... infrared analysers (IR)
 - HC_{FID}... flame ionization detector for total hydrocarbons
 - CH_{4FID}... flame ionization detector with catalyst for only CH₄
 - NO/NO_x...chemiluminescence analyzer (CLA)

The dilution ratio DF in the CVS-dilution tunnel is variable and can be controlled by means of the CO₂-analysis.

The measurements of summary particle counts in the size range 23-1000nm were performed with the CPC TSI 3790 (according to PMP).

For the exhaust gas sampling and conditioning a ViPR system (ViPR...volatile particle remover) from Matter Aerosol was used. This system contains:

- Primary dilution - MD19 tunable rotating disk diluter (Matter Eng. MD19-2E)
- Secondary dilution – dilution of the primary diluted and thermally conditioned sample gas on the outlet of evaporative tube.
- Thermoconditioner (TC) - sample heating at 300°C.

The overview of used PEMS is given in [Table 1](#).

Table 1. Overview of used measuring systems.

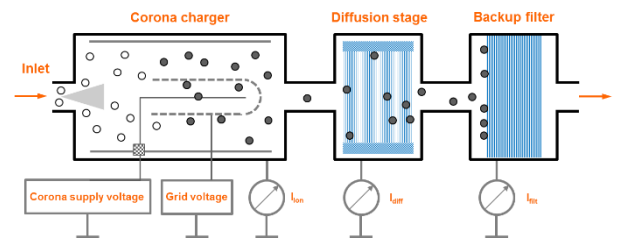
GAS PEMS

	HORIBA MEXA 7200	HORIBA OBS ONE	SEMTECH
	4x4 chassis dyno CVS	PEMS⊙ wet	PEMS⊙ dry
CO	NDIR	heated NDIR	NDIR
CO ₂	NDIR	heated NDIR	NDIR
NO _x	CLD	CLD	calculated
NO	CLD	CLD	NDUV
NO ₂	calculated	calculated	NDUV
O ₂	-	-	
HC	FID	-	electrochemical
PN	not measured	-	-
OBD logger	-	yes	yes
GPS logger	-	yes	yes
ambient (p, T, H)	yes	yes	yes
EFM	-	pitot tube	pitot tube (SEMTECH- EFM)

OBS - one H₂O monitored to compensate the H₂O interference on CO and CO₂ sample cell heated to 60°C

PN PEMS

As PN PEMS for Real Driving Emissions the NanoMet3-PS from Matter Aerosol-TESTO (NM3) was used. The exhaust gas conditioning, as described above for chassis dynamometer, is integrated in this analyzer and it indicates the solid particle number concentration and geometric mean diameter in the size range 10-700 nm. TESTO NanoMet3 presents several advantages like compactness, robustness, fast on-line response and it has been considered in the preparatory activities of on-coming RDE type approval in EU as a “Golden Instrument” (see [1]). This instrument works on the diffusion charging classifier principle (DiSC), which is represented in [Fig. 1](#).

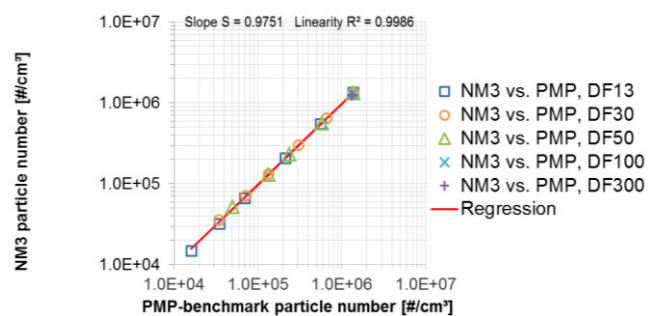


[Source: Testo]

Figure 1. Setup of the particle sensor DiSC

Operating principle of DiSC:

- Particles are labeled with positive charges in a unipolar charger, so that they can later be detected by the current they induce.
- Particles are deposited by diffusion in a "diffusion stage" and detected as an electrical current $D = I_{diff}$; Diffusion stage penetration is size-selective.
- Remaining particles end up in a filter stage and also produce an electrical current $F = I_{filt}$.
- DiSC Sensor measures both currents D and F simultaneously, with 1s time resolution.
- Measured ratio $D/F = I_{diff} / I_{filt} \rightarrow$ particle diameter.
- Charge per particle is a function of particle diameter \rightarrow once the particle diameter is known, DiSC computes the particle number from the total current $I_{diff} + I_{filt}$ and the flow rate.
- Diffusion charger DC signal correlates well with lung-deposited (alveolar or tracheobronchial) surface area.



[Source: Testo, PMP]

Figure 2. Correlation NanoMet 3 vs. PMP (GDM 70 nm; CAST soot generator)

The correlation of readings with a PMP-benchmark is very good. Example of a correlation at geometric mean diameter (70nm) is given in Fig. 2.

Engine test bench

The test engine used for comparisons of the flowmeters was an Iveco F1C engine with following data:

Manufacturer:	Iveco, Torino Italy
Type:	F1C Euro 3 / Euro 4
Displacement:	3.00 Liters
RPM:	max. 4200 rpm
Rated power:	100 kW @ 3500 rpm
Model:	4 cylinder in-line
Combustion process:	direct injection
Injection system	Bosch Common Rail 1600 bar
Supercharging:	Turbocharger with intercooling
Emission control:	none
Development period:	until 2000 (Euro 3/Euro 4)

The test bench is equipped with:

- Dynamic test dynamometer Kristl & Seibt
- Tornado Software Kristl & Seibt
- Fuel flow measurement AIC 2022
- Air mass meter ABB Sensiflow P
- Pressure transducers Keller KAA-2/8235, PD-4/8236
- Thermo-couples Type K.

There is also extensive equipment for measurement of legislated and non-legislated exhaust emission components, which was not used and will not be more specified for this part of work. Since this engine test stand is accredited according to ISO 17025, the used flowmeters, as well as all used measuring chains are subject of a continuous calibration and quality control.

Test Procedures

Driving cycles on chassis dynamometer

The vehicles were tested on a chassis dynamometer in the dynamic driving cycles: WLTC, Fig. 3, NEDC Fig. 4 and CADC, Fig. 5. The first WLTC of each test series was performed with cold start (20-25°C) and further cycles followed with warm engine. Between the cycles, always 3 minutes of constant speed of 80 km/h, in 4th gear, were performed as conditioning.

The braking resistances were set according to legal prescriptions; they were not increased i.e. responded to the horizontal road.

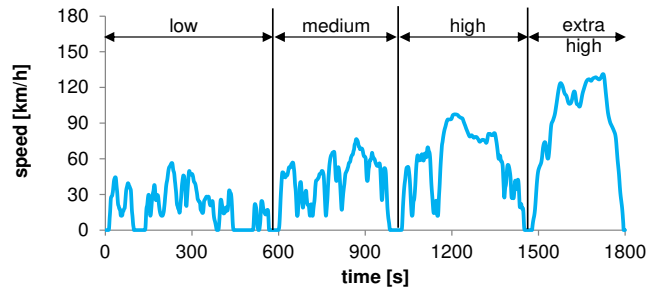


Figure 3. WLTC driving cycle

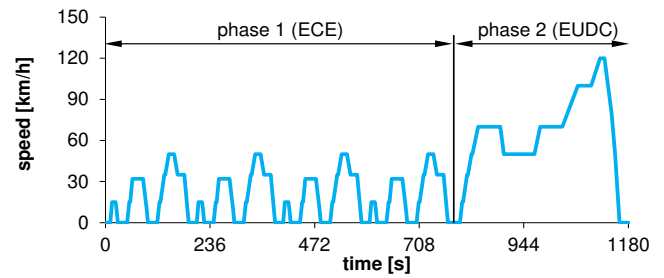


Figure 4. NEDC European driving cycle

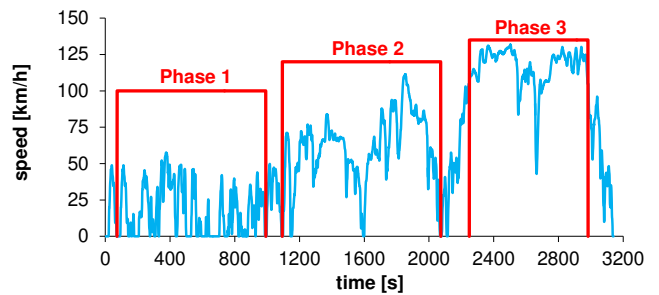


Figure 5. CADC driving cycle

On road testing

In order to reach the validity according to the actual requirements several road tests were performed. Finally, the used valid road circuit was always the same with approximately 1.5h duration and parts of urban, rural and highway roads. Fig. 6 represents an example of a road trip from the PN PEMS test program.

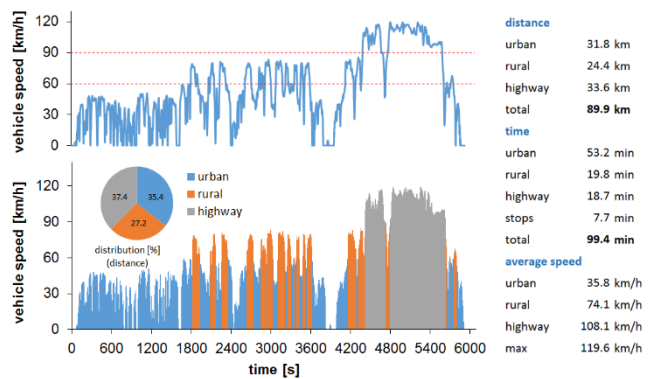


Figure 6. AFHB, road trip for RDE; vehicle 1, PEMS 2 & PN PEMS

Engine testing

The correlation tests of gas flow measuring devices were performed at 35 steady state operating points (OP) of the engine.

Tested cars

Fig. 7 shows the tested vehicles and the data of them are represented in the Table 2. Each vehicle was used for different working task:

- Vehicle 1 was a “golden vehicle” (GDI) of the inter-laboratory comparison tests with JRC,
- vehicle 2 (Diesel) was used for a comparisons of PN PEMS- and CPC-results,
- vehicle 3, GDI flex fuel vehicle (FFV) was used for correlations of PEMS with E10,
- vehicle 4 (Diesel) served for demonstration of impact of slope on the chassis dynamometer.

All vehicles were operated with the Swiss market fuels and with the lubricating oil, which was actually present in each vehicle.

Results and discussions

RDE & PN PEMS

Including the particle number (PN) measuring device in the portable emission measuring systems (PEMS) is an important objective of the EU legislation.

Table 2. Data of tested vehicles

Vehicle	① VW Golf TSI 1.2l gasoline	② Opel Astra 16V Diesel	③ Audi A4 2.0 TFSI FFV gasoline	④ Mercedes VITO Diesel
Number and arrangement of cylinder	4 in line	R 4	4 in line	4 in line
Displacement cm ³	1197	1994	1984	2143
Power kW	63 @ 4800rpm	60@ 4300 rpm	132@ 4000rpm	100 @ 3800rpm
Torque Nm	160 @ 1500-3500rpm	185@ 1800-2500rpm	320@ 1500rpm	310 @ 1400-2400rpm
Injection type	gasoline direct injection	Distribut or pump / DI	Direct Injection (DI)	Direct Injection (DI)
Curb weight kg	1129	1390	1570	2180
Gross vehicle weight kg	1229	1845	2065	3050
Drive wheel	2WD	2WD	2WD	Rear-wheel drive
Gearbox	m5	m5	m6	AT 5
First registration	10.03.15	1998	2010	16.11.10
Exhaust	Euro 5	Euro 2	Euro 5	Euro 5a



Vehicle ① VW Golf TSI 1.2l



Vehicle ② Opel Astra 16V in the laboratory



Vehicle ③ Audi A4



Vehicle ④ Mercedes VITO

Figure 7. The tested cars

The Swiss developments at ETHZ, FHNW and Matter Aerosol, which were supported by the Swiss Federal Office of Environment (BAFU) gave a strong contribution to the progress of portable PN-measurements.

2015/2016 inter-laboratory comparison test series (ILCE ... Inter-Laboratory-Comparison-Exercise) with PN-PEMS were organized and performed by the VELA (Vehicle Emissions Laboratory) of the EC-JRC, Ispra. For the tests a “golden vehicle” with a “golden PN-analyzer” (TESTO NanoMet3) have been circulated among different laboratories.

The comparison test series were also performed in Switzerland in the frame of collaboration between EC-JRC and BAFU.

A modern GDI car (vehicle 1) equipped with PEMS SEMTECH, both “golden” systems (Gas & PN) from the ILCE, were tested in standard test cycles (NEDC and WLTC) on the chassis dynamometer and on-road (RDE).

For the real-world testing a road circuit was fixed: approximately 1.5h driving time with urban/rural and highway sections. This circuit fulfils the actual RDE-requirements. A portable system for measurements of nanoparticles (TESTO NanoMet3) was included in the tests and the results were compared with CPC (PMP) on the chassis dynamometer.

Fig. 8 compares the emission results obtained on chassis dynamometer and in the road circuit with PEMS.

The average emission values, which are found with PEMS in on-road (warm) operation (RDE) are well responding to the average values in WLTC warm (measured with PEMS), which confirms that WLTC represents well the real driving behaviour.

The emissions measured with PEMS in repeated road driving circuit are generally well repetitive. Exceptions can happen due to extreme driving behaviour, special traffic situations or activities of vehicle electronic control (here especially NO_x).

Fig. 9 shows the comparisons of results obtained in WLTC warm in the present tests with the min/max/average values obtained during the JRC-ILCE. Regarding the results from stationary installation (CVS) – CO₂ (not represented here) and PN on the lowest side of the ILCE-dispersion range – it is assumed that the driving resistances of the chassis dyno were too low. Regarding the PEMS-results; nevertheless, this supposition does not seem to be right. The average values of NO_x and PN measured with PEMS in WLTC warm correlate very well with the average PEMS-values from ILCE.

Analysis of data from two RDE trips was performed by means of the JRC EMROAD program using the verification method of trip dynamics with moving averaging windows (MAW), [1,13].

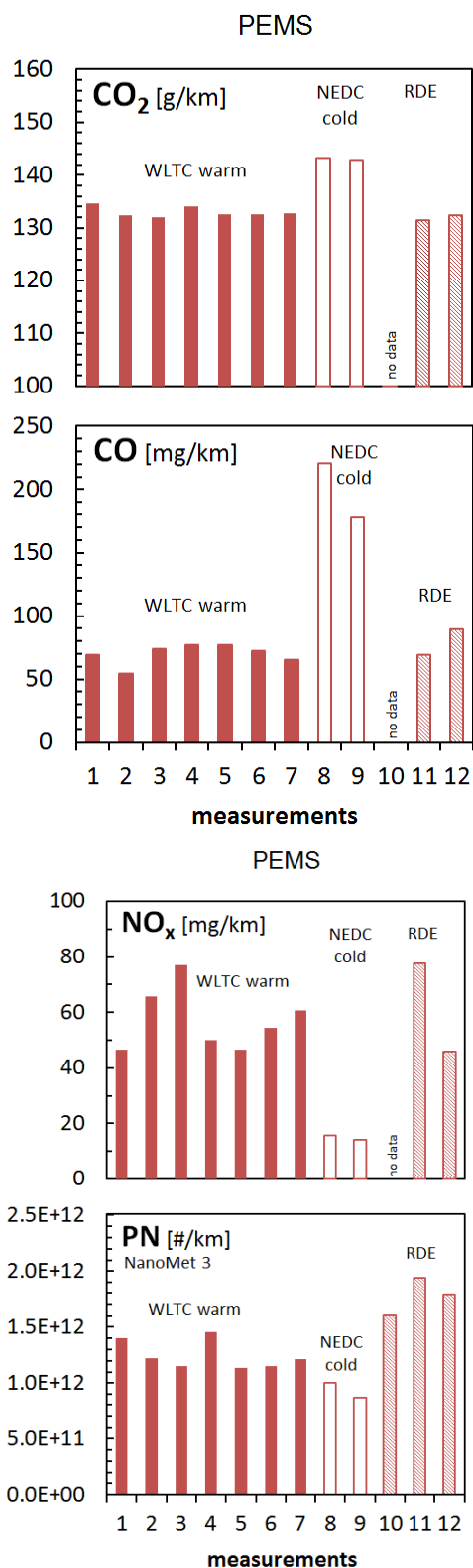


Figure 8. Comparison of emissions in WLTC- NEDC on chassis dynamometer and RDE on road measurements, vehicle 1, PEMS 2

Some explanations from [1] are:

The Moving Averaging Window method provides an insight on the real-driving emissions (RDE) occurring during the test at a given scale of speed. The test is divided in sub-sections (windows) and the subsequent statistical treatment aims at identifying which windows are suitable to assess the vehicle RDE performance.

The “normality” of the windows is concluded by comparing their CO₂ distance-specific emissions with a reference curve. The test is complete when the test includes a sufficient number of normal windows, covering different speed areas (urban, rural, motorway).

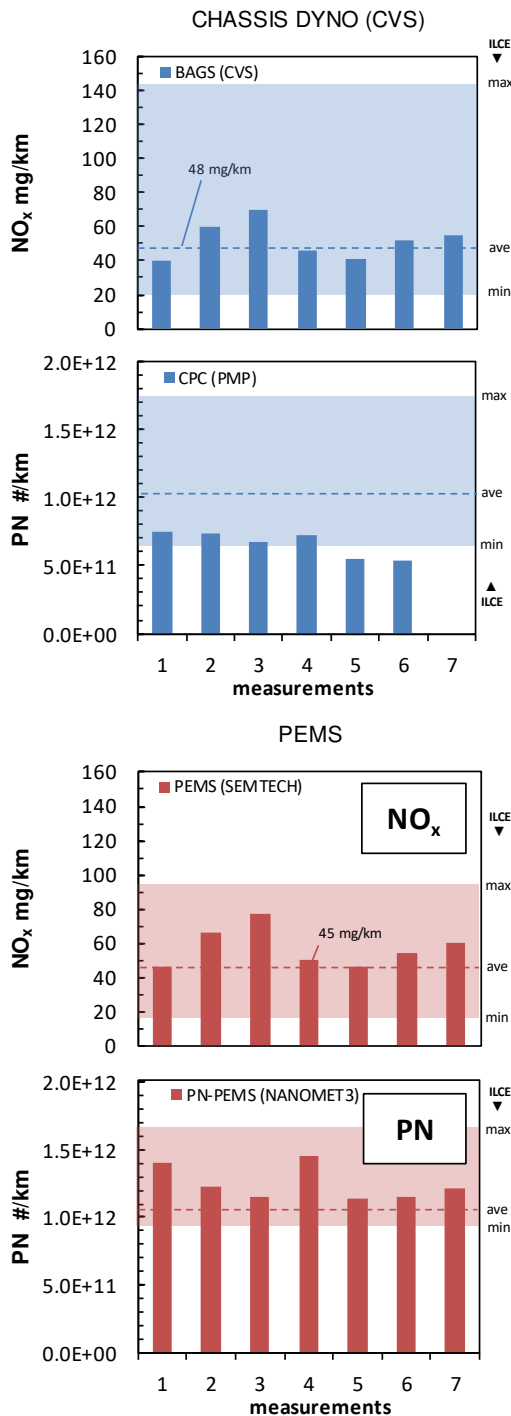


Figure 9. Comparison of Emissions in WLTC warm Chassis Dynamometer, vehicle 1, PEMS 2

During the evaluation the following steps are performed:

- Step 1 Segmentation of the data and exclusion of cold start emissions.
- Step 2 Calculation of emissions by sub-sets or “windows”.
- Step 3 Identification of normal windows.
- Step 4 Verification of test completeness and normality.
- Step 5 Calculation of emissions using the normal windows and weighted windows.

The following data are not considered for the calculation of the CO₂ mass, the emissions and the distance of the averaging windows:

- the periodic verification of the instruments and/or after the zero drift verifications
- the cold start emissions
- vehicle ground speed < 1 km/h
- any sections of the test during which the combustion engine is switched off.

The reference dynamic conditions of the test vehicle are set out from the vehicle CO₂ emissions versus average speed measured at type approval and referred to as “vehicle CO₂ characteristic curve”.

In Fig. 10 such CO₂ characteristic curves are represented for one of the evaluated trips. The trip and its dynamic conditions are normal, since the characteristic curves are in the primary tolerance of +/- 25% (of the average WLTC-CO₂-values).

The emissions resulting from EMROAD-evaluation are generally considerably lower, than the values of integral averages (without any exclusion). The differences are caused mainly by excluding the cold start emissions from the EMROAD-evaluation, Fig. 11.

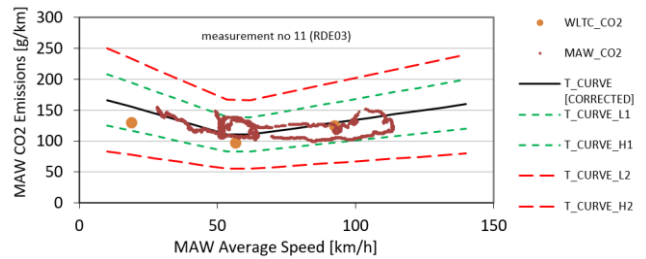


Figure 10. JRC / EMROAD test, normality verification (CO₂ vs speed, MAW... moving average windows)

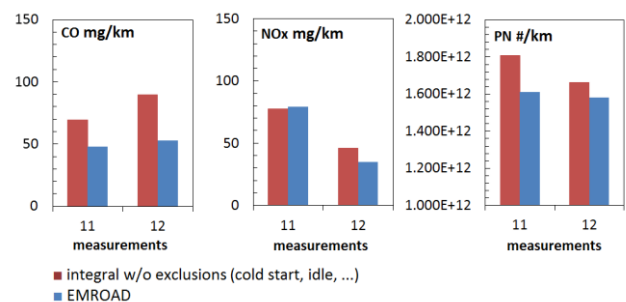


Figure 11. Comparison of results in RDE EMROAD vs integral calculation (SEMTECH & NanoMet 3)

Comparison NM3 – CPC

The PN-results obtained with NanoMet3 (NM3) were compared with the PN-results of a CPC on vehicle 2.

Fig. 12 illustrates an example of correlation of results obtained with CPC (according to PMP) and with NM3 in NEDC. A very good correlation of both measuring systems is demonstrated. The ability of NM3 to show higher peaks during the transients and also higher average values in the driving cycles is to explain with the fact, that NM3 is more sensitive in the lowest size range below 23nm, while CPC has a cut-off below 23nm.

Similar relationships of results NM3/CPC were confirmed with other vehicles (also GDI) at different operating conditions.

Fig. 13 shows on-line PN-courses with NM3 and CPC obtained at tailpipe (TP) and at the end of the CVS-tunnel during a constant operation of 80 km/h. The non-corrected values on the left side of the figure indicate that the diffusion losses between TP and CVS are higher for the CPC-measured aerosol. Consequently, there are higher PN-values measured with NM3 in CVS.

It is possible to find a constant correction factor for NM3, which evens out the differences of both results. This factor, see on the right side of this figure is different for TP and for CVS.

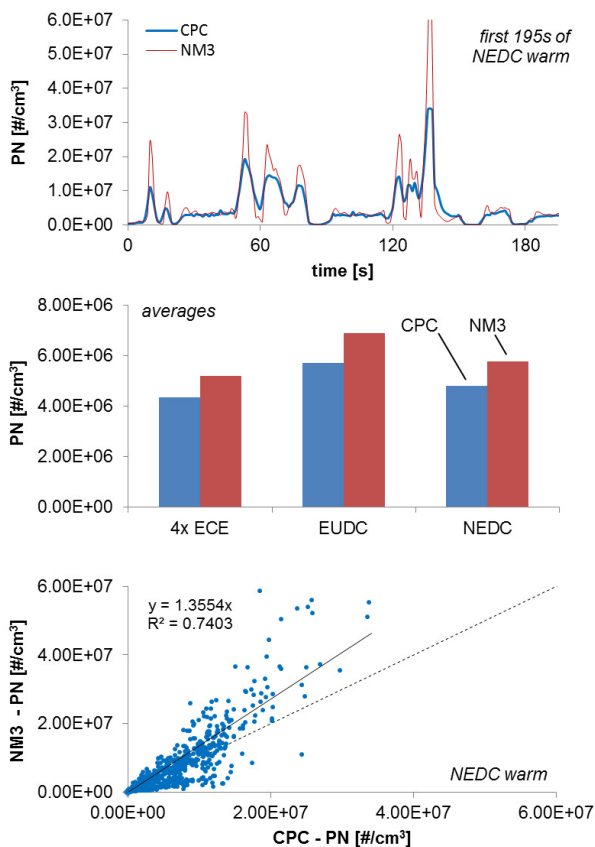


Figure 12. Particle counts concentrations measured simultaneously at tailpipe with NanoMet 3 (NM3) and with CPC.

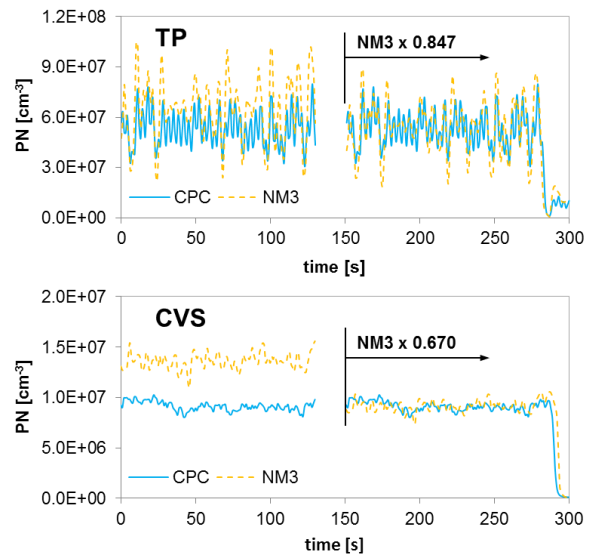


Figure 13. PN at tailpipe (TP) and in CVS tunnel by constant speed 80 km/h.

Similar exercise was performed for the transient operation (WLTC) and similar factors were found. They are: 0.662 for CVS and 0.885 for TP. Fig. 14 illustrates the effects of corrections in different phases of the WLTC.

As a lesson learned from these considerations, it can be said that it is possible to verify the PN PEMS results with CPC (PMP) on chassis dynamometer by repeating some WLTC_{warm} cycles, which were previously remarked to be also an excellent tool to corroborate the Gas PEMS, [8].

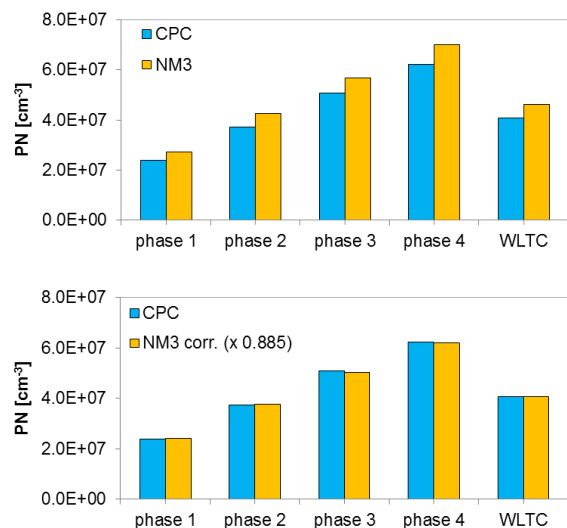


Figure 14. PN at tailpipe (TP) in WLTC.

Correlation of PEMS

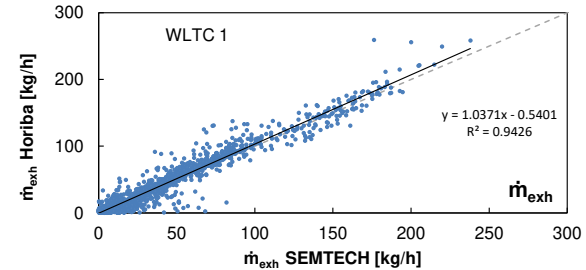
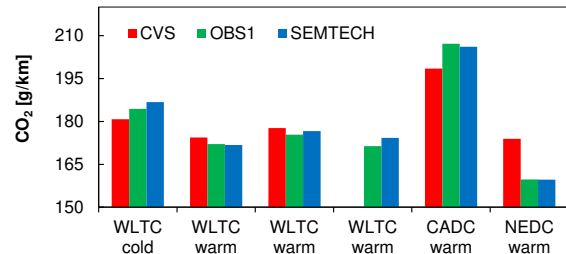
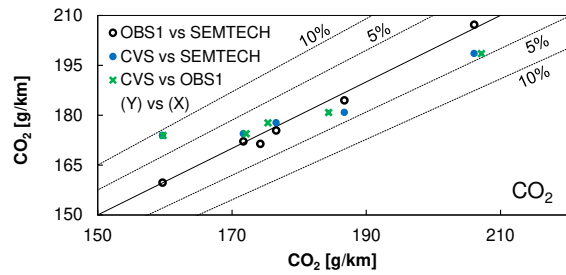
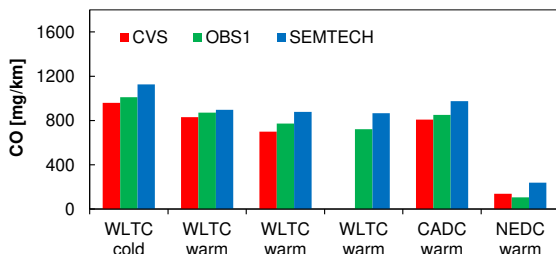
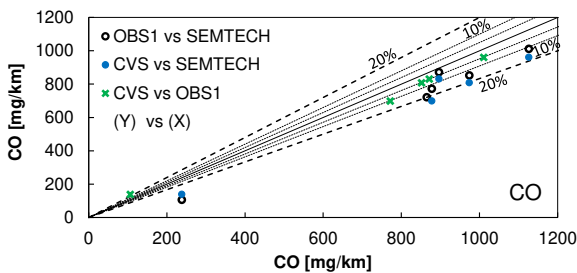
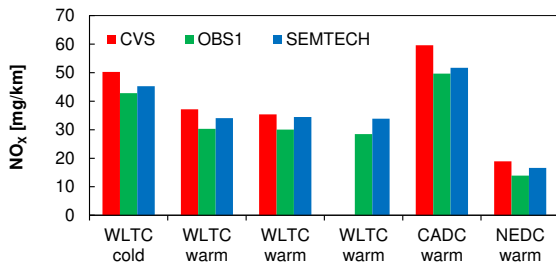
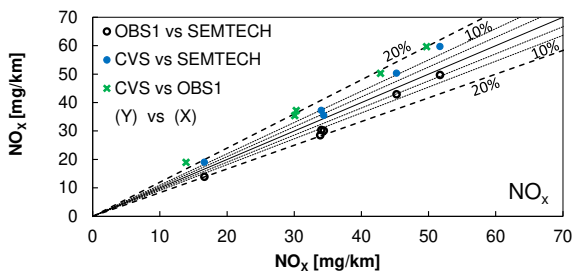
In this part of work comparison tests with two PEMS's – Horiba OBS1 and SEMTECH – were performed on chassis dynamometer in different driving cycles with vehicle 3. The results were correlated with the stationary installation with bag-sampling (called here as "CVS").

Fig. 15 shows correlations of NO_x, CO & CO₂ with the three systems measuring simultaneously in different driving cycles – WLTC_{cold}, 3x WLTC_{warm}, CADC_w and NEDC_w.

The visible tendencies are:

- both PEMS indicate slightly lower NO_x-values and higher CO-values, than CVS; for CO₂ there is no uniform trend,
- comparing the PEMS's between each other mostly higher readings result with SEMTECH, than with Horiba,
- for NO_x & CO most correlation values are in the dispersion range of 20%, for CO₂ in the range of 10%.

A comparison of exhaust gas mass flows measured with both PEMS's shows an excellent correlation. At the lowest flows there is the biggest dispersion of results.



Exhaust gas	Horiba OBS1 kg/test	Semtech kg/test	dev. %
WLTC 1	20.0	19.6	-1.9
WLTC 2	19.9	20.0	0.6
WLTC 3	20.2	20.2	-0.1
CADC	51.2	50.9	-0.6
NEDC	8.6	8.6	0.0

Figure 15. Comparison of emissions & exhaust flow measured with Horiba OBS1 and with SEMTECH in different driving cycles on chassis dynamometer.

Correlations on engine dynamometer

Correlation tests of Horiba OBS1 and engine test bench equipment were performed on the IVECO FIC engine at 35 stationary OP's. A major interest was about the accuracy of different Pitot Tube flowmeters.

Fig. 16 gives an example of correlation of \dot{m}_{exh} -results obtained with Pitot flowmeter (PF) and with the stationary installation. At idling, in the lowest range of flow-values there are the strongest deviations of PF-indications. This is a repetitive tendency in all tests. It can be explained with the difficulty to reach a repetitive-ness of measuring very low pressure increments, which in addition are influenced by the pulsation of flow.

Fig. 17 indicates that also during these comparison tests there were higher readings of some gaseous components (NO_x, NO₂, CO₂) with PEMS than with the stationary instruments.

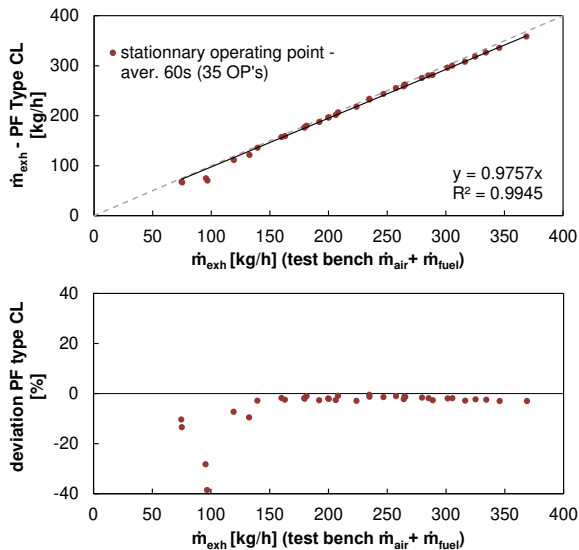


Fig. 16: Correlation of \dot{m}_{exh} – results measured with Pitot Tube Flowmeter (PF) and with engine test bench equipment at 35 OP's. OBS1, IVECO FIC, ulsd

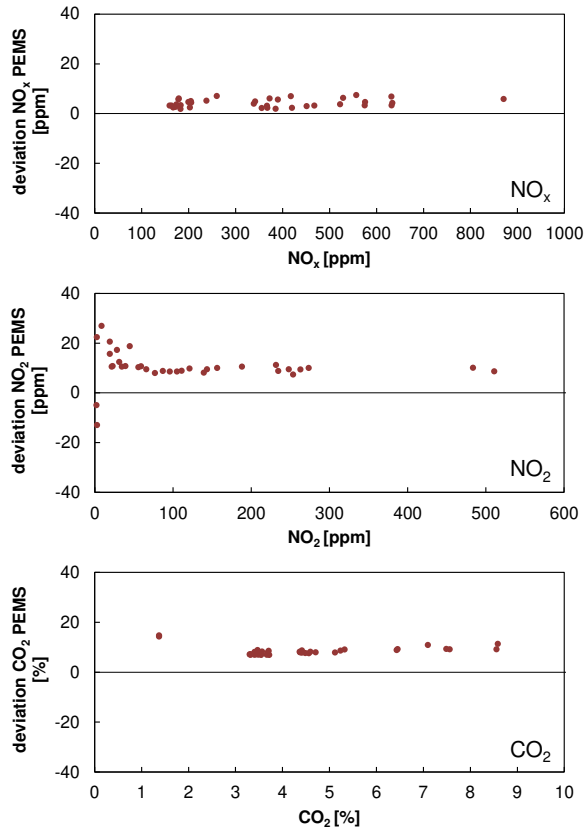
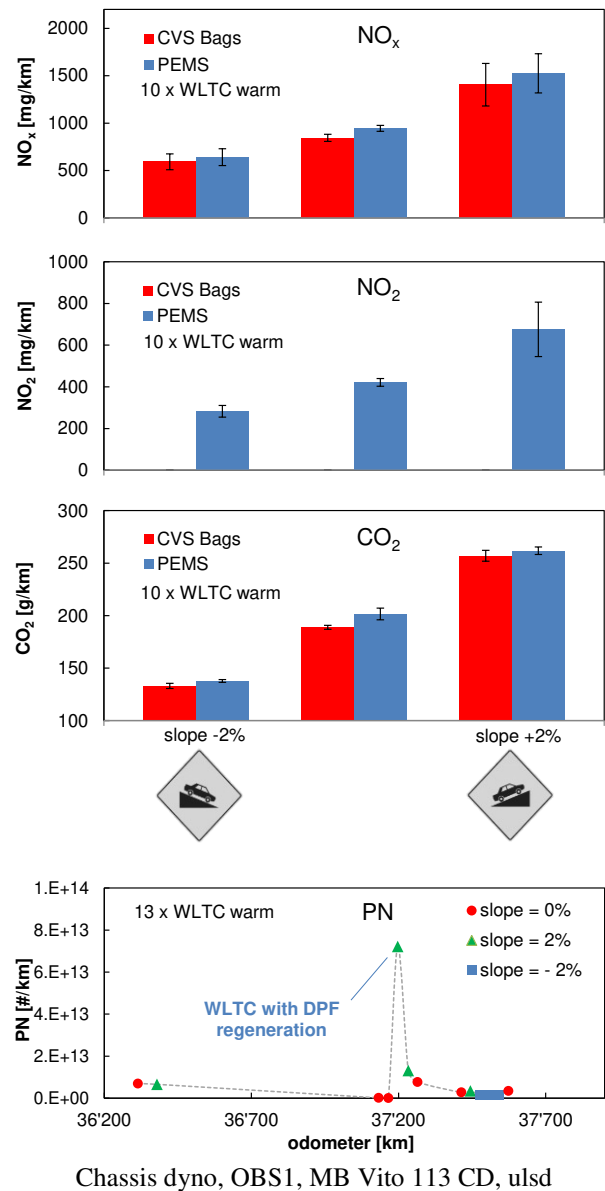


Fig 17: Deviations of gaseous emissions with PEMS and with test bench equipment at 35 OP's. OBS1, IVECO FIC, ulsd

Influences of slope on emissions

The driving resistance of chassis dynamometer was changed in order to simulate the slope +/- 2%. 10 x WLTC_{warm} was performed with vehicle 4 with different slope. The slope nevertheless was kept constant during the cycle.



Chassis dyno, OBS1, MB Vito 113 CD, ulsd

Figure 18. Influence of slope on emissions in WLTC warm

Fig. 18 confirms that the emissions of NO_x , NO_2 and CO_2 principally rise with the increased slope. The most observed tendency that PEMS indicates higher gas-values than CVS is confirmed for NO_x & CO_2 . Nanoparticle emissions are principally independent on slope. In one of the cycles the regeneration of DPF took place and this provoked a visible increase of PN in this one cycle.

It can be concluded, that the slope has an important impact on emissions and it should be considered during the reproduction of RDE driving cycles on the chassis dynamometer.

Conclusions

Following conclusions can be mentioned:

- the emissions CO , CO_2 , NO_x measured with PEMS are generally higher than the same emissions simultaneously measured in the same driving cycle

on the chassis dynamometer with the stationary measuring system (CVS),

- the average values of NO_x and PN measured with PEMS in WLTC warm (chassis dynamometer) correlate very well with the average PEMS-values from ILCE (on road),
- the PN-measuring device – TESTO NanoMet3 – is confirmed as a useful device for PEMS-application,
- the evaluation EMROAD with the moving averaging windows method showed that:
 - the trips were normal from the point of view of CO₂ vs. speed,
 - the driving circuit is valid,
 - the emission results from EMROAD are lower than the results of integration due to neglecting the cold start, near to zero speeds, engine stop periods and devaluation of "unnatural" windows.
- PN PEMS (TESTO NanoMet3) indicates higher peak values during cold start, or dynamic events and it depicts more sensitive the variations of speed of the driving cycle, than CPC (PMP),
- PN PEMS average values at transient operation were higher, than the average values measured with CPC,
- it is possible to verify the PN PEMS results with CPC (PMP) on chassis dynamometer by repeating some WLTC_{warm} cycles,
- the investigated GasPEMS correlate well to each other and they indicate higher CO₂-values, than the stationary installation,
- The flowmeters show the biggest dispersion of results in the lowest flow-range, which is typical for idling,
- Varying slope has clear influences on emissions and must be considered in the measuring procedures.

References

- [1] Official Journal of the European Union: Commission regulation (EU) 2016/427 of 10 March 2016, amending regulation (EC) No 692/2008.
- [2] COMMISSION REGULATION (EC) no 692/2008 of 18 July 2008 implementing and amending Regulation (EC) No 715/2007 of the European Parliament and of the Council on type-approval of motor vehicles with respect to emissions from light passenger and commercial vehicles (Euro 5 and Euro 6) and on access to vehicle repair and maintenance information
Available at: <http://eur-lex.europa.eu/legal-content/en/ALL/?uri=CELEX:32008R0692>
- [3] Darft of the Annex IIIa: *Verifying Real Driving Emissions amending Regulation (EC) No 692/2008 as regards emissions from light passenger and commercial vehicles (Euro 6)*.
- [4] Hofacker, A. *Abgasnorm und Wirklichkeit Eine Annäherung*. Springer: MTZ-Motortechnische Zeitschrift, January 2015, Vol. 76, Issue 2, pp 8-13.
- [5] Vlachos, T. G., Bonnel, P. und Weiss, M. *Die Bewertung des Abgasverhaltens von Fahrzeugen im realen Fahrbetrieb – Eine Herausforderung für die europäische Emissionsgesetzgebung*. 36. Internationales Wiener Motorensymposium, 2015.
- [6] Gerstenberg, J., Schyr, Ch., Sterzing-Oppel, S. and Trenkle, D. (2017) *RDE Engineering via Engine-in-the-loop Test-bench*. MTZ worldwide 78(2017), Nr. 6, p. 16-23.
- [7] Czerwinski, J., Zimmerli, Y., Comte, P. and Bütler, Th. *Experiences and Results with different PEMS*. Laboratory for IC-Engines and Exhaust Emission Control of the University of Applied Sciences, Biel-Bienne. TAP Paper, International Transport and Air Pollution Conference, May 24th-26th, 2016, Lyon, France.
- [8] Czerwinski, J., Zimmerli, Y., Comte, P., Cachon, L. and Riccobono, F. *Potentials of the portable emission measuring systems (PN PEMS) to control real driving emissions (RDE)*. 38. International Vienna Motor Symposium, 27-28 April 2017, VDI Fortschritt-Bericht Reihe 12, Nr. 802, Vol. 2.
- [9] Maschmeyer, H. und Beidl, C. *RDE Homologation – Herausforderungen, Lösungen und Chancen*. MTZ 77 (2016), Nr. 10, S. 84-91
- [10] Zellbeck, H., Walter, R., Stiegler, M. und Roß, T. *RDE – Der reale Fahrbetrieb auf dem hochdynamischen Motorenprüfstand*. MTZ 76 (2015), Nr. 2, S. 42-47
- [11] Röttger, D., Pérez-Guzmán, E., Vigild, Ch. and De Smet, F. *Feature Function Development for RDE in Diesel Engines*. MTZ 78(2017), Nr. 3, S. 46-51
- [12] Schröder, M., Baltes, N. and Danzer, J. *Impact of RDE Legislation on Test-bed Measurements*. MTZ worldwide 78(2017), Nr. 6, p. 28-35.
- [13] Giechaskiel B., Riccobono, F., Bonnel, P. *Feasibility study on the extension of the Real Driving Emissions (RDE) procedure to Particle Number (PN)*. European Commission, Joint Research Centre, ISBN: 978-92-79-51003-8 , ISSN: 1831-9424 , DOI: 10.2790/74218
- [14] Anderson, J., May, J., Favre, C., Bosteels, D. et al. *On-Road and Chassis Dynamometer Evaluations of Emissions from Two Euro 6 Diesel Vehicles*. SAE Paper 2014-01-2826. SAE Detroit, April 2014.
- [15] Kadijk, G., Elstgeest, M., Ligterink, N.E. and van der Mark, P.J. *Investigation into a Periodic Technical Inspection (PTI) test method to check for presence and proper function of Diesel Particulate Filters in light-duty diesel vehicles*. TNO report TNO(2017)R10530|1.0
- [16] Spreen, J.S., Kadijk, G. and van der Mark, P.J. *Diesel Particulate Filters for Light-Duty Vehicles: Operation, Maintenance, Repair, and Inspection*. TNO report TNO(2016)R10958

Abbreviation

AFHB	Abgasprüfstelle FH Biel, CH	LFE	laminar flow element
ASTRA	Amt für Strassen (CH)	MAW	moving averaging windows
BAFU	Bundesamt für Umwelt, (Swiss EPA)	MFS	mass flow sensor
BC	board computer	NEDC	New European Driving Cycle (ECE+EUDC)
CADC	Common Artemis Driving Cycle	NM3	NanoMet3
CAST	Combustion Aerosol Standard	NO	nitrogen monoxide
CD	chassis dynamometer	NO ₂	nitrogen dioxide
CLA	chemiluminescence analyser	N ₂ O	nitrous oxide
CLD	chemiluminescence detector	NO _x	nitric oxides
CPC	condensation particle counter	OBD	on-board diagnostics
CVS	constant volume sampling	OP	operating point
DAQ	data acquisition	PCRR	Particulate Counts Reduction Rate
DC	diffusion charging	PEMS	portable emission measuring systems
DF	dilution factor	PMP	EC Particle Measuring Program
DI	Direct Injection	PN	particle number
DiSC	diffusion charge size classifier	PN-PEMS	PEMS with PN measuring device
EC	European Commission	RDE	real driving emissions
ECE	Economic Commission Europe	TFZ	Technologie- und Förderzentrum für Nachwachsende Rohstoffe, Straubing, D
ECU	electronic control unit	TP	tailpipe
EFM	exhaust flowmeter	TWC	three way catalyst
EMPA	Eidgenössische Material Prüf- und Forschungsanstalt	ViPR	nanoparticle sample preparation with volatile particles remover
ETC	European Transient Cycle	WLTC	worldwide harmonized light duty test cycle
ETHZ	Eidgenössische Technische Hochschule Zürich	WLTP	worldwide harmonized light duty test procedure
EUDC	Extra Urban Driving Cycle	3WC	three way catalyst
FHNW	Fachhochschule Nord West Schweiz		
GDI	gasoline direct injection		
GMD	geometric mean diameter		
HC	unburned hydrocarbons		
ILCE	Inter- Laboratory-Comparison-Exercise		
JRC	Joint Research Centre (EC)		

Fuel Consumption and Emissions of Four Modern Passenger Cars under Real-World Driving Conditions

A. Dimaratos¹, G. Triantafyllopoulos¹, L. Ntziachristos¹, Z. Samaras^{1*}, P. Mock², Y. Bernard², J. Dornoff²

¹ Laboratory of Applied Thermodynamics, Aristotle University of Thessaloniki, P.O. Box 458, GR-54124, Thessaloniki, Greece, *Corresponding author: zisis@auth.gr

² International Council on Clean Transportation, Berlin, 10178, Germany

Introduction

Emissions of light-duty vehicles measured in laboratories under the current type-approval procedure are harshly criticized. The test based on the New European Driving Cycle (NEDC) is known for being unrepresentative of real-world driving conditions and vehicles to be specifically optimized for this protocol. Moreover, the fuel economy targets for the automotive sector are specified according to this procedure, although that it was not originally developed for this purpose (Tsokolis et al., 2016). This has resulted in a significant gap between the real-world fuel consumption and nitrogen oxide (NO_x) emissions, with the deviation reaching currently 42%, and expected to reach almost 50% in 2020 for the former, and up to 20 times for the latter (Tietge et al., 2015; T&E, 2015). The gap in fuel consumption will be partially addressed by the introduction of the Worldwide harmonized Light vehicles Test Procedure (WLTP) as new type-approval process (Tsokolis et al., 2015). Further, the recently developed Real Driving Emissions (RDE) on-road test will allow for a more realistic reporting of emissions from light-duty vehicles (ICCT, 2015).

The present work investigated the emissions of four modern passenger cars under actual and upcoming regulatory procedures in the laboratory, as well as on the road. The selected vehicles consisted of one B-segment direct injection gasoline vehicle equipped with a three-way catalyst (TWC), one D-segment diesel vehicle equipped with a Selective Catalytic Reduction (SCR) system and two diesel vehicles (one C-segment and one mid-size luxury) equipped with Lean NO_x Trap (LNT). Laboratory tests were conducted using both type-approval and more realistic vehicle specifications, such as corrected mass and rolling resistance, while on-road measurements included a RDE-compliant test and a more dynamic one that goes beyond the regulatory limits and covers a wider range of real-world conditions. An analysis of the deviations between laboratory and on-road tests is presented. Further, the different on-road tests (RDE-compliant and dynamic) are compared, focusing on specific findings such as the frequency of LNT regeneration events and the relevant NO_x emissions.

Methodology

Tested vehicles and equipment

Four Euro 6 vehicles of different segments and technology, all equipped with Start-Stop system, were tested in the context of the present study. All four vehicles were procured from rental companies and were checked for any malfunctions prior to testing. An overview of the technical specifications of the tested vehicles is provided in Table 1.

For the on-road testing, a Portable Emissions Measurement System (PEMS) was used. This was the AVL GAS PEMS iS with its system control unit and the associated sensors (Figure 1). The main technical characteristics of the PEMS equipment are given in Table 2. Apart from the exhaust emissions measured with the PEMS, the recorded data included information from the vehicle's ECU (through the OBD port), such as vehicle velocity, engine speed, intake air mass flow, lambda, engine coolant temperature, EGR rate, accelerator pedal position and battery voltage, as well as GPS and ambient data, such as the instantaneous position, altitude, ground velocity and ambient pressure/temperature/humidity.

Table 1: Technical specifications of the tested vehicles

Parameter	Mid-size luxury	C segment	D segment	B segment
MY & Chassis type	2015, Sedan	2016, Hatchback	2016, Station wagon	2015, Hatchback
Fuel & Engine	Diesel, 4-cyl	Diesel, 4-cyl	Diesel, 4-cyl	Gasoline, 4-cyl GDI
Drive & Transmission	RWD, Automatic	FWD, Manual	FWD, Manual	FWD, Automatic
Number of gears	8	6	6	7
Max power [kW]	140	81	125	66
Engine capacity [cm ³]	1995	1461	1956	1197
Start-stop	Yes	Yes	Yes	Yes
Euro class	6	6	6	6
Aftertreatment system	DOC, DPF, LNT	LNT, cDPF	cDPF, SCR	TWC
Type approval CO ₂ [g/km]	109	94	124	109
Mileage (start of testing) [km]	16,630	27,540	20,560	5,930



Figure 1: Up: The AVL GAS PEMS iS inside the trunk of the vehicle. Down: The GPS and ambient sensors on the roof of the vehicle.

Table 2: Technical characteristics of the AVL GAS PEMS iS

Gas	Range	Accuracy
CO	Linearized range: 0 – 49999 ppm	0-1499 ppm: ± 30 ppm abs
	Display range: 0 – 15% vol	1500-49999 ppm: $\pm 2\%$ rel.
CO ₂	0 – 20% vol	0-9.99% vol: $\pm 0.1\%$ vol abs
		10-20% vol: $\pm 2\%$ rel.
NO	0 – 5000 ppm	$\pm 0.2\%$ FS or $\pm 2\%$ rel.
NO ₂	0 – 2500 ppm	$\pm 0.2\%$ FS or $\pm 2\%$ rel.
O ₂	0 – 25% vol	$\pm 1\%$ FS

Testing routes and driving cycles

Two on-road routes and four driving cycles in the laboratory were included in the present experimental campaign. The first route (RDE route) for the on-road measurements has been designed according to the relevant regulation for RDE testing of light passenger and commercial vehicles. It consists of three separate parts, namely Urban, Rural and Motorway, driven in this order (Figure 2). Figure 3 presents the vehicle velocity and instantaneous altitude profile throughout the RDE route, while Table 3 summarizes the detailed characteristics of the testing routes, where it can be seen that the RDE route meets all the requirements of the regulation. The second route (Dynamic route) has been designed in order to represent a driving style with more dynamic characteristics than the previous one, including abrupt accelerations and braking phases. It also consists of Urban, Rural and Motorway parts (Figure 4), but these are not necessarily driven in a specified sequence. It includes uphill/mountain driving with the maximum altitude difference between the highest and the lowest point in the order of 500m, as shown in Figure 5. Table 3 summarizes the characteristics of the Dynamic route, where it is clearly shown that it does not comply fully with the regulation. It needs to be clarified that all on-road tests were run hot-started, i.e. with the engine and all the other engine components already in their nominal operating temperature.

Concerning laboratory testing, Figure 6 presents the velocity profiles of the driving cycles tested. NEDC and WLTC v5.3 were tested both cold and hot-started, while the Artemis cycles were run hot-started. Laboratory tests were run with the realistic road load determined after a coast-down test, while the NEDC was also repeated with the type approval (TA) settings, in order to confirm that the vehicles' emissions performance is compliant with their factory specifications.

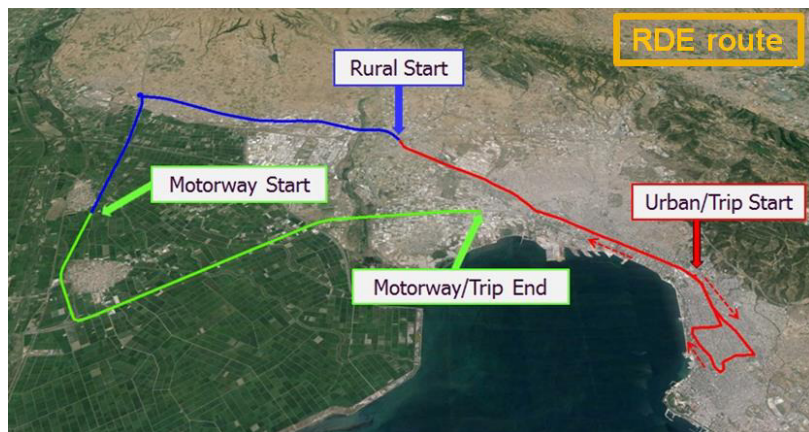


Figure 2: The route for measuring on-road real-world emissions, complying with the regulation

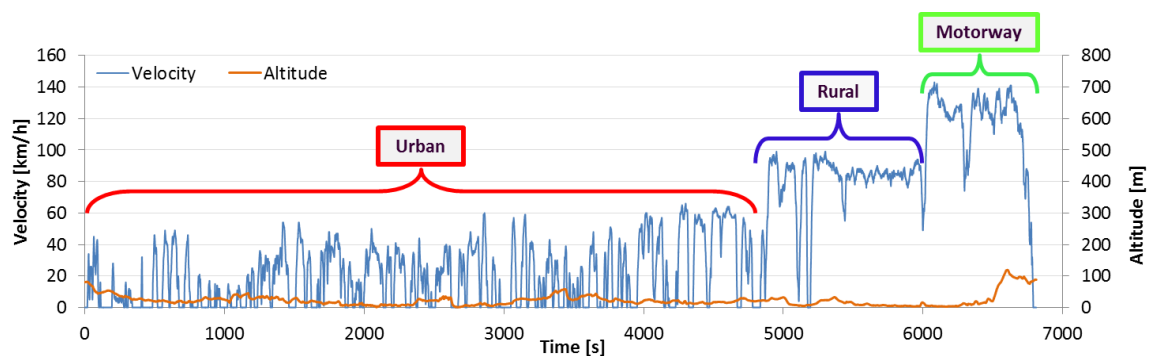


Figure 3: Vehicle velocity and altitude profile, following the RDE-compliant route

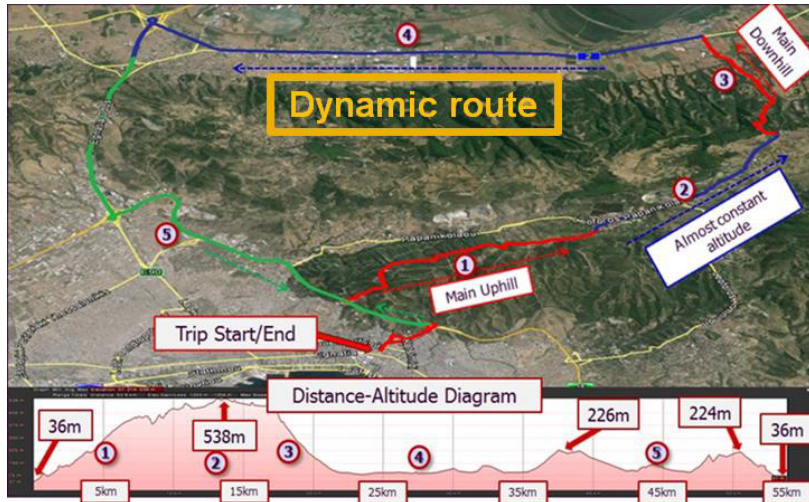


Figure 4: The route for measuring on-road real-world emissions during dynamic driving

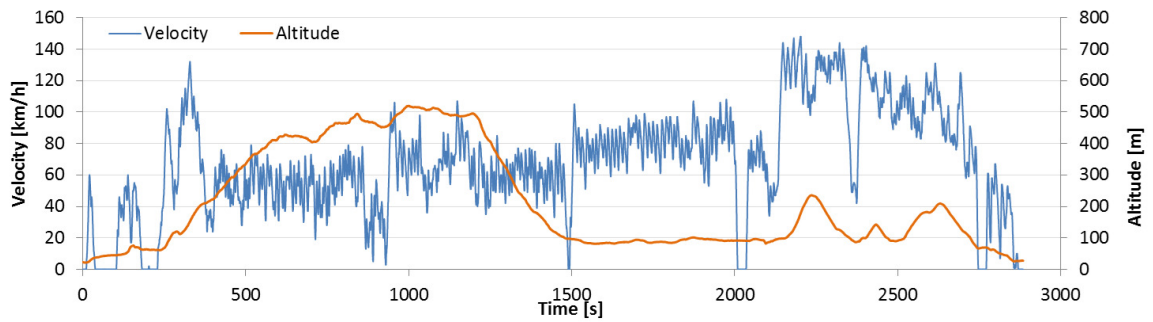


Figure 5: Vehicle velocity and altitude profile, following the Dynamic route

Table 3: Characteristics of the testing routes

Parameter	RDE route	Dynamic route	Regulation limits
Trip distance [km]	77	54	>48
Trip duration [min]	100-110	65	90-120
Maximum speed [km/h]	130	140	<145
Altitude difference end-start [m]	-10	0	< \pm 100
Max Slope (Uphill/Downhill) [%]	4.2/-6.5	11.7/-17.6	—
Cumulative positive elevation gain [m/100km]	500	1700	<1200
Road type sequence	Urban-Rural-Motorway	mixed	—
Road type distance share (Urban(U)-Rural(R)-Motorway(M)) [%]	U: 36.1 R: 32.5 M: 31.4	—	U: 29-44 R: 23-43 M: 23-43

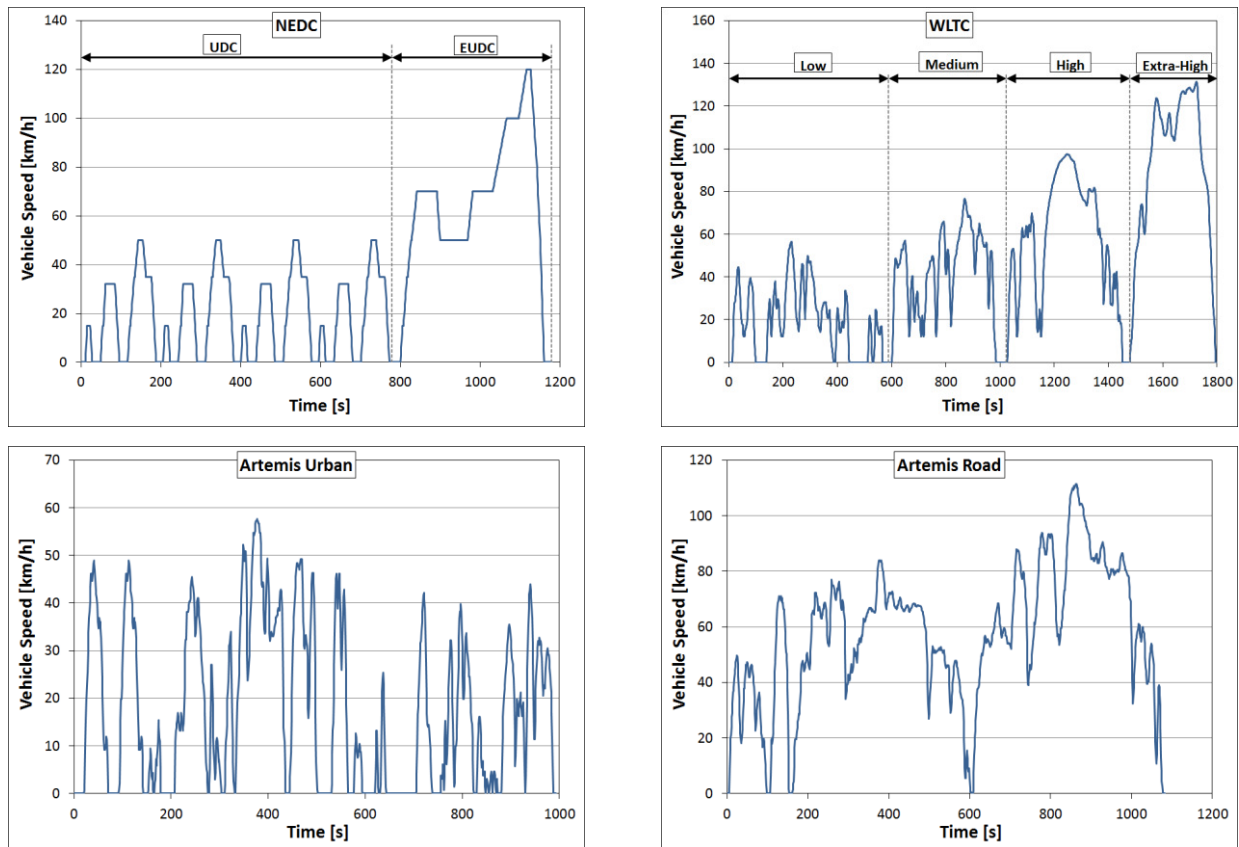


Figure 6: Vehicle speed profile for the driving cycles run in the laboratory

Results

The calculation of the final emission values, expressed in emission mass per travelled distance, were made following the prescriptions of the relevant regulations. The emission values for the laboratory tests were calculated following the NEDC and WLTC protocols. As regards the real-world tests, the emission values for the RDE compliant tests were made according to the Moving Averaging Window (MAW) method of the RDE regulation, whereas the emission values for the dynamic tests were calculated by simply dividing the total emission mass by the total travelled distance. Although that the MAW method was not applied in the dynamic tests, this is responsible only for a minor part of the emission difference between the two types of on-road tests. For example, in the case of CO₂ emissions, the different calculation method is responsible for about 3g/km CO₂ of the difference, whereas the distance between the RDE-compliant and the dynamic tests can be in the order of 50-100g/km CO₂ or even higher (Figure 7).

CO₂ Emissions

The measured CO₂ emission values of the four vehicles during the various tests are presented in Figure 7. Each bar represents the average CO₂ emissions of a specific test protocol/route. All three diesel vehicles presented higher CO₂ emissions following the RDE route compared to the NEDC TA, reaching up to 33% difference. For the gasoline vehicle the CO₂ emissions of the measured RDE route were similar with the ones measured during the NEDC TA tests. The reasons for this, initially unexpected observation, are the hot starting of the on-road tests, contrary to the cold-started NEDC, on the one hand, and the small difference between real-world and TA road loads for the specific vehicle, on the other.

Generally, the CO₂ emissions of the NEDC tests with real-world settings were consistently higher than the NEDC TA tests, up to 15%, for all the four vehicles. This is expected, since the TA settings include lower test mass and lower driving resistances than those of a typical real-world case. Since for the specific 1.2lt gasoline TWC vehicle, the difference between TA and

real-world road load is low, the corresponding deviation in CO₂ emissions is accordingly limited. The dynamic route CO₂ emission values are the highest of all tests for all vehicles, up to almost double than the RDE compliant test. This is expected since the frequent and harsh acceleration and braking events, as well as the high road slopes contribute to higher distance-specific engine power and load demands and thus higher fuel consumption and CO₂ emissions.

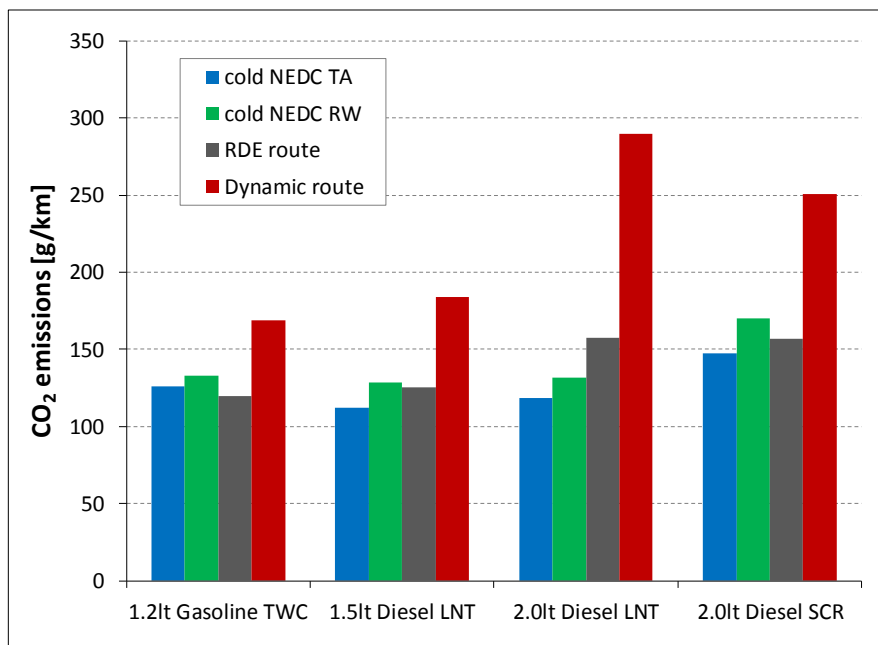


Figure 7: CO₂ emissions of the four vehicles during the various tests

NO_x Emissions

NO_x emission results have a much higher variance than the corresponding CO₂ emission values, since NO_x formation is strongly related to the combustion characteristics and the exhaust aftertreatment devices operation. The average NO_x emission results per test protocol/driving route are presented in Figure 8 for the four vehicles considered in this study.

The gasoline vehicle presents relatively low NO_x emissions following both the NEDC and the RDE compliant tests. These results demonstrate the high effectiveness of the TWC in limiting NO_x emissions in gasoline vehicles. NO_x emissions for this vehicle increase significantly in the dynamic test, reaching up to 170 mg/km.

On the other hand, all diesel vehicles presented significantly higher NO_x emissions than the gasoline one under all the tested conditions. During the NEDC TA tests, all diesel vehicles were within the Euro 6 limit, while some of them maintained the compliance with the limit even during the NEDC with realistic settings. At the latter case, NO_x emissions are expected to be higher, since the higher mass and driving resistance is translated into engine operation at higher loads.

Concerning the on-road tests, very significant differences are observed. Beginning with the RDE-compliant tests, NO_x emission results are one order of magnitude higher than the legislated Euro 6 limit, reaching values as high as 1.3 g/km (~16 times more than the Euro 6 limit). Even higher are the NO_x emissions during the dynamic route, with the highest values varying from 2.0 to 3.2 g/km (25 to 40 times higher than the Euro 6 limit). These results are a first indication that during real-world driving the LNT and SCR aftertreatment systems may not be as efficient as in laboratory conditions.

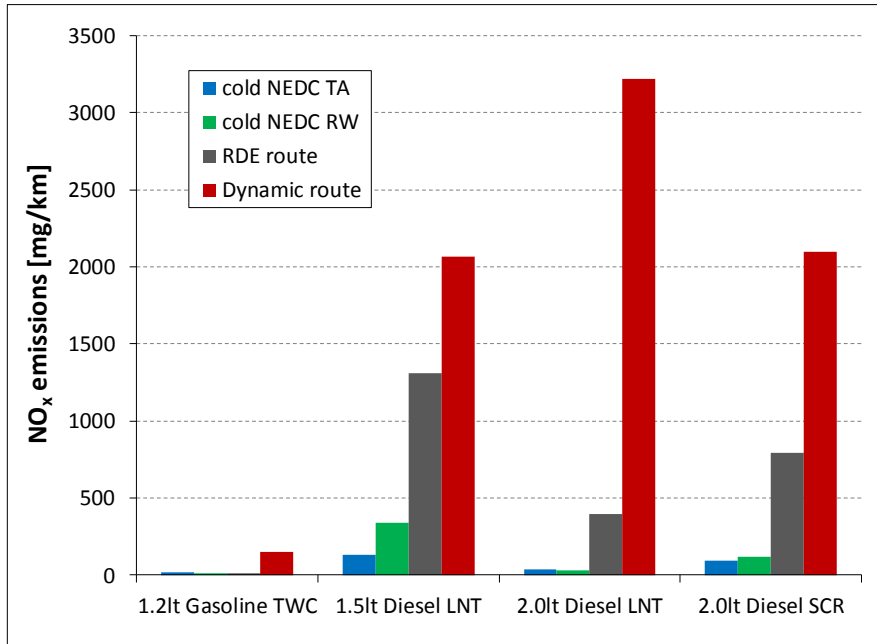


Figure 8: NO_x emissions of the four vehicles during the various tests

A more detailed look into NO_x emissions during the on-road tests is provided in Figures Figure 9 to Figure 12, which illustrate the instantaneous NO_x emissions in relation to vehicle dynamics, quantified by the combination of instantaneous vehicle velocity and acceleration, for all the four vehicles. In all the following figures, the left graph depicts the instantaneous NO_x emissions during the RDE-compliant test, while the right graph presents the corresponding emissions during the dynamic test. Both velocity and acceleration acquire higher values under the dynamic testing, owing to the abrupt acceleration and braking phases; accordingly, NO_x emissions are higher, as already explained. At the case of the gasoline vehicle, the differences between the two types of on-road testing are limited, indicating the effective operation of the TWC. The differences are mainly located in the area of medium velocity and high acceleration, as shown in Figure 9.

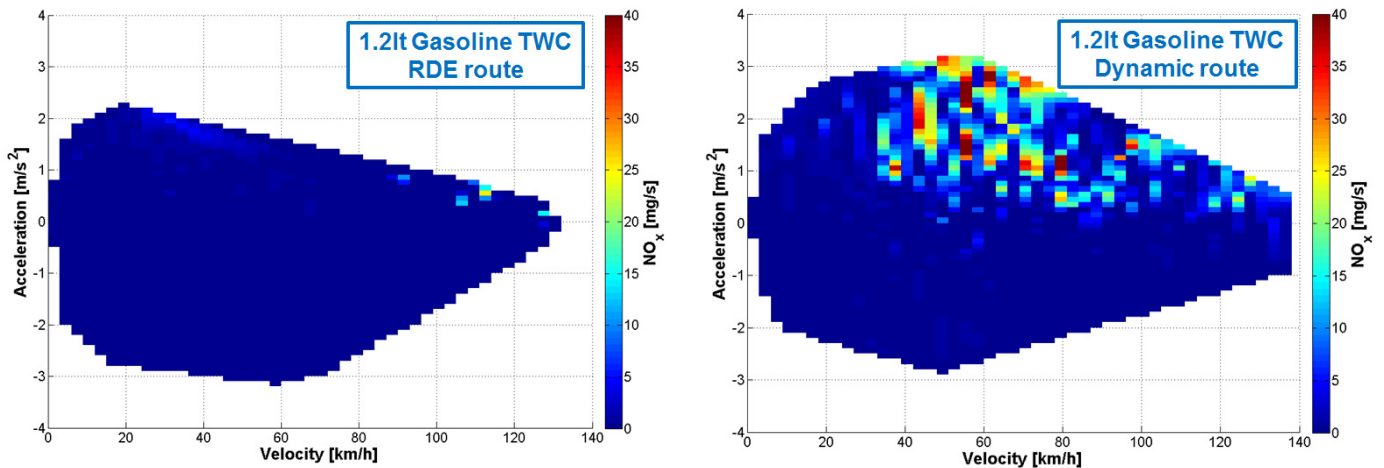


Figure 9: NO_x emissions of the 1.2lt gasoline TWC vehicle illustrated on the v x a plane

However, for all the diesel vehicles, the differences between the RDE-compliant and the dynamic tests are significant and are observed in the area of medium/high velocity and high acceleration (Figure 10 to Figure 12). Clearly, the higher engine loads associated with the abrupt driving during the dynamic test result in higher NO_x emissions. It is even interesting to notice that for the same combination of velocity and acceleration values, NO_x emissions can be

different between the two types of on-road testing, owing to the harsh transients experienced during the dynamic tests. Especially for the LNT equipped vehicles, another factor contributing to the different NO_x emissions is the LNT purges during each test. The 1.5lt and 2.0lt diesel vehicles experienced 9 and 10 LNT purges per 100km during the RDE-compliant test, respectively. Under the dynamic driving, the 1.5 diesel vehicle experienced 3 LNT purges per 100km, while the 2.0lt diesel one did not undergo a LNT purge at all.

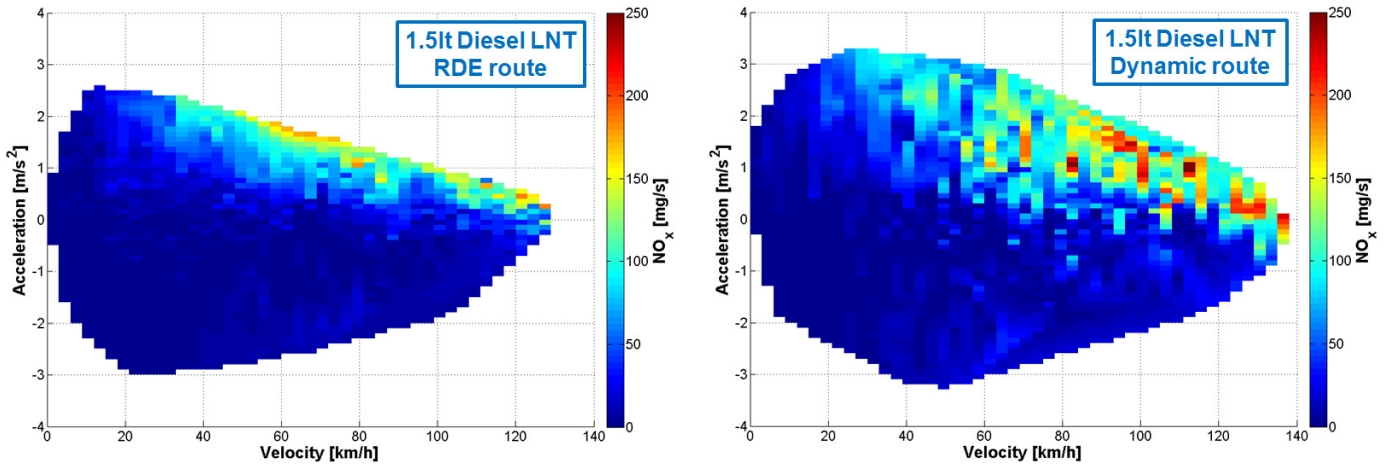


Figure 10: NO_x emissions of the 1.5lt diesel LNT vehicle illustrated on the $v \times a$ plane

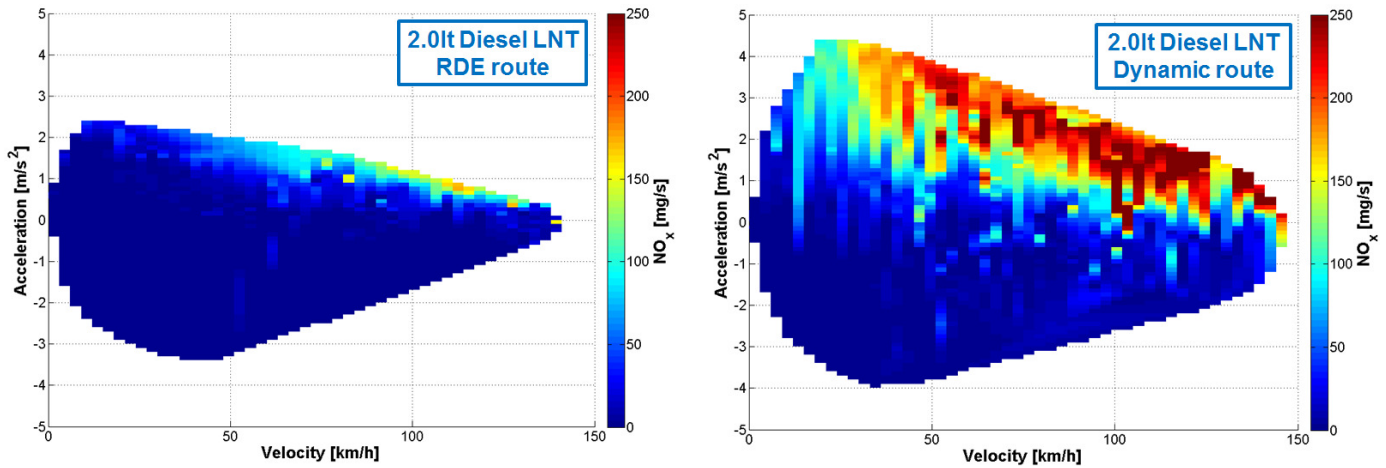


Figure 11: NO_x emissions of the 2.0lt diesel LNT vehicle illustrated on the $v \times a$ plane

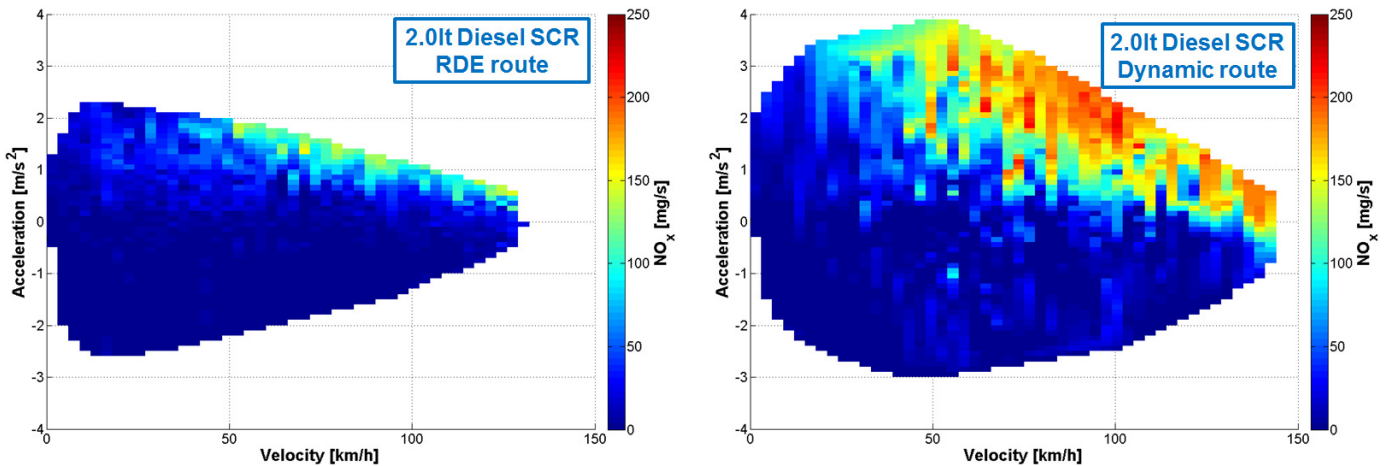


Figure 12: NO_x emissions of the 2.0lt diesel SCR vehicle illustrated on the $v \times a$ plane

CO Emissions

In almost all the conducted tests, CO emissions were negligible. For the case of diesel vehicles, this was somehow expected, since the engine-out CO emissions of diesel engines are low, and are further reduced by the oxidation catalyst activity (either a DOC or a catalytic DPF) that is enhanced by the fully warm conditions at the beginning of the on-road tests.

The only case with significant CO emissions was the dynamic testing of the gasoline vehicle, which resulted to emissions of up to 3 g/km. Figure 13 presents the instantaneous CO emissions in relation to vehicle dynamics, quantified again by the combination of instantaneous vehicle velocity and acceleration. The left graph of Figure 13 shows that CO emissions on the RDE route are almost negligible, whereas the right graph of Figure 13 demonstrates that the harsh accelerations that occur in medium to high velocities produce significant CO emissions. This can be attributed to the instantaneous fuel enrichment during abrupt transients, resulting in rich operation (the GDI engine of the specific vehicle is a stoichiometric one) and oxygen deficiency both in the combustion chamber and the TWC.

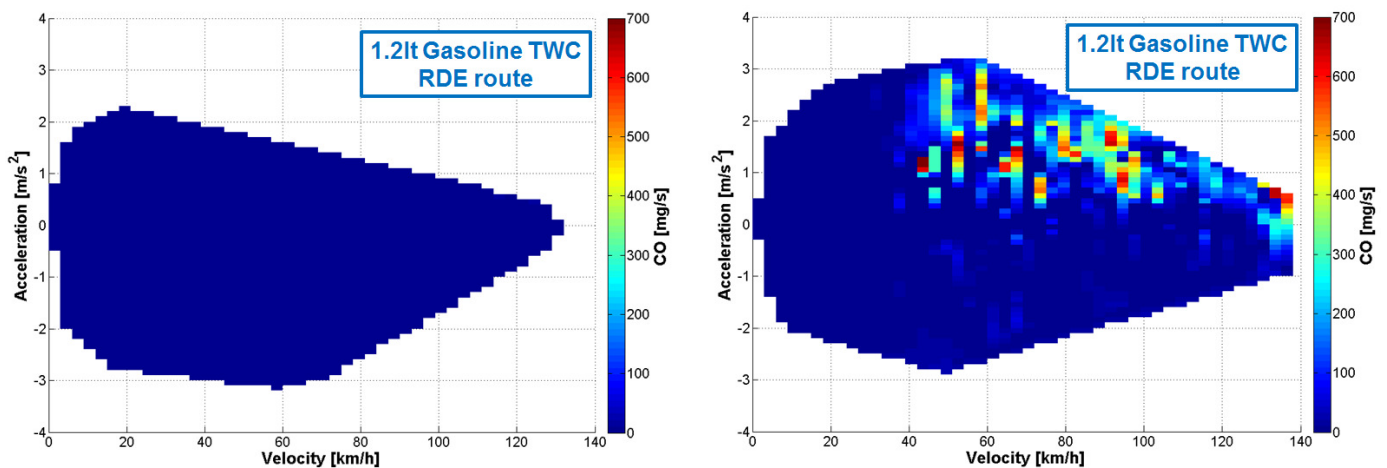


Figure 13: CO emissions of the 1.2t gasoline TWC vehicle illustrated on the $v \times a$ plane

Conclusions and future work

The present work investigated the emissions of four modern passenger cars under actual and upcoming regulatory procedures in the laboratory, as well as on the road. Three diesel vehicles with different exhaust aftertreatment systems and from different vehicle segments were tested, while the vehicle pool included also a gasoline vehicle equipped with a direct injection engine and a TWC. All vehicles were tested in the same RDE-compliant route, while an additional dynamic trip was also followed. The testing campaign assisted the assessment of the real-world behaviour of the tested vehicles and of different technologies. The different on-road tests (RDE-compliant and dynamic) were compared, focusing on specific findings such as the frequency of LNT regeneration events and the relevant NO_x emissions.

All diesel vehicles exceeded significantly the temporary NO_x conformity factor (CF) of 2.1, with extreme values experienced under dynamic driving. On the other hand, the gasoline vehicle remained below the Euro 6 NO_x limit when driven in the RDE route. However, it slightly exceeded the temporary NO_x CF value in the dynamic route, where it also presented high CO emissions.

The next steps of this activity include testing of other vehicles equipped with modern technologies, such as GDI lean-burn or GDI equipped with GPF, the inclusion of PN emissions in every vehicle during real-world measurements and cold-start on-road testing following the same, as well as additional routes and driving styles.

References

ICCT (2015), "The European Real-Driving Emissions Regulation", *Position Brief*.

Tietge U., S. Diaz, P. Mock, J. German, A. Bandivadekar and N. Ligterink (2015), FROM LABORATORY TO ROAD – A 2015 update of official and 'real-world' fuel consumption and CO₂ values for passenger cars in Europe, *ICCT White Paper*.

T&E (Transport & Environment) (2015), "Realistic real-world driving emissions tests: the last chance for diesel cars?", *RDE position paper*.

Tsokolis D., S. Tsiakmakis, G. Triantafyllopoulos, A. Kontses, Z. Toumasatos, G. Fontaras, A. Dimaratos, B. Ciuffo, J. Pavlovic, A. Marotta, Z. Samaras (2015), Development of a template model and simulation approach for quantifying the effect of WLTP introduction on light duty vehicle CO₂ emissions and fuel consumption, *SAE Technical Paper 2015-24-2391*.

Tsokolis D., S. Tsiakmakis, A. Dimaratos, G. Fontaras, P. Pistikopoulos, B. Ciuffo, Z. Samaras (2016). Fuel consumption and CO₂ emissions of passenger cars over the New Worldwide Harmonized Test Protocol, *Applied Energy*, 179, 1152-1165.

Diesel Particle Filter Tampering Detection during a Vehicle Periodic Technical Inspection

Authors, *F. Bijelić^{1,2*}, G. Pejić^{1,2} and Z. Lulić¹*

¹ Faculty of Mechanical Engineering and Naval Architecture, University of Zagreb, Ivana Lučića 5, HR-10000 Zagreb, Croatia, franjo.bijelic@cvh.hr

² Center for Vehicles of Croatia, Capraška 6, HR-10000 Zagreb, Croatia

Introduction

One of prerequisites for vehicle registration in EU countries is a positive Roadworthiness certificate. Vehicles are inspected and checked for deficiencies, environmental or mechanical at the periodic technical inspection (PTI). The goal is to keep the roads safe and ensure that vehicles don't pollute more than it is necessary. Center for Vehicles of Croatia (CVH) has the public authority to manage the organization and standardization of the PTI procedure in Croatia and also possesses an extensive vehicle database which was used in this study.

Personal vehicles (PCs) equipped with a diesel engine and their impact on particle matter (PM) emissions in Croatia are the focus of this study. Deficiencies in vehicles propelled by diesel engines can be costly to repair. Diesel particle filter (DPF) is the most expensive part in the exhaust system which is the main reason vehicle owners opt for its removal instead of buying a new one once it's determined to be faulty. PM are harmful emissions with adverse effects on health (Guttikunda and Goel, 2013; Li et al., 2017; Stockfelt et al., 2017) and the removal of DPF causes a significant increase in particle matter emissions from those vehicles (Theodoros et al., 2009; Tzamkiozis et al., 2010). Efforts in reducing PM emissions, beside emission regulations include banning and restricting traffic to cleaner vehicles in low emission zones (Malina C., 2015; Jiang et al., 2017). The impact of PM emissions on health is even greater in countries with an older vehicle fleet such as Croatia, where the average vehicle age exceeds 13 years (CVH, 2016). Amount of those emissions was shown in a study of NO_x and PM emissions for PCs for the period from 2007 to 2016 (Resetar et al., 2017). PCs equipped with diesel engines make up 46% (CVH, 2016) of the PCs fleet, and 22% (CVH, 2016) of those are PCs equipped with a DPF and high mileage. PCs equipped with a DPF and a high mileage odometer reading are our target group.

This study includes an emissions estimation for PM in PCs and a worst-case scenario estimation of PM emissions accounting for the DPF removal in PCs on the road today. Emission estimations were calculated using COPERT 5 (Computer Programme to calculate Emissions from Road Transport). PC fleet structure and activity data in form of odometer readings used were taken from the CVH database for the year 2016. The current emission test during PTI for PCs equipped with a diesel engine is conducted with an exhaust gas opacity meter which measures the optical properties of the exhaust gases expressed as a K value (smoke density). There is a correlation between K value and PM emissions (Mridul et al., 2008). This testing method, however, is insufficient for diesel engines from EURO 4 onwards because of the instruments resolution limit. Average K value data was calculated for PCs from the PTI emission tests.

PTI inspectors are required to visually check for the presence of the DPF, but they can't detect if a DPF was drilled out or removed from its housing. At this moment, there are no simple methods of detecting DPF tampering. For a method to be applicable during a PTI inspection it must be simple, fast and without any significant mechanical disassembly of the parts. Thermography, a non destructive testing (NDT) method was used as a tool to gather exhaust systems isolation temperature values in order to determine the method applicability for PTI.

Methodology and input data

To estimate the impact of DPF removal and determine its importance on PM emissions real vehicle data was used. Those include experimental measurements done during PTI and theoretical estimation using a specialised software. Emission tests during PTI for vehicles equipped with a diesel engine were conducted with exhaust gas opacity meters which measure the optical properties of the exhaust gases in form a K value. Since DPFs tend to fail on high mileage vehicle, average K value was calculated for vehicles with more then 100 000 km on the odometer.

Theoretical emission calculation was done using COPERT 5, a software program which serves as a tool for the calculation of emissions from road vehicles. Emissions calculated also include PM. Input data needed for PM calculation are vehicle technical, vehicle activity data and environmental data. Vehicle data, including vehicle activity data was taken from the CVH database. Data taken included the number of vehicles, their engine capacity and mileage values. Mileage values recorded during the PTI inspection are shown in figure 1. Vehicle activity data as mean speed and driving conditions percentage were estimated. Estimated values are shown in table 1. Environmental data in form of average temperature and relative humidity needed for the calculation were taken from the Globe program of Croatia (Jurić et al., 2012).

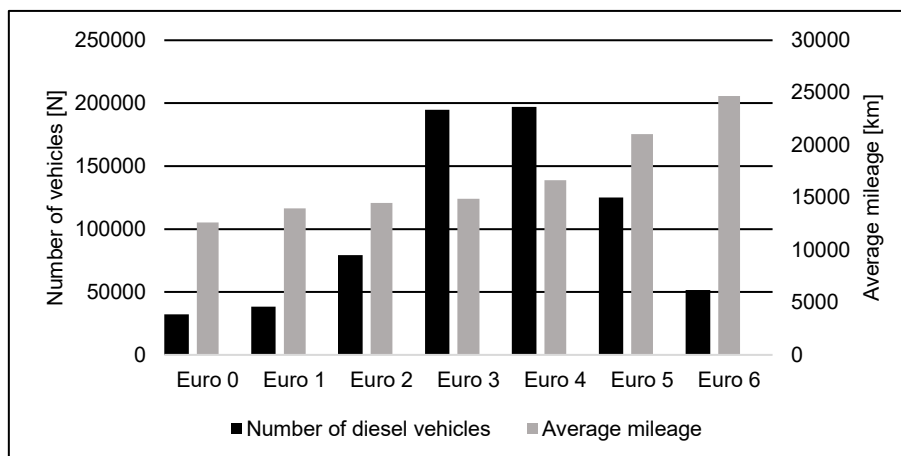


Figure 1: Number of PCs and their average annual mileage by EURO (Croatia, 2016)

Table 1: Mean speed and mileage driven per driving mode

DRIVING MODE	MEAN SPEED [kmh ⁻¹]	SHARE (%)
Urban Off Peak	38	20
Urban Peak	28	20
Rural	60	35
Highway	110	25

To incorporate PTI inspection guidelines, where methods used for vehicle inspection must be simple, fast and without any significant mechanical disassembly of the parts, a none destructive testing (NDT) was chosen. Thermography was used as a tool to gather exhaust systems isolation temperature values and to determine if there is a possibility for the method to detect DPF tampering and if it's suitable for PTI. Thermal camera used was FLIR E6.

Results

Emission tests during PTI for vehicles equipped with a diesel engine were conducted with exhaust gas opacity meters, results are shown in table 2. Average K value increases with vehicle mileage. Only EURO 5 and EURO 6 PCs were taken into account.

Table 2: Average measured K value during PTI depending on mileage for EURO 5 and EURO 6 vehicles in Croatia (CVH database 2016)

Mileage [km]	Average K value [m ⁻¹]
100 000 – 150 000	0,085
150 000 – 200 000	0,088
200 000 – 250 000	0,104
> 250 000	0,159

This testing method, however, is insufficient for low emission diesel engines from EURO 4 onwards because of the instruments resolution limit. Measurements far outside the bounds

(estimated K value of 0,2) could be an indicator of DPF manipulation, this requires further investigation.

PM10 (all particle matter up to 10 µm) emissions are shown in figure 2 and table 3. All EURO 5 and EURO6 PCs are equipped with a DPF, hence a significant decrease in PM10 emissions is visible for those categories.

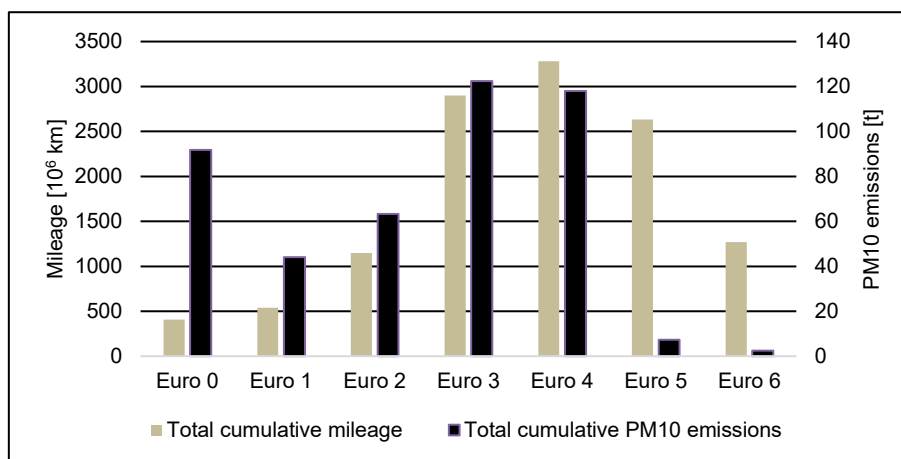


Figure 2 Total cumulative mileage and PM10 emissions of PCs by EURO

Table 3: Total Real Tailpipe PM10 emissions for diesel personal vehicle in Croatia 2016

EURO standard	Number of cars [N]	Average mileage [km]	PM10 emissions [t]
-	32 326	12 621	91,822
EURO 1	38 443	13983	44,102
EURO 2	79 279	14 498	63,316
EURO 3	194 883	14 879	122,378
EURO 4	196 935	16 653	117,969
EURO 5	124 985	21 063	7,378
EURO 6	51 430	24 683	2,495

Crude estimate of PM10 emissions for PCs with removed DPF was done by adding EURO 5 and EURO 6 vehicles to the EURO 4 emission category. Table 4 shows a significant increase in PM10 emissions with a cumulative difference of 130 tones.

Table 4: Total Tailpipe PM10 emissions for diesel personal vehicle in Croatia 2016 accounted for DPF removal

EURO standard	Number of cars [N]	Average mileage [km]	PM10 emissions [t]
-	32 326	12 621	91,822
EURO 1	38 443	13983	44,102
EURO 2	79 279	14 498	63,316
EURO 3	194 883	14 879	122,378
EURO 4	373 350	19 234	258,375
EURO 5	-	-	-
EURO 6	-	-	-

After assessing the importance of a DPF, thermography was used as a method for detecting tampering. At this stage reference data was gathered. That data shows us what thermal changes happen at idle engine speeds for vehicles equipped with DPFs and will serve as a reference point for developing a reliable method. Figure 3 and table 5 show temperature values for a vehicle with

a tampered DPF, as it is completely removed from the housing. A decreasing characteristic in temperature values was recorded along the DPF housing. This could be attributed to the shape of the DPF as the temperature tends to even out after the engine was working for a certain time.

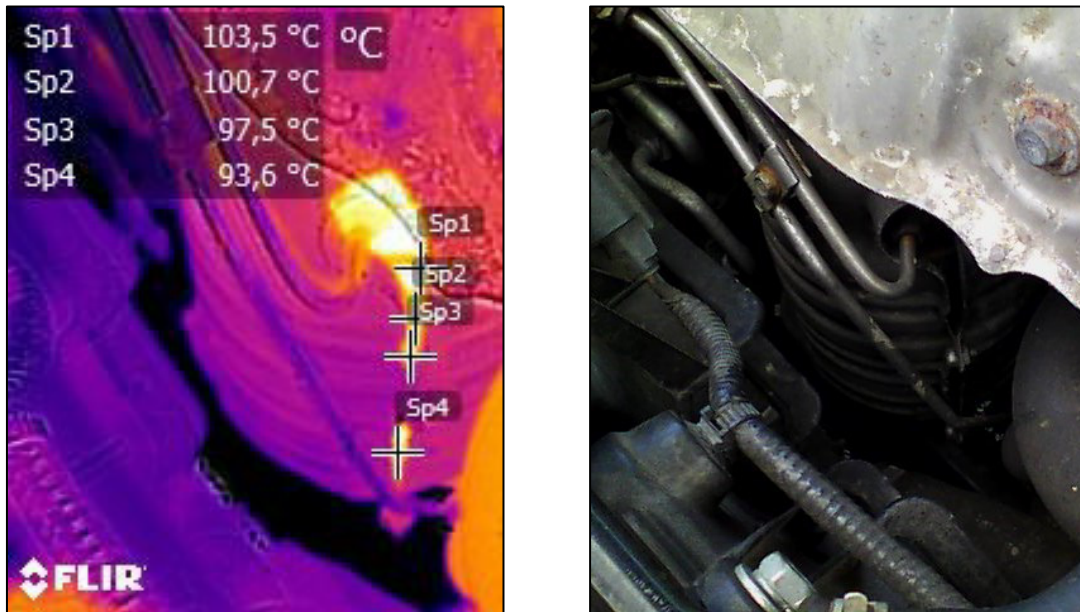


Figure 3: DPF housing thermal image (Honda Accord 2.2 i-CDTI 2009 with removed DPF)

Table 5: DPF housing (isolation) temperature values (Honda Accord 2.2 i-CDTI 2009 with removed DPF)

Measurement spot	Temperature [°C]
Sp1	103,5
Sp2	100,7
Sp3	97,5
Sp4	93,6

The vehicle equipped with the DPF shows temperature variations as shown in figure 4 and table 6.

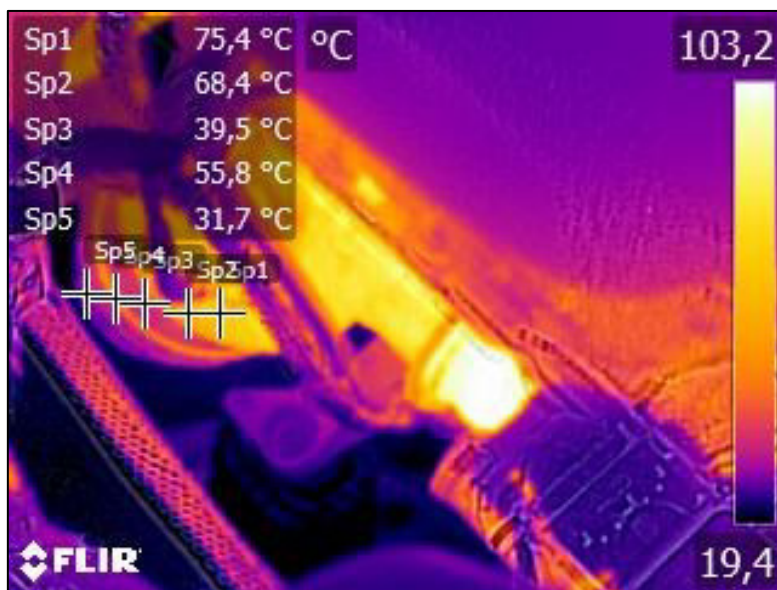


Figure 4: DPF housing thermal image (BMW 120D 2008 with DPF)

Table 6: DPF housing (isolation) temperature values (BMW 120D with DPF))

Measurement spot	Temperature [°C]
Sp1	75,4
Sp2	68,4
Sp3	39,5
Sp4	55,8
Sp5	31,7

The temperature suddenly drops two times, once at Sp3 and the second time at Sp5. The reason for this significant drop is the isolation created by the existing NO_x catalyst (Sp3) and DPF (Sp4). In detecting the complete removal of DPF thermography shows merit.

Conclusion

PCs equipped with a diesel engine and their impact on PM emissions in Croatia were a starting point for this study. Total emissions were calculated using real data collected from CVH. A crude estimate of the effects of DPF removal was established using COPERT 5 and it showed a significant increase in PM emissions from those vehicles. To get a more precise assessment of the DPF tampering impact additional data is needed. Data could be collected in form of questionnaires conducted on vehicle owners in PTI stations to estimate the share of DPF removal. DPF is the most expensive part in the exhaust system which is the main reason vehicle owners opt for its removal. Old average vehicle age, high mileage and purchasing power also contribute to the problem. As roadworthiness is a prerequisite for vehicle registration, PTI inspection is the ideal place to check for DPF tampering. Thermography was assessed as a method and it shows promise and a need for further exploration. Aside from the complete removal of DPF there are methods which just drill holes and therefore reduce the simplicity of thermography as tool for detecting tampering. One way to make the method suitable for different cases of tampering would be to create a temperature reference base of stock cars. Tampering is a current problem which only worsens with the increase in numbers of aging vehicles, especially in countries with a limiting purchase power as Croatia.

References

- Jurić, B., Lacković, D., Šegota, J., 2012. Mean annual temperatures and relative humidity in Zagreb [WWW Document] The GLOBE Program of Croatia. URL globe.pomsk.hr (accessed 9.26.17)
- Theodoros Tzamkiozis, Leonidas Ntziachristos*, Zissis Samaras 2009. Diesel passenger car PM emissions: From Euro 1 to Euro 4 with particle filter
Atmospheric Environment, Volume 44, Issue 7, March 2010, Pages 909-916
- Resetar, M., Pejic, G., Lulic, Z., 2017. Road Transport Emissions of Passenger Cars in the Republic of Croatia
Digital Proceedings of the 8th European Combustion Meeting. Dubrovnik, Croatia, 18-21 April 2017, pp. 2553–2558.
- Mridul G., Randall L. B., Daniel K. C., Peter D. B., Donald W. L. Particulate matter emissions and smoke opacity from in-use heavy-duty vehicles
Journal of Environmental Science and Health, Part A Toxic/Hazardous Substances and Environmental Engineering Pages 557-573 Published online: 15 Dec 2008
<http://dx.doi.org/10.1080/10934520009376986>
- Malina C., Scheffler F., The impact of Low Emission Zones on particulate matter concentration and public health
Transportation Research Part A: Policy and Practice, Volume 77, Pages 372-385, July 2015
<https://doi.org/10.1016/j.tr.a.2015.04.029>
- Guttikunda, S.K., Goel, R., 2013. Health impacts of particulate pollution in a megacity—Delhi, India. *Environmental Development* 6, 8–20. doi:10.1016/j.envdev.2012.12.002
- Stockfelt, L., Andersson, E.M., Molnár, P., Gidhagen, L., Segersson, D., Rosengren, A., Barregard, L., Sallsten, G., 2017. Long-term effects of total and source-specific particulate air pollution on incident cardiovascular disease in Gothenburg, Sweden.
Environmental Research 158, 61–71., doi:10.1016/j.envres.2017.05.036

Tzamkiozis, T., Ntziachristos, L., Samaras, Z., 2010. Diesel passenger car PM emissions: From Euro 1 to Euro 4 with particle filter

Atmospheric Environment 44, 909–916., doi:10.1016/j.atmosenv.2009.12.003

Jiang W., Boltze M., Groer S., Scheuven D., 2017. Impacts of low emission zone in Germany on air pollution levels

Transportation Research Procedia, Volume 25, Pages 3370-3382,
<https://doi.org/10.1016/j.trpro.2017.05.217>

Are GPFs effective for reducing genotoxic emissions of GDI vehicles?

M. Muñoz¹, R. Haag¹, K. Zeyer², J. Mohn², P. Comte³, J. Czerwinski³, N. Heeb¹

¹Laboratory for Advanced Analytical Technologies, Empa, Dübendorf, CH.

²Laboratory for Air Pollution / Environmental Technology, Empa, Dübendorf, CH

³IC-Engines & Exhaust Emissions Lab. Bern University of Applied Science, Nidau, CH.

Introduction

Gasoline Direct Injection (GDI) vehicles are quickly replacing traditional port fuel injection vehicles. It is estimated that 40-60% of all new gasoline vehicles will be powered by GDI engines by 2017 (Mamakos et al., 2013). However, several sources reported high emissions of particles for these vehicles exceeding the Euro 6 limit of 6×10^{11} particles/km (Commission Regulation, 2008).

In GDI engines, the fuel is injected at higher pressures and mixed less uniformly with the incoming air. Due to this stratified charging in the cylinders, rich mixtures near the spark plug and injector, and leaner mixtures further away are obtained. As a consequence of this inhomogeneous combustion, GDI vehicles release large numbers of soot-like nanoparticles of yet unknown toxicity. These particles are formed in cylinders possibly together with polycyclic aromatic hydrocarbons (PAHs) and are not combusted completely before release. GDI-particles are agglomerates with diameters of 20-90 nm. They are as small as those of diesel engines.

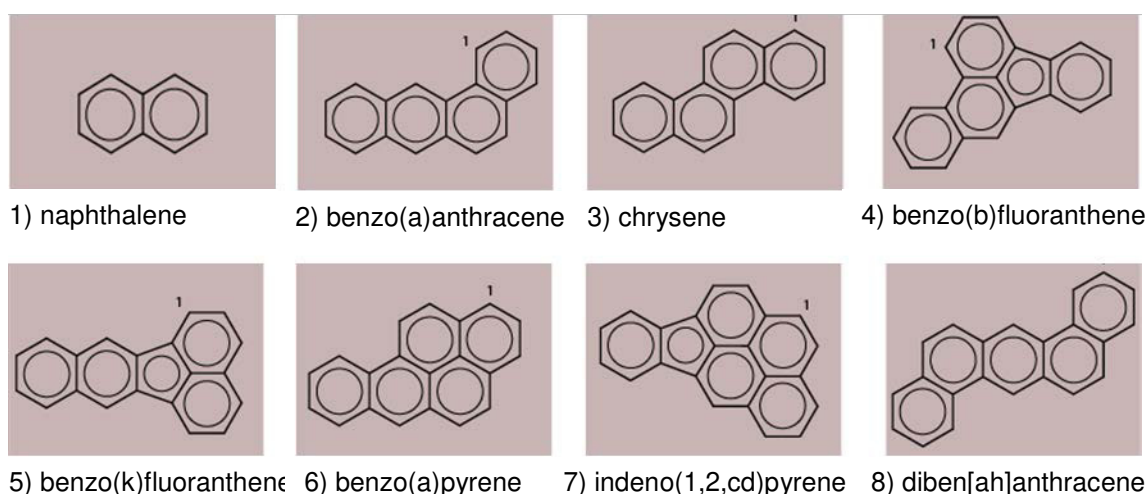


Figure 1: Chemical structures of the 8 genotoxic PAHs.

Certain PAHs and their nitro-derivatives are genotoxic either acting as direct mutagens or carcinogens or as precursors for carcinogens (WHO, 1998, 2004). Apart from their toxic and carcinogenic properties, PAHs are also considered as intermediates for soot formation (Muñoz et al., 2016; Raj et al., 2009). Due to low vapour pressures and similar chemical structures with extended aromatic systems, PAHs tend to adsorb on soot and are co-released with soot.

The WHO classified several PAHs as carcinogenic to humans, like Benzo(a)pyrene (BaP) which is a group 1 carcinogen. Figure 1 shows chemical structures of the 8 genotoxic PAHs. According to the US EPA, 16 PAHs are priority pollutants and 8 of them are carcinogenic (Figure 1). In the Gothenburg Protocol (United Nations Economic Commission for Europe, 2013) and the following directives and amendments the EU and its member states agreed to curtail

long-range transboundary air pollutants. Since 2004, an EU directive limits mean annual benzo(a)pyrene ambient air levels to 1 ng/m³ (European Parliament, 2004). It has been estimated recently that 20% of the European population is exposed to benzo(a)pyrene levels above the target value and 35% of all monitoring stations reported exceedances (European Environment Agency, 2016). It can be questioned, if benzo(a)pyrene levels will remain at current levels or increase in the next years due to additional emissions of the GDI technology. The Swiss occupational health and safety organization limits BaP exposure to 0.002 mg/m³ per work shift (Swiss National Accident Insurance Organization, 2016).

Technical solutions to reduce these toxic emissions are required. Particle filters are most promising. They are widely used for diesel vehicles and could be implemented in GDI vehicles as well. But particle filters may also support the formation of new pollutants, so-called secondary pollutants, during soot combustion. It is expected that the new GDI technology will produce changes in exhaust composition and associated with this new health risks for humans.

Materials and Methods

In this study, complete exhaust samples, including solid, condensed and gaseous fractions, have been collected from 7 GDI vehicles (GDI1-GDI7) representing technologies from Euro-3 to Euro-6, providing a robust GDI mean. A Euro-5 diesel vehicle with a particle filter (D-DPF) has been investigated too as a bench mark. All vehicles were tested at the chassis dynamometer of the UASB. Table 1 summarizes the main characteristics of the vehicles.

Table 1: Characteristics of the tested vehicles

	GDI1	GDI2	GDI3	GDI4	GDI5	GDI6	GDI7	D-DPF
Displacement (L)	1.834	1.390	1.598	1.596	1.598	1.199	1.395	1.560
Injection type	GDI	GDI	GDI	GDI	GDI	GDI	GDI	DI
EU-Legislation	Euro-3	Euro-4	Euro-5	Euro-5	Euro-5	Euro-6	Euro-6	Euro-5
Power (kW)	90 (5500 rpm)	118 (5800 rpm)	125 (6000 rpm)	132 (5700 rpm)	125 (6000 rpm)	81 (5500 rpm)	110 (6000 rpm)	84 (3600 rpm)

The vehicles were driven following the Worldwide Harmonized Light-Duty Vehicles Test Cycle (WLTC) under hot (hWLTC) and cold start conditions (cWLTC) (UNECE, 2013). Moreover, four different filters (two were non-coated and two were coated) were mounted after the three way catalyst (TWC) and were tested with one vehicle (GDI4-Euro5). Diluted exhausts were sampled from a CVS tunnel. In the laboratory, samples were analysed for PAHs following a multistep clean-up procedure described before (Muñoz et al., 2016). Analysis of PAHs is performed by gas chromatography and detection and identification of compounds were achieved by high resolution mass spectrometry in electron-impact ionization mode (GC/EI-HRMS).

The internal standard method is used for PAH quantification. Five concentrations containing deuterated compounds and 16 native PAHs were analysed to determine respective calibration curves and response factors.

Results and discussion

Figure 2 shows concentrations in ng/m³ of the sum of 7 genotoxic PAHs, excluding naphthalene. On the right of the figure, the x-fold increase of PAH emissions related to the diesel vehicle is indicated for each GDI vehicle and the mean of the fleet. The x-fold increase or decrease is also shown for each filter tested related to the vehicle without filter (GDI4).

The results reveal that the GDI fleet emits up to 50 times more genotoxic PAHs than the benchmark diesel vehicle, which was equipped with a DPF; with the GDI1 vehicle being the highest emitter (oldest technology). The later technologies (from Euro 4 to 6) emitted 2-7 times more PAHs than the diesel vehicle.

It can also be observed that variations among different vehicles are substantial and there is a trend toward reduced emissions from the oldest technology (Euro-3) to the newest (Euro-6). This trend can also be found in literature for older Euro legislation vehicles (Caplain et al., 2006).

Figure 2 also includes PAH emission data of the GDI4 vehicle equipped with different gasoline particle filters which were catalytically coated or non-coated. It is shown that with filters F1, F2 and F3 the emissions of GDI4 decreased by 9.5x-, 4x- and 3.5x-fold, respectively. However, genotoxic PAH emissions are still higher than those of the Diesel with DPF (~ 2 times) when using filters F2 and F3. With the non-coated filter F4, PAH emissions increased 3-fold compared to the reference level of GDI4 without gasoline particle filter, being more than 20 times higher than those for the diesel with DPF. A reason for this may be a storage/release phenomenon. This phenomenon has been observed before for other non-catalysed filters. The increased emissions could also be interpreted as the result of a PAH formation during soot combustion, which is to our opinion less likely, because the filter has no catalytic coating which would support the soot combustion.

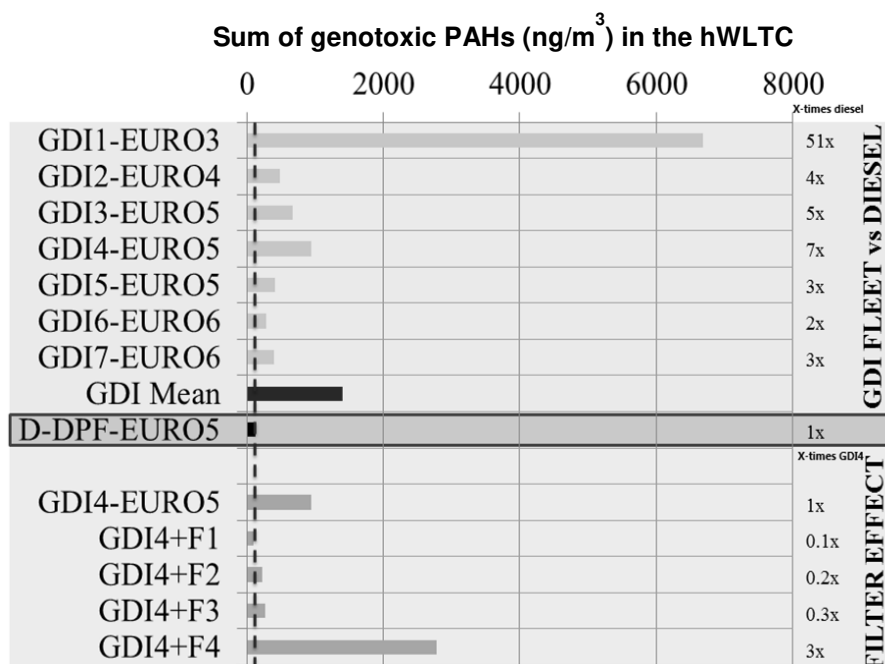


Figure 2: Exhaust concentrations of the sum of 7 genotoxic PAHs (ng/m³), excluding the naphthalene, in GDI vehicles without and with gasoline particle filters. The diesel vehicle with DPF (D-DPF) was used as a reference. GDI4 was tested with different prototype filters in the hWLTC. F1: Non-coated, F2: Coated, F3: Coated, F4: non-coated. The dash line indicates EU ambient limit value for PAHs (1 ng/m³).

It was observed that cold start PAH emissions are often higher than those at hot start. This cold start effect, however, is smaller for the genotoxic PAHs, where average cold and hot start emissions are similar.

In a parallel study, emissions were also collected during steady state conditions, operating the vehicle at specific driving loads. PAH emissions increase substantially at transient vehicle

operations. A similar increase in emissions is also observed with particles. It seems like particle and PAH emissions are correlated and are orders of magnitude higher during transient operations.

Patterns of genotoxic PAHs in vehicles exhaust were also investigated. It could be observed that these PAH patterns are similar to those found for diesel exhaust. This suggests that combustion conditions and formation of pollutants in GDI vehicles might be similar to those in diesel vehicles. These patterns are in most samples dominated by benzo(a)pyrene, the most carcinogenic PAH. It could be observed that, in those filters reducing total PAH emissions, PAH patterns remained similar as well

Conclusions

According to these results, the answer to the question raised in the title is clear. GDI vehicles need efficient catalytic filters in order to reduce the emissions of genotoxic PAHs to levels already achieved for current diesel vehicles. Moreover, a certification procedure similar to that undergone for DPF-approval should be performed with GPFs to comply with high quality parameters achieved for diesel filters.

Vehicle emission legislation should also include a limit or target value for benzo(a)pyrene and other genotoxic PAHs as exhausts of GDI- and non-filtered diesel vehicles exceed the ambient air target value of 1 ng/m^3 by two to three orders of magnitude.

Traditional port-fuel injection vehicles (PFI) are being replaced by the GDI-technology in many markets. It is expected that 50 million GDI vehicles, corresponding to 30% of the passenger car fleet, will operate on Europe's roads in 2020. Therefore, the transformation of fleets which were dominated by PFI-vehicles in the past to fleets with millions of GDI-vehicles is expected to increase atmospheric particle number (PN) and PAH burdens and related to this the genotoxicity of ambient air in traffic affected environments.

References

- Schwarz F.P., H. Okabe and J.K. Whittaker (1997), Fluorescence detection of sulphur dioxide in air at the parts per billion level, *Analytical Chemistry*, 46, 1024-1028.
- Staehelin J., J. Thudium (1994), Trends in surface ozone concentrations at Arosa (Switzerland), *Atmos. Environ.*, 28, 75-87.
- Caplain, I., Cazier, F., Nouali, H., Mercier, A., Déchaux, J.-C., Nollet, V., Joumard, R., André, J.-M., Vidon, R., 2006. Emissions of unregulated pollutants from European gasoline and diesel passenger cars. *Atmos. Environ.* 40, 5954-5966.
- Commission Regulation, 2008. Commission Regulation (EC) No 692/2008 of July 2008 implementing and amending Regulation (EC) No 715/2007 of the European Parliament and of the Council on type-approval of motor vehicles with respect to emissions from light passenger and commercial vehicles (Euro 5 and Euro 6), OJ L 199/1.
- European Environment Agency, 2016. Air quality in Europe - 2016 report. EEA, Denmark.
- European Parliament, 2004. Directive 2004/107/EC of the European Parliament and of the Council of 15 December 2004 relating to arsenic, cadmium, mercury, nickel and polycyclic aromatic hydrocarbons in ambient air, OJ L 23/3-16.
- Mamakas, A., Steininger, N., Martini, G., Dilara, P., Drossinos, Y., 2013. Cost effectiveness of particulate filter installation on Direct Injection Gasoline vehicles. *Atmos. Environ.* 77, 16-23.
- Muñoz, M., Heeb, N.V., Haag, R., Honegger, P., Zeyer, K., Mohn, J., Comte, P., Czerwinski, J., 2016. Bioethanol Blending Reduces Nanoparticle, PAH, and Alkyl- and Nitro-PAH Emissions and the Genotoxic Potential of Exhaust from a Gasoline Direct Injection Flex-Fuel Vehicle. *Environ. Sci. Technol.* 50, 11853-11861.
- Raj, A., Celnik, M., Shirley, R., Sander, M., Patterson, R., West, R., Kraft, M., 2009. A statistical approach to develop a detailed soot growth model using PAH characteristics. *Combust. Flame* 156, 896-913.
- Swiss National Accident Insurance Organization, 2016. Grenzwerte am Arbeitsplatz 2016.

UNECE, World Forum for Harmonization of Vehicle R.W., 2013. Proposal for a new global technical regulation on the Worldwide harmonized Light vehicles Test Procedure (WLTP), in: UNs Economic Commission Europe (Ed.), ECE/TRANS/WP.29/2014/27.

United Nations Economic Commission for Europe, 2013. 1999 Protocol to Abate Acidification, Eutrophication and Ground-level Ozone to the Convention on Longrange Transboundary Air Pollution, as amended on 4 May 2012, in: United Nations Economic Commission for Europe (Ed.), ECE/EB.AIR/114.

WHO, W.H.O., 1998. Environmental Health Criteria 202: Selected Non-Heterocyclic Polycyclic Aromatic Hydrocarbons, in: WHO (Ed.), WHO report number. International Program on Chemical Safety, World Health Organization, Geneva, Switzerland.

WHO, W.H.O., 2004. Environmental Health Criteria 229: Nitrogenated Polycyclic Aromatic Hydrocarbons, in: WHO (Ed.), WHO report number. International Program on Chemical Safety, World Health Organization, Geneva, Switzerland.

Drone-based measurement systems offer promising new methods for measuring Air Pollution Spatial Distribution – example results from a pilot study conducted in the Misox Valley of the Swiss Alps

J. D'Atri¹, M. Betschart¹, C. Ruckstuhl¹, M. Fengler² and H. Lötscher³

¹inNET Monitoring AG, Altdorf, Uri, 6460, Switzerland, datri.justin@innetag.ch

²Meteomatics AG, St. Gallen, St. Gallen, 9014, Switzerland

³Amt für Natur und Umwelt Graubünden, Chur, Graubünden, 7000, Switzerland

Summary

Building off some of the world's first air pollution characterization studies conducted with drones in 2014 in the Reuss Valley of the Swiss Alps, inNET Monitoring AG and Meteomatics AG led another drone-based air pollution measurement campaign in the Misox Valley of Switzerland in December 2016. This study, commissioned in partnership with the Amt für Natur und Umwelt Graubünden, was conducted to determine the effectiveness of using drones to evaluate the spatial distribution of air pollution (i.e. lung deposited surface area (LDSA)) within the well-studied Misox Valley. Using a specially designed drone equipped with temperature and air pollution sensors, the project was able to successfully measure the spatial dynamics of air pollution during a 2-day period where the Misox Valley was experiencing a strong winter inversion. Compared with the nearby fixed reference measurement stations, the drone measurements provided a first indication of how small-scale and subtle differences in meteorological parameters have a strong influence on the formation of weak ground-level inversion layers. Although the low number of drone flights to date do not offer conclusive evidence yet, promising initial results from the study suggest further opportunities for drone-based air quality studies including the further optimization of forecasting models.

Air Quality measurement with Drones – a novel approach

Recent developments in drone technology are now driving new air pollution measurement possibilities that can enable a better understanding of air pollution spatial distribution. Typical traditional measurement methods like fixed air quality measurement stations do not offer practical methods for accurately understanding the spatial distribution dynamics in a small valley like the Misox. Meteomatics AG, an innovative SME from St. Gallen Switzerland, has developed a specially designed drone that can measure in-situ parameters for air quality and other weather measurements like temperature, humidity, and wind. Being able to carry a payload up to 1kg for a period of 40 minutes, the MeteoDrone XL is equipped with onboard weather and air quality sensors in order to become a flying air quality measurement station – thus enabling never-before possible studies of spatial distribution of air pollution and other weather phenomena.



Figure 1: The MeteoDrone XL from Meteomatics AG used for measuring air pollution in the Misox Valley Switzerland case study.

Pilot Study Location – Misox Valley Switzerland

The narrow geographic shape of the Misox Valley, combined with the wood burning habits of the residents and the intersection of two important highways for pan-European transport (San Bernardino and Gotthard), frequently create air pollution conditions that exceed normal limits during winter (Sandradewi et al. 2008). The narrow valley sides and a distinct pool of cold air in winter, lead to pollutants being unable to mix within the air column sufficiently diffuse compared to flatter landscapes. In order to monitor such inversions and corresponding poor air quality conditions, the Amt für Natur und Umwelt (ANU) Graubünden operates a temperature profile on the northern slope south of valley in addition to two high-quality air quality monitoring stations. The two fixed air quality monitoring stations of San Vittore and Grono primarily permit the documentation of long-term changes in air pollution and limit value transgressions. On the other hand, these measuring stations do not allow the spatial distribution of pollutants to be determined both vertically and horizontally. Fortunately, advances in measurement technology and drones make it possible to carry out weather and air pollutant profile measurements using drones relatively easily.



Figure 2: Near-ground inversion layer showing air pollution cloud above the Misox Valley.

Pilot Study Objectives

In order to quantify the spatial dispersal of pollutants more precisely, the ANU Graubünden has commissioned Meteomatics AG and inNET Monitoring AG to carry out drone measurement flights in the Misox Valley and to compare the measured values collected with conventional measurements. The following case study will summarize results of the drone-based measurements carried out on the 6th and 7th of December 2016. The Misox case study focuses on the following objectives:

- Comparison of with the drone-based temperature profile vs. the ground based measurement on the north slope of the valley
- Altitude dependence of the pollutant load
- Spatial distribution of pollution levels
- Influence of meteorology on pollutant load.

Method and LDSA Measurement Parameter

During the in-situ drone flights, the pollutant parameter Lung Deposited Surface Area (LDSA) was measured. The LDSA stands for the sum of the total particle surface area per air volume, usually measured in $\mu\text{m}^2 \text{cm}^{-3}$. Since particle surface is relevant for health effects on the body, LDSA (although relatively rarely used in studies) is an insightful measurement for health and workplace safety studies. The parameter LDSA is therefore particularly suitable for analyses concerning particulate matter and the measurement of black carbon emissions, such as the conditions being investigated in the Misox Valley.

Pilot Study Results - Analysis of two-day Drone-based Measurement Campaign

Over the course of the two-day measurement campaign, 37 different drone measurement flights were carried out altogether on December 6th and 7th, 2016. At each flight location, the changes in temperature, relative humidity, dew point, air pressure, wind speed, wind direction and LDSA parameters were recorded throughout the duration of the drone's flight time

Analysis of 1st day results:

At the location of the San Vittore air quality station, four drone measurement flights were carried out on 06.12.2016 and 07.12.2016 (see Figure 3 to Figure 10). These figures display the temperature profile and the parameter LDSA as a function of the altitude during the course of the day. Throughout the day, the valley experienced a significant inversion with colder temperatures on the valley floor and warmer temperatures with increasing altitude. At no time, however could a decrease in temperature be observed with increasing altitude. Both measuring systems (temperature profile and drone) show a pronounced isothermal inversion. Furthermore, the temperature differences between what was recorded by the temperature profile and drones, appear to be systematic and can be explained by warmer temperatures in the middle of the valley (where the drone was flying) compared to the shadowy valley wall where the vertical temperature profile loggers are installed in San Vittore. While the temperatures on the valley floor hardly changed at all during the course of the day, they increased in altitude until after midday. These observations are not only valid for the study, but can be regarded as examples of the meteorological situation during large-scale inversion situations (Sandradewi et al. 2008).

The concentrations of particulate matter in the form of the parameter LDSA show two main characteristics - the concentrations rise in line with the temperature increase within the inversion, and as the drone measurement at 5.17 p.m. impressively demonstrates, probably also with the parallel firing activities of the households. During the first day, the peak LDSA measurement was located at an altitude of about 10-20m above ground. This is consistent with observations on site, according to which there was always an extremely pronounced haze layer just above ground level. Lastly, the LDSA values tend to zero as soon as the temperature gradient decreases and appears to be equal to the isotherm. Further horizontal spatial distribution analyses of the 1st day of the measurement campaign can be found in the appendix.

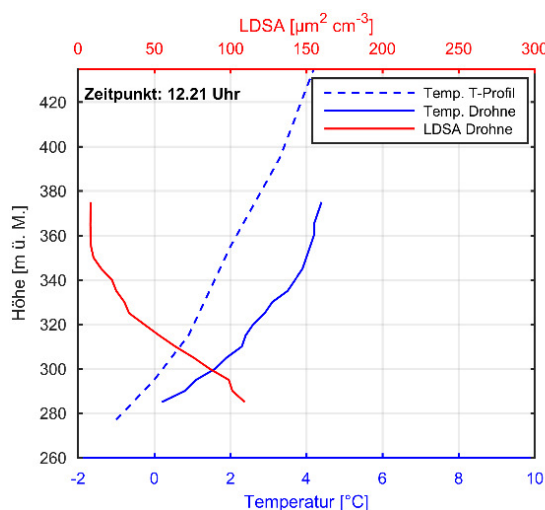


Figure 3: Flight data at 12:21 on 06.12.16

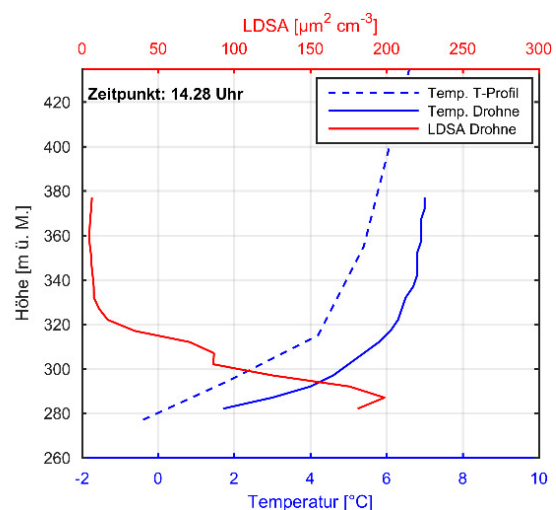


Figure 4: Flight data at 14:28 on 06.12.16

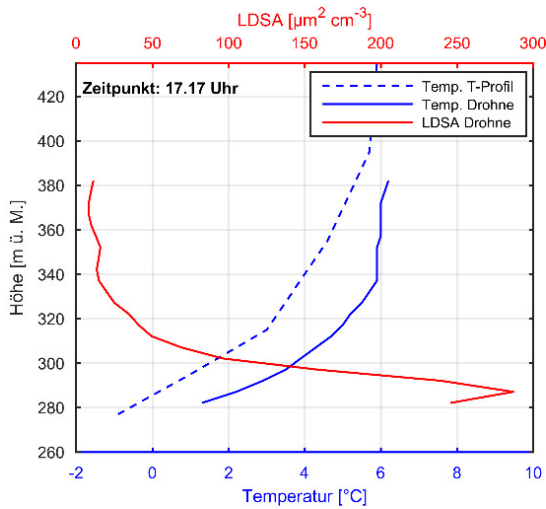


Figure 5: Flight data at 17:17 on 06.12.16

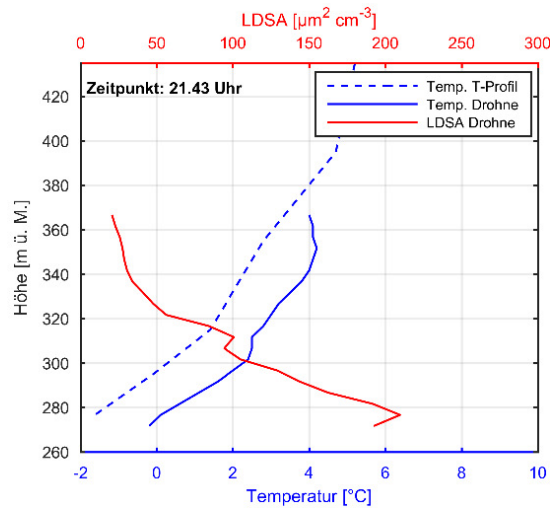


Figure 6: Flight data at 21:43 on 06.12.16

Analysis of 2nd day results:

On the second day, a similar but not identical picture presented itself on 07.12.2016. Again, a clear inversion situation was visible. The inversion increased during the course of the day with the maximum occurring during the afternoon. The LDSA values decrease with increasing altitude, whereas the values tend to zero as soon as the vertical temperature gradient decreases significantly. The highest concentrations of particulate matter are reached during the morning and at 8 p.m. Once again, the wood-firing activities appear to be the most obvious explanation. During the morning, a continuous firing activity pushes up particulate matter levels, in the afternoon the values decrease, and then increase further towards evening. Furthermore, there was no obvious intense haze layer just above the ground as observed on the first day. It is not possible to make a conclusive assessment of why this layer is missing. Apart from this small difference, the situations are generally comparable, but the wind speeds on the 2nd day (07.12.2016) were slightly higher than on the previous day. Additionally, the maximum LDSA concentrations were lower compared to the 1st day (06/12/2016). It is conceivable that, in addition to the general situation in the valley, the development of a local inversion layer near the ground is a decisive factor in the fact that the particulate matter values can be significantly higher a few metres above the ground (and thus, over the height of the fixed fine dust measuring stations). However, for the formation of such a very localized and strongly pronounced layer, various factors (temperature, relative humidity and wind speeds) need to be just right to create these conditions.

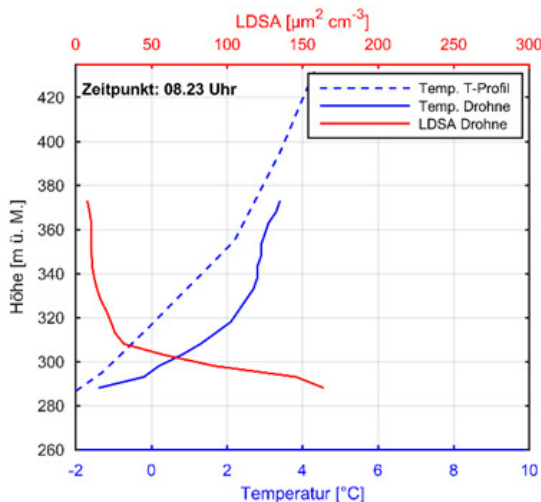


Figure 7: Flight data at 08:23 on 07.12.16

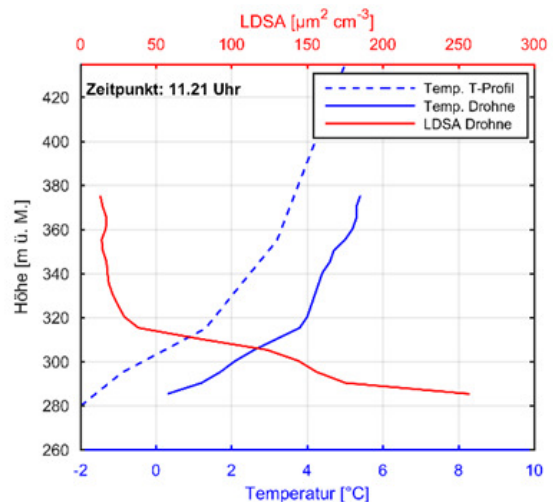


Figure 8: Flight data at 11:21 on 07.12.16

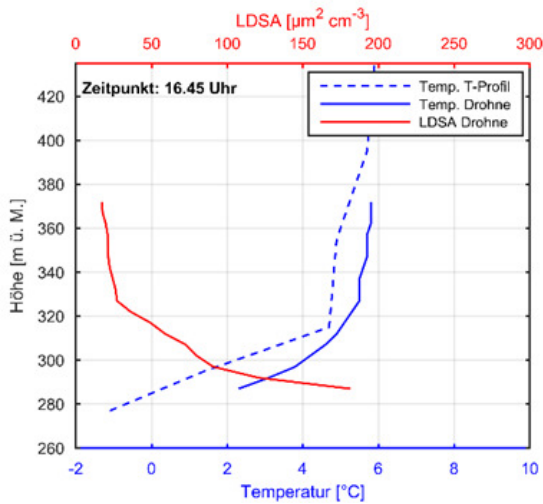


Figure 9: Flight data at 16:45 on 07.12.16

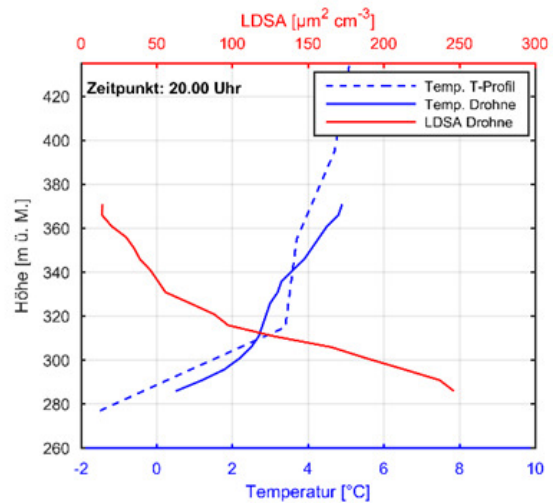


Figure 10: Flight data at 20:00 on 07.12.16

Comparison of Drone LDSA measurements with fixed air quality measurement stations:

In the following figures, parameters Black Carbon 6 (BC for the wavelength 880 nm), PM10, and the particle count are continuously recorded (based on 30 min values) from the two Misox Valley measurement stations locations, San Vittore (SV) and Grono (Gr). In order to compare the measurement station values with the in-situ drone measurements, the ground-level measurement of each individual drone flight is plotted as a single cross. Although the measuring heights between the stations and the drone flights differ considerably in some cases, the overall result is a detailed picture of the chronological progressions between the individual parameters over the two days. Furthermore, it is important to note that on the second day of the campaign (07.12.2016) the pollution level was slightly higher than on the first day. This can most likely be explained by the continued large-scale inversion situation.

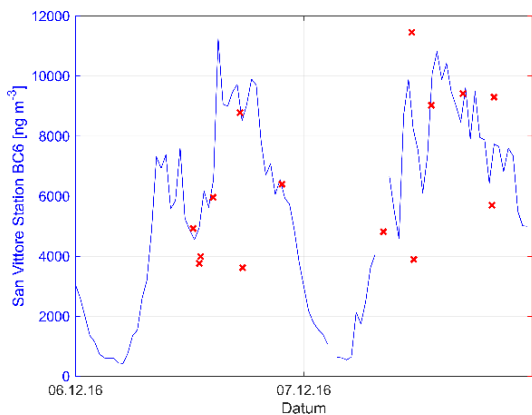


Figure 11: BC6 vs. Drone LSDA at SV

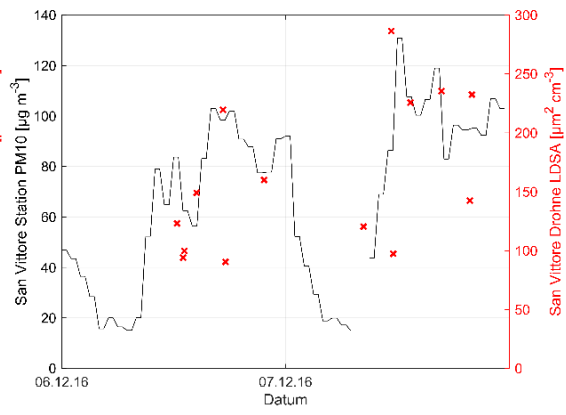


Figure 12: PM10 vs. Drone LSDA at SV

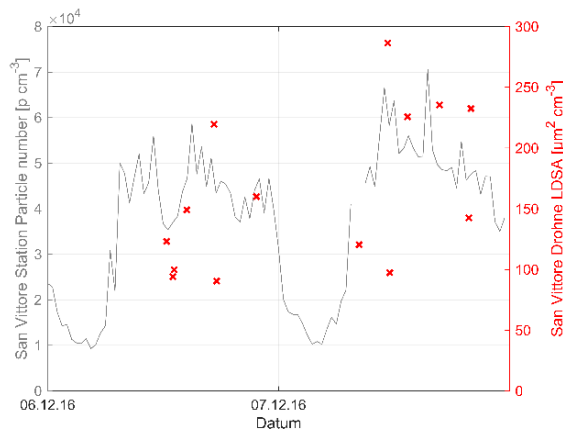


Figure 13: Particle Count vs. Drone LSDA at SV

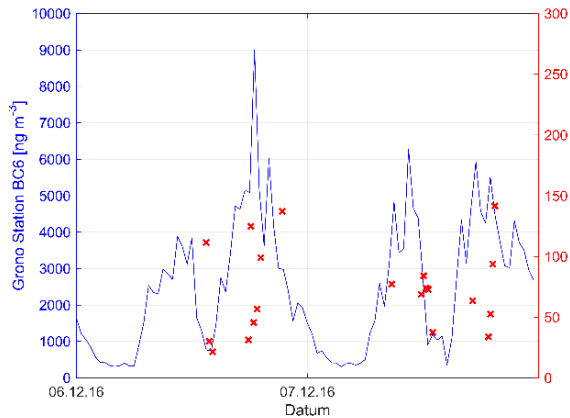


Figure 14: BC6 vs. Drone LSDA at Gr

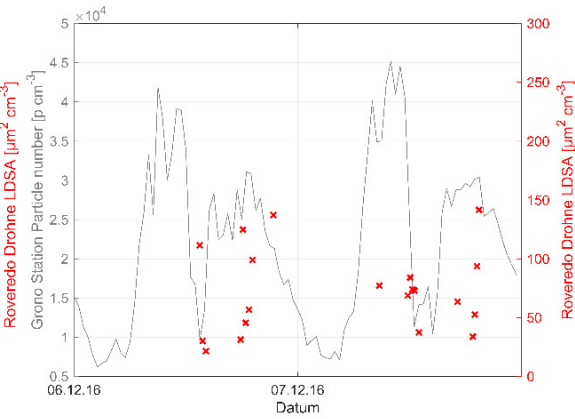


Figure 15: Particle Count vs. Drone LSDA at Gr

Conclusion

The drone measurement campaign in the lower Misox Valley has shown that detailed insights can be evaluated regarding the air quality situation with the help of pollutant and meteorological measurements. The spatial distribution of the measurements allows for an even better understanding of the interrelationships that lead to the formation of high concentrations of particulate matter, especially during strong winter inversions as observed in the pilot, than only with fixed measurement stations. Although, the drone measurements were well in line with the fixed station measurements, it became clear that due to the solar radiation, wind and humidity, there are sometimes large deviations compared to the fixed measurement stations. Furthermore, the temperature profile on the shadowy slope of the valley wall shows only the valid situation near the surface of the shadowy slope, but in the middle of the valley or on the opposite side where there is significantly more sun radiation, large deviations were again observed during the measurement campaign. Depending on the of drone flight location, these differences were also found in the wind, the humidity, and even the fine dust pollution in comparison to the ground stations. Most notably, the change in the gradient of the temperature seems to have a major influence on the spatial expansion of fine dust pollution within the inversion. In some cases, the measurement data suggests that the LSDA load is increased at ground level with increasing height until the temperature gradient changes. Although the low number of flights during the pilot study do not allow a conclusive assessment above the above inferences, these initial drone measurements provide the first indications of how small-scale and fine differences in meteorological parameters affect the formation of weak inversion layers near the ground.

Next Steps for further research in Drone-based in-situ air quality measurement

Even though the drone measurements over the two-day measurement campaign provide an initial overview of the spatial distribution of ambient air pollution, it is recommended that further studies carry out the drone measurement campaigns over a longer period of time in order to better explain the meteorological influences on air pollution. In addition, it is recommended to supplement the vertical flights with so-called horizontal flights in the valley in transverse and longitudinal directions. This could make it easier to assess the influence of wood firing systems on air pollution. An additional use of drone measurement could offer interesting insights when utilized, in explicit congestion situations with in a town, or in case of heavy traffic in order to monitor the air pollution influence of a nearby highway or traffic on observed air pollution spatial distribution.

Furthermore, in a follow-up project, it is planned that the data analysis tools first used with in the pilot study will be further optimized, in order to enhance and automate the data analysis process so standardized drone analyses can be created quickly and efficiently in the future.

In addition to leveraging automated analysis tools and horizontal flight paths, further studies could also evaluate the temperature profile data in more detail. The inversion intensity and the temporal development of the inversion throughout the year, should always be investigated more

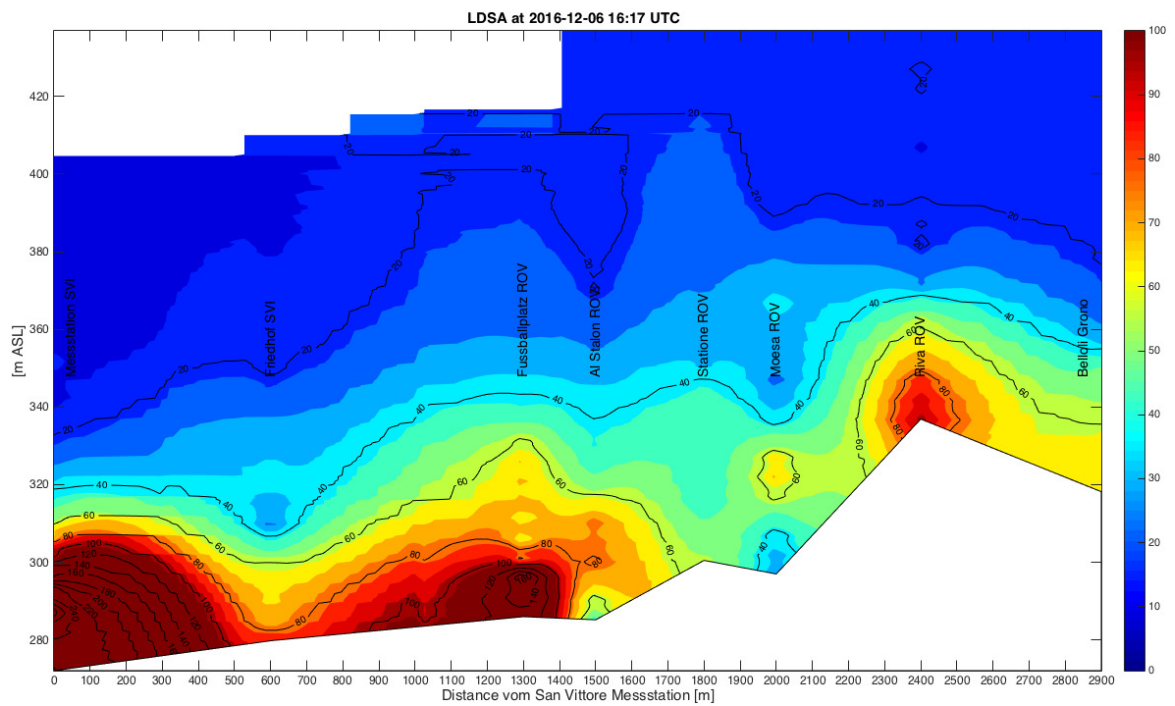
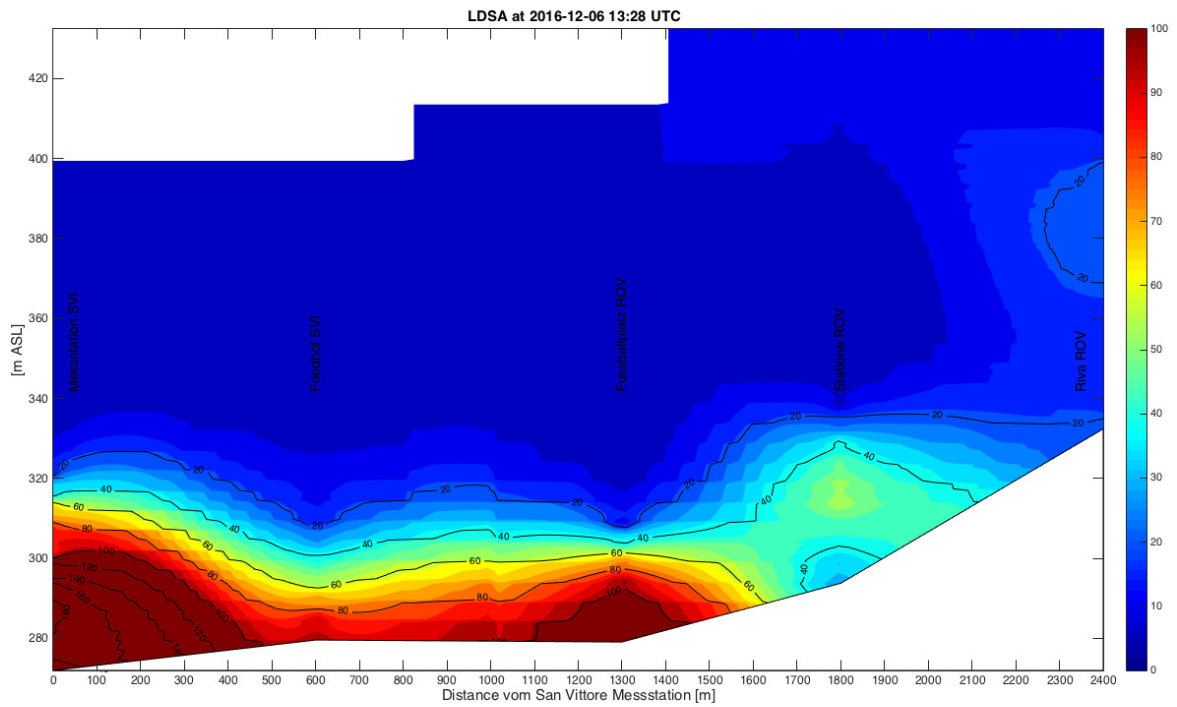
closely regarding the ambient air pollution situation due to air pollution's strong correlation with inversion conditions. The evaluation of measurement station data could also be supplemented by additional model analyses in order to identify the large-scale air movements and their influence on the air quality situation in the overall context (such as during the phenomena of alpine pumping). The first measurement campaign has shown that local and weak ground level inversions also have a massive impact on near-ground air quality. By combining more drone measurements with the existing elevation profile of the temperature, a more detailed inversion analysis for the communities of the lower Misox could be carried out. It is also conceivable that an analytical forecasting tool could be developed based on this data, which in combination with information from the weather models and the live values of the measuring stations, would allow for a detailed and short-term forecast of potentially unfavorable situations. This forecast could in turn be made available to the population or serve as a basis for further managing the overall air pollution context for a region.

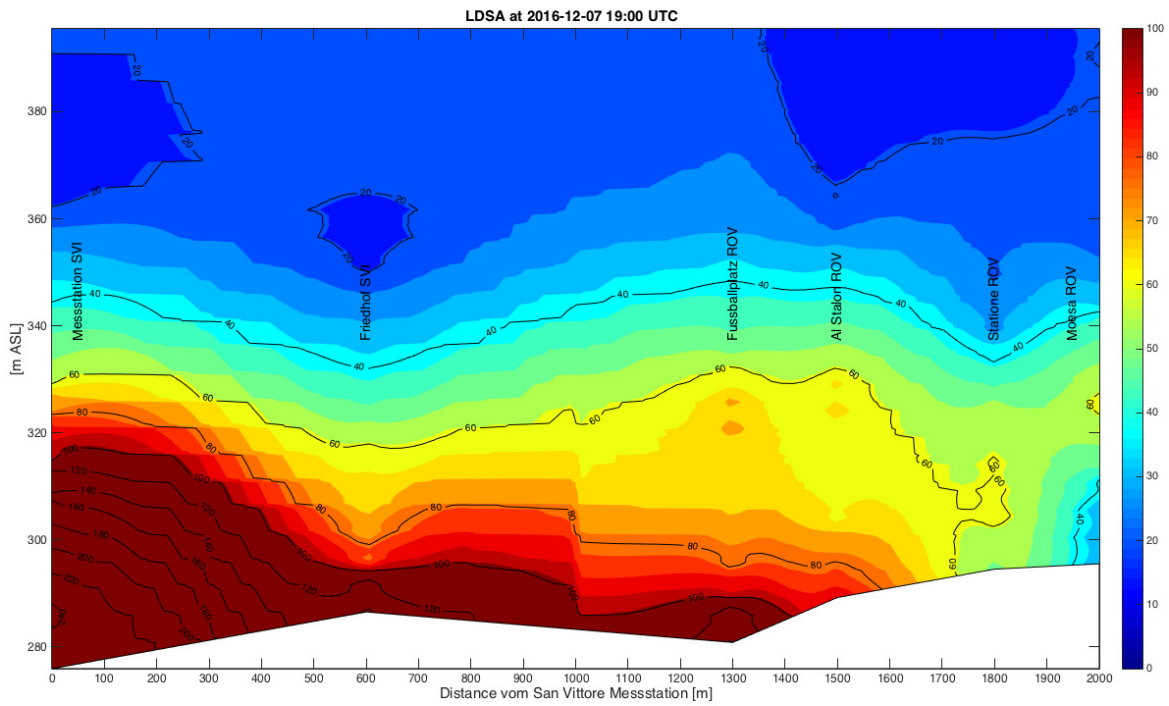
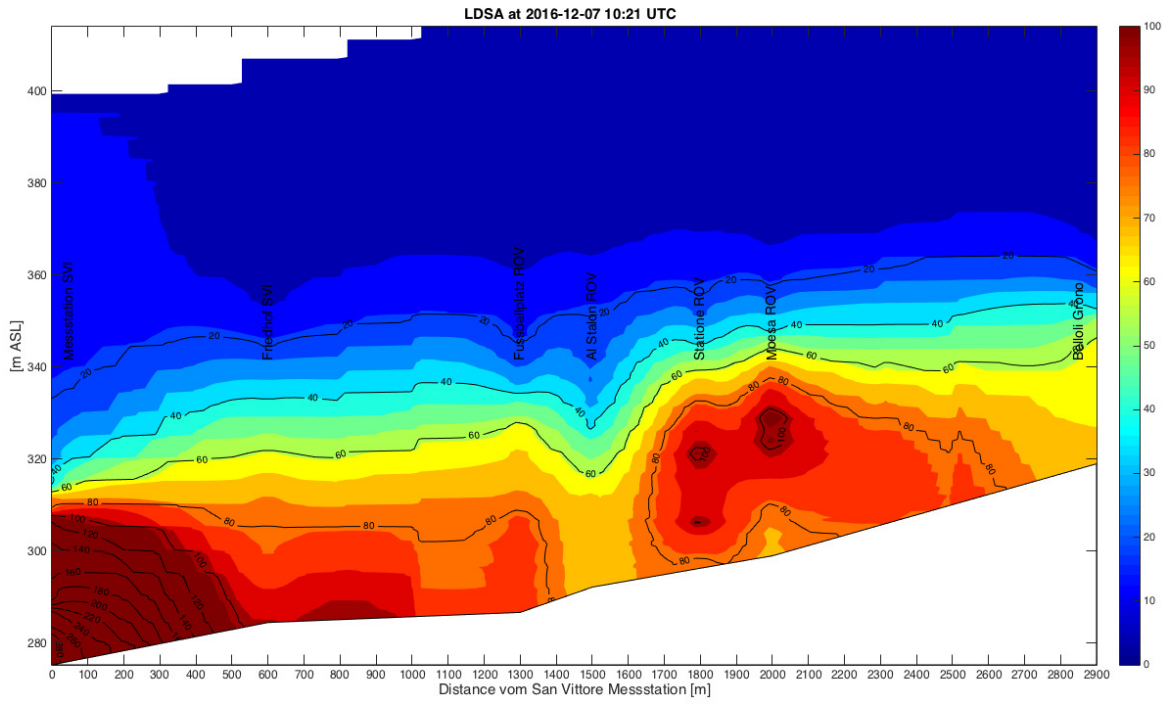
References

Sandradewi J., A.S.H. Prevot, E. Weingartner, R. Schmidhauser, M. Gysel, and U. Baltensperger (2008), A study of wood burning and traffic aerosols in an Alpine valley using a multi-wavelength Aethalometer, *Atmospheric Environment*, 42, 101-112.

Appendix

The following appendix figures display the LSDA spatial distribution across the valley axis starting with the measurement station on the left.





Assessment of urban hybrid buses performance in a megacity network

Christos Keramydas¹, Georgios Papadopoulos¹, Leonidas Ntziachristos^{2}, Ting-shek Lo³, Kwok-lam Ng³, Hok-lai Anson Wong³, Carol Ka-lok Wong³*

¹ Emisia S.A., 21 Antoni Tritsi Str., PO Box 8138, GR 57001, Thessaloniki, Greece

² Department of Mechanical Engineering, Aristotle University of Thessaloniki, PO Box 483, GR 54124, Thessaloniki, Greece, leon@auth.gr

³ Environmental Protection Department, Hong Kong SAR Government

Abstract

Fuel consumption and emission levels of six Euro VI hybrid-diesel double-deck buses tested on six regular city routes in the broader metropolitan area of Hong Kong are examined in this study. Six Euro V conventional diesel buses were also included in the trials (control group), so that a pair of different technology buses was assigned to each route. Measurements were conducted by employing portable emission measurement systems, which allowed for the collection of data covering a wide range of driving, operation, and ambient conditions. The average fuel consumption of the hybrid-diesel buses was found to be 6.1% lower. Air-conditioning, which was enabled for all vehicles during trials, limited the expected fuel consumption benefits of hybrid technology, especially in routes of low average speed. NO_x emission levels of hybrids were 93±5% lower than the ones of the conventional buses. The outcomes of this study show that the real-world fuel consumption benefits potentially offered by the hybrid technology are not as high as expected by such an advanced powertrain system.

Keywords: PEMS, hybrid technology, fuel consumption, double-deck buses, Euro V, Euro VI

Introduction

Hybrid buses are expected to offer improved fuel consumption than conventional ones (Lajunen, 2014). Fuel economy benefits offered by parallel- and series-hybrid buses have been verified in recent past through either simulation experimentation or the conduction of real-world driving trials. Merkisz and Pielecha (2010) reported a 15-18% lower fuel consumption of hybrid-diesel buses when compared to conventional buses, in Poznan, Poland, also denoting the impact of traffic conditions on fuel consumption. Hallmark et al. (2013) measured three hybrids and two conventional buses in Iowa, USA, and found a 11.8% higher on-road fuel economy for the hybrids. A higher fuel saving potential (up to 30%) is reported by Semercioglu et al. (2010), who comparatively tested one hybrid and one conventional bus in Sakarya, Turkey. Zhang et al. (2014), who analysed the on-road emissions of two Euro IV single-deck hybrid-diesel buses in Beijing as part of a total sample of 75 buses, reported a 29% benefit in fuel consumption for the hybrids over the conventional buses, but also a 50% increase in hybrid fuel consumption when shifting from an average driving speed of 25 km/h to that of 15 km/h, as well as the elimination of fuel consumption gains when air-conditioning was enabled. Consequently, the operation conditions appear to have a critical role in the final real-world fuel consumption benefits offered by the hybrid technology.

The Environmental Protection Department (EPD) of Hong Kong (HK) launched in 2008 one of the most widespread Portable Emission Measurement Systems (PEMS) campaigns around the world, which is dynamically evolving over time, having measured thus far 330 vehicles of different categories. In parallel, the Government of Hong Kong decided in 2014 on the financial support of the purchase of six Euro VI double-deck diesel-hybrid buses that was initially used for trials under regular operation conditions so as to assess their real-driving performance; this action was performed in the context of a campaign aiming at zero public transport emissions across the territory (The Government of Hong Kong Special Administrative Region, 2011).

Fuel consumption and emission levels of six Euro VI hybrid-diesel and six Euro V conventional-diesel double-deck buses, tested in the broader metropolitan area of Hong Kong, are examined in this study. The main goal of the study is to investigate and comparatively assess the fuel

economy efficiency of the hybrid buses under their regular real-world operation; conventional buses had the role of the control group in this study. A secondary goal is to explore the potential benefits of combining the hybrid and the Euro VI-related technologies. The overall scope of the analysis is to provide the necessary input to public authorities of municipalities around the world in order to support the respective decisions on the most appropriate and beneficial technologies that should be promoted for public transport in their areas.

Methods

Test vehicles and PEMS

The twelve double-deck buses that were employed in the trials are regular full-service buses and part of the fleet of two major public transportation providers in Hong Kong. The make of the buses is Alexander Dennis and the models are Enviro500 and Enviro500H, respectively, for the conventional and hybrid buses. The series-hybrid system of the hybrid-diesel buses is the BAE HDS200 HybriDrive System. Hybrid buses are of smaller engine size (6.7 [L]) than the respective conventional buses (8.9 [L]), and consequently, the engine rated power is also lower for the hybrids (204 [kW]) than the rated power of the conventional ones (243 [kW]). Both types of vehicles were equipped with a Selective Catalytic Reduction System (SCR), whereas, the equipment of hybrids additionally included a Diesel Particulate Filter (DPF) and an Exhaust Gas Recirculation (EGR) system. Gross vehicle weight was the same for all buses.

CO, CO₂, NO, NO₂, and HC emissions were measured using the commercially available SEMTECH-DS (Sensors, Inc.) PEMS system, whereas, the measurement of NH₃ and N₂O pollutants was performed using an A&D Technology Fourier Transform InfraRed spectrometer (FTIR). A SEMTECH EFM-2 or EFM-HS (Sensors, Inc.) exhaust flowmeter was employed for the measurement of the real-time exhaust gas flowrate. Additional data recordings included the date/time of the recording, global positioning system data, on-board diagnostics and engine management data, and gaseous and particulate pollutant concentrations. Instrument calibration and verification were performed based on the specifications of ISO 16183 (ISO, 2002), US EPA (US EPA, 2015) and the European Commission (EU, 2011). PEMS zero level was set every hour, practically at the beginning and end of each route, using zero gases, while audit was performed every three hours, and span twice a day at concentrations comparable to the range of the emissions.

Design of trials, testing routes, and calculation methods

The trials conducted during the first half of 2015 resulted in the collection of 140 hours of field data. Six original city routes were selected, representative of the Hong Kong traffic conditions and road patterns, including either completely urban, a combination of urban and highway, or mostly highway driving. A pair of one conventional bus and one hybrid bus was allocated to each route. Buses were driven by professional drivers. The “bus trailing” mode on a fixed route was employed in the experimentation. The bus load was set to 50%-60% of the respective maximum vehicle payload. Each bus performed at least three (3) round-trips. The start/stop engine function was enabled for two of the hybrid buses. Air-conditioning was constantly on during testing.

Instantaneous fuel consumption rates were calculated based on the PEMS real-time emissions of CO₂ and carbon-related pollutants (CO and HC) by properly modifying the respective standardized carbon balance methodology for diesel combustion (UN, 2013), as illustrated in equation 1 (Zhang et al., 2014). In this equation, FR is the instantaneous fuel consumption rate [g/s]; ER_{THC} , ER_{CO} , and ER_{CO_2} are the instantaneous emission rates [g/s] of HC, CO, and CO₂ pollutants, respectively, and WC is the carbon fraction of fuel (0.861 for diesel).

$$FR = \frac{0.861 \times ER_{THC} + 0.429 \times ER_{CO} + 0.273 \times ER_{CO_2}}{W_C} \quad (\text{Eq. 1})$$

The instantaneous power was calculated with equation 2:

$$P = \frac{1}{2} \rho C_d A v^3 + \tau_0 g m v + (m_{tare} \lambda + m_{load}) v a + m g v s i n a + P_{aux} \quad (\text{Eq. 2})$$

In equation 2, ρ is the air density [kg/m^3], C_d is the aerodynamic drag coefficient ($C_d=0.45$), A is the frontal bus area ($A=10.6$ [m^2]), v is the vehicle speed [m/s], τ_0 is a rolling resistance coefficient ($\tau_0 = 0.007$), g is the gravitational acceleration ($g=9.81$ [m/s^2]), m is the vehicle mass including loading, i.e. $m = m_{tare} + m_{load}$, with m_{tare} the tare mass of the vehicle and m_{load} the mass of the measurement devices and the ballast mass used to account for passengers. The term λ stands for the equivalent inertia of rotational masses ($\lambda=0.1$ for conventional and $\lambda=0.15$ for hybrid buses, to take into account the additional rotating mass of electrical devices for hybrids). P_{aux} can be significant in case that the air condition is constantly on to cool the passenger cabin for buses operating in hot and humid climates, like in Hong Kong (Shek and Chan, 2008); a fixed consumption of 25 [kW] (Bottiglione et al., 2014) was considered.

Results and Discussion

Driving, operation, and ambient testing conditions

Table 1 presents the driving, operation and ambient conditions during trials. The main operational and ambient parameters are similar for the two groups of buses (p-values range from 0.23 to 0.88); statistically significant differences are also marked on the table. This fact allows for more reliable conclusions with respect to the potential benefits of the hybrid technology since the assessment of the performance of the hybrid buses in this study is conducted in a comparative manner to their conventional diesel counterparts. Engine speed differences in routes #2 and #3 are due to the activation of the start-stop engine function for the respective hybrid buses.

Table 1: Overview of the mean driving, operation and ambient conditions per route and bus.

Route #	Speed [km/h]	Positive acceleration [m/s^2]	Positive power [kW]	Engine speed [rpm]	Exhaust temperature [$^{\circ}\text{C}$]	Ambient temperature [$^{\circ}\text{C}$]	Height gain [%]	Height st. dev. [m]
Euro V Conventional								
1	8.1	0.29	35.6	849	241	26.7	0.43	2.2
2	12.1	0.34	43.4	877	242	21.7	0.64	1.3
3	12.7	0.45	48.5	892	246	17.4	1.16	21.8
4	14.2	0.43	53.7	n.a.	274	19.7	1.88	30.3
5	16.3	0.32	56.1	960	299	32.1	2.24	21.8
6	29.5	0.32	61.2	1060	309	28.8	0.83	20.0
Euro VI Hybrid								
1	8.2	0.40 [†]	39.4	939 [†]	286 [†]	31.6 [†]	0.40	2.4
2	12.5	0.40 [†]	46.8	710 [†]	241	18.9 [†]	0.60	1.4
3	13.3	0.47	53.4	751 [†]	260	20.5 [†]	1.14	21.4
4	14.0	0.42	54.1	881	274	18.7	1.88	30.1
5	15.1	0.34	54.7	973	293	32.1	2.20	20.9
6	28.7	0.29 [†]	62.5	1055	316	26.4 [†]	0.82	20.3

st. dev.: standard deviation; n.a.: not available for complete route due to data recording issues; [†] mean is statistically different to corresponding value of Euro V test

Fuel consumption levels

Table 2 presents the estimated fuel consumption [$\text{kg}/100\text{km}$] and tailpipe CO_2 emission levels [g/km] per vehicle and route, as well as the associated relative differences between the hybrid-diesel and the conventional-diesel technology per pair of buses travelling on the same route. The conventional buses exhibited a fuel consumption that varied from 45 to 96 [$\text{kg}/100\text{km}$], whereas fuel consumption of the diesel-hybrid buses ranged from 42 to 111 [$\text{kg}/100\text{km}$]. Fuel consumption of hybrid buses appeared to be lower by $6.1 \pm 12.4\%$ than their paired conventional buses (non-significant, $p=0.34$). The maximum benefit associated with the hybrid technology was 19% and it was observed on route #2, while a handicap of 16% was detected on route #1. The mean fuel consumption level of the hybrid double-deck buses was approximately 45-65% higher than the Euro IV hybrid single-deck buses measured in Beijing (Zhang et al., 2014).

Table 2: Estimated distance-based fuel consumption and CO₂ tailpipe emission levels per route and pair of buses (conventional/hybrid).

Route #	Fuel consumption [kg/100km]			CO ₂ tailpipe emissions level [g/km]		
	Conventional Euro V buses	Hybrid Euro VI buses	Relative difference [%]*	Conventional Euro V buses	Hybrid Euro VI buses	Relative difference [%]*
1	96	111	16	3001	3491	16
2	67	54	-19	2110	1700	-19
3	68	58	-15	2141	1833	-14
4	72	65	-10	2269	2050	-10
5	69	68	-1	2169	2149	-1
6	45	42	-7	1407	1312	-7

* Reference group: Euro V conventional buses

Gaseous pollutants emission levels

The estimated distance-based emission levels and a brief description of the routes, in terms of vehicle speed, exhaust temperature, ambient temperature, and altitude, are shown in Table 3. Euro VI buses appear to have significantly lower gaseous emission levels outperforming their Euro V counterparts in all pollutants, but N₂O. NO_x emissions gains attributed to Euro VI-related technologies are estimated to 93±5% (p=0.00). NO emissions seem to offer a higher benefit of 96% than the 78% one calculated for NO₂, and so the NO₂/NO_x ratio of Euro VI buses is higher than the one observed for Euro V buses (0.48±0.26 versus 0.31±0.04). CO and THC benefits attributed to Euro VI buses are also remarkable and estimated to an average of 67±12% and 73±10%, respectively (p=0.00). Euro VI N₂O emission levels appeared to be 4 times higher than the ones of the Euro V buses (p=0.08). Most of the NH₃ concentrations were lower than the respective detection limit of the measurement instrument for both Euro standard groups.

Table 3: Distance-based emission levels of basic pollutants per bus and route.

Route #	Route characteristics	Emission Factors [g/km]							
		NO _x	NO	NO ₂	CO	THC	NH ₃ [*]	N ₂ O [*]	CO _{2e}
Euro V (conventional) buses									
1	SL/EL/AM/HM	26.64	21.74	4.89	8.78	0.10	5.5	72	3020
2	SM/EL/AL/HL	9.55	8.26	1.29	9.24	0.07	11.9	221	2168
3	SM/EL/AL/HH	10.62	9.55	1.07	6.91	0.08	4.0	181	2190
4	SM/EM/AL/HH	8.81	7.96	0.84	5.10	0.07	-	-	2269
5	SM/EH/AH/HH	12.95	10.55	2.40	4.52	0.03	3.4	94	2194
6	SH/EH/AM/HH	6.58	5.45	1.13	2.24	0.03	2.2	59	1422
Euro VI (hybrid) buses									
1	SL/EM/AH/HM	4.08	0.64	3.44	3.55	0.04	4.6	1177	3803
2 [£]	SM/EL/AL/HL	0.21	0.20	0.02	1.26	0.02	7.3	265	1770
3 [£]	SM/EM/AL/HH	0.48	0.37	0.10	1.81	0.01	2.4	494	1964
4	SM/EM/AL/HH	0.42	0.34	0.07	1.55	0.02	2.4	421	2162
5	SM/EH/AH/HH	0.70	0.13	0.58	1.92	0.01	2.7	540	2292
6	SH/EH/AM/HH	0.64	0.41	0.22	0.99	0.01	1.7	294	1390

* NH₃ and N₂O are reported in [mg/km];[£] The "start-stop" engine function was enabled.

Route characteristics are reported in a XY form where X denotes each of the variables Speed (S), Exhaust temperature (E), Ambient temperature (A), or Height standard deviation (H) and Y the respective level Low (L), Moderate (M), or High (H).

Table 4 presents the power-based emission factors [g/kWh] of regulated pollutants. One Euro VI bus exceeds the respective euro standard NO_x limit. All Euro VI vehicles conform with the regulated CO and THC euro standard emission limits. The highest concentration observed for NH₃ was 0.71 [ppm], significantly below the respective regulated limit of 10[ppm].

The Euro VI hybrid bus travelling on route #1 provides an interesting example of tuning the overall emission control system, as its exhaust gas temperature was retained at a higher level compared to the respective Euro V conventional bus, probably due to the engine thermal management activated in order to ensure a high SCR NO_x conversion efficiency. The fuel consumption implications of such a kind of operation are evident, and the respective trade-off between NO_x emissions and fuel consumption has been established in the relevant heavy-duty vehicles literature (Gabrielsson, 2014).

In Euro VI buses, when taking into account the 100-years global warming potential of N₂O (GWP_{100,N2O}= 265) and calculating the total CO₂ equivalent emissions (Table 3) (IPCC, 2014), N₂O appears to contribute an average of 5.9% (maximum 8.1% on route #1) to the respective total greenhouse gases, counterbalancing the protentional CO₂ exhaust benefits at a certain level.

Table 4: Power-based emission levels of regulated pollutants (per tested bus and route) and euro standard limits.

		Emission Factors [g/kWh]		
		Euro VI (hybrid) buses		
1	SL/EM/AH/HM	0.94 ⁺	0.85	0.01
2 [£]	SM/EL/AL/HL	0.04	0.40	0.01
3 [£]	SM/EM/AL/HH	0.13	0.55	0.00
4	SM/EM/AL/HH	0.12	0.48	0.00
5	SM/EH/AH/HH	0.21	0.64	0.00
6	SH/EH/AM/HH	0.32	0.53	0.01
EU Emission Standards for Heavy-Duty Diesel and Gas Engines: Transient Testing		0.46	4.00	0.16

+ Emissions are higher than the respective Euro standard limit; § The limit refers to non-methane hydrocarbons (NMHC); £ The "start-stop" engine function was enabled.

Comparative assessment of diesel-hybrid buses over different city routes

The particular characteristics of each route appear to have a critical role in fuel consumption gains offered by diesel-hybrid buses over the conventional diesel technology. The benefits of the hybrid technology are clear in routes #2, #3, and #4, marginal for routes #5 and #6, whereas the fuel consumption of the route #1 diesel-hybrid bus is higher than the respective conventional one.

The routes with the three lowest average ambient temperatures of 20 [°C], exhibit a 15% lower fuel consumption for hybrids, compared to the three routes of moderate and high ambient temperatures of 30 [°C], where fuel consumption is 3% higher for hybrids. This remark provides evidence on the significance of the impact of air-conditioning on fuel efficiency of the hybrid buses, given the direct association of ambient temperature to air-conditioning loads. The average fuel consumption of hybrids driving on routes #1 and #5, i.e. the high ambient temperature routes, is higher by 52% compared to the respective fuel consumption of the hybrid buses traveling on routes #2, #3, and #4, i.e. the high ambient temperature routes. Zhang at al. (2014), also reported a similar increase in fuel consumption of 48%, on average, when air-conditioning was enabled, whereas Muncrief et al. (2012) measured a 20% increase.

Routes #2 and #3, where the engine start-stop operation was enabled, appear to have the highest hybrid technology fuel consumption benefits, i.e. 20% and 15% respectively. Indicatively, when considering the hybrid bus assigned to route #4 of similar conditions of speed and ambient temperature, but with the function disabled, the fuel consumption benefits drop to 10%.

The positive road gradient of a route seems to have a significant negative impact on the hybrid powertrain benefits; route #5 is an example of such an effect. Route #5 has the highest elevation gain (2.2%) among the testing routes, whereas ambient and operational parameters are similar for both types of buses (p-value ranges from 0.11 to 0.93). The fuel consumption difference between the two technologies is almost zero -0.9 ± 2.9 [kg/100km], i.e. -1% (p=0.81).

The comparison of routes #1 and #5, where the hybrid buses were tested under – practically – the same ambient conditions, provides some evidence on the effect of vehicle speed on fuel consumption. More specifically, the fuel consumption of the hybrid bus travelling on the medium speed (15 [km/h]) route appear to be 63% higher than the fuel consumption of the hybrid bus driving on the low speed (8 [km/h]) route of 43 ± 3 [kg/100km] (p=0.00); this finding is in agreement with the respective results of Zhang et al. (2014). This difference was lower but also statistically significant (sig.=0.00) in the case of the respective conventional buses (28 ± 3 [kg/100km] or 39%).

Conclusions

In this study, six Euro VI diesel-hybrid transit buses and six Euro V diesel double-deck transit buses were tested employing Portable Emissions Measurement Systems under their regular city routes in the broader Hong Kong metropolitan area. Fuel consumption and gaseous pollutants emission levels were comparatively assessed based on the real-driving data collected. The effect of ambient, operation, and driving conditions on fuel consumption and emissions performance of the buses tested were also investigated.

The fuel consumption difference between diesel-hybrid buses and conventional diesel ones, as measured per single route, was on average $-6.1 \pm 12.4\%$, ranging from -19% to +16%, and statistically non-significant. The NO_x, CO, and THC emission levels of the diesel-hybrid buses were lower, on average, by 93%, 67%, and 72%, respectively, than their conventional counterparts. The EGR system that the Euro VI buses are equipped with, along with the high-efficiency SCR system, appear to be responsible for the respective lower NO_x levels. The general hybrid operation, including engine shut-off at idle in some of the routes, did not seem to have a significant impact on the performance of Euro VI buses. The diesel-hybrid buses exhibited a NO₂/NO_x ratio of 48% that was 17% higher than the Euro V buses.

The expectations for significantly lower fuel consumption of the Euro VI hybrid technology than the diesel conventional one, as they have been shaped based on the hybrids experience in other metropolitan cities worldwide, have not been met in the case of Hong Kong. However, remarkable reductions in NO_x emissions are offered compared to the respective Euro V technology. The hybrid technology benefits in Hong Kong appear to be limited mainly due to the high energy consumption of air-conditioning imposed by the, constantly, relatively high ambient temperatures during the year along with the creeping operation speeds and positive road gradients for some of the city routes.

Acknowledgements

The study is implemented in the framework of the project entitled “Provision of Services for Analysing Vehicle Emission Data collected by Portable Emission Measuring Systems” (ref. #16-00280), sponsored by the Hong Kong Environmental Protection Department (HK EPD). The authors are grateful for the data and the technical support provided by their HK EPD colleagues. The contents of this paper are solely the responsibility of the authors and do not necessarily represent official views of the sponsors.

References

- Bottiglione F., T. Contursi, A. Gentile and G. Mantriota (2014), The fuel economy of hybrid buses: the role of ancillaries in real urban driving, *Energies*, 7, 4202–20. doi:10.3390/en7074202.
- European Commission (2011), Regulation (EU) 582/2011 with respect to emissions from heavy duty vehicles Euro VI, *Official Journal of the European Union L 167*, 2011.
- Gabrielsson P.L.T. (2004), Urea-SCR in automotive applications, *Top. Catal.*, 28, 177–84. doi:10.1023/B:TOCA.0000024348.34477.4c.

- Hallmark S.L., B. Wang and R. Sperry (2013), Comparison of on-road emissions for hybrid and regular transit buses, *J. Air Waste Manage. Assoc.*, 63, 1212–20. doi:10.1080/10962247.2013.813874.
- IPCC (2014), Climate Change 2014: Synthesis report. Contribution of working groups I, II and III to the Fifth Assessment Report of the Intergovernmental Panel on Climate Change [Core Writing Team, R.K. Pachauri and L.A. Meyer (eds.)]. Geneva, Switzerland: 2014.
- ISO (2002), Standard: ISO 16183: Heavy-Duty Engines Measurement of Gaseous Emissions from Raw Exhaust Gas and of Particulate Emissions using Partial Flow Dilution Systems under Transient Test Conditions, *International Organization for Standardization*.
- Lajunen A. (2014), Energy consumption and cost-benefit analysis of hybrid and electric city buses, *Transp. Res. Part C Emerg. Technol.*, 38, 1–15. doi:10.1016/j.trc.2013.10.008.
- Merkisz J. and J. Pielecha (2010), Emissions and fuel consumption during road test from diesel and hybrid buses under real road conditions, *2010 IEEE Veh. Power Propuls. Conf.*, IEEE; 1–5. doi:10.1109/VPPC.2010.5729035.
- Muncrief R.L., M. Cruz, H. Ng and M. Harold M (2012), Impact of auxiliary loads on fuel economy and emissions in transit bus applications, *SAE 2012 World Congress & Exhibition*. doi:10.4271/2012-01-1028.
- Semercioglu H., A. Bal and S. Soylu (2010), Examination of real world operating conditions and emissions of a hybrid city bus, *Int. Conf. Energy Automot. Technol.*, Istanbul, Turkey: 2010.
- Shek K.W. and W.T. Chan (2008), Combined comfort model of thermal comfort and air quality on buses in Hong Kong, *Sci. Total Environ.*, 389, 277–82. doi:10.1016/j.scitotenv.2007.08.063.
- The Government of Hong Kong Special Administrative Region, Press Release: LCQ18: Pilot green transport fund 2011. <http://www.info.gov.hk/gia/general/201111/02/P201111020178.htm> (accessed January 1, 2017).
- UN (2013), Agreement Concerning the Adoption of Uniform Technical Prescriptions for Wheeled Vehicles Addendum 100: Regulation No. 101. *United Nations*: 2013.
- US EPA (2015), Subpart J - Field Testing and Portable Emission Measurement Systems, CFR Part 1065, Title 40, Vol. 33. Environmental Protection Agency.
- Zhang S., Y. Wu, H. Liu, R. Huang, L. Yang, Z. Li, L. Fu and J. Hao (2014), Real-world fuel consumption and CO₂ emissions of urban public buses in Beijing, *Appl. Energy*, 113, 1645–55. doi:10.1016/j.apenergy.2013.09.017.

Emission Inventory of Non-Road Mobile Machineries (NRMM) – First results for the Republic of Croatia

M. Pečet¹, M. Bunjevac¹, and Z. Lulić¹

¹ Department of IC Engines and Mechanical Handling Equipment, Faculty of Mechanical Engineering and Naval Architecture, University of Zagreb, Ivana Lučića 5, 10002 Zagreb, Croatia, mp195277@stud.fsb.hr

Abstract

The largest number of non-road machinery in the Republic of Croatia has no any systems for reducing harmful emissions and greenhouse gases. That emission represents the obvious danger for public health.

Directive 97/68/EC is the first European directive to address the problem of non-road mobile machinery. It included non-road mobile machines from chainsaws, construction machinery and power generators to locomotives and inland navigation vessels. Nowadays, non-road mobile machinery is subject to Regulation 2016/1628 of the European Council, and Parliament, which sets out a clear division of non-road mobile machinery by categories and limits for each harmful and greenhouse emissions are given.

The aims of this paper are the analysis of the number of imported non-road mobile machines in the Republic of Croatia in last three years, calculation of harmful emissions for some specific non-road mobile machines. The primary objective is to give the proposal for producing an inventory of non-road mobile machinery.

It is estimated that harmful emissions from non-road mobile machinery, especially particulate matter, are the main cause of respiratory system disease which causes 70 deaths per 100,000 people in the Republic of Croatia. The lung cancer is the leading cause of cancer death in the world, and it is believed that one of the main reasons is the particulate matter with diameter up to 2,5 μm .

Keywords: non-road mobile machinery, emissions inventory, Directive 97/68/EC, Regulation 2016/1628

Introduction

Europe Union first addressed problem of non-road mobile machinery with Directive 97/68/EC¹ which states that all persons should be effectively protected against recognized health risks from air pollution and that this necessitates, in particular, the control of emissions of nitrogen dioxide (NO₂), particulates (PT) - black smoke, and other pollutants such as carbon monoxide (CO); whereas with regard to the prevention of tropospheric ozone (O₃) formation and its associated health and environmental impact, the emissions of the precursors nitrogen oxides (NO_x) and hydrocarbons (HC) must be reduced; whereas the environmental damage caused by acidification will also require reductions inter alia on the emission of NO_x and HC.

Nowadays, non-road mobile machinery is subject to Regulation 2016/1628¹ where non-road mobile machines are defined as any mobile machine, transportable equipment or vehicle with or without bodywork or wheels, not intended for the transport of passengers or goods on roads, and includes machinery installed on the chassis of vehicles intended for the transport of passengers or goods on roads.

There is no publicly available inventory of non-road mobile machinery yet in the Republic of Croatia. This paper will present ideas and first steps for making an adequate inventory and proposed methodology to maintain it.

¹Directive 97/68/EC¹ of the European Parliament and of the Council of 16 December 1997 on the approximation of the laws of the Member States relating to measures against the emission of gaseous and particulate pollutants from internal combustion engines to be installed in non-road mobile machinery

1. Objectives

The primary aim of this paper is to give the proposal for a more efficient model for collecting data about non-road mobile machinery. The long-term goal is to create a reliable and consistent non-road mobile machinery inventory.

Due to CLRTAP (Convention on Long-range Transboundary Air Pollution) non-road mobile machinery is divided into categories according to their purpose and a typical representative is shown for each category in Figure 1.

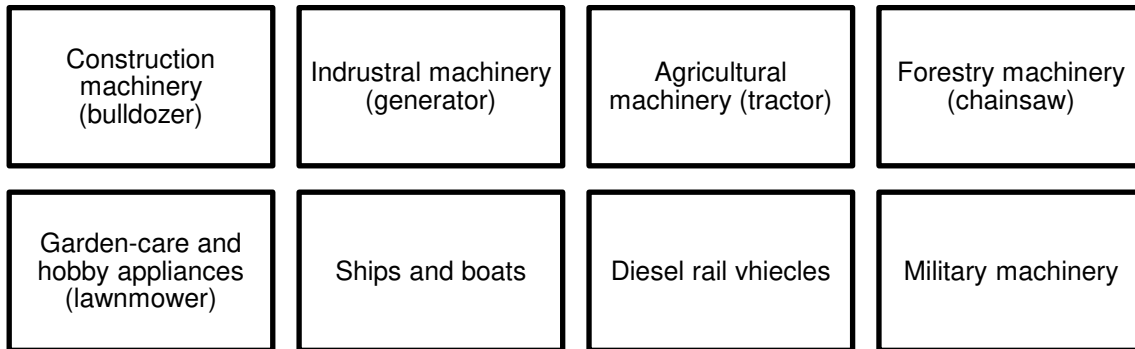


Figure 1: Non-road mobile machinery divided into groups by CLRTAP

There is also a division of non-road mobile machinery made by Europe Parliament and Council which separates non-road mobile machinery as it will be shown in the sequel.

- 1) "Category NRE":
 - a) engines for non-road mobile machinery intended and suited to move, or to be moved, by road or otherwise;
 - b) engines having a reference power of less than 560kW used in place of Stage V categories IWP, IWA, RLL or RLR;
- 2) "Category NRG": engines having a reference power that is greater than 560 kW, exclusively for use in generating sets; engines for generating sets other than those having those characteristics are included in the categories NRE or NRS, according to their characteristics;
- 3) "Category NRSh": hand-held SI engines having a reference power that is less than 19 kW, exclusively for use in hand-held machinery;
- 4) "Category NRS": SI engines having a reference power that is less than 56 kW and not included in category NRSh;
- 5) "Category IWP":
 - a) engines exclusively for use in inland waterway vessels, for their direct or indirect propulsion, or intended for their direct or indirect propulsion, having a reference power that is greater than or equal to 19 kW;
 - b) engines used in place of engines of category IWA provided that they comply with Article 24(8);
- 6) "Category IWA": auxiliary engines exclusively for use in inland waterway vessels and having a reference power that is greater than or equal to 19 kW;
- 7) "Category RLL": engines exclusively for use in locomotives, for their propulsion or intended for their propulsion;
- 8) "Category RLR":

- a) engines exclusively for use in railcars, for their propulsion or intended for their propulsion;
- b) engines used in place of Stage V engines of category RLL;
- 9) "Category SMB": SI engines exclusively for use in snowmobiles; engines for snowmobiles other than SI engines are included in the category NRE;
- 10) "Category ATS": SI engines exclusively for use in ATVs and SbS; engines for ATVs and SbS other than SI engines are included in the category NRE.

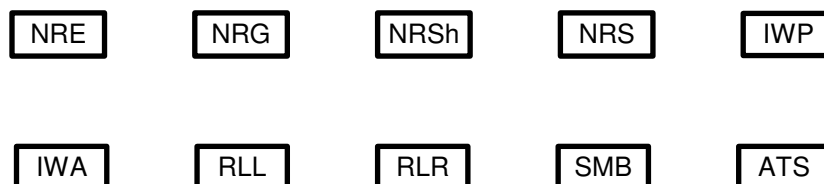


Figure 2. Non-road mobile machinery divided into categories by Directive 2016/1628

2. Methodology

General approach

In the Republic of Croatia, it is tough to compile detail non-road mobile machines inventory due to continued neglecting about new non-road mobile machinery that is coming on the market, but also old non-road mobile machines that are in use for a while. There is a small improvement in collecting data about machines that are imported in last few years but nothing significant enough to start a detailed inventory.

The United Nations Economic Commission for Europe (UNECE) Guidelines for reporting emissions and projections data define a set of quality criteria. To make the quality inventory it must be transparent, consistent, comparable, complete and accurate.

There is no data about the life of that machines and their usage. Also, it is not known are all imported machines immediately delivered to the buyer, or they sit in some warehouse until someone buys them.

Second, in the Republic of Croatia, according to EU criteria, 78,6 % of the population lives in rural areas, and most of them are engaged in agriculture and forestry activities in which non-road mobile machines are used but none of that machines are registered, and it is very challenging to determine their exact number.

Also, fishing is one of the most important maritime activities. In the Republic of Croatia, there are 7 746 fishermen registered for the commercial fishery with a similar number of vessels used for fishing. That vessel also can be taken into consideration when talking about non-road mobile machines. There is a considerable number of coastal population is engaged in maritime activities such as fishing for personal needs and sports fishing and both non-road mobile machines are used as means of transport.

Thirdly, a small number of the non-road mobile machines are in city areas where population uses them for maintenance of green sectors such as parks.

¹ Regulation (EU) 2016/1628 of the European Parliament and the Council of 14 September 2016 on requirements relating to gaseous and particulate pollutant emission limits and type-approval for internal combustion engines for non-road mobile machinery, amending Regulations (EU) No 1024/2012 and (EU) No 167/2013 and amending and repealing Directive 97/68/EC

General data

According to data given by Croatian Chamber of Economy for 2013. Some imported non-road mobile machines in the Republic of Croatia is 44 023 with the value of 170 million €, which makes about 0,4 % of Croatian GDP.

In figure 2 is shown import of non-road mobile machinery from 2013 to 2016. This data is not very reliable because there is no distinctive division of non-road mobile machinery in categories. First, a clear and unambiguous division of non-road machinery in groups is needed so one machine type cannot be placed in two categories. Today, due to the insufficient education of customs officers the same machine can be put in one machine category and by another customs officer in the entirely different group. That is why collected data is inconsistent and cannot be a basis for making an accurate inventory of non-road mobile machines.

There is need to maintain data about new non-road machines that are placed in explanation and that machines which are already in usage. Nowadays, the problem is there is no such agency and data about non-road mobile machinery is split between various legal entities such as Croatian Chamber of Economy, Croatan Bureau of Statistics, Ministry of Finance and Tax administration. There is need to establish a framework for needs of homologation according to European regulations and market surveillance.

As a possible solution, it should be considered founding specialized Department or Agency to deal with making inventor of non-road mobile machinery and their harmful emissions inventory. In the Republic of Croatia, all vehicles are in the domain of State Office for Metrology, and it would be logical to establish a department that will be responsible for collecting and maintaining data about non-road mobile machinery.

As an alternative to the previous option is to outsource job like in many members of Europe Union to a specialized institution which can collect data, measuring harmful emissions and making a detailed inventory of non-road mobile machinery.

Directive 97/68/EC of the European Parliament and the Council of the Republic of Croatia is transposed as a National Rulebook for the Vehicle Technical Inspection 401.2, and currently, there are bylaws about homologation for the non-road mobile machinery is in the preparation.

Trade channels must be defined so no machine can be imported by the worldwide distributor or by individual so no one machine can be imported without being placed in the inventory of non-road mobile machinery, with that prerequisites for systematic data collection about non-road mobile machinery wants to be created.

Another major problem is an assessment of lifespan and number of working hours for each non-road mobile machine so the inventory of emissions for non-road mobile machinery can be made. Some prediction can be done but with little certainty. A lot of machines are already in use for few decades such as tractors with no technology such as catalysts, and they contribute to harmful emissions a lot.

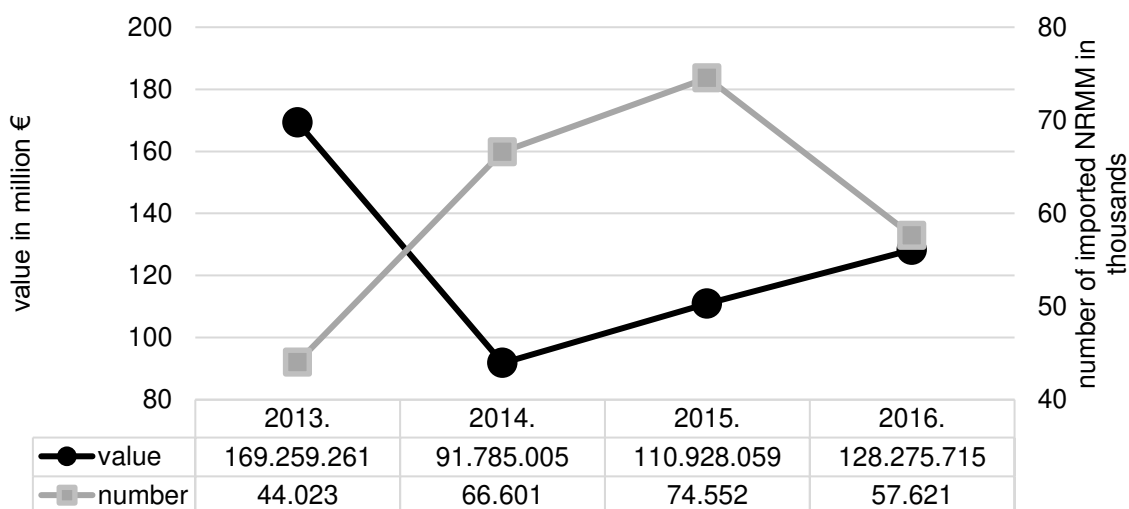


Figure 3: Value and number of imported non-road mobile machinery by year

With the aim of identification, the lifetime of non-road mobile machine general “Stihl” distributor for the Republic of Croatia was interviewed. They helped to describe the path of each non-road mobile machine produced by them as it is shown in Figure 3. A world-renowned German manufacturer of chainsaws and other machines for forestry and garden-care equipment “Stihl” which is in business over 90 years is a synonym for reliable and quality tools in the Republic of Croatia.

New machines in most of the cases are manufactured in a factory near Stuttgart, Germany. After detailed inspection and convincing that everything is right machines are placed in the central warehouse and distributed to general importer when they are needed. Now comes the part of distributing procedure that needs to be improved and that is crossing the border with non-road mobile machines and customs officer needs to divide them into categories so collected data in future is consistent and precise enough to maintain inventory. Machines are placed in general distributor warehouse and distributed to the stores across the country when stores need them depending on demand. The last step in the flow chart is exploitation of machines in real-world conditions.

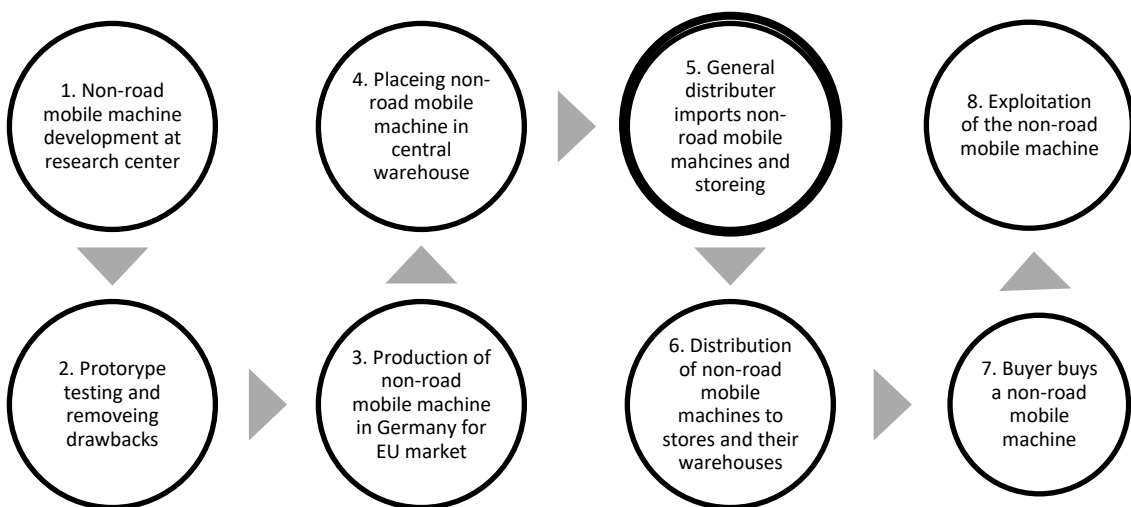


Figure 4: Flow diagram for lifetime of non-road mobile machine

General approach

Exhaust emissions from non-road mobile machinery arise from the combustion of diesel, gasoline, and LPG. The non-road mobile machinery sources which account for most of the emissions by European Environment Agency are construction machinery, agricultural mobile machinery, residential and commercial mobile machinery and military machines. A flowchart is shown in Figure 4, all that machines are placed in non-road mobile machinery box.

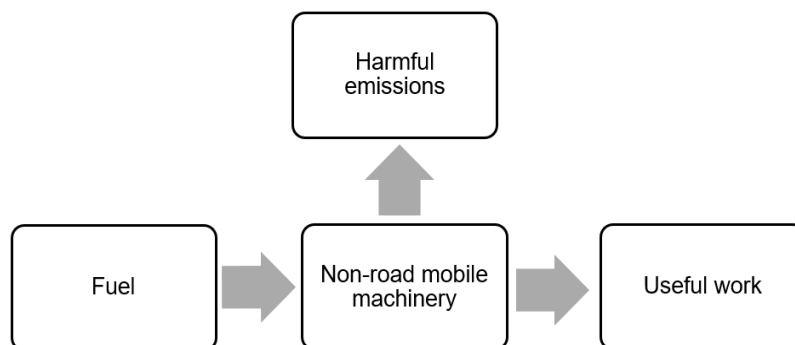


Figure 5: Flowchart for the contribution of NRMM categories to combustion emissions

The procedure presented in Figure 5 is used for selecting the appropriate methods for estimating the emissions from non-road mobile machinery. The basic concepts are if detailed information is available then use it as much as is possible and if the source category is the principal source, then Tier 2 or Tier 3 method should be utilized for estimating emissions.



Figure 6. Decision tree for choosing method for calculating harmful emissions dependable about available data according to EMEP guide

Estimated harmful emissions

For evaluation of the emission of harmful emission Tier 3 method is used. The non-road mobile machinery is disaggregated to the equipment level, including specific operational data and size of an engine. Rather than providing EFs regarding emissions per unit of fuel consumed, the hours of operation are required, and the EFs are presented as emission emissions per kW hour.

$$E = N \times \text{HRS} \times P \times (1 + \text{DFA}) \times \text{LFA} \times \text{EF}_{\text{Base}} \quad (1)$$

Where:

- E = mass of emissions of pollutant i during inventory period;
- N = number of engines (units), the machinery/vehicle population - this is split into different technology levels and power ranges;
- HRS = annual hours of use, the annual working time – this is a function of the age of the equipment/vehicles; therefore, for each subcategory, individual age-dependent usage patterns can be defined,
- P = engine size (kW), the power – this is a function of the power distribution of the vehicles/machinery; therefore, for each subcategory, an individual power distribution can be defined within given power ranges;
- DFA = deterioration factor adjustment, this is a function of the power range of the vehicles/machinery and the technology level;
- LFA = load factor adjustment, this is a function of technology level;
- EF_{Base} = Base emission factor (g/kWh), the emission factor – this is, for each pollutant, a function of technology levels and power output.

In the Republic of Croatia, there are many construction fields, so a lot of construction equipment is used every day so specific emission of four-stroke spark ignited digger will be calculated. In one year there are around 2500 working hours on construction site. Estimated power for the construction machine is around 150 kW (generator sets, loaders, bulldozers, etc.). Estimated load factor is 0,7 because machines do not use maximum power all the time but just occasionally. Default emission factors are taken out EMEP guide and their value is EF_{NOx}=0,4 g/kWh, EF_{VOC}=0,13 g/kWh, EF_{CH4}=0,003 g/kWh, E_{CO}=1,5 g/kWh, EF_{N2O}=0,035 g/kWh, EF_{NH3}=0,002 g/kWh, EF_{PM}=0,025 g/kWh, EF_{PM10}=0,025 g/kWh, EF_{PM2,5}=0,025 g/kWh, EF_{BC}=0,018 g/kWh. With total number around 50 000 construction machines their estimated harmful emissions are E_{NOx}=5 250,00 t, E_{VOC}=1706,25 t, E_{CH4}=39,38 t, E_{CO}=19 687,50 t, E_{N2O}=459,38 t, E_{NH3}=26,25 t, E_{PM}=328,13 t, E_{PM10}=328,13 t, E_{PM2,5}=328,13 t, E_{BC}=236,25 t.

In the mountain areas of the Republic of Croatia, there is a lot of population that are lumberjacks, and their primary tool is professional chainsaw that is powered by two-stroke spark ignited motors. By looking at “Stihl” professional chainsaw catalog, the average power of chainsaw is 5 kW. In one year there are around 700 working hours for each chainsaw. Estimated load factor is 0,75 because maximum power is used only for a part-time. Default emission factors are taken out EMEP guide and their value is EF_{NOx}=0,03 g/kWh, EF_{VOC}=0,10 g/kWh, EF_{CH4}=0,07 g/kWh, E_{CO}=418 g/kWh, EF_{N2O}=0,001 g/kWh, EF_{NH3}=0,002 g/kWh, EF_{TSP}=2,6 g/kWh, EF_{BC}=0,13 g/kWh. With total number around 15 000 chainsaws their estimated harmful emissions are E_{NOx}=2,36 t, E_{VOC}=787,5 t, E_{CH4}=55,13 t, E_{CO}=3291,75 t, E_{N2O}=0,79 t, E_{NH3}=0,16 t, E_{TSP}=204,75 t, E_{BC}=10,24 t.

In last 20 years around 600 000 lawnmowers were imported. Estimated lifetime of a single lawnmower is five years, and every year it is working for approximately 30 hours. Nowadays, their number is around 250 000, and average power is around 3 kW. Estimated load factor is 0,9 because maximum power is used only for a part-time. Default emission factors are taken out EMEP guide, and their value is EF_{VOC}=341 g/kWh, EF_{CO}=532 g/kWh, EF_{NOx}=4 g/kWh, EF_{TSP}=10 g/kWh, EF_{FC}=791 g/kWh. estimated harmful emissions are E_{VOC}=7672,50 t, E_{CO}=11 970,00 t, E_{NOx}=90,00 t, E_{TSP}=225,00 t, E_{FC}=17 797,50 t.

For calculating harmful emissions from railways, Tier 1 method is used because known data is fuel consumption of compression-ignited engine and emission factors. Estimated fuel consumption for 2015 is 21 830 tons of diesel fuel by Croatan Bureau of Statistics. While calculating emissions with this method, it can be challenging to obtain even the most basic activity data such as fuel use, for the different mobile machinery sectors. This is because the fuel used by mobile machinery in a source area is not commonly reported as an amount that is resolved from the industry total fuel use.

$$E = FC \times EF \quad (2)$$

Where:

E = mass of emissions of pollutant i during inventory period;

FC = the fuel consumption for each fuel (diesel, LPG, four-stroke gasoline, and two-stroke gasoline) for the source category;

EF = the emission factor for this pollutant for each fuel type.

Default emission factors are taken out EMEP guide and their value is $EF_{CO_2}=3,14$, $EF_{NO_x}=0,0524$, $EF_{CO}=10,7$, $EF_{NMVOC}=4,65$, $EF_{TSP}=1,52$, $EF_{PM_{10}}=1,44$, $EF_{PM_{2,5}}=1,37$ and their estimated harmful emissions are $E_{CO_2}=68\,564$ t, $E_{NO_x}=1\,144$ t, $E_{CO}=234$ t, $E_{NMVOC}=102$ t, $E_{TSP}=33$ t, $E_{PM_{10}}=31$ t, $E_{PM_{2,5}}=30$ t.

Total harmful emission calculated for these examples amounts $E_{NO_x}=6\,486,36$ t, $E_{VOC}=1\,166,25$ t, $E_{CH_4}=94,51$ t, $E_{CO}=35\,183,25$ t, $E_{N_2O}=460,17$ t, $E_{NH_3}=26,41$ t, $E_{PM}=328,13$ t, $E_{PM_{10}}=359,13$ t, $E_{PM_{2,5}}=368,13$ t, $E_{BC}=246,50$ t.

3. Conclusions

Nowadays, as previously mentioned, there is no inventory of non-road mobile machinery in the Republic of Croatia which is a precondition for creating detail harmful emission inventory. To perform that task, some tasks need to be carried out so inventory can be created such as establishing of Agency for Non-Road Mobile Machineries which would collect and maintain data about machines that are imported and already in use.

Estimated emission need verification with measured data because now data for calculating harmful emission are just assumptions. Calculated harmful emissions makes about third of emission produced by mobile road machinery in Croatia, for example in 2015 was 21,7 kt of NO_x according to (*Resetar, M., Pejic, G., Lulic, Z., 2017.*) by road machines and approximately 6,49 kt by non-road mobile machinery.

Acknowledgments

The authors wish to thank Croatian Chamber of Economy for providing data about the import of non-road mobile machinery in the Republic of Croatia and "Unikomerc" for describing a lifetime of the non-road mobile machine.

References

Benedikt Notter, Philipp Wüthrich, Jürg Heldstab 2016. An emissions inventory for non-road mobile machinery (NRMM) in Switzerland, in Digital Proceedings of the 21st International Transport and Air Pollution Conference "TAP 2016", Lyon, France, 24th-26th May 2016, pp.447-460

Directive 97/68/EC¹ of the European Parliament and of the Council of 16 December 1997 on the approximation of the laws of the Member States relating to measures against the emission of gaseous and particulate pollutants from internal combustion engines to be installed in non-road mobile machinery

EMEP/EEA air pollutant emission inventory guidebook – 2016; <http://www.eea.europa.eu/publications/emep-eea-guidebook-2016>

Regulation (EU) 2016/1628 of the European Parliament and the Council of 14 September 2016 on requirements relating to gaseous and particulate pollutant emission limits and type-approval for internal combustion engines for non-road mobile machinery, amending Regulations (EU) No 1024/2012 and (EU) No 167/2013 and amending and repealing Directive 97/68/EC

Resetar, M., Pejic, G., Lulic, Z., 2017. Road Transport Emissions of Passenger Cars in the Republic of Croatia, in: Digital Proceedings of the 8th European Combustion Meeting. Dubrovnik, Croatia, 18-21 April 2017, pp. 2553–2558.

Moped emissions in urban areas

P. van Mensch^{1*}, A.R.A. Eijk¹, N.E. Ligterink¹,

¹ Research Group Sustainable Transport and Logistics, TNO, PO Box 96800, 2509 JE The Hague, the Netherlands, presenting author: pim.vanmensch@tno.nl

Keys-words: *Mopeds, ISC, emission factors, testing, urban, speed limiters, Euro 5, PEMS, on-road, tampering, fleet composition, L-category, 2-stroke, 4-stroke*

Background

Road-traffic emissions are significant contributors to air quality degradation. In particular in urban areas traffic emissions affect the human living space. Although mopeds correspond only to a rather small fraction of total road transport activity, they are an important contributor to HC emissions in specific areas. In particular, many inhabitants of metropolitan areas in the Netherlands complain about driving behaviour, noise and stench of mopeds. At the same time mopeds become increasingly popular, in some cities the number of mopeds almost doubled over the last decade. The ubiquitous smell of mopeds in busy inner cities does raise concern over possible negative health effects.

Moped fleet composition in the urban area

To calculate the contribution of mopeds to local air pollution and in order to quantify the stench problem of mopeds, TNO investigated the moped fleet composition in two large Dutch cities (Eijk et al., 2016). Several locations were selected and license plate cameras were installed to register license plates and vehicle speed. The license plates of all mopeds passing the selected locations were registered 24 hours a day, 7 days a week. The information of the Dutch road authority and the help of the moped importers was used to determine the moped fleet composition, see Figure 1. Ten thousands of mopeds were registered during several scans in various cities.

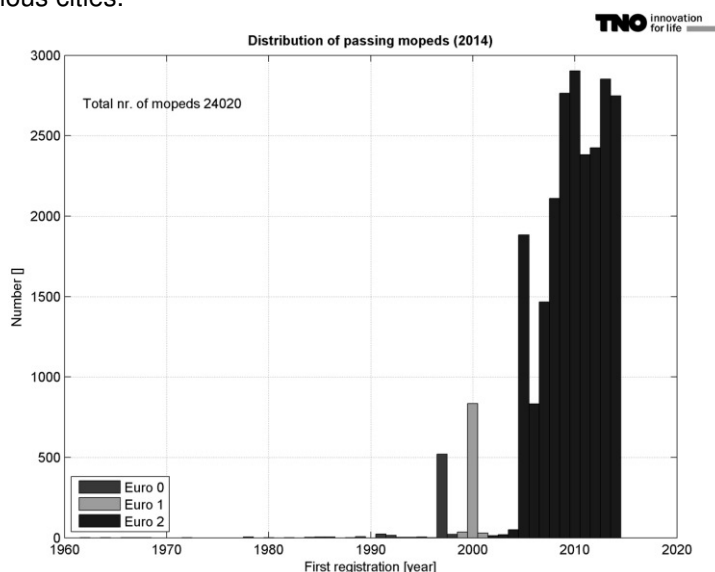


Figure 1: Age distribution of passing mopeds in a specific city (Eijk et al., 2016).

Dutch moped fleet composition:

In the Netherlands two different categories of mopeds are available:

- Mopeds with a maximum construction speed of 45 km/h, used with helmet, on the road
- Mopeds with a maximum construction speed of 25 km/h, used without helmet, on the bicycle lanes

Both categories are sold with 2-stroke and 4 stroke engines, approved according to different Euro standards 0, 1 and 2. For accurate calculation of the total moped emissions, these typical moped categories have been distinguished in the moped vehicle fleet scans.

Maximum construction speed and number of mopeds in the Netherlands

Mopeds with a maximum construction speed of 25 km/h have become increasingly popular over the last 5 to 10 years, this is indicated by figure 2. This indicates a shift from long-distance, regional transport to inner-city use of mopeds. In the Netherlands, these mopeds (max. speed of 25 km/h) do have specific advantages over the 45 km/h mopeds: it is allowed to drive these mopeds on all bicycle lanes in cities and it is not mandatory to wear a helmet. Drivers of mopeds (max. speed 45 km/h) sometimes are allowed on bicycle lanes in specific urban areas, but normally drive on the roads with the cars. Furthermore, it is mandatory to wear a helmet.

Statistics Netherlands has performed a large survey on the ownership and usage of mopeds in the Netherlands (Ewalds, et al., 2013). On 17 million people, nationally, there are over 1 million mopeds, which has been an increasing number over decades. This is one of the highest numbers in Europe. Furthermore, there is an increase in the annual mileage of mopeds, approaching an average of 4000 km/annum.

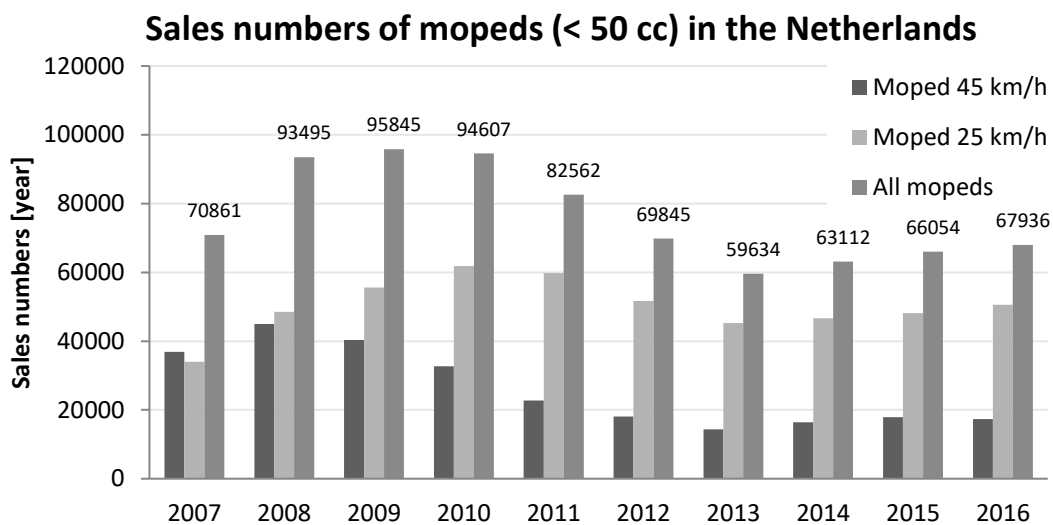


Figure 2: Sales numbers of mopeds in the Netherlands (Source Bovag)

Different Euro classes

Based on the date of first registration and the European emission legislation, mopeds can be classified according to the different Euro emission standards. The majority of the mopeds registered by the license plate cameras are Euro 2 mopeds. A limited number of Euro 0 and Euro 1 mopeds remain driving in the cities. Although the Euro 3 emission standard was introduced in 2014, Euro 3 mopeds have seldom been sold and are rarely seen in the Netherlands. This is a result of the emission legislation, after the introduction of the Euro 3 standard, manufacturers were still allowed to sell Euro 2 mopeds.

2-stroke versus 4-stroke

In general, the emission performance of 2- and 4-stroke engines is quite different. Accurate emission calculations require detailed insight in the share of 2- and 4-stroke engines in the fleet. This important characteristic is unfortunately not registered by the Dutch road authority (RDW). Quite some mopeds, even of the same make and model, are sold with both 2-stroke and 4 stroke engines. Therefore, relevant moped importers and dealers were asked for help to determine this characteristic for all registered mopeds. Up to 2010, an important share of the moped fleet was equipped with a 2-stroke engine. From 2011, new mopeds are mainly equipped with 4-stroke engines.

Moped modifications

Since the first moped entered the market, enthusiastic owners started to modify their mopeds to increase maximum acceleration and/or maximum vehicle speed. The modifications range from

removing speed limiters (especially 25 km/h mopeds) up to modified carburettors, injection/ignition systems, exhaust systems, engine capacity and so on. During the license plate scan period, not only license plates were registered, but vehicle speed as well. This information is used to estimate the number of modified vehicles on the road.

A large share of the 25 km/h mopeds pass the license plate cameras driving at speeds well above 30 km/h, as shown in the speed distribution of 25 km/h mopeds in figure 3. Although the official construction speed is limited to 25 km/h, some of these mopeds travel up to 60 km/h, and in some cases even up to 80 km/h (city centre). The 45 km/h mopeds show similar behaviour, as also displayed in figure 3. A large share of these vehicles passes at speeds ranging from 45 up to 60 km/h, in rare cases even up to 80 km/h. This shows that speed reduction measures are removed very frequently and some mopeds are modified in a more advanced way.

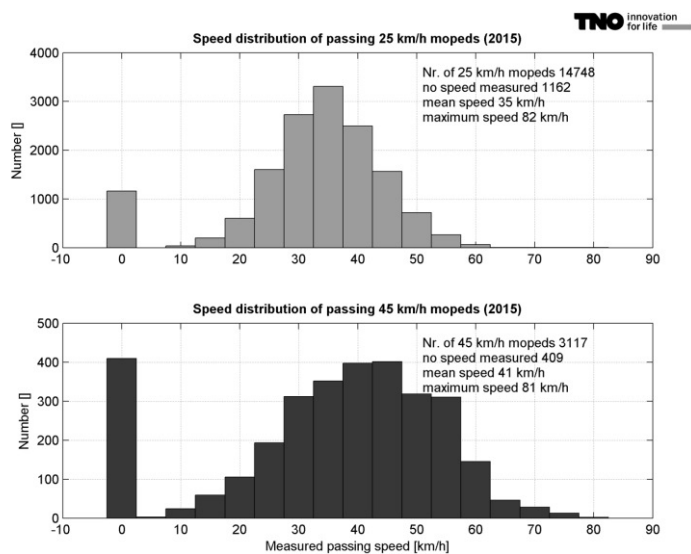


Figure 3: vehicle speed of mopeds with an official 25 and 45 km/h construction speed when passing the license plate camera (Eijk et al., 2016).

Typical issues with mopeds in the Netherlands

Speed limiters

These aforementioned mopeds with a construction speed of 25 km/h are a typical Dutch moped configuration. The majority of these mopeds with a maximum construction speed of 25 km/h are technical similar to mopeds with a maximum speed of 45 km/h. However, the maximum speed has been reduced by simplistic technical solutions. These simple measures to reduce the maximum speed of mopeds usually raise emission levels and fuel consumption, when this maximum speed is reached.

Commonly applied speed limiters for 4-stroke mopeds are 'engine speed limiters' (often applied for vehicles which use a carburettor for the fuel supply) and 'variomatic limiters' (transmission ratio limiters). Both types of speed limiters have a negative effect on fuel consumption (Hensema et al., 2013). The engine speed limiter delays the ignition timing for the combustion in order to restrict the engine speed. By doing so, a large part of the fuel is combusted not delivering engine power, resulting in a high fuel consumption. By driving only just below the limited speed, the negative effect of the engine speed limiter reduced. It is commonly known that in real-world driving conditions, most drivers will drive those vehicles in full-throttle operation and thus with an activated speed delimiter. The engine speed limiter especially has a negative effect at maximum speed.

In figure 4 a graph of the fuel consumption visualizes the increase in fuel consumption for various configurations of mopeds. Driving a moped without speed limiters at maximum allowed speed of

25km/h was the most fuel efficient. The delimited 25 km/h version was 3.5 times more fuel efficient than the standard 25 km/h version (Hensema et al., 2013).

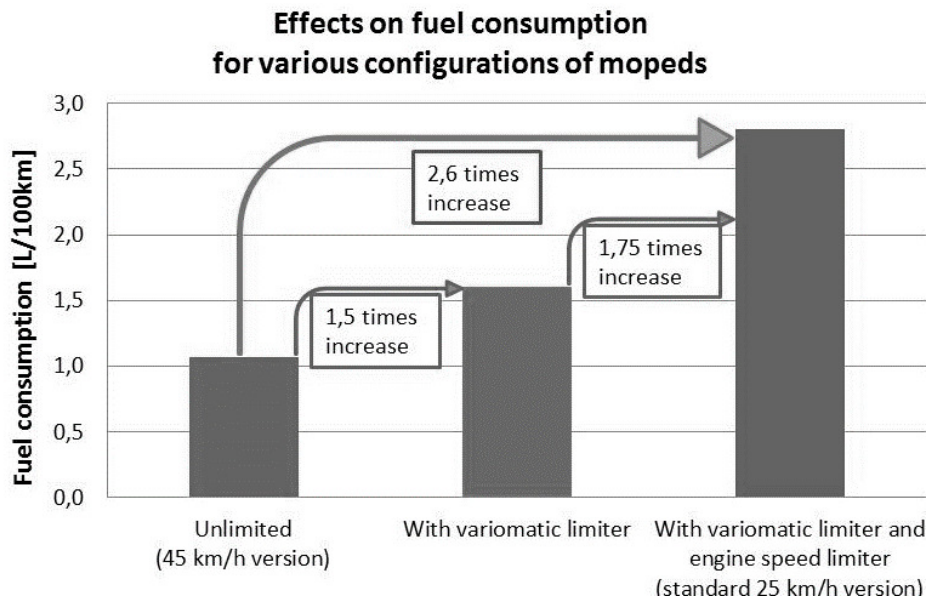


Figure 4: Visualization of the increase in fuel consumption for various configurations of mopeds (Hensema et al., 2013).

Modified fuel nozzle to meet client expectations

Based on discussions with several dealerships of mopeds in the Netherlands, it is suspected that many new mopeds are adjusted by dealerships before the new moped is handed over to its first owner (Ntziachristos et al., 2017). The dealerships claim that they make this adjustment in order to deliver a vehicle to the client that meets the client expectations: a moped with a smooth-running engine that starts and drives well under all conditions. This adjustment often involves replacement of the fuel nozzle by a larger one, this applies to vehicles with an engine with a carburettor. According to the dealers, the client expectations for drivability often cannot be met without the adjustments. However, this means that those vehicles are not compliant to the type approval specifications anymore, though they are representative for many vehicles in-use. Still, as a result, emissions of the vehicle that is delivered to the end-user may not comply to the emission requirements anymore. The conformity of production (CoP) requirements ensure that vehicles are compliant when they leave the factory. These adjustments are made after production and cannot be detected with the current set of type approval procedures. However, this phenomenon may result in a large number of in-use vehicles that are not compliant to the emission requirements during their full lifetime.

But, the anti-tampering provisions of Regulation (EU) No 168/2013 are more stringent than in the Directive 97/24/EC, which may affect the size of the issue for Euro 4 and Euro 5 compliant mopeds. Moreover, the size of the issue might be different with introduction of vehicles which have more advanced engines technologies to comply with the Euro 5 emission limits (Ntziachristos et al., 2017).

Typical emissions from mopeds

Based on the moped fleet composition and appropriate emission factors, the contribution of mopeds to the total traffic emissions and local air pollution can be calculated. This requires an extensive and reliable set of emission factors (van Zyl et al., 2015). As mentioned before, mopeds come in many different types. The current emission factors per type of moped with urban driving are shown in graphs of figure 5 for multiple emission constituents. In this figure, the main bars represent the emission factors of standard (modern) vehicles. The upper and lower stripes represent extensively tampered mopeds and delimited mopeds respectively. The displayed stripes for the passenger cars represent an average passenger car (2015). In the table below, a distinction is made of the main type of mopeds with their typical emission characteristics. These typical emission characteristics are based on the emission factors. In addition, the effect on fuel consumption is added for some types.

Table 1. Typical emission characteristics per type of moped

Type of moped	Typical emission characteristics
45 km/h mopeds: 2-stroke	In general more polluting than 4-stroke, especially high HC and particle emissions. The CO emissions are generally lower than with 4-stroke mopeds.
45 km/h mopeds: 4-stroke	Less polluting than 2-stroke mopeds. However, CO emissions can be excessively high.
25 km/h mopeds	Higher emissions and higher fuel consumption than 45 km/h mopeds.
Delimited 25 km/h mopeds	Comparable emissions and fuel consumption as 45 km/h mopeds.
Extensively modified/tampered mopeds resulting in very high vehicle speeds	Depending of the stage of tampering, an excessive increase of emissions is possible, in particular when the exhaust is replaced.

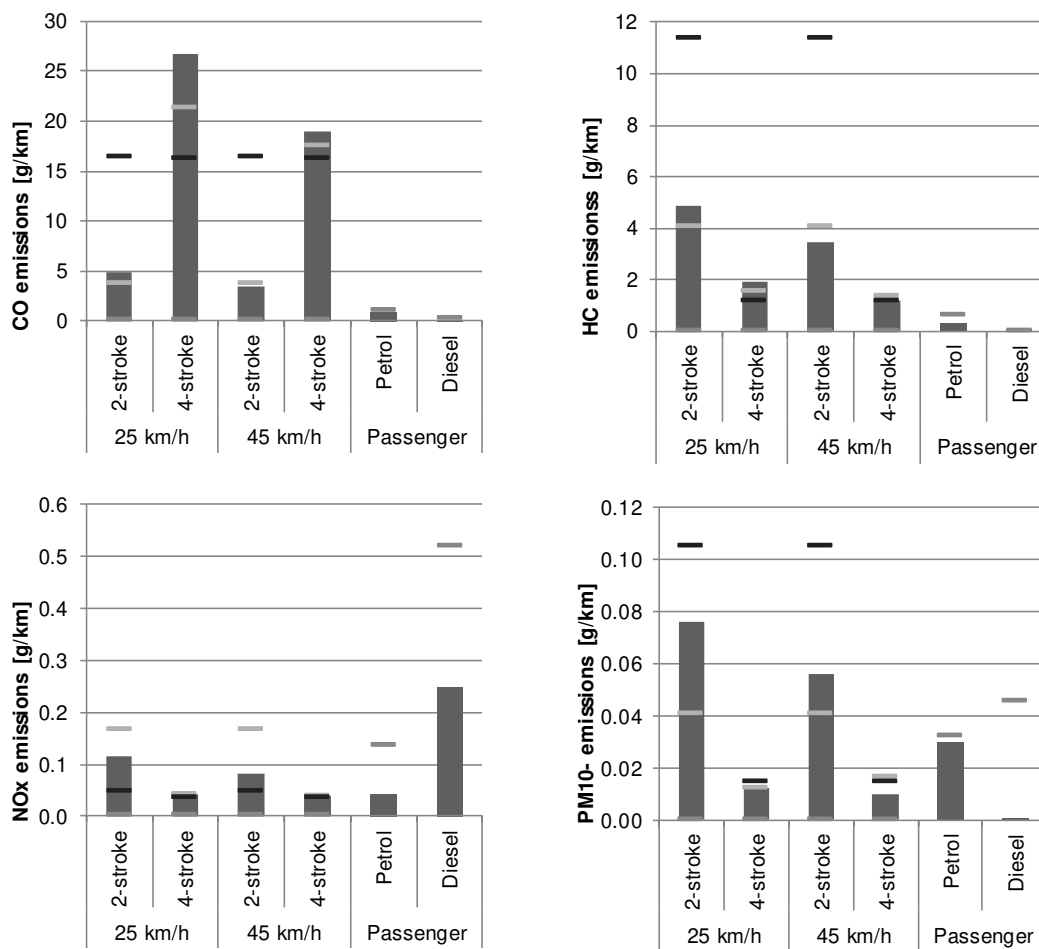


Figure 5: The current emission factors per type of moped with urban driving

New insights from recent measurements

To refine the most important, detailed emission factors, TNO has collected new emission data in two measurement projects. In the first project, nineteen Euro 2 mopeds, both 4-stroke and 2-stroke mopeds, were tested on the chassis dynamometer (Ntziachristos et al., 2017). Nine of these mopeds were in-use 4-stroke mopeds from the Netherlands. Three models with high sale volumes were selected. Three mopeds per selected model have been located at various official dealerships. The original anti-pollution components, i.e., the exhaust system, of these vehicles were still present. Moreover, the condition of these vehicles was checked at the dealerships before the vehicle was delivered to the emission test centre. However, some vehicles do not have a complete maintenance record since not all vehicles went for maintenance to the same workshop during their lifetime. The procedure for Type I testing as described in Annex II of Regulation (EU) No 134/2014 is used for these tests. Every vehicle drove a precondition cycle before the actual test. The preconditioned vehicles drove two WMTC's with a cold start.

The graph in figure 6 shows a comparison between the emission results of measured in-use 4-stroke mopeds and the Euro 2 emission limits, as a function on the vehicle's mileage. The conformity factor is determined by dividing the emission results of the test (WMTC) by the applicable Euro 2 emission limit. Each marker shape represents a vehicle model. It should be noted that the formal Type I test with which these vehicles should comply, was not driven. This means that these figures do not represent formal in-service-conformity of the tested vehicles.

The experimental results of the Euro 2 mopeds in this study showed some excessively high CO emissions for the 4-stroke mopeds, though, relatively low CO emissions were measured as well. The HC and NO_x emission performance of these 4-stroke mopeds were in general similar to the Euro 2 emission limits. However, other Euro 2 vehicles with a 2-stroke engine which were tested in another task of this study showed significantly higher HC emissions than the 4-stroke mopeds. Moreover, these emissions were often higher than the previously described emission factors for HC. Most of these other mopeds were not provided by dealerships.

The CO emission performance varies significantly per vehicle model. Moreover, the CO emission performance can vary greatly as well between the three tested vehicles of one model. On the contrary, the HC + NO_x emission performance per vehicle model does not show significant variations. Furthermore, the emission performance does not vary greatly between the three tested vehicles of one model. For these tested vehicle, there is no clear relationship between the emission performance and the period that vehicles are in service. The emissions are either high or low, once the vehicle has driven more than 10% of its defined useful life mileage.

The vehicles are tested by using the WMTC, which is not the applicable Type I driving cycle for the tested vehicles. However, such excessive exceedances are cannot solely be the result of changing the driving cycle to the WMTC. It is not clear whether a part of the selected vehicles have modified fuel nozzles, which then might cause higher emissions. Hence, it not clear if these high emissions can be the related to the potentially made adjustments. The high emissions can also be the result of fast degraded anti-pollution devices, as there are no durability requirements for the tested vehicles yet, or a combination of these two issues. Alternatively, ineffective Conformity of Production (CoP) can also be a possible cause, which is less probable. It is important to introduce measures for in use vehicles in order to prevent such high emissions.

In general, these results from this study are in line with the previously described emission factors.

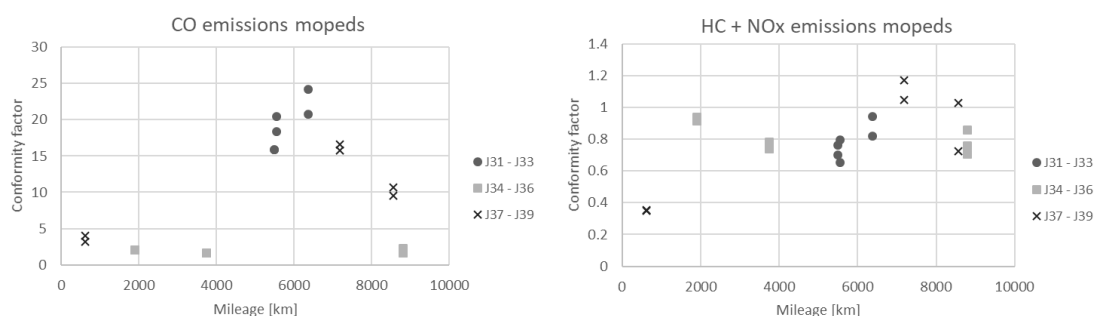


Figure 6: A comparison between emission results and the Euro 2 emission limits as a function on the vehicle's mileage (Ntziachristos et al., 2017).

During the second project, sixteen mopeds are measured. A wide range of common vehicle types was selected, ranging from Euro 2 to Euro 3, 2-stroke to 4-stroke, new and used and from fuel injection to carburettor. These measurements showed similar results for the emissions of 4-stroke mopeds as described before. However, the vehicles which use electronic fuel injection, rather than a carburettor, showed CO emissions which were significantly lower. On the contrary, the 2-stroke mopeds showed on average higher HC and PM emissions than the current emission factors.

Policy instruments for lowering emissions of mopeds

European legislation

In order to reduce emissions from mopeds, the European Commission introduced several stages of emissions control regulation since 1997. Directive 97/24/EC defined emissions limits up to the Euro 3 step. Since 2017, the Euro 4 step is implemented with more stringent emission limits. Moreover, the Euro 4 step has a comprehensive package of environmental tests, including durability requirements, a fuel permeability test and a crankcase emission test. The intention has been not only to make sure that new vehicle models become increasingly clean when placed to the market but also that they remain so throughout their useful life. In 2020 the Euro 5 step will be implemented. In this step, the emission limits are comparable with the emission limits for Euro 6 passenger cars. Moreover, the WMTC, a more dynamic test cycle, is introduced for mopeds.

Type approval process

Mopeds are certified for emission performance according to European regulations. For mopeds on the road, there are very few safeguards against deterioration of emission performance and modifications which will affect the emissions. Though, in comparison with current situation, this issue is improved with the Euro 5 step.

In principle, the sale of mopeds should be supervised by the inspection authority to ensure the proper functioning of the products sold. However, there is no exact guideline or standard to check against. Consequently, the inspection is restricted to the documentation with the moped registration.

Environmental zones

One of the possible policy measures of a local government is the introduction of an environmental zone. This zone should exclude especially the high emitting mopeds, loud (older) mopeds are possibly excluded as well. Emission factors of the relevant specific moped classes therefore became very important. Older and especially older 2-stroke mopeds are known for their high (HC) emissions. Based on these emission factors, the city of Amsterdam plans to introduce an environmental zone in 2018 for mopeds with a first registration date before 2011. In this way, nearly all mopeds with 2-stroke engines will be excluded from the environmental zone of Amsterdam. More cities in the Netherlands consider environmental zones for mopeds as well. Electrically powered mopeds seem a good alternative, but are not available on large scale (and at low costs) as yet.

Future testing methods: In-service-conformity (ISC) and on road measurements

ISC

The measurement results as shown in this paper clearly show the need to control emissions of in-use vehicles, as some of the emission results are excessively high. These measurements are performed with Euro 2 mopeds where no durability requirements apply. However, in case durability and/or CoP requirements are not fully effective at the Euro 5 stage, ISC implementation can be an effective measure to remedy this problem (Ntziachristos et al., 2017). With these more stringent limits in Euro 5, the condition of the anti-pollutant devices will become increasingly important. Ineffective anti-pollution devices can easily cause relatively high exceedances of the emission limits.

On-road measurements

To improve the overall environmental performance assessment in the type-approval procedure, off-cycle emission testing can be added. A method to assess off-cycle emissions are on road tests with a Portable Emissions Measurement System (PEMS). By introducing such requirements, exhaust emissions of more comprehensive driving conditions than the laboratory test cycle can be assessed. This means a test trip which covers a larger part of the engine load area, but also different ambient conditions, different road types, etc. In addition, the chance that vehicles are optimized for a defined emission laboratory test cycle and the risk of cycle beating significantly decrease when on-road measurement requirements are introduced into the type approval process.

It is technically feasible to adopt a test procedure for on-road testing by using PEMS measurements (Ntziachristos et al., 2017). However, the accuracy of the determined mass emissions is not as high as for passenger cars measured with PEMS.

A regular PEMS, which is commonly used for light- and heavy-duty vehicles, is often too heavy and too bulky for usage on L-category vehicles, in particular for two-wheeled vehicles. For example, the typical weight of the main unit only, is often already more than 30 kg. A heavy and bulky PEMS makes installation more difficult and may influence the driveability and the test results. Moreover, PEMS is a stand-alone measurement device with a standalone power supply, which makes the packaging of PEMS even more challenging when a large battery or a generator is required. A stand-alone power supply is needed because the use of the vehicle's electric power output could influence the emission performance. Another complexity is the proper mounting of an exhaust flow meter. In particular for mopeds, very little space is available around the vehicle to mount the exhaust flow meter in a proper and safe manner.

For the afore-mentioned reasons, a PEMS with low energy consumption, low weight and limited dimensions is desirable for mopeds. It should, however, be noted that the following compromises are often made to make this low weight and low energy consumption possible:

- exhaust flow is not directly measured;
- there are no heated lines;
- the set of analysers differ from a 'regular' PEMS. In particular the measurement principle for HC, NDIR instead of FID, may affect the accuracy.

Since an exhaust flow is required to obtain absolute emissions in grams per kilometre, this PEMS estimates the flow based on the speed-density method. The inlet air flow can be calculated by measuring the engine speed, manifold absolute pressure (MAP) and inlet air temperature (IAT). Then, the exhaust flow can be estimated based on the inlet air flow.

The availability of commercially viable PEMSs suitable for small vehicles, including mopeds, is rather low in comparison to the light- and heavy-duty vehicles sector (Zardini et al., 2016).

Discussion

With the attention for NO_x emissions from diesel vehicles, because of the European NO₂ air-quality standards, other emissions have been put in the background. However, the emissions of mopeds form a special category, for which automotive measurement standards are less suitable. The mixture of hydrocarbons and particulates from the tailpipe has been considered by many as a toxic cocktail, which should deserve proper attention. In particular, with the growing metropolitan use of mopeds, the exposure of humans to these emissions at street level may require its own standard. Different parties have looked at different non-regulated aspects of moped emissions. In Switzerland, the volatile fraction in the particulates is considered most relevant, and the condensation and accumulation over time has been investigated by, for example, the PSI (Platt et al., 2014). In the Netherlands health experts considered the exposure of cyclists to the particulates from the exhaust of mopeds on the bicycle lane in urban environment (Boogaard & Hoek, 2008). TNO has measured emissions at the side of bicycle lanes, combined with license plate recognition and speed cameras.

All studies raise the concern for the mixture of particulates and hydrocarbons from the exhaust gas of mopeds. However, on details the result differs, mainly because of the non-standard measurement technologies used to address the issue of the exposure of the toxic mixture. They

generally assume specific transport process and processes for its health risk. In a simpler approach, one could say the petrol of a moped is emitted partly unburned, and the composition of the petrol with about 0.8% benzene, and 25% polyaromatics, is sufficient concern for the health of cyclists who share the lane with mopeds which can emit up to 10 g/km hydrocarbons. The cyclists will inhale the gases deeply with the exercise. Whether the pollutants are gases, droplets, or particulates, is only of secondary concern. In this respect, the total national emissions may be limited, but still represent a health risk due to the high exposure rates in the busy urban environment. People use mopeds to avoid road traffic congestion, by using the bicycle lanes next to the pedestrians and houses.

Due to the more stringent legislation for Euro 4 and 5 mopeds, it is expected that a large part of such new mopeds will carry more complex and more durable engine technology. Potentially this should secure a lower level of emissions during the useful life of a vehicle. However, this should be monitored.

ISC and on-road tests are possible methods to monitor in-use and on-road emission levels of mopeds. It can be considered to perform ISC testing by application of an on-road test, rather than the applicable type I test. By combining these two test procedures, the real-world emission performance of in-use vehicles are thoroughly secured in the most representative way (Ntziachristos et al., 2017).

Within the ISC requirements for passenger cars, the manufacturer is responsible for the ISC of the type approved vehicle models. However, when the ISC-programme is performed under full guidance of the manufacturer, there still is a potential risk that 'prepared' vehicles are used. Instead, representative in-use vehicles deployed in various real-world circumstances, should be randomly selected. By using representative in-use vehicles, any commonly applied adjustments at dealerships which can influence the exhaust emissions, are revealed as well. Ideally, the ISC-verification testing is performed by the TAA independent from the vehicle manufacturer. As a compromise, TAAs could randomly perform a part of the ISC-verification testing to prevent the risk of having non-compliant vehicles on a precautionary basis.

References

- Boogaard, H. and G. Hoek, *Blootstelling aan ultrafijnstof tijdens fietsen en autorijden in Nederlandse steden*, 2008, Universiteit Utrecht, P-UB-2008-02.
- Eijk, A.R.A., Mensch, P. van, and Cuelenaere, R.F.A., 2016. *Brommers in de stedelijke leefomgeving Status rapport*, TNO Report 2016 R10093, Delft, Netherlands.
- Ewalds, D., Moritz, G. and Sijstermans, M., *Bromfietsen in Nederland*, CBS (Statistics Netherlands) report 2013 (Dutch).
- Hensema, A., Mensch, P. van, and Vermeulen, R., 2013. *Tail-pipe emissions and fuel consumption of standard and tampered mopeds*, TNO Report 2013 R10232, Delft, Netherlands.
- Ntziachristos, L., Vonk, W., Papadopoulos, G., van Mensch, P., 2017. *Effect study of the environmental step Euro 5 for L-category vehicles*, TNO Report 2017 R10565, The Hague, Netherlands.
- Platt, S.M. et al, *Two-stroke scooters are a dominant source of air pollution in many cities*, Nature Communications, 13 May 2014.
- Zyl, S. van, Van Mensch, P., Ligterink, N., Droge, R. and Kadijk, G., 2015. *Update emission model for two-wheeled mopeds*, TNO Report 2014 R11088, Utrecht, Netherlands.
- Zardini, A., Clairotte, M., Lanappe, G., Giechaskiel, B. and Martini, G., 2016. *Preparatory work for the Environmental Effect Study on the Euro 5 step of L-category vehicles*, European Commission Joint Research Centre.

The Influence of Passenger Car Population and Their Activities on NO_x and PM Emissions (Data from Croatia)

M. Rešetar^{1*}, G. Pejić¹, P. Ilinčić² and Z. Lulić²

¹ Centre for Vehicles of Croatia, Capraška 6, Zagreb, HR-10000, Croatia, marko.resetar@cvh.hr

² Faculty of Mechanical Engineering and Naval Architecture, University of Zagreb, Ivana Lučića 5, Zagreb, HR-10002, Croatia

Introduction

For the past few years special attention has been given to harmful road transport emissions, nitrogen oxides (NO_x) and particulate matter (PM). Exposure to increased concentrations of NO_x and PM emissions is known to cause respiratory ailments, heart diseases, stroke and can be the cause of premature death (Guttikunda and Goel, 2013; Li et al., 2017; Stockfelt et al., 2017). The time series results of real driving emission measurements have shown a significant difference in NO_x emissions of diesel cars compared to the type approval limit values. However, this does not apply to petrol cars (Chen and Borken-Kleefeld, 2014). Remote sensing measurements indicate that NO_x emissions from Euro 5 petrol cars are about a factor of 20 lower than Euro 0 cars. However, there has not been a significant change in NO_x emission reduction for diesel cars from Euro 0 to Euro 5 (Carslaw and Rhys-Tyler, 2013). Particulate matter emissions are rising in many of the world's populated cities and exceeding World Health Organization guidelines (Guttikunda and Goel, 2013; Ma and Jia, 2016). However, the emission control policies implemented in the last decade could result in noticeable reduction in PM emissions (Wang et al., 2017). Not only policy measures, but also the implementation of DPF (Diesel Particulate Filter) technology on vehicles enabled a large reduction in PM emissions (Tzamkiozis et al., 2010). However, some countries like Croatia have an aged vehicle fleet and exhaust PM emissions have a significant role in total emissions. The most severe problem is found in urban areas with high traffic density. One of the methods to reduce NO_x and PM emissions in urban areas is to introduce a low emission zones. The study from the University of Sydney shows the impact of London's low emission zone on NO_x and PM₁₀ emissions (Ellison et al., 2013). Not only tailpipe exhaust emissions but also non-exhaust PM emissions (road dust resuspension, road surface wear, abrasion of tyres, brakes and clutch) have a significant impact on air quality in urban areas (Amato et al., 2016; Pant and Harrison, 2013). Although electric vehicles are not included in this study, exploitation of such vehicles also results in non-exhaust emissions. Because of the significantly larger mass of electric vehicles in comparison to vehicles equipped with an internal combustion engine, electric vehicles generate more non-exhaust emissions than conventional vehicles (Timmers and Achten, 2016).

Most popular vehicle emission models such as COPERT (Computer Programme to calculate Emissions from Road Transport), HBEFA (The Handbook Emission Factors for Road Transport) and VERSIT+ are used for estimating road transport emissions (Borge et al., 2012; Smit et al., 2007). By applying these emissions models, it is possible to estimate emissions generated on a defined geographic area in a given time period. Air pollutant emissions from on-road vehicles in China for the time period from 1999 to 2011 were estimated using COPERT emission model (Lang et al., 2014). Considering that NO_x RDE from Euro 6 diesel cars exceed emission levels used in COPERT by two times, it was necessary to update NO_x emission factors (EFs) (Ntziachristos et al., 2016). In Croatia, an emissions study has already been made, which, among other things, provided NO_x and PM emissions of passenger cars (PCs) for the period from 2007 to 2016 (Resetar et al., 2017). In order to apply COPERT model, a significant amount of input data must be acquired. Therefore, a top-down approach is used in order to determine national emissions and the most important data, along with emission factors, is precisely related to the PC fleet structure and activity data.

Based on the above-mentioned information it is obvious that NO_x and PM emissions present a major problem today with diesel cars as the major source of the above pollutants. Therefore, the study focused on the influence of PC population and their activities on NO_x and PM emissions in the Republic of Croatia. For relevant PC subcategories, emissions and implied emission factors for pollutants NO_x and PM for the year 2016 were calculated using COPERT 5 computer program.

Methodology and input data

The processed data on the PC fleet that underwent technical inspection in 2016 was collected from the database of Centre for Vehicles of Croatia (CVH), the company whose primary activity is performing periodical technical inspections on vehicles in Croatia. This is a unique database that contains data on all vehicles registered in Croatia, including periodical technical inspection data and annual vehicle activity data. These data have the greatest impact on the calculation of emissions and as such were used as COPERT 5 input data. Activity data taken into account means annual mileage along with mean lifetime cumulative mileage, whereas the assumed circulation data taken into account means the speed and the percentage of mileage driven by vehicles of each emission level per driving mode (urban/rural/highway). In addition to the above data, input data also included environmental information with monthly values of average minimum and maximum temperatures as well as relative humidity. Tier 3 methodology, which is described in *EMEP/EEA air pollutant emission inventory guidebook*, was applied in the scope of this research (Ntziachristos and Samaras, 2016). A simplified form of COPERT emissions calculation model is shown in Figure 1.

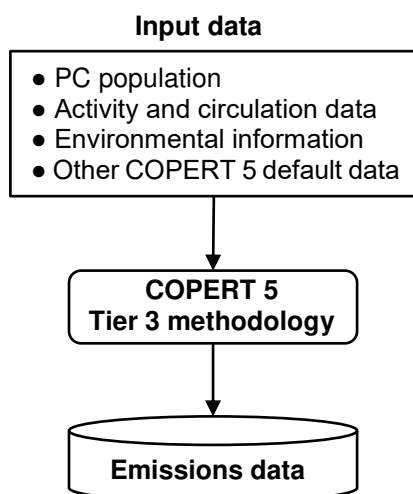


Figure 1: COPERT emissions calculation model.

Passenger car population and their activity data for the year 2016 were processed and prepared for COPERT calculation. Figure 2 shows PC population, mean annual activity and total annual activity for petrol and diesel PCs in 2016, according to each of the European emission standards. Over 779,000 petrol and over 718,000 diesel cars were registered in Croatia in 2016. Almost 61,000 other vehicles included hybrid, LPG bi-fuel and CNG bi-fuel cars, while 224 registered cars were electric. If we look at the top-left chart in Figure 2, it can be noted that there is a numerically small difference between the total number of petrol and diesel cars. Older cars, up to Euro 4, are mainly petrol, while newer cars, Euro 5 and Euro 6, are mainly diesel. There are roughly twice as many Euro 2 petrol cars as there are Euro 2 diesel cars. The top-right chart in Figure 2 indicates that diesel cars are exploited much more than petrol cars. When comparing all petrol and diesel PCs, diesel cars drive 6,750 km a year more than petrol cars. It is also apparent that newer vehicles, both petrol and diesel, are exploited much more than older vehicles. In order to calculate emissions on an annual basis, it was necessary to consider total annual activity (bottom chart in Figure 2). Total annual activity is the product of PC population and mean annual activity. This data is very useful because it shows a fleet's activity in a broader sense. Although the number of petrol cars is greater than the number of diesel cars, due to considerably greater exploitation of diesel cars compared to petrol cars, diesel cars drive 1.53 times more kilometres a year than petrol cars. The main causes of significantly higher activity of diesel cars are lower fuel consumption and lower fuel costs when compared to petrol cars.

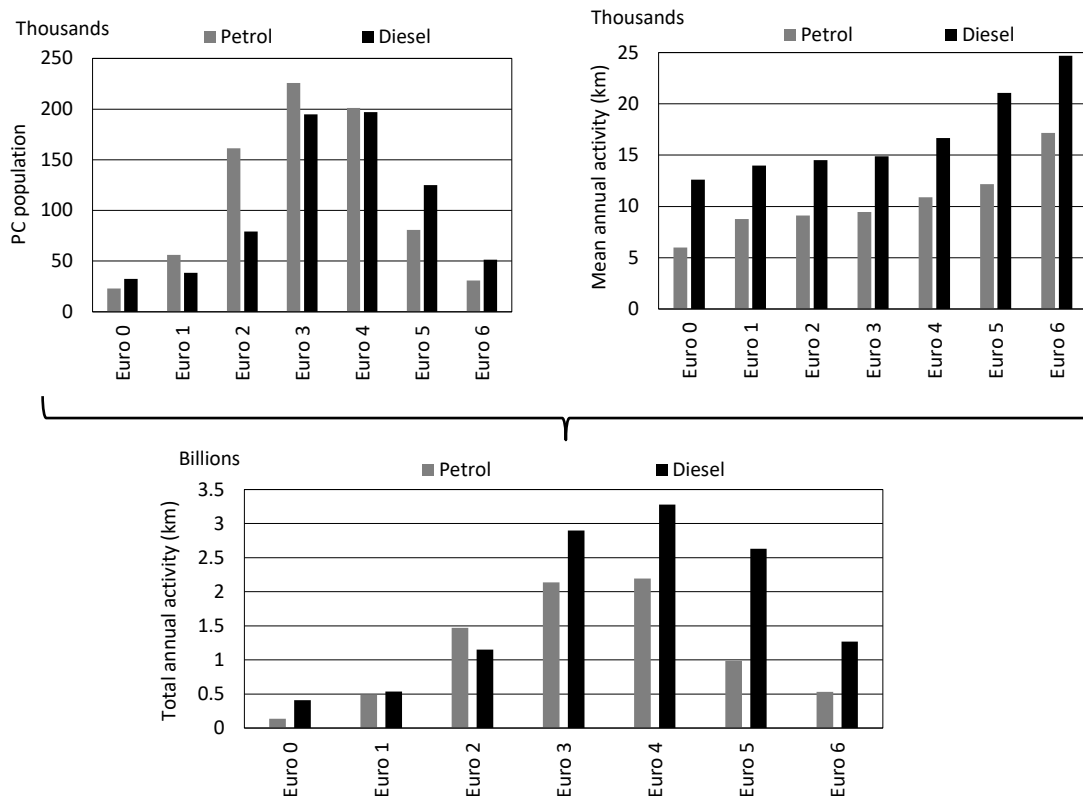


Figure 2: Population, mean annual activity and total annual activity for petrol and diesel PCs in 2016, according to European emission standards.

As mentioned above, circulation data were taken as an assumption. Therefore, the distribution of emissions generated in separate driving modes (urban/rural/highway) has not been considered. This paper presents total emissions generated in all mentioned driving modes. Table 1 shows the mean speed and the percentage of mileage driven by vehicles per driving mode (urban/rural/highway).

Table 1: The mean speed and percentage of mileage driven by vehicles per driving mode.

DRIVING MODE	MEAN SPEED (km/h)	SHARE (%)
Urban Off Peak	38	20
Urban Peak	28	20
Rural	60	35
Highway	110	25

Environmental information includes monthly values of average minimum and maximum temperatures as well as relative humidity. The data were taken from *The GLOBE Program of Croatia* and are shown in Table 2 (Jurić et al., 2012).

Table 2: Monthly values of average minimum and maximum temperatures as well as relative humidity (data for Zagreb, 2012).

	Jan	Feb	Mar	Apr	May	Jun	Jul	Aug	Sep	Oct	Nov	Dec
Min Temp (°C)	0.7	-0.2	4.5	10	12.5	16.9	18.1	19	16.4	8	2.2	2.1
Max Temp (°C)	5.6	6.4	13	20.4	24.1	27.5	28.6	30.3	26.8	16.1	7.1	7.9
Relative Humidity (%)	68	56	44	48	49	52	49	45	47	56	75	70

Results

Total (hot and cold) NO_x emissions from both petrol and diesel PCs in 2016 according to each Euro emission standard (Euro 0 to Euro 6) are calculated and presented in the top-left chart in Figure 3. Emissions are expressed in kilotons (kt). The top-right chart in Figure 3 shows implied NO_x EFs for petrol and diesel cars. Implied NO_x EFs are defined as total NO_x emission produced by cars with the relevant Euro standard, divided by the total annual activity of these cars. Nitrogen oxides EFs are provided in grams per kilometre (g/km). The comparison between implied NO_x EFs and type approval limit values for both petrol and diesel cars are presented in the bottom charts in Figure 3.

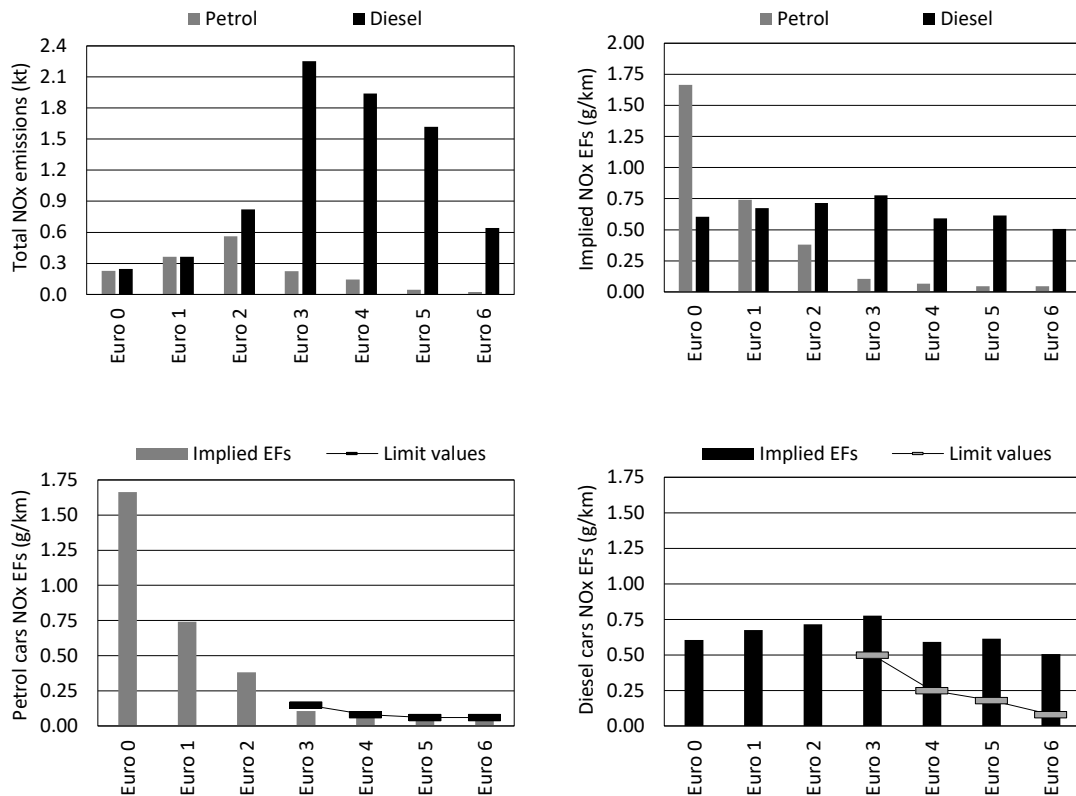


Figure 3: Total NO_x emissions, implied NO_x EFs and comparison of calculated NO_x EFs with type approval limit values.

Tailpipe emission of particulate matter PM₁₀ from both petrol and diesel PCs in 2016 according to each Euro emission standard (Euro 0 to Euro 6) are calculated and presented in the top-left chart in Figure 4. Emissions are expressed in tons (t). The top-right chart in Figure 4 shows implied PM₁₀ EFs for petrol and diesel cars. Implied PM₁₀ EFs are defined as total PM₁₀ emission produced by cars with the relevant Euro standard, divided by the total annual activity of these cars. Particulate matter EFs are provided in milligrams per kilometre (mg/km). The comparison between implied PM₁₀ EFs and type approval limit values for both petrol and diesel cars are presented in the bottom charts in Figure 4.

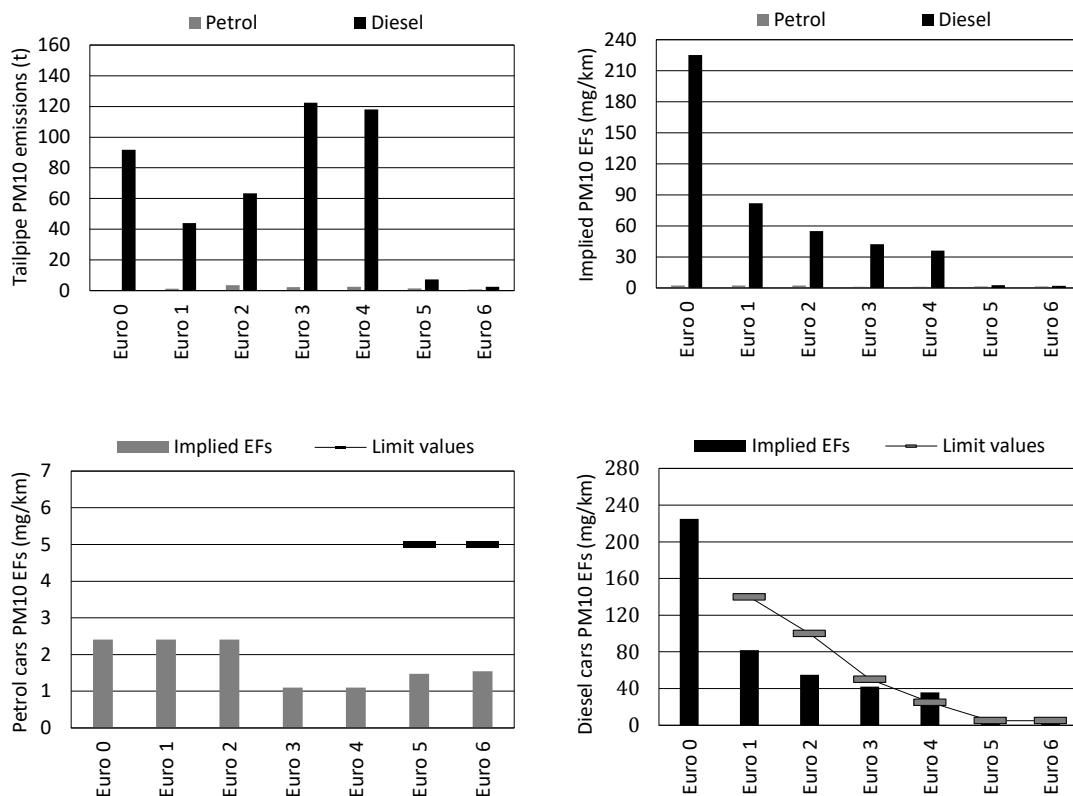


Figure 4: Tailpipe PM10 emissions, implied PM10 EFs and comparison of calculated PM10 EFs with type approval limit values.

Discussion and conclusions

The study investigated the influence of PC population and their activities on NO_x and PM emissions. As petrol and diesel PCs made up 96 % of the Croatian PC fleet in 2016, only these two PC subcategories were taken into account. Petrol cars make up 52 %, while diesel cars make up 48 % of the total number of vehicles considered. However, petrol cars drive 40 %, while diesel cars drive 60 % of the total annual mileage considered. Euro 3, Euro 4 and Euro 5 diesel cars are exploited much more than other PCs and these vehicles generated more than 60 % of total NO_x emissions of PCs. It is evident from Figure 3 that Euro 3/4/5/6 diesel cars exceed type approval limit values. Although diesel Euro 6 implied NO_x EF is the lowest in total diesel PC subcategory, its value exceeds Euro 6 emission limit by more than 6 times. Euro 0 petrol cars have the biggest implied NO_x EF, but the number of these vehicles is negligible compared to other PC subcategories. In addition, this subcategory is only marginally exploited. Regarding PM10 emissions, petrol cars do not play a significant role. Diesel cars Euro 0 up to, and including, Euro 4 emission standard produced 95 % of tailpipe PM10 emissions. It is only with the implementation of DPF technology on diesel Euro 5 and Euro 6 cars enabled that the PM emissions were significantly reduced. In order to reduce NO_x and PM emissions, it is necessary to lower the number of diesel PCs and/or their activity. The introduction of levies for diesel PCs is a method that would surely contribute to a reduced number of diesel vehicles and consequently to reduction of NO_x and PM emissions. In Croatia most levies are being considered through the carbon dioxide (CO₂) as a criterion. Diesel vehicles, due to lower fuel consumption compared to petrol cars, have the advantage when CO₂ EFs are taken as a criterion. But along with CO₂ as a criterion, it is necessary to introduce additional criteria related to harmful emissions, primarily NO_x and PM. Therefore, it is necessary to change the national policy measures. In order to decrease emissions, the vehicle fleet has to be renewed as well, by replacing older second-hand vehicles with new ones with low emissions. This would require definite national policy measures which would introduce tax cuts for new vehicles, while new tax levies would be redirected to older, mostly technically faulty and environmentally unfit vehicles, and specifically to the import of such vehicles.

References

- Amato, F., Favez, O., Pandolfi, M., Alastuey, A., Querol, X., Moukhtar, S., Bruge, B., Verlhac, S., Orza, J.A.G., Bonnaire, N., Le Priol, T., Petit, J.-F., Sciare, J., 2016. Traffic induced particle resuspension in Paris: Emission factors and source contributions. *Atmospheric Environment* 129, 114–124. doi:10.1016/j.atmosenv.2016.01.022
- Borge, R., de Miguel, I., de la Paz, D., Lumberras, J., Pérez, J., Rodríguez, E., 2012. Comparison of road traffic emission models in Madrid (Spain). *Atmospheric Environment* 62, 461–471. doi:10.1016/j.atmosenv.2012.08.073
- Carlaw, D.C., Rhys-Tyler, G., 2013. New insights from comprehensive on-road measurements of NO_x, NO₂ and NH₃ from vehicle emission remote sensing in London, UK. *Atmospheric Environment* 81. doi:10.1016/j.atmosenv.2013.09.026
- Chen, Y., Borken-Kleefeld, J., 2014. Real-driving emissions from cars and light commercial vehicles – Results from 13 years remote sensing at Zurich/CH. *Atmospheric Environment* 88, 157–164. doi:10.1016/j.atmosenv.2014.01.040
- Ellison, R.B., Greaves, S.P., Hensher, D.A., 2013. Five years of London's low emission zone: Effects on vehicle fleet composition and air quality. *Transportation Research Part D: Transport and Environment* 23, 25–33. doi:10.1016/j.trd.2013.03.010
- Guttikunda, S.K., Goel, R., 2013. Health impacts of particulate pollution in a megacity—Delhi, India. *Environmental Development* 6, 8–20. doi:10.1016/j.envdev.2012.12.002
- Jurić, B., Lacković, D., Šegota, J., 2012. Mean annual temperatures and relative humidity in Zagreb [WWW Document]. The GLOBE Program of Croatia. URL globe.pomsk.hr (accessed 9.26.17).
- Lang, J., Cheng, S., Zhou, Y., Zhang, Y., Wang, G., 2014. Air pollutant emissions from on-road vehicles in China, 1999–2011. *Science of The Total Environment* 496, 1–10. doi:10.1016/j.scitotenv.2014.07.021
- Li, L., Lei, Y., Wu, S., Chen, J., Yan, D., 2017. The health economic loss of fine particulate matter (PM 2.5) in Beijing. *Journal of Cleaner Production* 161, 1153–1161. doi:10.1016/j.jclepro.2017.05.029
- Ma, X., Jia, H., 2016. Particulate matter and gaseous pollutions in three megacities over China: Situation and implication. *Atmospheric Environment* 140, 476–494. doi:10.1016/j.atmosenv.2016.06.008
- Ntziachristos, L., Papadimitriou, G., Ligterink, N., Hausberger, S., 2016. Implications of diesel emissions control failures to emission factors and road transport NO_x evolution. *Atmospheric Environment* 141, 542–551. doi:10.1016/j.atmosenv.2016.07.036
- Ntziachristos, L., Samaras, Z., 2016. EMEP/EEA Air Pollutant Emission Inventory Guidebook.
- Pant, P., Harrison, R.M., 2013. Estimation of the contribution of road traffic emissions to particulate matter concentrations from field measurements: A review. *Atmospheric Environment*. doi:10.1016/j.atmosenv.2013.04.028 Review
- Rešetar, M., Pejić, G., Lulić, Z., 2017. Road Transport Emissions of Passenger Cars in the Republic of Croatia, in: *Digital Proceedings of the 8th European Combustion Meeting*. Dubrovnik, Croatia, 18-21 April 2017, pp. 2553–2558.
- Smit, R., Smokers, R., Rabé, E., 2007. A new modelling approach for road traffic emissions: VERSIT+. *Transportation Research Part D: Transport and Environment* 12, 414–422. doi:10.1016/j.trd.2007.05.001
- Stockfelt, L., Andersson, E.M., Molnár, P., Gidhagen, L., Segersson, D., Rosengren, A., Barregard, L., Sallsten, G., 2017. Long-term effects of total and source-specific particulate air pollution on incident cardiovascular disease in Gothenburg, Sweden. *Environmental Research* 158, 61–71. doi:10.1016/j.envres.2017.05.036
- Timmers, V.R.J.H., Achten, P.A.J., 2016. Non-exhaust PM emissions from electric vehicles. *Atmospheric Environment* 134, 10–17. doi:10.1016/j.atmosenv.2016.03.017
- Tzamkiozis, T., Ntziachristos, L., Samaras, Z., 2010. Diesel passenger car PM emissions: From Euro 1 to Euro 4 with particle filter. *Atmospheric Environment* 44, 909–916. doi:10.1016/j.atmosenv.2009.12.003
- Wang, J., Zhao, B., Wang, S., Yang, F., Xing, J., Morawska, L., Ding, A., Kulmala, M., Kerminen, V.-M., Kujansuu, J., Wang, Z., Ding, D., Zhang, X., Wang, H., Tian, M., Petäjä, T., Jiang, J., Hao, J., 2017. Particulate matter pollution over China and the effects of control policies. *Science of The Total Environment* 584–585, 426–447. doi:10.1016/j.scitotenv.2017.01.027

Urban Public Transport Systems Analysed in Terms of Land Use Considering CO₂ Emissions: the Case of Vienna, Austria

Andreas Gassner¹; Jakob Lederer², Markus Ossberger³, Johann Fellner⁴

^{1,2,4} CD Laboratory for Anthropogenic Resources, Institute for Water Quality, Resource, and Waste Management, TU Wien, Vienna, Austria; Corresponding author:

Andreas.Gassner@tuwien.ac.at

² Wiener Linien GmbH & Co KG, Vienna, Austria

Abstract

As the world urbanizes cities all over the globe have been constantly growing. Directly linked to the population growth of cities are increasing traffic and steadily raising land prices. Compared to the increase of many commodities observed during last decades land prices in cities have experienced significantly higher gains, indicating its overall scarcity. One option to cope with increasing traffic and scarce land availability is to strengthen public transport systems, as they are characterized by lower land use and higher transportation capacities. Besides the direct land use within the city borders transportation systems also cause land use in the hinterland, for example for the extraction of raw materials, for energy supply or for the sequestration of emitted carbon dioxide.

The study at hand investigated different land uses of a public transport network taking the case study of Vienna and its three main modes of public transport (subway, tram, and bus). The land uses distinguished were the **direct land use** within the city (for tracks, garages, etc.), the **direct land use in the global hinterland** (to provide energy and resources), and the land needed to sequestrate the CO₂ emissions emitted. For the latter a distinction between the CO₂ emissions from direct energy consumption (**operational energy CO₂ hinterland use**), and from CO₂ embodied in goods and materials (**embodied CO₂ hinterland use**) was made. The overall land use of the public transport system was finally determined and illustrated using an extended ecological footprint (EF) analysis.

The results obtained indicate that the operational energy CO₂ hinterland use, which accounts for the energy consumption, contributes most to the overall land use (550 km²), followed by the embodied CO₂ energy hinterland use (150 km²) and the direct hinterland use (16 km²). The direct land use within the city covers an area of around 6.2 km² (1.5% of city area) which corresponds to 1% of the ecological footprint (EF). Divided by transport mode, the subway has the largest EF (51%) followed by busses 20%, trams 19%, and services 10%. However, calculation of the EF per performance unit changes this ranking: the bus uses round 1.7 times the area per person kilometer traveled compared to subway.

On the basis of these results, the reduction of land use of Vienna's public transport network can be planned. It can be argued that that the knowledge about the mentioned lands and by what degree they are caused by specific inventory categories is essential to find reduction measures. Finally, our findings are essential to ensure sustainable development of the urban public transport.

1. Introduction

Urbanization leads to growing cities, until 2050 the current share of 50% of the global population living in urban areas will further increase to 80% (UN-DESA, 2014). The latter is also responsible for a significant share of cities' overall resource consumption and CO₂ emissions, which leads to a large land use for providing resources (e.g. energy, construction materials) and sequestrate CO₂. To reduce traffic area, emissions and resource consumption public transport is widely propagated, as it allows transporting more passengers over the same cross section per hour (Whitelegg, 1993) and fewer emissions are emitted per person kilometre travelled.

Public transport systems like in Munich, Paris, Shanghai and Vienna comprise mainly busses, trams, subways and railways. Therein, subways have the advantage of requiring less above-ground land within a city (Pfaffenbichler, 2001; Randelhoff, 2014) while providing high transportation capacity at the same time. On the other hand, they require more materials than tramways or bus lines, i.e. for the construction of tunnels (Andrade and D'Agosto, 2016; Lederer et al., 2016a, 2016b; Li et al., 2016), which impact on direct land consumption in the cities'

hinterland for the supply of raw materials (e.g. land for gravel pits), goods (e.g. land for cement production plants), and energy (e.g. land for coal mines necessary to supply cement production or power plants to generate electricity for concrete mixing). In addition to this direct land and hinterland consumption, sustainable urban development planning should furthermore consider the compensation of greenhouse gas (GHG) emissions (e.g. CO₂ sequestration by forests). This land requirement can be assessed by means of the so-called “ecological footprint”, which should always be set in context with the overall life-cycle emissions as specified in several frameworks and studies (e.g. (European Commission, 2012; Matthews et al., 2008; Wackernagel and Beyers, 2010). Several studies (e.g. (Barrett and Scott, 2003; Bhandari et al., 2014; Chi and Stone, 2005; Lederer et al., 2016b; Tuchschnid, 2009)) have already assessed the contribution from public transport systems or partial transport modes to the emissions of a region or urban area. However, none of these studies have analyzed the contribution to the overall direct land use and the different land uses in hinterlands of each transport mode.

With respect to above mentioned aspects, the overall objective of the study at hand is to provide a detailed analysis of land consumption of an urban public transport system. To fulfill this objective, different land uses of an urban public transport network are investigated. The land uses distinguished were the direct land use within the city (for tracks, garages, etc.), the direct land use in the global hinterland (to provide energy and resources), and the land needed to sequester the CO₂ emissions emitted. For the latter a distinction between the CO₂ emissions from direct energy consumption (operational energy CO₂ hinterland use), and from CO₂ embodied in goods and materials (embodied CO₂ hinterland use) was made. The overall land use of the public transport system was finally determined and illustrated using an extended ecological footprint (EF) analysis.

Vienna’s public transport system has been investigated as a case study. Considered is an integrated transport system of one provider operating three different transport modes, yielding a unique set of data. The fact that this type of transport system and operation is prevailing at least in European cities of comparable size (van Egmond et al., 2003) underlines the relevance of the study at hand. For the study, real inventory and energy-consumption data were used.

2. Material and methods

In the case study city of Vienna, the share of public transport of the modal split was 39% in 2013 (Wiener Stadtwerke Holding AG, 2013a). 85% of the overall passenger kilometers traveled (PKT) by public transport was provided by WIENER LINIEN GmbH & Co KG (Österreichisches Institut für Raumplanung (ÖIR), 2014). In the study at hand, only the service covered by this provider is considered. In the reference period from 2012-2013, which was used in this study, the provider operated a network of 5 subway lines, 29 tram lines, and 109 bus lines, characterized by a length of 79 km, 172 km and 700 km, respectively. Additionally, service buildings (e.g. administration) are part of the operators assets and have been considered in the present study.

The overall land consumption of Vienna’s public transport system has been determined using an extended ecological footprint (EF) analysis approach based on several studies (Borucke et al., 2013; Global Footprint Network, 2009; Rees, 1992; Wackernagel et al., 2005; Wackernagel and Rees, 1996). While most EF studies quantify the overall land required on a global scale, the study at hand distinguished direct land use and the land use in global hinterland. The hinterland is divided in the three categories: direct hinterland use, embodied CO₂ hinterland use, and operational energy CO₂ hinterland use

To calculate the land use categories mentioned, different data were utilized. The direct land use was determined using spatial data processed by a geographic information system (GIS). To assess the hinterland demand, an ecological footprint (EF) calculation was performed. Thereto the software SimaPro and the therein implemented database Ecoinvent was utilized. For the determination of the incorporated land use due to the provision of materials and goods (for the infrastructure of the public transport system), a material inventory was created. Direct land use caused either by material or energy use was subsumed under the category of direct land use. The total land use (ecological footprint) was calculated by combining all four land use categories. Finally, the results obtained were referred to the transport capacity, seat km provided (SKP), and the actual performance in terms of passenger kilometers traveled (PKT). Figure 1 summarizes the method of the study at hand.

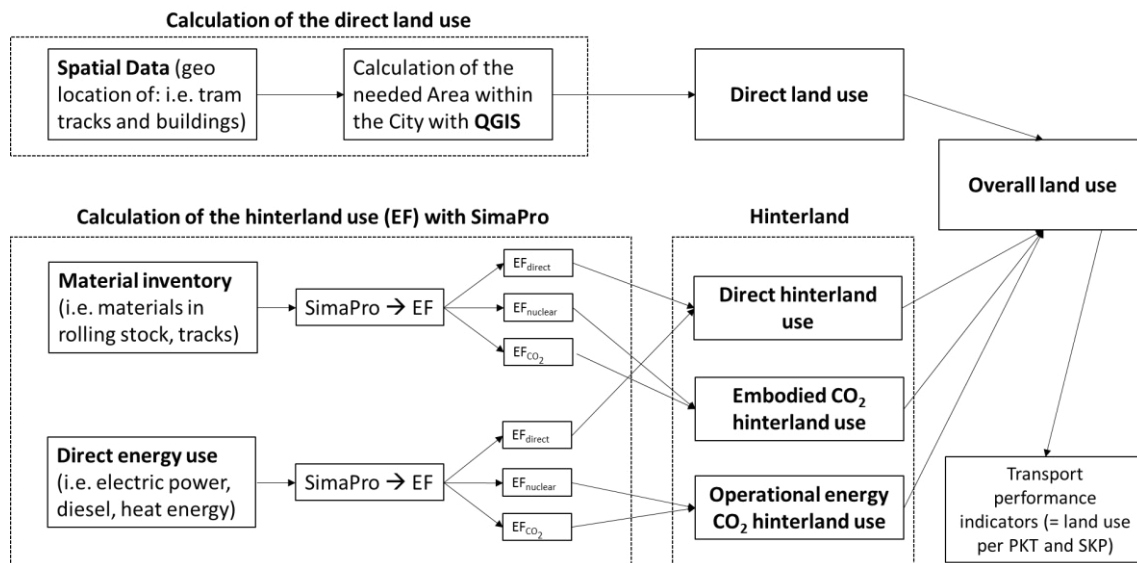


Figure 1: Calculation method and resulting land use categories

2.1. Direct land use

To calculate the direct land use within the city, all surface areas in use by the public transport provider were identified considering the transport modes subway, tram, and bus, including service buildings (depots, garages and administration). Therefore spatial data provided by the city of Vienna (Federal Chancellery and Vienna City Administration, n.d.) and GIS data sets of the operator were used. The data was evaluated and processed using the open source software QGIS (Version 2.16.2). For each transport mode the network was divided into areas in use below and above ground, whereas only the latter were regarded as direct land use. Detailed information which data is used per transport mode is provided below:

- Tram: Data from the Municipal Department 28 - Road Management and Construction (MA 28), in detail the so called Straßeninformationssystem (SIS) provides the basis for the direct land use of the tram lines (MA 28, n.d.). The spatial data for buildings (i.e. train depots, engineering rooms, social rooms, and other services) was retrieved from the operator. The stops are on public areas due that reason they are not in that database, the area used is calculated separately on the basis of the number of stops.
- Subway: The direct land use for the subway was determined using spatial datasets provided by the operator. The basic data set includes all civil engineering constructive works (tunnels, bridges, elevated track sections).
- Bus: The area for the bus network was determined by using vector data for the bus lines from Wiener Linien (Wiener Linien GmbH & Co KG, 2015). Transversal to the vector of the bus lines, a puffer was set to create a raster layer, distinguishing manually between sections where busses travel solely in one direction and those which are used for travel in both directions. According to bus standards, the width of the puffer was chosen at 3.5 m for sections in one direction and 6.5 m for sections used in both directions (MA 18, 2011). The bus stops were calculated separately on the basis of the number of stops.
- Services: As some buildings (e.g. main administration building and main garage) cannot be allocated to one single mode of transport, their areas are treated separately in the study at hand. The spatial data is provided by the operator.

2.2. Calculation of the hinterland

In order to assess direct hinterland use, first the quantity and composition of materials (including goods) consumed were determined. Therefore, data provided by the operator were categorized and a material inventory (see section 2.3) was created. Based on the material inventory, direct

hinterland use was calculated using the software SimaPro (version: 7.2.3). In addition, the software was also used to determine the EF for the inventory.

SimaPro uses the Ecoinvent database, which includes not only all preceding chains of materials and energy for manufacturing these materials, but also the associated land uses (Hischier et al., 2010). The method implemented in SimaPro distinguishes three environmental impact categories associated with land use ($EF = EF_{\text{direct}} + EF_{\text{CO}_2} + EF_{\text{nuclear}}$). The categories are divided in direct land occupation (EF_{direct}) and indirect land occupation (EF_{CO_2} and EF_{nuclear}). The indirect land occupation is related to nuclear energy use (EF_{nuclear}) and to the sequestration of CO₂ emissions from fossil energy use (EF_{CO_2}) (Hischier et al., 2010). Contrary to the common application of SimaPro, direct hinterland consumption due to material and associated energy supply is presented separately from the hinterland used to sequester CO₂ emissions related to the production of materials. In other words, the total direct hinterland consists of the direct land occupation calculated from materials (and goods) used and the direct land occupation related to direct energy use. The hinterland land use categories are given in global hectares per time [gha/a]. A normalization was made in categories where materials and goods were used over a longer period than one year. For this reason, the results of the calculation (land use) for these categories were divided by assumed life spans that derive from economic depreciation. The economic life spans were defined by the financial accounts department based on legal regulations and are individual for each asset category.

2.3. Inventory data to calculate the hinterland

To assess direct hinterland use and the embodied CO₂ energy hinterland use, first a material inventory of all used goods and materials by Wiener Linien has to be determined. An overview of the inventory of Wiener Linien, the categories and sources used, is presented in Table 1. Inventory data from the public transport provider were collected, assessed and categorized. Thereby the following data groups were identified: (i.) buildings, (ii.) mobile and immobile assets, (iii.) rolling stock, (iv.) consumer goods, (v.) waste.

The respective quantity of goods within the data groups had to be linked with the material composition of each good. Besides information collected during previous studies (Gassner, 2013; Lederer et al., 2016a, 2016b; Ott et al., 2010), material intensities were taken from literature and the Ecoinvent database. The categorization of goods and its linkage to material intensities was very diverse for each data group due to the available data, but also due to different features. In general, the formulae applied have in common that information on quantities of goods (e.g. section length, number of goods) is multiplied by specific material intensities of these goods (e.g. copper in wire, concrete in buildings).

Due to resource constraints, similar infrastructures and appliances were clustered in joint categories, and representative elements of these categories were analyzed and subsequently the data have been up-scaled to account for all elements of the respective category.

The inventory data was divided wherever applicable into traffic modes and services. For the categories consumer goods and waste, for instance, an allocation to traffic modes was not accomplished. Hence, both are accounted for in the category services. The inventory data contain physical assets like buildings and rolling stock and nonphysical assets like thermal heat or electric power. For the physical assets, the material intensity and material composition were investigated. To calculate the environmental impact of nonphysical assets (power supply) the overall energy mix had to be identified.

Table 1: Inventory Data Wiener Linien – Data categories and sources

Data Category	Transport mode	Description	Source Material intensity and mass
General buildings	Tram, subway, bus, services	Storage buildings and administrative buildings	(Hoffmann et al., 2011; Kellenberger et al., 2007)
Subway construction	Subway	Subway constructions, inkl. 104 metro stations	(Lederer et al., 2016a).
Tram Tracks	Tram	Own calculation on the basis of the single-track standard cross-section.	(Wiener Linien GmbH & Co KG, 2012a)

Mobile and immobile assets	Tram, subway, bus, services	Allocation to the mode of transport with cost categories. In total around 36,500 assets are in use within the company. An ABC-analysis was performed to exclude non relevant assets. In total 18,000 assets were finally merged to 162 different categories .	The 162 categories have subsequently been evaluated for their composition using literature data, own calculations or expert interviews.
Rolling stock	Subway	700 subway trains, three different types (types V, U, and T)	(Bomardier, n.d.; Siemens AG, 1998; Struckl, 2007; Wiener Linien GmbH & Co KG, 2012b; Wiener Stadtwerke Verkehrsbetriebe, 1985)
Rolling stock	Tram	525 tram cars that divide into three types (A, B, and E)	(Pamminger and Adamek, 2010; Siemens AG, 2004a, 2004b; Spielmann et al., 2007; Wiener Linien GmbH & Co KG, 2013; Wiener Stadtwerke Verkehrsbetriebe, 1984)
Rolling stock	Bus	Three different types of busses are in operation, namely 223 low-floor normal buses, 234 low-floor articulated buses and 12 low-floor battery-powered buses (2-door).	(Gassner, 2013; Siemens AG, 2012; Wiener Linien GmbH & Co KG, 2013)
Consumer goods	Services	The purchasing department provided data on low-value assets and consumer goods. An ABC-analysis was performed and around 46,000 various articles remained. For all remaining goods, their mass was calculated. In general, the consumer goods can be allocated to a few main material groups. For instance, the majority of maintenance materials like screws, bolts and track wheels were made of steel. 64 consumer good material categories were identified.	Each type were allocated to an Ecoinvent process (e.g. Rainforced steel, paper, motor oil etc.)
Waste	Services	The annual amounts of waste arising were grouped by the type of waste. Each type of waste is defined by a waste code. 63 different types of waste were generated by Wiener Linien in the year 2012.	Each type were allocated to an Ecoinvent processes.

To assess the operational energy CO₂ hinterland use, first the total operational energy demand has to be determined. The respective data, which comprises the electricity for the subway and tram operations, fuel for busses, heat for the subway stations and electricity for buildings and services, was retrieved from the operator (c.f. Table 2). In the second step, data on the energy mix for the production of operational energy was obtained. The electricity supplier of the transport provider “Wien Energie” reported the overall energy mix for electric power in 2012 as follows: 46.62% hydropower, 44.99% natural gas, 3.74% wind and solar power, 0.08% power from renewable sources, 3.62% biomass energy, and 0.94% biogas (Keuschnig, 2014). The energy mix for the district heating was: 5,8% biomass energy, 14,3% waste heat (from industry), 17,8% waste incineration, 62,1% combined heat and power generation (natural gas) (Wiener Stadtwerke Holding AG, 2013b). By inserting this data in SimaPro, the operational energy CO₂ hinterland use was calculated, the operational energy CO₂ hinterland use is given in global hectares for one year [gha/a].

Table 2: Total energy consumption 2012 Wiener Linien in Megawatt hour (MWh); own representation based on data from Wiener Linien - (Rumpeltes and Reeps, 2013) and (Keuschnig, 2013).

Energy and Fuels	Megawatt hour (MWh/a)
Electric power consumption	426,647
District heating heat consumption	67,537

Liquid Petroleum Gas (LPG)	191,927
Natural gas	5,082
Diesel	7,518
Gasoline	215

2.4. Calculation of Transport performance indicators

The results were normalized to the transport performance. The total land use per year were divided by the amount of kilometers travelled (PKT) by all passengers of the public transport system. In order to consider not only the PKT but also the transport capacity offered by the operator, another normalization was performed using the seat kilometer provided (SKP). The data about the transport performance was taken for PKT (Österreichisches Institut für Raumplanung (ÖIR), 2014) and for SKT (Österreichisches Institut für Raumplanung (ÖIR), 2013).

3. Results

Results show that the direct land use within the city of Vienna covers with 6.2 km² around 1.5% of the city area. Altogether, the three land uses in the global hinterland are 115 times larger than the direct land use in the city. Therein, the operational energy CO₂ hinterland use contributes most to overall land use, followed by the embodied CO₂ hinterland use and the direct land use in the global hinterland. The resulting overall land use calculated was ~725 km² per year which equals around 175% of the city area. (cf. Figure 2).

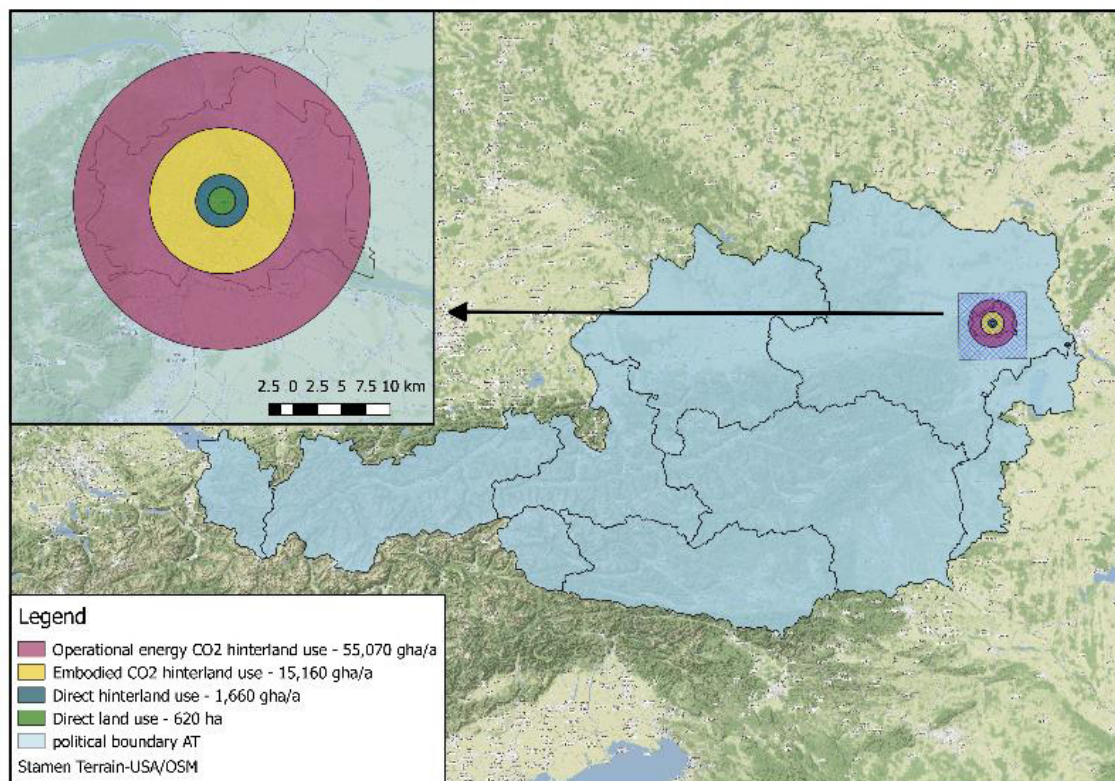


Figure 2: Land use of the public transport system in Vienna divided by land category

In Figure 3 the overall land use for the three transport modes are presented. Beside annual land use, the results are presented with respect of the transport performance in m²/PKT and m²/SKP. The comparison of the transport modes shows that the subway requires with 51% the largest share of the overall land use followed by bus (20%), and tram (19%). The remaining 10% are for services (e.g. office buildings) that can't be allocated to one of the aforementioned modes. For services a land use of around 7,000 gha/a was calculated, this number is included in the overall land use of urban public transport of Vienna.

The results indicate that the subway shows the largest overall land use of all transport modes. However, when considering at land use per performance unit, this ranking of the transport modes changes. Due to the high transport performance of the subway and tram, both perform better than the bus. The transport mode bus needs around 1.7 times the area per PKT and 2.5 times the area per SKP compared to the subway.

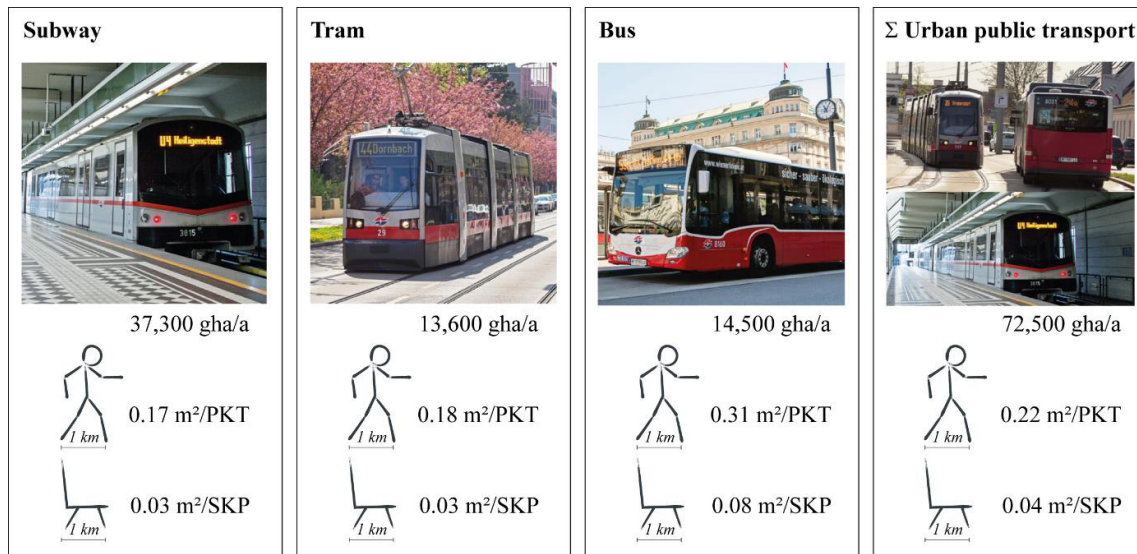


Figure 3: Overall land use divided by transport mode, land use per functional unit

4. Conclusion

A new approach for the analysis of land use of urban public transport systems is presented. The introduced classification of direct land use of transport systems distinguishes between local and global level. The results emphasize that when the land required for the sequestration of CO₂ emissions are included in the analysis of land use, energy consumption and building materials of the urban public transport system investigated are dominating the overall land use. A significant decrease in the EF can only be reached by reducing the hinterland EF. The result is not only relevant for Vienna, but also for other European cities of comparable size, as most of them have multi-modal transport systems similar to that in Vienna (van Egmond et al., 2003). In contrast to case studies which investigated one special transport mode such as rail transit (Li et al., 2016), high-speed rail (Chang and Kendall, 2011) or subway (Andrade and D'Agosto, 2016), the study at hand considered an integrated transport system of one provider operating three different transport modes, yielding a unique set of data. In absolute figures, the subway shows the largest contribution to the EF as well as to three out of four subcategories of the EF (except the direct land use). The total contribution of trams, busses, but also services is much lower, even though the network length of trams and busses is two and ten times larger, respectively. One reason for that is the material and energy intensive engineering work in subways, which has also been observed by Anderson (Anderson et al., 2015). Another reason is the traction energy consumed. However, when referring the results to the passengers transported, the subway has the lowest EF of all three modes of transport offered by the transport provider. In both cases, however, the question is if these results can guide decision making on whether a city of the size of Vienna should focus more on subway, tram or bus extension. This question is difficult to answer as the three transport modes are interlinked to each other in a network of main transport axes along densely populated areas (subways) and a small boned network of tram and bus lines in less densely populated areas connected to the main axes. The dense network of feeder lines guaranties nearby accessibility to the public transport network for the passengers (Ostermann et al., 2016).

Acknowledgment

The work presented is part of a large-scale research initiative on anthropogenic resources (Christian Doppler Laboratory for Anthropogenic Resources). The initiative is supported by the

References

- Anderson, J.E., Wulffhorst, G., Lang, W., 2015. Expanding the use of life-cycle assessment to capture induced impacts in the built environment. *Build. Environ.* 94, 403–416. doi:10.1016/j.buildenv.2015.08.008
- Andrade, C.E.S. de, D'Agosto, M. de A., 2016. Energy use and carbon dioxide emissions assessment in the lifecycle of passenger rail systems: the case of the Rio de Janeiro Metro. *J. Clean. Prod.* 126, 526–536. doi:10.1016/j.jclepro.2016.03.094
- Barrett, J., Scott, A., 2003. The Application of the Ecological Footprint: A case of passenger transport in Merseyside. *Local Environ.* 8, 167–183. doi:10.1080/1354983032000048488
- Bhandari, K., Advani, M., Parida, P., Gangopadhyay, S., 2014. Consideration of access and egress trips in carbon footprint estimation of public transport trips: Case study of Delhi. *J. Clean. Prod.* 85, 234–240. doi:10.1016/j.jclepro.2014.05.013
- Bomardier, n.d. Niederflur U-Bahn-Stadtbahntriebwagon für Wien und Köln (English: low-entry subway train for Vienna and Cologne). Vienna.
- Borucke, M., Moore, D., Cranston, G., Gracey, K., Iha, K., Larson, J., Lazarus, E., Morales, J.C., Wackernagel, M., Galli, A., 2013. Accounting for demand and supply of the biosphere's regenerative capacity: The National Footprint Accounts' underlying methodology and framework. *Ecol. Indic.* 24, 518–533. doi:10.1016/j.ecolind.2012.08.005
- Chang, B., Kendall, A., 2011. Life cycle greenhouse gas assessment of infrastructure construction for California's high-speed rail system. *Transp. Res. Part D Transp. Environ.* 16, 429–434. doi:10.1016/j.trd.2011.04.004
- Chi, G., Stone, B., 2005. Sustainable Transport Planning: Estimating the Ecological Footprint of Vehicle Travel in Future Years. *J. Urban Plan. Dev.* 131, 170–180. doi:10.1061/(ASCE)0733-9488(2005)131:3(170)
- European Commission, 2012. Organisation Environmental Footprint Guide, European Commission-Joint Research Centre-Institute for Environment and Sustainability. doi:doi:10.3000/19770677.L_2013.124.eng
- Federal Chancellery and Vienna City Administration, n.d. data.gv.at [WWW Document]. URL <https://www.data.gv.at> (accessed 10.1.16).
- Gassner, A., 2013. Vergleich des Ökologischen Fußabdruckes von Bussen unterschiedlicher Antriebstechnologien (English: Comparison of the ecological footprint of buses of different drive technologies). University of Natural Resources and Life Sciences, Vienna.
- Global Footprint Network, 2009. Ecological Footprint Standards 2009. Oakland: Global Footprint Network.
- Hischier, R., Editors, B.W., Althaus, H., Bauer, C., Doka, G., Dones, R., Frischknecht, R., Hellweg, S., Humbert, S., Jungbluth, N., Köllner, T., Loerincik, Y., Margni, M., Nemecek, T., 2010. Implementation of Life Cycle Impact Assessment Methods, ecoinvent report No. 3, v2.2. Dübendorf, CH. doi:citeulike-article-id:4863951
- Hoffmann, M., Krause, T., Martin, J., Kuhlmann, W., Pick, J., Olk, U., Schlösser, K.H., Streit, W., Winkler, N., 2011. Zahlentafeln für den Baubetrieb (English: Figures for the construction operation), 8., überar. ed. Vieweg + Teubner, Wiesbaden.
- Kellenberger, D., Althaus, H.-J., Jungbluth, N., Künniger, T., 2007. Life Cycle Inventories of Building Products. Final report ecoinvent data v2.0 No.7, Swiss Centre for Life Cycle Inventories. Dübendorf, CH.
- Keuschnig, E., 2014. Energiemix-Strom 2012 (English: overall energy mix - electric power 2012), unpublished. Vienna, AUSTRIA.
- Keuschnig, E., 2013. Betriebsdaten Energieverbrauch 2012 (English: Operating energy consumption 2012), Wiener Linien GmbH & Co. Vienna, AUSTRIA.
- Lederer, J., Kleemann, F., Ossberger, M., Rechberger, H., Fellner, J., 2016a. Prospecting and Exploring Anthropogenic Resource Deposits: The Case Study of Vienna's Subway Network. *J. Ind. Ecol.* 0, n/a-n/a. doi:10.1111/jiec.12395
- Lederer, J., Ott, C., Brunner, P.H., Ossberger, M., 2016b. The Life-Cycle Energy Demand and Greenhouse Gas Emissions of High-Capacity Urban Transport Systems: A Case Study From Vienna's Subway Line U2. *Int. J. Sustain. Transp.* 10, 120–130. doi:10.1080/15568318.2013.869704
- Li, Y., He, Q., Luo, X., Zhang, Y., Dong, L., 2016. Calculation of life-cycle greenhouse gas emissions of urban rail transit systems: A case study of Shanghai Metro. *Resour. Conserv. Recycl.* doi:http://dx.doi.org/10.1016/j.resconrec.2016.03.007
- MA 18, 2011. Projektierungs_Handbuch: Öffentlicher_Raum, Stadtentwicklung Wien, Magistratsabteilung 18. Wien. doi:10.1017/CBO9781107415324.004
- MA 28, n.d. Straßeninformationssystem SIS (English: Road information system) [WWW Document]. Magistr. 28 - Grup. Aufgrabungen und Inf. URL https://www.wien.gv.at/wudk/internet/wuisbatch/Prod/html/detail_15066096.html (accessed 10.4.16).
- Matthews, H.S., Hendrickson, C.T., Weber, C.L., 2008. The Importance of Carbon Footprint Estimation Boundaries. *Environ. Sci. Technol.* 42, 5839–5842. doi:10.1021/es703112w
- Ostermann, N., Rollinger, W., Kehr, J., 2016. Handbook Public Transport - Handbuch ÖPNV Schwerpunkt Österreich, 1. Auflage. ed. TZ-Verlga & Print GmbH, Hamburg.
- Österreichisches Institut für Raumplanung (ÖIR), 2014. Verkehrsleistung Wien 1970 bis 2013 (English: Transport performance Vienna from 1970 to 2013), unpublished. Vienna, AUSTRIA.

- Österreichisches Institut für Raumplanung (ÖIR), 2013. Fahrleistungen 2012 [Mio. Platz-km/Jahr] (English: Transport Performance 2012 [m. PKT/Year], unpublished. Vienna, AUSTRIA.
- Ott, C., Kral, U., Brunner, P.H., 2010. Vom Ökologischen Fußabdruck zum Ressourcen- und Umweltmanagement am Beispiel der Wiener Linien (ÖFRU) (English: From the ecological footprint to resource and environmental management). Vienna, AUSTRIA.
- Pamminger, R., Adamek, H., 2010. Integration von Umweltaspekten in den Produktentwicklungsprozess von Straßenbahnen (English: Integration of environmental aspects into the product development process of trams), in: Rießberger, K. (Ed.), *Moderne Schienenfahrzeuge* : 39. Tagung. Siemens, Graz, AUSTRIA, p. 208.
- Pfaffenbichler, P.C., 2001. Means of transport and structures. *Wiss. Umwelt Interdiszip. Verkehr und Mobilität* 3, 35–41.
- Randelhoff, M., 2014. Vergleich unterschiedlicher Flächeninanspruchnahmen nach Verkehrsarten (pro Person) (English: Comparison of different land use per means of transport (per person)) [WWW Document]. URL <http://www.zukunft-mobilitaet.net/78246/analyse/flaechenbedarf-pkw-fahrrad-bus-strassenbahn-stadtbahn-fussgaenger-metro-bremsverzoegerung-vergleich/> (accessed 8.25.16).
- Rees, W.E., 1992. Ecological footprints and appropriated carrying capacity: what urban economics leaves out. *J. Compos. Mater.* 33, 928–940. doi:0803973233
- Rumpeltes, H., Reeps, H., 2013. Betriebsdaten Heizenergie - Fernwärme, Erdgas (English: Operational heating energy - district heating, natural gas), Wiener Linien GmbH & Co. Vienna.
- Siemens AG, 2012. Elektrobus der Wiener Linien - Technische Daten (English: Electric bus of Wiener Linien - technical data). Vienna.
- Siemens AG, 2004a. Detailed plan ULF 197-4A1. Vienna.
- Siemens AG, 2004b. Detailed plan ULF 197-6B1. Vienna.
- Siemens AG, 1998. Prototypzug U-Bahn Wien V-Wagen Technische Information (English: Prototype subway train type "V" Vienna, technical information). Vienna, AUSTRIA.
- Spielmann, M., Bauer, C., Dones, R., Tuchschnid, M., 2007. Transport Services Data v2.0, Swiss Centre for Life Cycle Inventories. Villigen and Uster.
- Struckl, W., 2007. Green Line - Umweltgerechte Produktentwicklungsstrategien für Schienenfahrzeuge auf Basis der Lebenszyklusanalyse des Metrofahrzeuges Oslo (English: GreenLine - Environmentally sound product development strategies for rail vehicles based on the lifecycle). TU Wien.
- Tuchschnid, M., 2009. Carbon Footprint of High-Speed railway infrastructure (Pre-Study). Zürich.
- UN-DESA, 2014. World Urbanization Prospects: Revision 2014.
- van Egmond, P., Nijkamp, P., Vindigni, G., 2003. A comparative analysis of the performance of urban public transport systems in Europe. *Int. Soc. Sci. J.* 55, 235–247. doi:10.1111/1468-2451.5502005
- Wackernagel, M., Beyers, B., 2010. *Der Ecological Footprint. die Welt neu vermessen* (English: The Ecological Footprint.). Europäische Verlagsanstalt.
- Wackernagel, M., Monfreda, C., Moran, D., Wermer, P., Goldfinger, S., Deumling, D., Murray, M., 2005. National Footprint and Biocapacity Accounts 2005 : The underlying calculation method. *Land use policy* 21, 231–246.
- Wackernagel, M., Rees, W.E., 1996. *Our ecological footprint: reducing human impact on the earth*. Gabriola Island, BC [u.a.] : New Society Publ.
- Whitelegg, J., 1993. *Transport for a Sustainable Future: The Case for Europe*. Belhaven Press, London.
- Wiener Linien GmbH & Co KG, 2015. Öffentliches Verkehrsnetz - Liniennetz - Wien (English: Public transport network - Line network - Vienna) [WWW Document]. data.gv.at. URL <https://www.data.gv.at/katalog/dataset/36a8b9e9-909e-4605-a7ba-686ee3e1b8bf> (accessed 6.15.16).
- Wiener Linien GmbH & Co KG, 2013. Facts and Figures. Vienna.
- Wiener Linien GmbH & Co KG, 2012a. Regelpläne der Wiener Straßenbahn B6-B63-3-1004 (English: Construction plans of the tram tracks - Vienna: type: B6-B63-3-1004), Bau- und Anlagenmanagement - Abteilung Bahnbau. Vienna.
- Wiener Linien GmbH & Co KG, 2012b. Unternehmensinfo Alles über uns (English: Company information: All about us). Vienna.
- Wiener Stadtwerke Holding AG, 2013a. Bericht aus dem Nachhaltigkeitsmanagement der Wiener Stadtwerke (English: Report from the sustainability management of Wiener Stadtwerke). Vienna, AUSTRIA.
- Wiener Stadtwerke Holding AG, 2013b. Geschäftsbericht 2012 (English: Annual Report 2012). Vienna, AUSTRIA.
- Wiener Stadtwerke Verkehrsbetriebe, 1985. Technische Beschreibung U-Bahn Wien Type U1.1 (English: Technical description Subway Train Vienna Type "U1.1"), SGP Abteilung S/B 21. Vienna.
- Wiener Stadtwerke Verkehrsbetriebe, 1984. Detailed plan Gelenktriebwagen E2. Vienna.

Photocatalytic tunnel coatings: evaluation of their efficiency with time

C. Paglia¹, C. Mosca¹, S. Antonietti¹ and A. Jornet¹

¹ Institute of Materials and Constructions (IMC), DACD - SUPSI, CH-6952 Canobbio, Switzerland

Keywords: photocatalysis, road tunnel, coating.

Presenting author email: christian.paglia@supsi.ch

1. Introduction.

Ever since the photocatalytic properties of titanium dioxide (TiO₂) were discovered (Fujishima A., Honda K., 1972), its application has been widely studied in numerous research projects. Experiments carried out in laboratories have shown that TiO₂ is highly reactive and it can therefore be chemically activated by sunlight (UV component) and is effective at reducing some atmospheric pollutants, in particular nitrogen oxides (NO_x). In the construction industry, this knowledge has led to great enthusiasm as well as to the development and widespread marketing of so-called photocatalytic products (Cassar, 1998). These products contain the photocatalyst TiO₂ in powder form inside their matrix or dispersed in a solution used in surface treatment. Photocatalytic construction materials have a wide range of applications: cement, plaster, paint, textile membranes, etc. These products have been promoted by highlighting their capability of reducing atmospheric pollutants in urban environments, their highly hydrophilic and self-cleaning properties, and their capability of maintaining the colour and brightness of surfaces over time.

In the scientific field, interest for applications of photocatalysis has sharply increased, as is shown by the presence of some important research projects that have developed and experimented on the products (*PICADA 2002-2005*, *PhotoPAQ 2010-2014*, *PIER 2008*), as well as by the high number of research studies published in the last 15 years (Beeldens, A. and D. Van Gemert, 2004; Guerrini G.L., Peccati E., 2007; Chen J., Poon C-S, 2009).

Despite the wide scope of the research literature, some important issues remain open, mainly about the duration of the long-term effectiveness in reducing atmospheric pollutants (Gürol, 2006); the duration of the surfaces containing or treated with TiO₂; data acquisition systems; and procedures for the measurement of photocatalytic behaviour.

In this context, and in response to the many requests from our Commissioners, the Institute for Materials and Construction conducted an experimental study in 2012, with the aim of assessing the effectiveness over time of some photocatalytic products available in the market and used as surface coating in road tunnels.

2. Objective of the study.

The applicability of photocatalytic products for the creation of road tunnel coatings is seen as an important opportunity to contribute to environmental

sustainability, while allowing for savings in terms of maintenance and cleaning costs and, at the same time, contributing to the improvement of the quality of air.

In particular, when planning road tunnels, the *Department for Territory of Ticino* had to decide whether to use photocatalytic or traditional coatings. Products available on the market show promising data about their capability of reducing pollutants and dirt pickup, however, their costs are up to 20% higher than those of non-photocatalytic products. Therefore their use needs to be carefully considered. Moreover, photocatalytic products used in a closed environment, like road tunnels, require a lighting system that needs to be integrated with UV lamps to activate TiO₂ and at the same time needs to provide adequate lighting for road safety.

The *Institute for Materials and Construction* (Imc) tested the performance of some products available in the market and assessed a decrease in their main performance (photocatalytic activity and dirt pickup) as well as an increased maintenance work. The latter is a very important aspect of road tunnels, where there is a need to maintain light reflection and lighting uniformity at very high levels, both during normal operation and in case of emergency.

The research presented in this paper is highly applied and aims at assessing the behaviour over time of the efficiency of six products available in the market (a skim plaster and five types of paint) at reducing atmospheric pollutants. These products were suggested by the *Department for Territory* with the aim of estimating the cleaning times necessary to maintain the anti-pollution properties.

3. Instrumentation and methodology.

For the research, samples were prepared to measure the photocatalytic reduction rate of nitrogen oxides in the air, in compliance with UNI 11247:2010. The analytical method used was based on chemiluminescence; photoactivity tests were carried out on the products with NO_x (NO+NO₂) enriched air, so as to simulate a likely degree of atmospheric pollution.

3.1 Preparation of samples and location within the tunnel.

The samples had a surface of 6400 mm² and a thickness of about 10 mm, as provided for by UNI 11247:2010. In order to use standard supports, the *Imc* prepared all samples in cement mortar, on which the respective manufacturers applied their products in accordance with their protocols.

The method described in the UNI regulation provides that the test be performed on two different samples of the same material. Therefore, for each tested product, 5 couples of samples were prepared to measure the reduction rate at certain pre-determined time interval: initial test at $t=0$, then after 1 month, 3, 6 and 12 months. For one year, the samples remained in a road tunnel in Lugano with a traffic of 8 million vehicles/year, with an average daily transit of about 22,000 passengers. Logical scheme of the experiment is shown in figure 1.

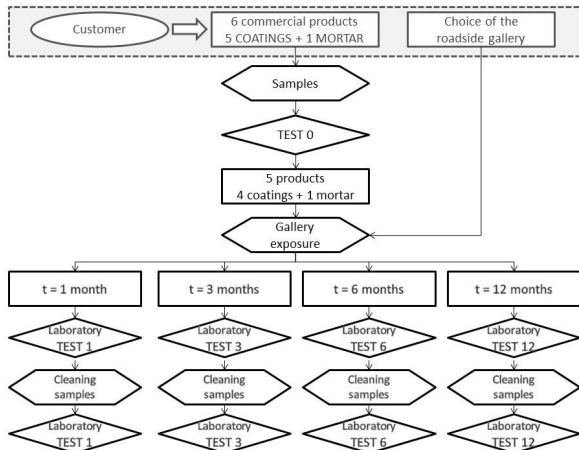


Figure 1. Logical scheme of the experiment.

3.2 Testing method and instruments.

The photocatalytic capacity of the different products was measured by determining the reduction activity of nitrogen oxides in the air.

The instrumentation, which was set up according to the provisions of UNI 11247:2010, was made up of a glass reaction chamber with a volume of 3 litres \pm 20%, inside which the sample was placed. In the reaction chamber, there was a continuous and constant inflow of 5 litres/min of a mixture of air and NO_x (NO+NO₂). A chemiluminescence analyser took a sample of the flowing fluid from the reaction chamber and measured the concentration of NO_x. The concentration of nitrogen oxides was measured by the analyser at three different times: before entrance into the reaction chamber (C_A); inside the reaction chamber with the sample being in the dark (C_B); inside the reaction chamber with the sample being irradiated with a UV lamp with a power of 300 W and a light emission of 365 nm, with a radiant flux on the surface of the sample of 20 ± 1 W/m² (C_L). The measurement procedure is outlined in figure 2.

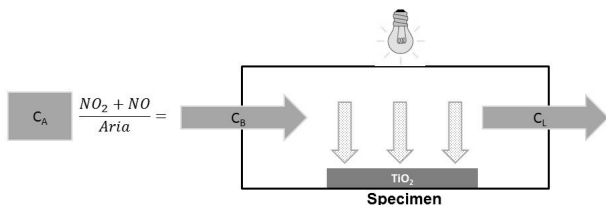


Figure 2. Test method scheme.

The photocatalytic activity in reducing NO_x is determined as the percentage difference between the

initial concentration in the dark (C_B) and the final concentration after 40 minutes of irradiation in stationary conditions (C_L).

The photocatalytic reduction rate (A_C) is defined by the formula:

$$\bar{A}_C[\%] = 100 * \frac{I_N}{I} * \frac{S_N}{S} * \frac{C_B - C_L}{C_B}$$

I_N e I = nominal Irradiance (20W/m²) e measured irradiance.

S_N e S = nominal area of the sample (64 cm²) measured area of the sample.

C_B = measured concentration of NO_x with UV lamp off (ppb).

C_L = measured concentration of NO_x with UV lamp on (ppb).

The result is a dimensionless index representing the decomposition rate of NO_x due to the UV radiation on the surface of the sample.

The characteristics of the results of each test are shown in figure 3.

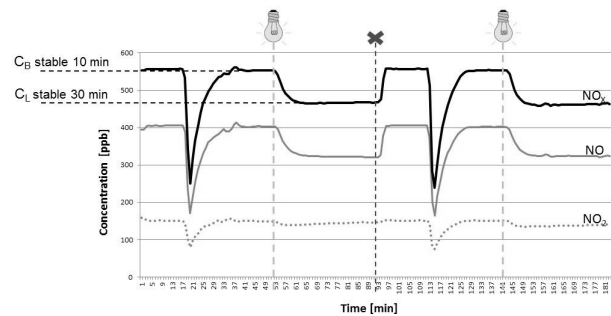


Figure 3. Implementation of photocatalytic activity measurement.

It can be seen that the concentration of pollutants remains constant until the UV lighting is activated, and then changes in the concentration are recorded until a new stationary condition is reached.

4. Analysis and interpretation of the results.

4.1 Initial test.

The photocatalytic capacity of the different products was initially measured, so as to select the products that were to be placed in the tunnel for a year. 6 products were tested: 5 types of paint with micron thickness (a, b, c, e, f) and one skim plaster with a thickness of about 2-3 mm (d).

Table 1 shows the results of the initial test.

Product	a	b	c	d	e	f
A_C [%]	16	20	17	35	29	4

Table 1. Degradation of nitrogen Oxides in the air at $t=0$.

The reduction rates of the products varied between 4 and 35%; five products had an interesting reduction rate and were therefore selected to be placed in the tunnel (a, b, c, d, e).

4.2 Placing the samples in the tunnel.

Inside the tunnel, the samples were placed in a row on a support with an inclination of about 40°. The

surface of the samples was lightened by UV lamps (type TL-D 36W BLB 1SL Philips) positioned at right angles to the samples, so as to irradiate the surface of the samples with a radiation intensity of about 10 W/m² (figure 4).



Figure 4. Samples placed in roadside Gallery with UV lamp system.

4.2 Measurement of the photocatalytic activity over time of samples with dirt deposited on them.

The photocatalytic activity of the products was measured in a laboratory at determined exposure time (1 month, 3, 6 and 12 months). The activity was measured on the samples taken from the tunnel both before removing any dirt from their surface and after removing it by using a brush and water.

Figure 5 reports the results of the tests, which show that as exposure time increased, the pollutant reduction capacity decreased.

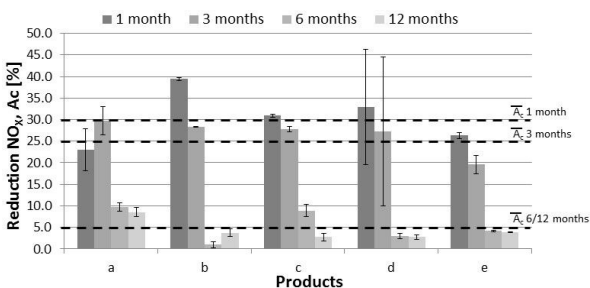


Figure 5. Degradation of NO_x in the air to the timing of 1, 3, 6, 12 months.

After one month, the average value of the reduction was about 30%, which, within the dispersion of the results, was comparable with the results of the initial tests on the samples.

After three months of exposure, a slight reduction of about 5% in the photocatalytic efficiency occurred. Between three and six months of exposure, products with dirt deposited on their surface lost about 20% of their efficiency. The same data were confirmed after one year of exposure in the tunnel.

Therefore, the decrease in the values is rather small after an exposure of three months in the tunnel. So in order to maintain the efficiency of the photocatalytic properties, cleaning should be carried out every three

months. After three months, all the products suffered a considerable decrease in their anti-pollution capacity.

4.3 Cleaning the samples and measuring dirt pickup.

When the samples were taken to the laboratory for the tests after the exposure times the different products had dirt pickups with a tendency of the dry films to attract considerable amounts of dirt on their surface. Therefore, the dirt deposits were removed using a brush and then weighted (figure 6).

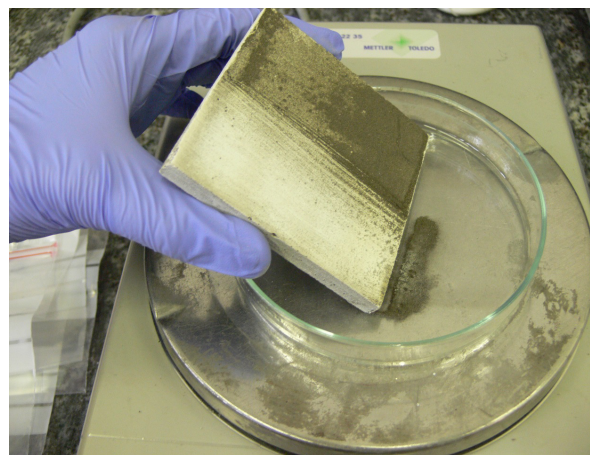


Figure 6. Removal of dirt deposited on the surface of the samples.

Figure 7 shows the analysed data expressed in g/m².

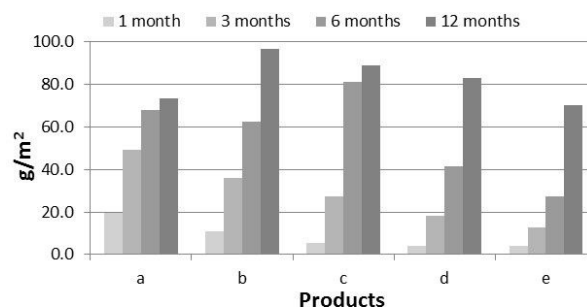


Figure 7. Dirt deposited in to the relationship exposure time.

The dirt amount increased with exposure time; dirt pickup in the first month was minimal, but the difference in the dirt deposition of the products could already be observed.

By correlating the different data it could be observed that, after one month, dirt pickup was minimal and did not seem to affect pollutant reduction properties. After three months of exposure, dirt pickup was higher and there was a slight loss in the pollutant reduction efficiency. After six months, dirt covered the entire surface, thus compromising the photocatalytic properties.

4.4 Measurement of photocatalytic activity over time of the samples cleaned in the laboratory.

The pollutant reduction rate was also measured after removing the dirt deposited on the surface. The dirt was first removed using a brush, then the surface was washed with water using a common multi-purpose manual water sprayer. Before repeating the tests to determine the pollutant reduction, the samples were dried in an oven at about 40 °C until their mass was constant.

Figures (fig. 8-11) below show the results of the tests performed at the set time intervals; the value of the pollutant reduction of the samples is shown both with and without dirt deposited on them.

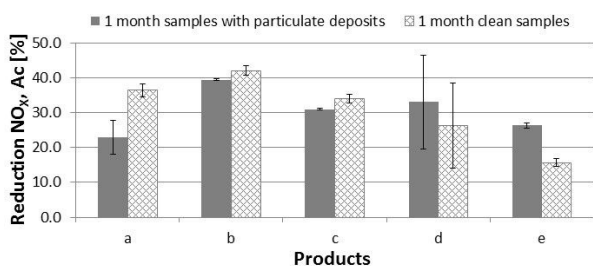


Figure 8. NO_x reduction after 1 month.

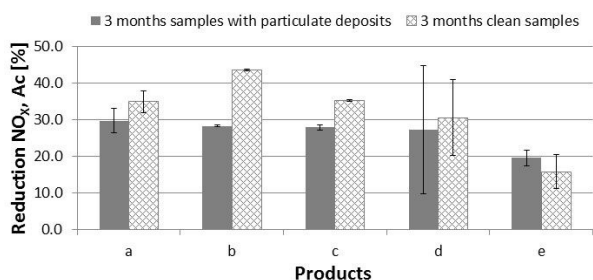


Figure 9. NO_x reduction after 3 months.

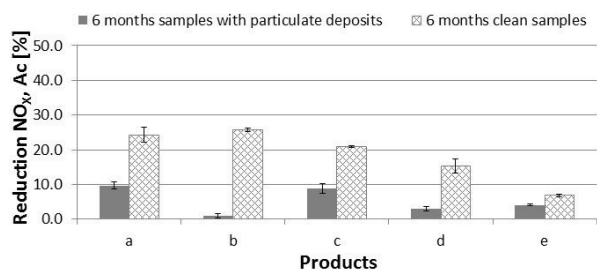


Figure 10. NO_x reduction after 6 months.

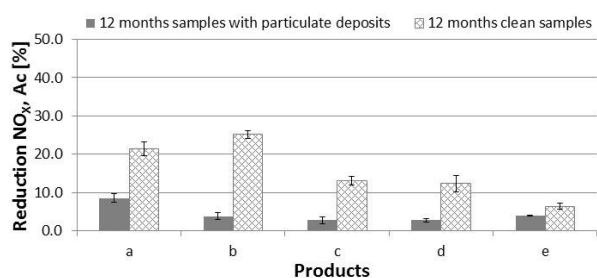


Figure 11. NO_x reduction after 12 months.

After cleaning the surface of the samples, it was observed that those exposed for one month recovered

their photocatalytic properties, except for products (d and e), which actually showed an unexpected behaviour, as there was no sign of recovery. The same trend was observed on the samples exposed for 3, 6 and 12 months.

Within statistical errors, the two samples that had the lowest dirt pickup showed no recovery or small recovery in their pollutant reduction capacity. This result may hint at an efficiency loss in the system; however, to demonstrate such loss further details about the product are needed.

In general, it can be said that the products with a higher dirt pickup showed a higher recovery in their pollutant reduction capacity when washed.

5. Conclusion.

The tests carried out highlighted that the dirt deposited on the surface of the samples reduced the photocatalytic efficiency of the products analysed. A significant decrease (about 20%) in the pollutant reduction capacity was observed between three and six months of exposure time. These results should be taken into account when planning the cleaning cycles of the tunnel surface.

All other things being equal, the different products showed different dirt pickup amounts; for some products, removing the dirt deposited on the surface of the samples by washing with water allowed to recover part of the nitrogen oxide reduction capacity. This conclusion, however, strictly depends on the exposure times used in the test and, therefore, at the moment, it cannot be predicted how long this trend is maintained.

The influence of some parameters relating to the products tested, like: the size of TiO₂ particles, the type of support, and the thickness of the layer applied onto the surface should be studied further to better understand some unexpected results.

Photocatalytic materials offer interesting opportunities; in fact, the capability of reducing nitrogen oxides has been shown in laboratory trials. However, before using these products in a widespread and intensive manner, on site further analysis of costs and benefits should be carried out. In particular, it is important to thoroughly analyse the context in which photocatalytic products are to be applied and keep in mind the factors that influence their anti-pollution properties. Studies published more recently (Gallus M. et al., 2015; Boonen E. et al., 2015; Guo M-Z., Maury-Ramirez A., Poon C.S., 2015) do not deny that the photocatalytic process has positive effects, however, the application of products that have photocatalytic properties in real contexts showed that a critical role in the preservation of anti-pollution properties over time depends on the substrate (e.g. by using smooth substrates, dirt pickup can be minimised). Moreover, it was also shown that photocatalytic activity is more efficient: when there is a higher concentration of NO_x; when the average relative humidity of the air is lower than 60%; when the average wind speed is low, which allows for higher times of reaction between pollutants and TiO₂; and when there is a high active surface/air volume ratio.

Finally, to activate the photocatalytic process, it is crucial to have a radiation level in the UV range (between 300 and 400 nm); to make to most of the anti-pollution properties of these products, a study should be carried out on how to use the properties of TiO₂ in the range of visible light.

- Fujishima, A. and Honda, K. (1972), *Electrochemical photolysis of water at a semiconductor electrode*, Nature, 238, 1972, pp. 37-38.
- Fujishima, A., Hashimoto, K. and Watanabe, T., *TiO₂ Photocatalysis: Fundamentals and its Applications*, BKC Inc., 1999.
- Cassar L., Pepe C. (1998), *Hydraulic Binder and cement compositions containing Photocatalyst Particles*, European Patent No. WO 9805601, Febbraio 12.
- Cassar L. (2004), *Photocatalysis of Cementitious Materials: Clean Buildings and Clean Air*, MRS Bulletin, Maggio 2004, pp. 328-331.
- Beeldens, A. and D. Van Gemert (2004), *Experimental investigation of efficiency of TiO₂-cement coating for self-cleaning and air purification*. RILEM Proceedings pro041 (RILEM International Symposium on Environment-Conscious Materials and Systems for Sustainable Development), pp. 353-359.
- Guerrini G.L., Peccati E. (2007), *Photocatalytic cementitious roads for depollution*, International RILEM Symposium on Photocatalysis, Environment and Construction Materials - TDP 2007, pp. 179-186.
- Maggos T. et al. (2008), *Photocatalytic degradation of NO_x in a pilot street canyon configuration using TiO₂-mortar panels*, Environ Monit Assess 136, pp. 35-44.
- Chen J., Poon C-S (2009), *Photocatalytic construction and building materials: from fundamental to applications*, Build Environ 44, Elsevier, pp. 1899-1906.
- Chen J., Poon C-S (2009), *Photocatalytic construction and building materials: from fundamental to applications*, Build Environ 44, Elsevier, pp. 1899-1906.
- Ohama Y., Van Gemert D. (2011), *Application of titanium dioxide photocatalysis to construction materials. State-of-the-Art Report of the RILEM Technical Committee 194-TDP*, Springer, XII; p. 48.
- Gurol M.D. (2006), *Photo-catalytic construction materials and reduction in air pollutants*, report Environmental Engineering, San Diego State University, <http://www.csus.edu/calst/frfp/photocatalytic.pdf>.
- Norma UNI 11247, *Determinazione dell'indice di abbattimento fotocatalitico degli ossidi di azoto in aria da parte di materiali inorganici fotocatalitici: metodo di prova in flusso continuo*, 2010.
- Alaimo G., Enea D., Guerrini G.L., Bottalico L. (2012), *Experimental evaluation of the durability of innovative cementitious coatings: photocatalytic activity and colour*, Proceedings of SPIE, vol. 8409-138.
- Boonen E., Beeldens A., (2014), *Recent Photocatalytic Applications for Air Purification in Belgium*, Coatings, 4, pp. 553-573.
- Guo M-Z., Maury-Ramirez A., Poon C.S., (2015) *Photocatalytic activities of titanium dioxide incorporated architectural mortars: Effects of weathering and activation light*, Building and Environment 94, pp. 395-402.
- Gallus M. et al. (2015), *Photocatalytic abatement results from a model street canyon*, Environmental Science and Pollution Research, Springer.
- Gallus M. et al. (2015), *Photocatalytic de-pollution in Leopold II tunnel in Brussels: NO_x abatement results*, Building and Environment 84, Elsevier, pp. 125-133.
- Boonen E. et al. (2015), *Construction of a photocatalytic De-polluting field site in the Leopold II tunnel in Brussels*, Environmental Management 155, Elsevier, pp. 136-144.

Consumer Acceptance and Societal Climate Benefits of Electric Vehicles: Insights from Individual Travel Patterns in China, U.S., and Europe

Xiaoyi He^{1,*,#}, Shaojun Zhang^{2,*,#}, Ye Wu^{1,3}, Timothy J. Wallington⁴, Michael A. Tamor⁴, K. Max Zhang², Xi Lu^{1,3}, Jiming Hao^{1,3}

¹ School of Environment, State Key Joint Laboratory of Environment Simulation and Pollution Control, Tsinghua University, Beijing 100084, P. R. China. hexy13@mails.tsinghua.edu.cn.

² Sibley School of Mechanical and Aerospace Engineering, Cornell University, Ithaca, New York 14853, USA

³ State Environmental Protection Key Laboratory of Sources and Control of Air Pollution Complex, Beijing 100084, P. R. China

⁴ Research and Advanced Engineering, Ford Motor Company, 2101 Village Road, Dearborn, MI 48121, USA

Abstract

Electrification of transportation is expected to play a critical role in realizing the 2°C climate target of the Paris Agreement. Climate and consumer benefits of electric vehicles (EVs) differ amongst individuals due to the diverse travel patterns, which also vary with country. Such heterogeneity raises the need for better portfolio strategies regarding mass adoption of EVs. We developed an integrative assessment model using travel profiles of 1789 passenger vehicles in China, U.S., and Europe to quantify the location-specific individual distributions of potential consumer savings and greenhouse gas (GHG) emission mitigation from the spread of EVs. Our results depict a cross-region positive synergy between consumer and climate benefits that consumers who could save more costs from conventional vehicles-to-EVs switching would also tend to reduce GHG emissions. Lower battery costs will change the present unfavorable situation of long-range (300 km) battery electric vehicles (BEV300), which will be more economically advantageous than conventional vehicles and plug-in hybrid electric vehicles (PHEVs) in 2030. We identify future priority BEV300 consumers, a cohort with significant cost savings (top 25%), can mitigate 58-70% cradle-to-grave GHG emissions. Climate benefits from electrification are expected to be strengthened by offering a massive storage capacity as vehicle batteries for the power grid to accommodate variable renewable sources.

Introduction

Electric vehicles (EVs), defined here as battery electric vehicles (BEVs) and plug-in hybrid electric vehicles (PHEVs), are important options to address global climate change and local air pollution (IEA, 2017; Ke, W., et al., 2017). The IEA's scenario limiting global warming to 2°C (2 Degree Scenario, 2DS) includes 140 million EV sales by 2030. Ownership cost, charging infrastructure development, and policy incentives are critical factors that determine whether such a growth in EV sales will occur. The climate benefits from electrification hinge on how many EVs are sold and how intensely they are used. EV acceptance and climate benefits need to be evaluated individually to develop customer-focused technology and policy recommendations. To address this need, travel pattern data from 1789 light-duty passenger vehicles in China (Beijing), U.S. (Atlanta, Minneapolis, and Seattle), and Europe (Germany) were analysed. The individual EV acceptance potential was estimated based on the comparative difference in total cost of ownership (TCO) between EVs and internal combustion engine vehicles (ICEVs). Particularly for BEVs, the battery range limitation is further taken into account comparing with an inconvenience threshold when they are not sufficient for long-distance travels and need to be substituted by alternative transportation options. The individual greenhouse gas (GHG) emission mitigation potentials were characterized to understand the heterogeneity among various potential EV adopters.

Methods

The multiday disaggregated vehicle activity datasets are from personal travel survey in five metropolitan areas (Beijing, Atlanta, Minneapolis, Seattle, and five German cities as one cluster; in form of megacity or urban agglomeration) from three important automotive markets (He, X. et

al. 2016; Tamor, M. et al. 2013). Detail travel trajectory profiles from 1789 conventional personal vehicles were obtained by using GPS data loggers, and data collection lasted at least one month for each vehicle to cover the multiday variation. We applied an individual trip chain distribution (ITCD) model consisting of an exponential distribution and a Gaussian distribution, which represent habitual trips and random trips respectively. This ITCD model includes charging at home (overnight residential charging exclusively) and charging at the mid-point of habitual travel (usually at workplace). We assume that individual travel patterns are unchanged when switching from ICEV to EV, and the trips that exceeds BEV range are covered by alternative transportation. The ITCD function of each vehicle has been normalized to a one-year basis for TCO estimation.

We applied the comparative TCO between EV and ICEV to estimate the potential acceptance depending on each individual's travel pattern. The comparative TCO considers major attributes relevant to the economic completeness of vehicle electrification, including initial fixed vehicle cost exclusive of battery cost, tax and other initial fees, incremental cost of high-voltage battery system, potential electrified mileage, improved fuel economy, fuel price, and one-time economic incentives (e.g., purchase subsidies). Vehicle cost is estimated based on a generic mid-size passenger car over the entire vehicle lifetime of 15 years. We select a mid-size light-duty passenger car as a representative vehicle which is popular in all the vehicle markets considered in the present work. Further work is warranted for other light-duty vehicle classes (e.g., compact cars, sport-utility vehicles, and trucks) and for medium- and heavy-duty vehicles to provide a more complete picture of the potential scope and benefits of electrification of the on-road vehicle fleet. Costs of future vehicle technologies were estimated based on component manufacture cost²⁴ with a markup factor to indicate retail price. For BEV adopters, we include the cost on alternative transportation options when the BEV is incapable of covering long-distance travel. The annual cost items of all vehicles are estimated with cash flow discounted to the base year (2015). The heterogeneity of travel patterns among individual vehicle users would influence the potential electrified mileage and capability of operating an BEV, which is simulated according to each vehicle and each day. Four generic EV models varying by powertrain type and all electric range (PHEV20, PHEV50, BEV150 and BEV300) are considered. If an individual has a lower TCO using PHEV than the ICEV counterpart, we define this user as a potential PHEV adopter. We consider the range-limit-caused inconvenience as an additional threshold to define potential BEV adopters. One potential BEV adopter should not only have a lower TCO than using ICEV but also limited number of days in one year when this user's driving distance exceeds battery range. The region-specific EV acceptance level is defined as the proportion of potential EV adopters in the total amount of travel investigation samples in that region.

C2G GHG emissions, including emissions during fuel production, vehicle operation and vehicle manufacture, are calculated according to individual travel patterns. The upstream emissions of fuel production (grams of CO_{2e} per unit gasoline, diesel or electricity) were estimated using the GREET2016 model, with consideration of the local energy generation mix and generation efficiency. For the vehicle manufacture processes, we employed the BatPac model to determine battery composition for each powertrain configuration, which provided the GREET2016 model with input data to further estimate GHG emissions over production activities of components, battery and fluids as well as those in the assembly, disposal, and recycle processes. Finally, we calculated individual C2G GHG emission reductions on a yearly basis to characterize their climate change mitigation potentials if switching to various EV technologies.

Results and discussion

Inspection of regional-specific TCO over vehicle lifetime (15 years) reveal important factors in the cost-competitiveness of EVs. First, as the all-electrified range (AER) increases, battery costs account for a substantial fraction of the TCO (47-64% for 300 km AER BEVs). Although monetary incentives are available for BEV purchases, they are not sufficient to fully offset the battery cost. Second, the fuel price differential between conventional liquid fuels and electricity affects the competitiveness of EVs. U.S. cities have more expensive electricity and less expensive gasoline than Beijing, which decreases the economic attractiveness of EVs. Third, alternative transportation options are required by BEV adopters when their travel distance exceeds the AER and the costs for alternative transport differ substantially for the different regions. Beijing has an economic and convenient public transportation system, which is a

favorable factor for electrification. Minneapolis does not, and the cost for alternative transport is a major factor in the total cost of ownership for the BEV150.

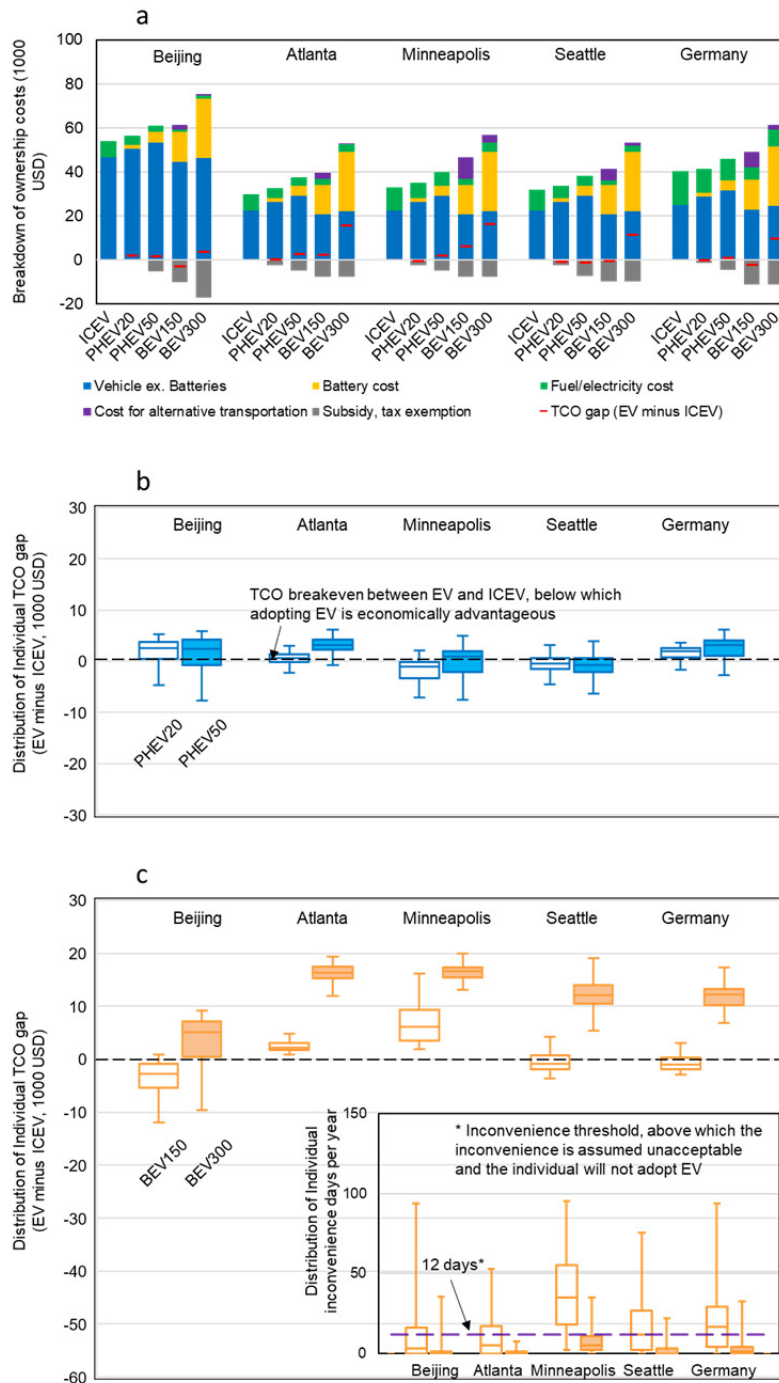


Figure 1: Breakdown of total cost of ownership (TCO) for internal combustion engine vehicles (ICEVs), PHEVs and BEVs (panel a); and box-whisker plots of individual TCO gaps between EVs (PHEVs in panel b and BEVs in panel c) and ICEVs in 2015. Vehicle cost is modeled based on a generic mid-size passenger car. In Beijing and U.S. cities, EVs are compared to gasoline ICEVs. In Germany, EVs are compared to a 50%/50% mix of gasoline and diesel passenger vehicles. EVs are assumed to be fully charged overnight at home.

Lower battery costs are essential for mass adoption of BEVs, particular for BEVs with large AERs (e.g., BEV300). Currently with high battery cost, BEVs with small-sized batteries (e.g., BEV150) could be a reasonable option in regions with economic and convenient alternative transportation systems and with strong EV-favorable policies. This is demonstrated by the sensitivity analysis of acceptance potential to various inconvenience thresholds and charging availability levels. By varying the inconvenience thresholds from low tolerance (1 day per year) to high tolerance (52 days per year), we observe that the acceptance levels of BEV150 increase by 45%-74%. This finding could help quantify the benefits from non-monetary incentives. For example, BEVs in Beijing are exempted from local traffic management that prohibit regular ICEVs from urban areas one weekday per week. If BEV users in Beijing tolerated the same inconvenience level as ICEV users (~52 days per year), the acceptance level of BEV150 would increase to 80%, the highest acceptance among all cities in this study. It is also estimated that additional workplace charging provides a modest increase in acceptance potentials (0-14%) for BEV and small to none for PHEVs.

Existing evaluations of GHG emission reductions from electrification are based on macroscale and aggregated travel profiles. Some recent studies have emphasized the heterogeneity of travel patterns across various cities and drivers (Björnsson, L.-H. & S. Karlsson, 2015; Cai, H. & Xu, M., 2013). However, the aggregated inputs in these studies still implicitly ignore the intra-city heterogeneity across individuals and have limited capability of designing customized electrification strategies. Taking BEV300 for example, the median values of C2G GHG emission reductions based on detailed individual travel profiles could be lower than those based on aggregated average travel profile by up to 15% depending on location (see Figure 2).

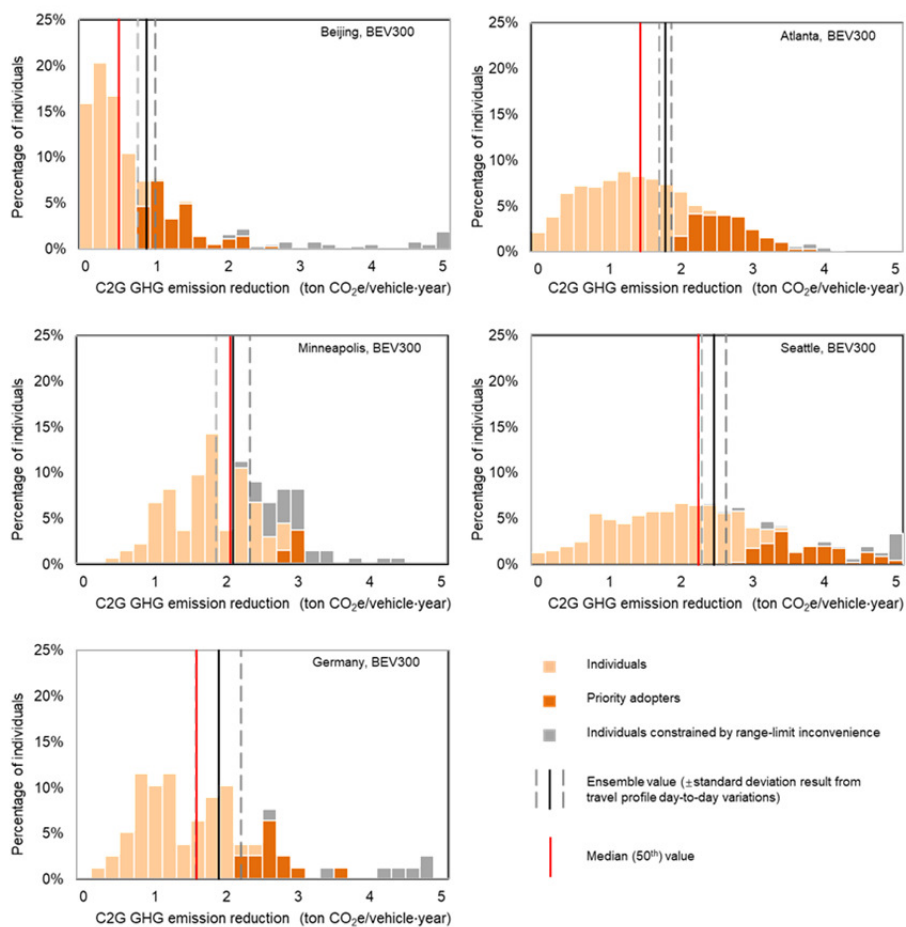


Figure 2: Comparison of different evaluation approaches (see Supplementary Section 1.2 for details) to estimate C2G GHG emissions reduction of BEV300 in five places. This study estimates C2G GHG emission reductions at individual level (*shown as bars*), based on multiday disaggregated travel profiles; the top 25% individuals that could gain most TCO savings from

adopting EV were selected out as priority EV adopters and their average C2G GHG emission were demonstrated as *dark orange bars*, among which some were constrained by range-limit convenience and hence not considered as probable adopters (*grey bars*).

Previous studies usually aggregate individual travel profiles into ensemble level (see *black lines*), which implicitly assume every driver follows the same travel pattern as the aggregated average. This could lead to bias in estimating C2G emission of EVs, especially when it comes to probable adopters. Dotted lines represents standard deviations resulted from day-to-day travel profile variations. The U.S. National Household Travel Survey (NHTS) has involved personal travel investigation where single-day travel records of each participant are gathered. This endeavor is expected to compensate amend the impact from lacking individual heterogeneity. Our reproduced individual travel profiles using a quasi-NHTS approach suggest that the day-to-day variation in travel profiles could still lead to normalized standard deviations of 3%~16%.

More importantly, as discussed above individual driving behaviors lead to a wide range of acceptance levels for EVs, Figure 2 further demonstrates a universal cross-region tendency except for BEV150s in Minneapolis that individual drivers who gain larger economic benefits in terms of TCO savings would also have greater climate change mitigation potentials. Here we define the top 25% high TCO-savers as “*priority EV adopters*”. These *priority PHEV adopters* are likely to be associated with high annual mileage levels, who could have more electrified mileage and mitigate more GHG emissions. Results show that these *priority PHEV adopters* could reduce more GHG emissions than the rest users by 80% to 279%, depending on local features (e.g., mileage, power system carbon intensity). The *priority BEV adopters* would reduce GHG emissions by 40% to 220% across various places, except for the BEV150 case in Minneapolis. Thus, the G2G emission mitigation potentials may be underestimated if evaluations are based on average travel profiles, because “*priority EV adopters*” are estimated to be more economically motivated for electrification. Meanwhile, we identify a part of individuals who are constrained by range-limit-inconvenience hence not considered as BEV adopters (grey bars in Figure 2). They could have achieved higher emission reductions if they were willing to tolerate more than 12 days per year inconvenience. The availability of convenient, economic, and low-carbon alternative transportation options facilitate an e-mobility future.

References

- Björnsson, L.-H. & S. Karlsson. Plug-in hybrid electric vehicles: How individual movement patterns affect battery requirements, the potential to replace conventional fuels, and economic viability. *Applied Energy* 143(0): 336-347 (2015).
- Cai, H. & Xu, M. Greenhouse gas implications of fleet electrification based on big data-informed individual travel patterns. *Environmental Science & Technology* 47(16): 9035-9043 (2013).
- He, X., et al. Individual trip chain distributions for passenger cars: Implications for market acceptance of battery electric vehicles and energy consumption by plug-in hybrid electric vehicles. *Applied Energy* 180: 650-660 (2016).
- Ke, W., et al. Assessing the Future Vehicle Fleet Electrification: The Impacts on Regional and Urban Air Quality. *Environmental Science & Technology* 51(2): 1007-1016 (2017).
- International Energy Agency. Global EV outlook (2017). Available from URL: <https://www.iea.org/publications/freepublications/publication/GlobalEVOutlook2017.pdf>
- National household travel survey. U.S. Department of Transportation. Federal Highway Administration. <http://nhts.ornl.gov/>. Cited June, 2017.
- Needell, Z. A., et al. Potential for widespread electrification of personal vehicle travel in the United States. *Nature Energy* 1: 16112(2016).
- Tamor, M. A., Gearhart, C. & Soto, C. A statistical approach to estimating acceptance of electric vehicles and electrification of personal transportation. *Transportation Research Part C: Emerging Technologies* 26: 125-134 (2013).

The Greenhouse gases, Regulated Emissions, and Energy use in Transportation (GREET) Model, version 2016. Developed by the U.S. Argonne National Laboratory. Available at url: <http://greet.es.anl.gov/>

The battery performance and cost (BatPaC) model. Developed by the U.S. Argonne National Laboratory. Available at url: <http://www.cse.anl.gov/batpac/index.html>

Physico-chemical characterization of fine and ultrafine non-exhaust particles generated by road traffic in urban and suburban environment

A. Beji¹, K. Deboudt¹, P. Flament¹, M. Fourmentin¹, S. Khaldi², B. Muresan², A. Thomasson³

¹Laboratory of Physics and Chemistry of the Atmosphere (LPCA), Université du Littoral Côte d'Opale, Dunkerque, 59140, France

²The French Institute of Science and Technology for Transport, Development and Networks (IFSTTAR), Marne la Vallée, 77447, France.

³ATMO Auvergne-Rhône-Alpes, Saint Martin d'Hères, 38400, France

Keywords: atmospheric aerosol, non-exhaust particles, roadside, air quality.

Presenting author email: asmabeji@gmail.com

Atmospheric particulate matter has well-known adverse effects on human health and climate. Road transport is one of the most important sources of particulate matter, and is considered to be involved in all major air pollution events in urban and suburban environments. Some studies have shown clear contributions of non-exhaust emissions to traffic particles. These emissions consist essentially in particles produced by abrasion from brakes, road wear, tires wear and vehicle induced resuspension of deposited road dust.

In this context, this work is focused on the contribution of non-exhaust particles to the roadside air quality, for different driving situations associated with different studied sites:

- in a braking situation (near a toll barrier) with a rural background
- in a braking situation (traffic jam) with an urban background
- in a continuous driving flow situation with a rural background
- in a continuous driving flow situation with an urban background

Atmospheric aerosols were collected by cascade impaction upwind and downwind from the road, for each studied site (Lyon and Grenoble, France), mainly for individual particle analysis by Scanning Electron Microscopy (SEM-EDX). Complementary measurements were also performed, especially particle size distributions with optical particle counters (OPC) and electrical mobility sizers (SMPS and FMPS), NO_x concentrations and black carbon concentrations with an aethalometer.

A special attention was paid to atmospheric dynamic considering meteorological data and turbulence state of the Atmospheric Boundary Layer (ABL).

In case of low ABL, with a clearly established local wind direction, perpendicular to the road, typically in the morning, a major evolution of the size distribution is evidenced, due

to the contribution of traffic emissions. Downwind the road two major modes centred on 200-300nm and 2-3µm and not present upwind, are observed (Figure 1). At the opposite, typically in the afternoon, a low whirlwind and a high ABL limit the impact of traffic emissions on downwind particle concentrations.

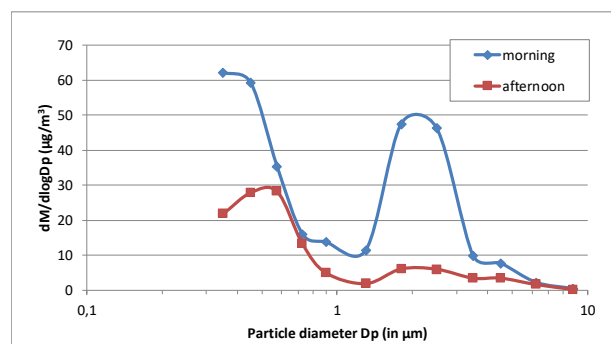


Figure 1. Example of particle mass-size distribution measured downwind from the road at the "Saint Priest" station with an OPC (continuous driving flow in a rural background).

In addition, a large number of particles per sample (typically 1,000) were observed by automated SEM-EDX to yield representative results. A significant input of iron-rich particles is observed at the downwind sites, notably for particle diameters larger than 1 µm, probably coming from non-exhaust emissions. Particles containing iron are also detected in submicron particles, but with lower iron concentrations. The elemental maps of this last kind of particles illustrated iron oxide compounds internally mixed with carbonaceous compounds.

Acknowledgment: This work was supported by the French Environment and Energy Management Agency (ADEME), CAPTATUS Project, grant Corcea n°1566C0016.